JAERI-M
84-007

# ROSA-III 200% DOUBLE-ENDED BREAK INTEGRAL TEST RUN 901

## (FULL ECCS ACTUATION)

February 1984

Hideo NAKAMURA, Kanji TASAKA, Yasuo KOIZUMI
Yoshinari ANODA, Hiroshige KUMAMARU, Hideo MURATA
Mitsuhiro SUZUKI and Masayoshi SHIBA

日本原子力研究所
Japan Atomic Energy Research Institute

JAERI-Mレポートは，日本原子力研究所が不定期に公刊している研究報告書です。
入手の問合わせは，日本原子力研究所技術情報部情報資料課（〒319-11茨城県那珂郡東海村）あて，お申しこしください。なお，このほかに財団法人原子力弘済会資料センター（〒319-11 茨城県那珂郡東海村日本原子力研究所内）で複写による実費領布をおこなっております。

JAERI-M reports are issued irregularly.
Inquiries about availability of the reports should be addressed to Information Section, Division of Technical Information, Japan Atomic Energy Research Institute, Tokai-mura, Naka-gun, Ibaraki-ken 319-11, Japan.



編集兼発行　日本原子力研究所
印　　刷　いばらき印刷㈱

JAERI-M 84-007

# ROSA-III 200% Double-Ended Break Integral Test RUN 901
## ( Full ECCS actuation )

Hideo NAKAMURA, Kanji TASAKA, Yasuo KOIZUMI
Yoshinari ANODA, Hiroshige KUMAMARU, Hideo MURATA
Mitsuhiro SUZUKI and Masayoshi SHIBA

Department of Nuclear Safety Research,
Tokai Research Establishment, JAERI

(Received January 11, 1984)

This report presents the experimental data of RUN 901, a 200% double-ended break test at the recirculation pump suction line with the ROSA-III test facility. The ROSA-III test facility is a volumetrically scaled (1/424) system of the BWR/6. The facility has the electrically heated core, the break simulator and the scaled ECCS (Emergency Core Cooling System). The MSIV closure and the ECCS actuation were tripped by the liquid level in the upper downcomer. The channel inlet flows were measured by differential pressure transducers installed at the channel inlet orifices of the fuel assembly No.4. The PCT (Peak Cladding Temperature) was 780 K occured during the blowdown phase in RUN 901. The whole core was quenched after the ECCS actuation and the effectiveness of ECCS has been confirmed.

Keywords: BWR, LOCA, ECCS, Integral Test, ROSA-III Program,
200% Double-Ended Break, PCT, Fuel Assembly No. 4

JAERI－M 84－007

# ROSA－Ⅲ 200％両端破断総合実験；RUN901
## （全ECCS作動）

日本原子力研究所東海研究所安全工学部
中村　秀夫・田坂　完二・小泉　安郎
安濃田良成・熊丸　博滋・村田　秀男
鈴木　光弘・斯波　正誼

（1984年1月11日受理）

本報は，ROSA－Ⅲ実験装置を用いた，再循環ポンプ入口配管での200％両端破断実験RUN901の実験結果について記述したものである。ROSA－Ⅲ実験装置は，BWR／6型原子炉の炉心を電気加熱ヒーターで模擬した実炉との体積比（1／424）の装置である。RUN901において，すべての非常用炉心冷却系（ECCS；Emergency Core Cooling System）が作動させられた。上部ダウンカマ水位信号により主蒸気隔離弁閉鎖およびECCS作動が行われた。炉心入口流量は炉心入口オリフィスに取り付けた差圧伝送器によって測定された。RUN901の最高被覆管温度は780Kで，ブローダウンの際に生じた。全炉心はECCS作動後クエンチECCSの有効性が確認された。

Contents



# 目　　次

LIST OF TABLES



LIST OF FIGURES

## ABBREVIATIONS

| | |
|---|---|
| ADS | Automatic Depressurization System |
| AT | Air Tank |
| AV | Air Actuation Valve |
| (2)B | (2) inches Pipe of Schedule 80 |
| BN | Boron Nitride |
| BWR | Boiling Water Reactor |
| CA | Chromel-Alumel |
| CCFL | Counter Current Flow Limiting |
| CHV | Check Valve |
| CP | Conductivity Prove |
| CV | Control Valve |
| CWT | Cooling Water Tank |
| D | Differential Pressure |
| d | Diameter |
| DF | Density of Fluid |
| DL(+100) | Elevation (+100 mm) from the Bottom of PV |
| ECCS | Emergency Core Cooling System |
| ESF | Engineered Safety Features |
| EX | Heat Exchanger |
| F | Flow Rate |
| Fig. | Figure |
| FS | Full Scale |
| FW | Feedwater |
| FWLF | Feedwater Line Flashing |
| FWP | Feedwater Pump |
| FWT | Feedwater Tank |
| HPCS | High Pressure Core Spray |
| HPCSP | High Pressure Core Spray Pump |
| HPCST | High Pressure Core Spary Tank |

| | |
|---|---|
| HPWP | High Pressure Water Pump |
| ID | Inner diameter |
| INC 600 | Inconel 600 |
| JP | Jet Pump |
| K | Kelvin |
| kg | Kilogram |
| kPa | Kilopascal |
| kW | Kilowatt |
| L | Liter |
| LB | Liquid Level in Channel Box |
| LBWR | Large Boiling Water Reactor |
| LL | Liquid Level |
| LOCA | Loss-of-Coolant Accident |
| LOCE | Loss-of-Coolant Experiment |
| LP | Lower Plenum |
| LPCI | Low Pressure Coolant Injection |
| LPCIP | Low Pressure Coolant Injection Pump |
| LPCIT | Low Pressure Coolant Injection Tank |
| LPCS | Low Pressure Core Spray |
| LPCSP | Low Pressure Core Spary Pump |
| LPCST | Low Pressure Core Spary Tank |
| LPF | Lower Plenum Flashing |
| LTP | Lower Tie Plate |
| M | Momentum Flux |
| m | Meter |
| mm | Milimeter |
| MLHR | Maximum Linear Heat Rate |
| MPa | Megapascal |
| MRP | Main Recirculation Pump |
| MSIV | Main Steam Isolation Valve |
| MSL | Main Steam Line |

| | |
|---|---|
| MW | Megawatt |
| N | Rotation Speed |
| OR | Orifice |
| P | Pressure |
| | Power |
| PCT | Peak Cladding Temperature |
| PV | Pressure Vessel |
| PWT | Pure Water Tank |
| QOBV | Quick Opening Blowdown Valve |
| QSV | Quick Shut-off Valve |
| RCN | Rapid Condencer |
| ROSA | Rig of Safety Assessment |
| rpm | Revolution per Minute |
| S | Signal |
| s | Second |
| Sch | Schedule |
| SUS | Stainless Steel |
| T | Temperature |
| T/C | Thermocouple |
| TC | Temperature of Fluid |
| TF | Temperature of Fuel |
| TS | Temperature of Structure Material |
| UTP | Upper Tie Plate |
| V | Valve |
| VF | Void Fraction |
| W | Watt |
| WL | Water Level |
| WSP | Water Supply Pump |

## 1. Introduction

The Rig of Safety Assessment (ROSA)-III program was initiated in 1976 to study the thermal-hydraulic behavior of a Boiling Water Reactor (BWR) during a posturated Loss of Coolant Accident (LOCA) with the Emergency Core Cooling System (ECCS) actuation and to provide the data base to evaluate the predictability of computer codes developed for reactor safety analysis. The ROSA-III test facility was fabricated in 1978 and consisted of the volumetrically scaled (1/424) primary system of a 3800 MW BWR/6-251 with the electrically heated core, the break simulator and the scaled ECCS[1].

Special emphasis is made on the following objectives in the ROSA-III program:

(1) to provide the system data required to improve and evaluate the analytical methods currently used to predict the LOCA response of large BWRs. The performance of the Engineered Safety Features (ESFs), with particular emphasis on ECCSs, and the quantitative margins of safety inherent in performance of the ESFs are of primary interest.

(2) To identify and investigate any unexpected event(s) or threshold(s) in the response of either the plant or the ESFs and develop analytical techniques that adequately describe and account for such unexpected behavior.

The information acquired from Loss of Coolant Experiments (LOCEs) is thus used for evaluation and development of LOCA analytical methods and assesment for the qualitative margins of safety of ESFs in response to a LOCA.

RUN 901, conducted on April 8, 1981, was an acceptance test of the fuel assembly No. 4 and simulated a 200% double-ended break at the recirculation pump suction line with the assumption of full ECCS actuation as designed.

The fuel assembly No. 4 was improved from No. 3 to simulate the core of the BWR/6 more realistically and to obtain more information about the thermal-hydraulic phenomena inside shroud. Major improved items are followings and the comparison of four fuel assemblies are also listed in Table 1.1.

1) The local peaking factor in a channel is introduced as shown in Fig. 2.7.
2) The channel inlet orifice is simulated by one hole (44 $\phi$ ID) each channel.
3) The upper end of the channel box is lengthened.
4) The differential pressures across the channel inlet orifices and the bypass holes are measured to measure the core inlet flow rate.
5) Number of conduction probes are increased to measure the mixture level more accurately.
6) Thermo-couples above and below the upper tie plate are increased to measure the counter current flow limiting (CCFL) behavior.
7) Thermo-couples are installed on the channel box wall outside to measure the liquid behavior in the core bypass.

The specific objectives of RUN 901 are as follows.

(1) To provide test data of a 200% double-ended break test at the recirculation pump suction line with full ECCS actuation.
(2) To confirm the closure of the flow path between inside and outside the core shroud.
(3) To confirm the trip signals by the liquid level probes in the upper downcomer for the Main Steam Isolation Valve (MSIV) closure and the ECCS actuation in a large break test.
(4) To confirm the function of the new instrumentation installed in the fuel assembly No. 4.

In this report, all the data obtained in RUN 901 are presented. The processed data like mass inventory in the pressure vessel are also given.

## 2. ROSA-III Test Facility

The ROSA-III test facility is a volumetrically scaled (1/424) BWR system with an electrically heated core designed to study the response of the primary system, the core and the ECCS during the postulated LOCA. The test facility is instrumented such that various thermal-hydraulic parameters are measured and recorded during the test. Details of the instrumentation are described in Section 3.

The test facility consists of four subsystems. These subsystems are : (a) the pressure vessel, (b) the steam line and the feedwater line, (c) the recirculation loops and (d) the ECCS. Figures 2.1 through 2.3 illustrate configuration of the test facility, the pressure vessel internals and the piping schematics, respectively. Table 2.1 compares the major dimensions of the ROSA-III test facility to the corresponding dimensions of the reference BWR system.

The ROSA-III pressure vessel includes various components in it simulating the internal structures of the reactor vessel in the BWR system as shown in Fig. 2.4. The interior of the vessel is divided into the core, the lower plenum, the upper plenum, the downcomer annulus, the steam separator, the steam dome and the steam dryer. The core is consisted of four model fuel assemblies of half length and a control rod simulator. Each fuel assembly contains 62 heater rods (Fig. 2.5) and 2 water rods spaced in a 8 x 8 square array and supported by spacers and upper and lower tie plates. The heater rod is heated electrically with chopped cosine power distribution along the axis as shown in Fig. 2.6. The effective heated length is 1880 mm, one half of the active length of a BWR fuel rod. The electric power supplied to the model fuel assembly "A" is 1.4 times larger than the power supplied to each of the other assemblies. The heater rods in each assembly are divided into three groups in terms of heat generation rate as shown in Fig. 2.7. The relative power generation rate of a heater rod in each group is 1.1,

1.0, and 0.875 respectively. The orifice plates are inserted at the core inlet to control the core inlet flow[1].

The steam line is connected to the steam dome of the pressure vessel. A control valve is installed in the steam line to control the steam dome pressure in steady state before the initiation of the tests. The steam line has a branch in which the automatic depressurization system is installed. The operation of valves in the steam line is described in Sec. 4. The feedwater is supplied from the feedwater tank (FWT) through the feedwater line and the feedwater sparger below the steam separator.

Figure 2.8 shows the recirculation lines consisted of two loops. Each line is furnished with a pump and two jet pumps. The jet pumps are installed outside the pressure vessel to simulte the relative volume and the relative height to the core. Two break simulators and a quick shut-off valve (QSV) are installed in one of these loops to simulate the various break conditions. Each break simulator consists of a nozzle or a orifice to determine the break size and a quick opening blowdown valve (QOBV) to initiate the test. The break mode (double-ended or split), the break size and the break location can be changed. The diameter of the largest nozzle and orifice available is 26.2 mm. Figure 2.8 shows two QOBVs, a QSV and flow nozzles installed upstream of the QOBVs. Several flow nozzles and orifices of different size are prepared to vary the break size.

The ROSA-III test facility is furnished with all kinds of the ECCS available in the BWR system, i.e., the High Pressure Core Spray (HPCS), the Low Pressure Core Spray (LPCS), the Low Pressure Coolant Injection (LPCI), and the Automatic Depressurization System (ADS). The HPCS and the LPCS provide the cooling water from the top of the core. The LPCI injects the cooling water into the core bypass. Each ECCS consists of a pump, a tank, piping, and a control system.

Reference (1) serves more detailed information on the facility.

## 3. Instrumentation

The instrumentation of the ROSA-III is designed to obtain thermal-hydraulic data during the simulated BWR LOCA. The data obtained from the experiments will contribute to the assessment of the analytical computer code. Table 3.1 summarizes instrumentation used in RUN 901.

Tables 3.2 and 3.3 show the measurement list of RUN 901 and the core instrumentation list, respectively. Instrumentation locations are shown in Fig. 3.1 through Fig. 3.7.

Typical measured parameters in the ROSA-III are pressure, differential pressure, flow rate, electric power, pump speed, fluid and metal temperatures, collapsed liquid level, two-phase mixture level, coolant fluid density, on-off type signals and so on.

Pressure and differential pressure transducers are two-wire, direct-current type which convert diaphragm displacement to electric capacitance. The pressure lead pipes are either the standard single, cylindrical pipes used in conjunction with condensate pots, or dual concentric cylinders capable of the circulation of cooling water to prevent flashing of the fluid.

The flow rate is measured either by an orifice or a venturi type flow meter depending on the fluid condition and measurement location.

The temperatures of the fluid, structural material and fuel rod cladding are measured with Chromel-Alumel thermocouples (CA T/C) of 1.6 or 0.5 mm $\phi$.

Liquid levels are measured by either differential pressure transducers, described above or needle type electrical conductivity probes (CP) developed in the ROSA-III program. The probes are distributed along the vessel hight to detect the existence of water or vapor at different levels.

The electric power supplied to the simulated fuel rods is controlled to follow the predetermined function of time and measured by

a fast response electric power meter.

Pump speed is measured by a pulse generator integral of the pump. On-off signals such as selected valve positions, decay heat and pump coastdown simulation initiations and so on are detected in order to record the exact actuation time.

Fluid density in the pipe is measured by means of gamma-ray densitometers. Preliminary studies indicate that a three-beam densitometer should be used to determine the flow regime. Figures 3.7 and 3.8 show the beam directions of the three-beam and the two-beam gamma densitometers, respectively. The gamma-ray source is $^{137}Cs$ and the detector is a water cooled NaI (Tl) scintillation counter.

Momentum flux is measured by a drag disk as shown in Fig. 3.9. The combination of signals from a drag disk and a gamma densitometer is used to determine the two-phase flow rate as shown in Fig. 3.10.

The data acquisition system ( DATAC 2000B, Iwasaki Tsūshinki Co. ) scans all the 700 channels of signals with the frequency up to 30 Hz. The data recorded on magnetic tape are processed by the FACOM M200 system computer at JAERI by off-line control. After evaluation, for example by comparing the initial and final pressure values with standard values, the data is reprocessed using the correct conversion factors as determined from the consistency examination.

More detailed information on the instrumentation and the data processing procedure are available in Reference (2).

## 4. Test Conditions and Procedure

RUN 901 is a 200% double ended large break test at the recirculation pump suction in the recirculation line. The break area is determined by inserting an nozzle upstream of the QOBV as shown in Figs. 4.1 and 3.9. Blowdown is initiated by opening the QOBV and closing the QSV placed between the two break simulators. The initial conditions of the test are as follows: The steam dome pressure is 7.29 MPa, the lower plenum temperature is 552 K giving the subcooling of 10.5 K, the core inlet flow rate is 16.0 kg/s, the core heat generating rate is 4.045 MW. The estimated quality at the core outlet is 13.9%. The detailed conditions are summerized in Table 4.1.

To conduct the test, makeup water (pure water) is pumped into the primary system of the test facility and electric power is supplied to the core to heat the water in the system and to achieve the saturation condition in the upper portion of the pressure vessel. The core power is 4.045 MW before the break initiation and is 45% of the steady state power 9 MW based on the conservation of the power to volume ratio in the reference BWR. The core power is changed during the transient after the break initiation as shown in Fig. 4.2. The power is kept constant for the first 7.0 seconds and reduced along the curve shown in the figure which simulated the total heat transfer rate in the core of the reference BWR (the delayed neutron fission power, the decay power of fission products and actinides and the stored heat in the nuclear fuel) neglecting the stored heat of ROSA-III heater rod[3]. The maximum linear heat rate of the peak power rod is 16.5 kW/m before the break initiation.

The schematics of the main steam line and the feedwater line are shown in Figs. 4.3 and 4.4. The main steam line of the ROSA-III has three branches: (1) steady flow branch, (2) ADS branch and (3) transient branch. Before the break initiation CV-130 in the steady flow branch

controls the steam flow to maintain the steam dome pressure constant and CV-1 and CV-2 are opened to provide steam to the heat exchanger to heat the feedwater. At the break initiation, the steam flow is switched to the transient branch by closing AV-168, CV-1 and CV-2 and opening AV-165 in RUN 901. Then the MSIV is simulated by AV-165 in the transient branch. The steam flow before MSIV closure is limited by an orifice OR5 of 16.8 mm ID (Inner Diameter) installed upstream of AV-165. Tables 4.2 and 4.3 show the characteristics and the control sequence of steam discharge line valves in the present test, respectively.

The details of the feedwater line is shown in Fig. 4.5. The feedwater is terminated at 2 s after the break by closing AV-112 in the feedwater line. However, the feedwater remained in the piping between the valve AV-112 and the feedwater sparger below the steam separator in the pressure vessel.

The coolant recirculation pumps are tripped to start coasting dowm at the break initiation.

The liquid level signal in the dowmcomer is used to actuate the ECCS and to close the MSIV. The downcomer level in the steady state operation is set at the scram level L3 (5.00 meters above the bottom of the pressure vessel) and L1 and L2 levels are 4.25 meters and 4.76 meters, respectively. The L2 level signal is used to close the MSIV with a time delay of 3 s and to actuate the HPCS with time delay of 27 s. The L1 level signal is used to actuate the LPCS, the LPCI and the ADS with time delay of 40 s, 40 s and 120 s, respectively. The above lag times of 3 s , 27 s, 40 s and 120 s are used in a safety analysis of the reference BWR[4]. The LPCI and the LPCS could inject cooling water after the primary system pressure is reduced below 2.16 MPa and 1.57 MPa, respectively. Specified system pressures for actuating the LPCS and the LPCI were decided from the pump characteristics used in the safety analysis of the reference BWR [5]. The test was terminated after all the core is quenched at 127 s after the break initiation.

## 5. Data Processing

In RUN 901, the data acquisition by DATAC 2000B was started 95 s before the break initiation and terminated 788 s after the break initiation. The data acquisition frequency was 10 Hz. The test data was processed and reduced to 1000 data points for computer plotting. The time span and frequency of the reduced data for plotting were 300 s and 3.3 Hz, respectively.

The test data are shown in Figs. 5.1 through 5.186. In these figures, the measured quantity is identified by the channel number and the alphabetic characters (Ref. Table 3.2).

The major test sequences and events observed in RUN 901 are summarized in Table 5.1.

Figures 5.1 through 5.6 show the pressure data in the pressure vessel and in the recirculation loop. Figures 5.7 through 5.36 show differential pressure data between various positions in the pressure vessel and the recirculation loop. Figures 5.37 and 5.38 show the liquid levels in the pressure vessel and in the tanks. Figures 5.39 through 5.45 show the flow rates. Differential pressures across orilfices and venturies shown in Figs. 5.46 through 5.56, are useful to check out the flow rate instrumentation. Figure 5.57 shows the power supplies to the core with the maximum capacities of 2100 and 3150 kW. The revolution speeds of the recirculation pumps are shown in Fig. 5.58. On-off signals such as the break initiation signal and the valve positioning signals are shown in Figs. 5.59, 5.60 and 5.61. Figures 5.62 through 5.71 show the fluid densities measured by the gamma densitometer. Figures 5.72 through 5.74 show momentum fluxes measured by drag disks. Figures 5.75 through 5.83 show the fluid temperatures at various positions in the loops. The fuel rod cladding temperature and the surface temperatures of the water rods and the channel boxes measured at Positions 1 through 7 are given in Figs. 5. 84 through

5.112. Figures 5.113 through 5.159 show the fuel rod cladding temperatures in a different manner. Figures 5.160 through 5.164 show the fluid temperatures at the inlet and outlet of the channel box. The surface temperatures of the channel box are shown in Figs. 5.165 through 5.171, comparing the data at the same elevation. The fluid temperature in the lower plenum was not measured in RUN 901 with the fule assembly No. 4. The liquid level signals in the core, the upper and lower plena, the guide tube and the downcomer are shown in Fig. 5.172 through 5.186. The Peak Cladding Temperature (PCT) distribution in the core is given in Table 5.2

Quantities obtained from reduction of the test data are shown in Fig. 5.187 through 5.218.

Figures 5.187 shows the estimated liquid level in the pressure vessel obtained by reducing the conductivity probe signals in Figs. 5.172 through 5.186. Figures 5.188 and 5.189 show transients of the dryout front and the quenching front. Figures 5.190 through 5.193 show the average density claculated from the data measured by the three-beam or two-beam gamma densitometers. The beam configurations of gamma densitometers installed in the ROSA-III facility are shown in Figs. 3.7 and 3.8. The average density is claculated as an arithmetic mean of the densities in multi directions with the weight of the cord length.

For the three beam densitometer at the jet pump outlet spool piece,

$$\rho_{av} = 0.3221\rho_A + 0.43\rho_B + 0.2479\rho_C \qquad (5.1)$$

where,

$\rho_{av}$ : average density obtained from the three-beam gamma densitometer,

$\rho_A$ : density measured by beam A (bottom),

$\rho_B$ : density measured by beam B (middle),

$\rho_C$ : density measured by beam C (top).

For the two-beam densitometer at the break spool piece,

$$\rho_{av} = 0.5863\,\rho_A + 0.4137\,\rho_B \qquad (5.2)$$

where,

$\rho_{av}$ : average density obtained from the two-beam gamma densitometer,

$\rho_A$ : density measured by beam A (bottom),

$\rho_B$ : density measured by beam B (top).

Figures 5.194 through 5.196 show the flow rates at upstream sides of the break in the recirculation loop. The flow rate is computed from the drag disk data and the gamma densitometer data using the following equation,

$$G = C_D\, A\sqrt{\rho_{av} \cdot \rho v^2} \qquad (5.3)$$

where,

$G$ : mass flow rate,

$C_D$ : drag coefficient ( =1.13),

$A$ : flow area ( $=1.923 \times 10^{-3}$ m$^2$),

$\rho_{av}$ : average density from gamma densitometer,

$\rho v^2$ : momentum flux from drag disk.

The break flow is derived from the flow rate in the recirculation loop as follows,

$$G_B = G_P + G_V \qquad (5.4)$$

where,

$G_B$ : break flow,

$G_P$ : flow rate at the pump side of the break,

$G_V$ : flow rate at the vessel side of the break.

The break flow rate based on the high range drag disk data is shown in Fig. 5.197.

Figures 5.198 through 5.208 show the fluid flow rates at the main

steam line, the channel inlet orifices, the bypass hole and the jet pump outlets. The fluid flow rates are calculated from the test data which are the pressure drop across the orifices or venturi flow meters and the liquid density obtained from the temperature and the pressure condition. The equation used for the calculation is as follows:

$$G = C_D A\sqrt{2g \cdot \rho_\ell \cdot \Delta P} \qquad (5.5)$$

where,

G : flow rate (kg/s)

$\Delta P$ : pressure drop ($mmH_2O$)

$C_D$ : discharge coefficient,

= 0.6552 (the orifice to measure the steam discharge flow rate)

= 0.4761 (the channel inlet orifice)

= 0.8032 (the bypass hole)

= 0.7383 (the orifice to measure the jet pump outlet flow rate)

= 1.1260 (the venturi tube to measure the jet pump outlet flow rate)

A : flow area ($m^2$)

= $2.875 \times 10^{-3}$ (the orifice to measure the steam discharge flow rate)

= $1.521 \times 10^{-3}$ (the channel inlet orifice)

= $1.758 \times 10^{-4}$ (the bypass hole)

= $1.133 \times 10^{-3}$ (the orifice to measure the jet pump outlet flow rate)

= $9.095 \times 10^{-4}$ (the venturi tube to measure the jet pump outlet flow rate)

g : gravitational acceleration (=9.807 $m/s^2$)

$\rho_\ell$ : density of the single-phase fluid ($kg/m^3$)

This calculation method is not applicable for two-phase flow condition after the LPF initiation at the channel inlet orifice, the bypass hole and the jet pump outlet. The calculated value shows only a trend in

two-phase flow condition. Total channel inlet flow rate presents the sum of four channel inlet flow rates.

Figure 5.209 and 5.210 show the collapsed water level outside and inside the shrond. The collapped water level is obtained from the differential pressure in the pressure vessel. The differential pressure may include the flow resistance effect, however, the flow resistance becomes negligible after completion of the recirculation pump coastdown.

Figures 5.211, 5.212 and 5.213 show the fluid mass inventories in the pressure vessel. The fluid mass inventory is determined from the density and the volumes of liquid outside and inside the shroud,

$$M = \rho_\ell \cdot Q \tag{5.6}$$

where,

M : fluid inventory,

$\rho_\ell$ : liquid density estimated from the satulation temperature and/or pressure,

Q : liquid volume calculated from the liquid level.

The volume Q ($m^3$) outside the shroud is given below as a function of height.

$$\begin{aligned}
Q &= 0 && (\quad L \leq 0.494) \\
Q &= 0.0225\,L - 0.0111 && (0.494 \leq L \leq 1.384) \\
Q &= 0.0697\,L - 0.0769 && (0.384 \leq L \leq 1.519) \\
Q &= 0.0801\,L - 0.1980 && (3.355 \leq L \leq 4.250) \\
Q &= 0.2443\,L - 0.8959 && (4.250 \leq L \leq 4.413) \\
Q &= 0.2611\,L - 0.9700 && (4.413 \leq L \leq 4.578) \\
Q &= 0.2504\,L - 0.9211 && (4.578 \leq L \leq 4.654) \\
Q &= 0.2375\,L - 0.8610 && (4.654 \leq L \leq 4.815) \\
Q &= 0.2866\,L - 1.0974 && (4.815 \leq L \leq 4.915) \\
Q &= 0.3396\,L - 1.3580 && (4.915 \leq L \leq 5.143) \\
Q &= 0.3607\,L - 1.4665 && (5.143 \leq L \leq 5.365)
\end{aligned} \tag{5.7}$$

$Q = 0.3848\ L - 1.5960 \quad (5.365 \leq L \leq 5.955)$

$Q = 0.7111 \quad (5.955 \leq L)$

The volume Q ($m^3$) inside the shroud is given below as a function of height.

$$
\begin{aligned}
Q &= 0 && (L \leq 0.0) \\
Q &= 0.2350\ L && (0.0 \leq L \leq 0.497) \\
Q &= 0.1245\ L + 0.0549 && (0.497 \leq L \leq 1.354) \\
Q &= 0.0698\ L + 0.1290 && (1.354 \leq L \leq 3.589) \\
Q &= 0.1648\ L - 0.2120 && (3.589 \leq L \leq 3.744) \\
Q &= 0.1963\ L - 0.3299 && (3.744 \leq L \leq 4.243) \\
Q &= 0.0196\ L + 0.4199 && (4.243 \leq L \leq 4.578) \qquad (5.8) \\
Q &= 0.0186\ L + 0.4244 && (4.578 \leq L \leq 4.654) \\
Q &= 0.0410\ L + 0.3201 && (4.654 \leq L \leq 5.099) \\
Q &= 0.0196\ L + 0.4292 && (5.099 \leq L \leq 5.365) \\
Q &= 0.5344\ L && (5.365 \leq L)
\end{aligned}
$$

The total fluid mass inventory in the pressure vessel is obtained as the summation of the mass inventory outside and inside the shround. The initial mass inventory before the break initiation is estimated as 640 kg.

Figure 5.214 shows the mass decrease by the fluid discharge from the break and the fluid mass recovery by the ECCS water and the feedwater injections. The variation of fluid mass inventory with time is calculated by the following equation,

$$M = \int_0^t \{G + \rho_1 \cdot (W_H + W_L + W_I) + \rho_2 \cdot W_F\}\, dt \qquad (5.9)$$

where,

M : mass accumulation,

G : steam discharge flow rate,

$\rho_1$ : density of satulated liquid at 315 K,

$\rho_2$ : density of satulated liquid at 489 K,

$W_H$ : volumetric flow rate of the HPCS,

$W_L$ : volumetric flow rate of the LPCS,

$W_I$ : volumetric flow rate of the LPCI,

$W_F$ : volumetric flow rate of the feedwater

Figure 5.215 shows the fluid mass discharged from the break. The fluid mass discharge $M_B$ is calculated as follows neglecting the change of the fluid mass inventory in the loops,

$$M_B = (M_P)_i - M_P + M_F \tag{5.10}$$

where,

$M_B$ : fluid mass discharged from the break,

$(M_P)_i$ : fluid mass inventory in the pressure vessel (= 640 kg),

$M_P$ : fluid mass inventory in the pressure vessel,

$M_F$ : net fluid mass increase by the ECCS, the feedwater flow and the steam discharge flow.

Figure 5.216 shows the break flow calculated from the fluid mass inventory in the pressure vessel. The break flow is estimated from the mass inventory as follows,

$$G_B = \frac{d}{dt} M_B \tag{5.11}$$

where,

$G_B$ : break flow,

$M_B$ : fluid mass discharge from the break.

## 6. Test Results

The fundamental thermal-hydraulic phenomena observed in RUN901 are descrived in this section.

### 6.1 Pressure Response

The system pressure measured in the lower plenum is shown in Fig. 6.1, which is a typical pressure response in the system in RUN901.

The pressure decreased during the initial 8 s because of discharge of coolant from the breaks and the steam line. After the MSIV closure the system pressure began to recover. The system pressure again started to drop rapidly after the recirculation line uncovery (RLU) in the downcomer because the steam started to be discharged directly through the vessel side break and the volumetric flow rate from the breaks became much larger than the vapor generation rate in the core. The Lower Plenum Flashing (LPF) started at 17.0 s after the system pressure lowered to the saturation pressure of 6.4 MPa corresponding to the lower plenum fluid temperature of 553 K. The Feedwater Line Flashing (FWLF) started at 64.8 s after the system pressure lowered to the saturation pressure of 2.15 MPa corresponding to the feedwater temperature of 216 K. The depressurization rate was reduced by the steam generation after the LPF and the FWLF. HPCS, LPCS, LPCI and ADS in RUN901 were actuated at 31.5 s, 65.6 s, 90.9 s and 127.7 s, respectively. However, ECCS actuation affected the system pressure little.

### 6.2 Differential Pressure

The differential pressure measured between the top and bottom of the pressure vessel is shown in Fig. 6.2. The figure indicates that the flow through the core-shroud decreased rapidly after break and became nearly stagnant when the liquid level in the downcomer decreased to the jet pump suction nozzle at 9.5 s. The upward flow after the LPF and the downward flow after the FWLF were observed inside the shroud, respectively.

The collapsed liquid level in the downcomer calculated from the downcomer head is shown in Fig. 6.3. The measuring range is separated at 3900 mm from the pressure vessel bottom (ECC spray line nozzle elevation, Fig. 3.2). A large acceleration loss in the lower downcomer head was observed immediately after break induced by a large downward flow

in the downcomer. Actuation signals for ECCS were given by the upper downcomer level and the system pressure. The liquid level in the downcomer decreased to L2 and L1 level at 3.2 s and 7.4 s, respectively, and HPCS, LPCS, LPCI and ADS were actuated at 31.5 s, 65.6 s, 90.9 s and 127.7 s, respectively. Actuations of LPCS and LPCI were delayed because of the pump head limitation and the high system pressure. The LPCS was started when the system pressure decreased to 2.23 MPa and LPCI to 1.61 MPa.

The lower downcomer head measured in ROSA-III test conducted before RUN901 increased immediately after LPCI actuation because of the flow path between the downcomer and the core bypass. In RUN901 the lower downcomer head didn't increase immediately after LPCI actuation and closure of the flow path between the downcomer and the core bypass was confirmed.

## 6.3 Coolant Flow Rate

The coolant flow rate through the channel inlet orifices and bypass holes were calculated from the differential pressures across the channel inlet orifices and bypass holes as shown in Figs. 5.199 through 5.203. These differential pressures were obtained by new pressure lead tubes installed in the fuel assembly No. 4. The channel inlet flow decreased rapidly after the break and became nearly stagnant. After the LPF initiation at 17.0 s after the break initiation the flow through the orifices became two-phase flow, therefore, the calculated flow rate with fixed form loss constant became incorrect giving only the trend. The flow through the channel inlet orifices was upward between the LPF and the FWLF because of the Counter Current Flow Limiting (CCFL) at the channel inlet orifices. After the FWLF initiation the flow changed downward temporarily because the rapid steam generation in the feedwater line reduced the depressurization rate resulting in the decrease in the steam generation rate in the lower plenum and the CCFL breakdown at the orifice. Therefore, the mixture in the core lowered. The flow through the bypass hole was reversed immediately after the break initiation and the reverse flow continued until the core shroud became almost filled up with the liquid.

Steam discharge flow rate calculated from the differential pressure data shown in Figs. 5.46 through 5.48 are presented in Fig. 5.198. As descrived in Section 4, the flow path was changed from the steady flow

branch to the transient branch at the break initiation and the steam discharge flow rate decreased with the system pressure fall. Steam discharge was terminated at 9.2 s due to the MSIV closure and started again at 128.2 s after the break initiation because of ADS actuation. The anomalous behavior of ADS steam discharge flow rate shown in Fig. 5.39 was caused by the insensitive range of the process flow meter at low flow rate.

Feedwater injection rate is shown in Fig. 6.4. The FWLF initiated at 64.8 s after break. Feedwater injection rate after FWLF is incorrect because the feedwater flow became two-phase flow.

Injection flow rates of HPCS, LPCS and LPCI are shown in Fig. 6.5. The measured ECCS flow rates were reasonable.

## 6.4 Liquid Level

Figure 5.187 shows the estimated liquid (mixture) levels in the pressure vessel obtained from the signals of the conductivity probes installed in the fuel assembly and the downcomer. The liquid level in the core dropped below position 3 because of the sudden decrease in the channel inlet flow after the break initiation. After the LPF initiation the liquid level recovered to the top of the core. The liquid level decreased again by the mitigation of the LPF and after the FWLF the liquid level dropped rapidly below position 6. After the LPCS actuation the liquid level in the core began to recover by the bottom-up reflooding and was completed to recover till 100 s after the break initiation in every channel. The whole core uncovery didn't occur in RUN901 with HPCS actuation. The channel inlet of every channel box was filled with two-phase fluid throughout the test.

The liquid level in the lower plenum was formed after the LPF initiation because the generated steam accumulated in the upper part of the lower plenum. In the figure the three separated liquid levels were observed at the same time in the upper plenum, the core and the lower plenum because the CCFL occured at the upper tie plate and the channel inlet orifice. The liquid level in the lower plenum rose to the top at 132 s after the break initiation because of the gradual accumulation of water in the lower plenum due to injection of the subcooled liquid into the core shroud by the ECCS and the fall back water from the core due to CCFL break down at the channel inlet orifices. The CCFL break down

occured at the channel inlet orifices of the average power channels B and C at about 125 s after the break initiation and resulted in the flow reversal at the channel inlet orifices and the temporary level drop in the core. After the CCFL breakdown the channel inlets of the channels B and C were filled with subcooled liquid as shown in Figs. 5.181 and 5.182. The core and the lower plenum had been filled up with water at 135 s after the break initiation.

The liquid level in the downcomer decreased rapidly after the break initiation. Jet pump suction and recirculation pump suction were uncovered at 9.6 s and 12.0 s, respectively. The liquid level in the downcomer measured by the conductivity probes has not such influences of the acceleration loss as in the level measurement by the downcomer head.

6.5 Fuel Rod Surface Temperature

The dryout and quenching transients in channels A and C are shown in Figs. 5.188 and 5.189. These transients were estimated from the fuel rod surface temperature transients shown in Figs. 5.84, 5.86, 5.88, 5.90, 5.100, 5.101, 5.102 and 5.103. The estimated mixture levels in the A and C channels shown in Fig. 5.184 are also presented in Figs. 5.185 and 5.186, respectively.

Following observations were obtained by comparing the surface temperatures at seven elevations and the dryout and quenching transients. The dryout and quenching transients were closely related to the mixture levels in the channel as shown in Figs. 5.188 and 5.189. The fuel rod surfaces at Position 1 through 3 dried out when the mixture level dropped below the Position 3 in the core. After the LPF initiation at 17.0 s after the break initiation the fuel rod surfaces were rewetted following the mixture level recovery to the top of the core. The fuel rod surfaces began to dryout again by the level fall because of mitigation of the LPF. After the FWLF initiation the top-down quenching was observed in the upper part of the core especially at the fuel rods located near the corner of the channel box. The fuel rod surfaces were finally quenched by reflooding after the LPCI actuation. The propagation of the dryout fronts after mitigation of the LPF corresponded well to the fall of the mixture level, whereas the quenching was delayed from reflooding especially at high power location Position 3 in channel A as shown in Fig. 5.188.

The Peak Cladding Temperature (PCT) in RUN901 was 780 K and was observed at 18.3 s at Position 2 of the peak power rod A11 in the peak power channel A as shown in Table 5.2. The PCT in RUN901 occured during the short dryout period before the LPF initiation and the temperature rise was more significant in the corner rods A11 and A88 as shown in Figs. 5.139 through 5.145. The highest temperature after mitigation of the LPF was 654 K recorded at 87.3 s after break at Position 3 of C13 rod in the average power channel C. Because the mixture level in the core after mitigation of the LPF was lower in the average power channels than in the peak power channel, the dryout was earlier and the quenching was later in the average power channel than in the peak power channel.

All fuel rod surface temperatures below midplane of the core stayed below the initial temperature before break except at Position 4 of the A37 rod because the mixture level in the core dropped below Position 4 only for a short time period after the FWLF initiation at 64.8 s owing to the HPCS actuation.

## 6.6 Density, Momentum Flux and Discharge Flow

Figures 5.190 and 5.191 show the area averaged fluid densities at the JP outlet in the intact and broken loops, respectively. Both figures show the same tendency that the density began to decrease gradually after the LPF initiation at 17.0 s. After the FWLF initiation the density recovered temporarily and began to increase gradually after the LPCI actuation at 90.9 s. The fluid density was not fully recovered even when the core shroud was completely covered with ECC water.

Figures 5.192 and 5.193 show the area averaged fluid densities at the pump side and the vessel side of the break, respectively. The density at the pump side of the break decreased rapidly from a single phase liquid density after the break initiation because of the rapid depressurization in the recirculation line between the break and the jet pump drive nozzles. The density at the vessel side of the break stayed at the single phase liquid density until the uncovering of the recirculation pump suction line nozzle in the downcomer at 12.0 s after the break initiation. After the 130 s the density of the vessel side of the break began to increase gradually because of an outflow of the coolant from the core shroud.

Figures 5.72 through 5.74 show the momentum flux at the break but the test data in Figs. 5.72 and 5.74 which show the momentum fluxes at

the pump side of the break measured by a low range drag disk and at the vessel side of the break measured by a high range drag disk, respectively, were saturated. Therefore the calculated discharge flow shown in Figs. 5.194 and 5.196 are incorrect during the period in which the momentum fluxes are saturated. The steady state flow directions are defined as negative at the pump side of the break and as positive at the vessel side of the break. The flow direction at the pump side of the break was reversed immediately after the break initiation.

This break flow measurement using drag disks and gamma densitometers has an error of at least ±20%.

The break flow calculated from a change of the mass inventory inside the pressure vessel are shown in Fig. 5.216. However, the calculated break flow was affected by the friction and acceleration terms in the differential pressure measured to estimate the liquid levels in the pressure vessel.

## 7. Conclusions

In this report, all the available test data obtained in a 200% double-ended break LOCA test RUN 901 were presented with information on the ROSA-III test facility, instrumentation and the test procedure. The explanations of the test results were also given.

RUN 901 was an acceptance test of the fuel assembly No. 4 and was conducted successfully with the assumption of full ECCS actuation. The ROSA-III test facility and its instrumentation worked well through the test. The conclusions obtained in RUN 901 are as follows.

(1) The fundamental thermal-hydraulic phenomena during a double-ended break LOCA have been clarified.

(2) The PCT is 780 K, which is observed at Position 2 of the All rod and 18.3 s after the break initiation during the blowdown phase. All fuel rods are quenched after the LPCI actuation and the effectiveness of ECCS for core cooling has been confirmed in RUN 901.

(3) There is a strong correlation between the mixture level transient in the core and the fuel rod surface temperature transients. The CCFL at the upper tieplate and the channel inlet orifice play an important role in the mixture level transient in the core, upper plenum and lower plenum.

(4) New differential pressure transducers installed at the channel inlet orifices of the fuel assembly No. 4 functioned properly to measure the channel inelet flow.

(5) The trip signals by the liquid level in the upper downcomer functions successfully for the MSIV closure and the ECCS actuation in a large break test.

(6) Closure of the flow path between inside and outside the core shroud has been confirmed.

Acknowledgment

The authors are grateful to H. Asahi, T. Odaira, T. takayasu, S. Sekiguchi, Y. Kitano and T. Numata of Nuclear Engineering Corporation for their assistance in conducting the experiment and K. Yamano, H. Gotoh and K. Hiyama of Information System Laboratory Corpolation for preparing the data plots and T. Kurosawa of Nihon Computer Bureau Corporation for preparing the report. The authors are also indebted to N. Abe of Nippon Atomic Industry Group Corporation Co., Ltd. for his valuable discussion in preparing the report.

References

(1) ANODA, Y et.al., "ROSA-III System Description for Fuel Assembly No. 4", JAERI-M 9363 (1981).

(2) SOBAJIMA, M. et.al., "Instrumentation and Data Processing for ROSA-III Test" (in Japanese), JAERI-M 8499 (1979).

(3) ABE, N., et. al., "Electric Power Transient Curve for ROSA-III Tests", JAERI-M 8728 (1980).

(4) "General Electric Standard Safety Analysis Report, BWR/6", DOCKET-STN-50531-22, General Electric Company.

(5) "BWR Blowdown Emergency Core Cooling Program, Preliminary Facility Description Report for the BT/ECC1A Test Phase", GEAP-23592, NRC-2 (1977).

Acknowledgment

The authors are grateful to H. Asahi, T. Odaira, T. takayasu, S. Sekiguchi, Y. Kitano and T. Numata of Nuclear Engineering Corporation for their assistance in conducting the experiment and K. Yamano, H. Gotoh and K. Hiyama of Information System Laboratory Corpolation for preparing the data plots and T. Kurosawa of Nihon Computer Bureau Corporation for preparing the report. The authors are also indebted to N. Abe of Nippon Atomic Industry Group Corporation Co., Ltd. for his valuable discussion in preparing the report.

References

(1) ANODA, Y et.al., "ROSA-III System Description for Fuel Assembly No. 4", JAERI-M 9363 (1981).

(2) SOBAJIMA, M. et.al., "Instrumentation and Data Processing for ROSA-III Test" (in Japanese), JAERI-M 8499 (1979).

(3) ABE, N., et. al., "Electric Power Transient Curve for ROSA-III Tests", JAERI-M 8728 (1980).

(4) "General Electric Standard Safety Analysis Report, BWR/6", DOCKET-STN-50531-22, General Electric Company.

(5) "BWR Blowdown Emergency Core Cooling Program, Preliminary Facility Description Report for the BT/ECC1A Test Phase", GEAP-23592, NRC-2 (1977).

Table 1.1 Comparison of Fuel Assemblies

| | 1st | 2nd | 3rd | 4th |
|---|---|---|---|---|
| Active Core Length (m) | | 1.880 | | |
| Number of Fuel Rods | 252 | 252 | 248 | 248 |
| Number of Water Rods | 4 | 4 | 8 | 8 |
| Rods Array | | 8 x 8 square | | |
| Fuel Rod O.D. (mm) | 12.52 | 12.52 | 12.27 | 12.27 |
| Fuel Rod Pitch (mm) | 16.26 | 16.26 | 16.16 | 16.16 |
| Peaking Factor | | | | |
| Local P.F. | 1.0 | 1.0 | 1.0 | 1.1 |
| Axial P.F. | 1.4 | 1.4 | 1.4 | 1.4 |
| Radial P.F. | 1.0 | 1.0 | 1.4 | 1.4 |
| Side Entry Orifices | | | | |
| Number of Holes | 48 | 48 | 48 | 4 |
| Diameter (mm) | 9.5 | 6.29 | 6.5 | 44.0 |
| Total Area ($cm^2$) | 34.02 | 14.92 | 15.93 | 60.82 |
| Leak Holes | | | | |
| Number of Holes | 8 | 8 | 8 | 8 |
| Diameter (mm) | 8.6 | 7.66 | 9.2 | 9.14 |
| Total Area ($cm^2$) | 4.65 | 3.69 | 5.32 | 5.25 |
| Guide Tube Holes | | | | |
| Number of Holes | 4 | 4 | 4 | 4 |
| Diameter (mm) | 5.3 | 4.9 | 5.12 | 7.48 |
| Total Area ($cm^2$) | 0.88 | 0.75 | 0.82 | 1.76 |
| Conducted Test RUNs | 701 ~ 703 | 704 ~ 710 | 731 ~ 7341<br>801 ~ 827 | 901 ~ |

Table 2.1 Primary Charecteristics of ROSA-III and BWR/6

| | BWR* | ROSA-III | BWR/ROSA-III |
|---|---|---|---|
| Number of Recirc. Loops | 2 | 2 | 1 |
| Number of Jet Pumps | 24 | 4 | 6 |
| Number of Separators | 251 | 1 | 251 |
| Number of Fuel Assemblies | 848 | 4 | 212 |
| Active Fuel Length (m) | 3.76 | 1.88 | 2 |
| Total Volume ($m^3$) | 621 | 1.42 | 437 |
| Power (MW) | 3,800 | 4.40 | 864 |
| Pressure (MPa) | 7.23 | 7.23 | 1 |
| Core Flow (kg/s) | $1.54 \times 10^4$ | 36.4 | 424 |
| Recirculation Flow (l/s) | 2,970 | 7.01 | 424 |
| Feedwater Flow (kg/s) | 2,060 | 4.86 | 424 |
| Feedwater Temp. (K) | 489 | 489 | 1 |

* BWR/6-251

Table 3.1 ROSA-III Instrumentation Summary List

| ITEM | SENSOR | NUMBER | NOTE |
|---|---|---|---|
| Pressure | Pressure Transducer | 20 | |
| Differential Pressure | DP Cell | 60 | PV and Loop 44<br>Level Measurement 5<br>Flow Meter 11 |
| Fluid Temperature | CA Thermocouple | 129 | Primary Loop 23<br>DTT 4<br>Tie Rod 28<br>Upper Plenum 10<br>Lower Plenum 10<br>Tie Plate 40<br>Bypass 14 |
| Fuel Rod Temperature | CA Thermocouple | 213 | |
| Slab Surface Temperature | CA Thermocouple | 70 | Core Barrel 24<br>Pressure Vessel 3<br>Channel Box 35<br>Shroud Support 8 |
| Slab Inner Temperature | CA Thermocouple | 9 | JP Diffuser 4<br>PV Wall 5 |
| Volumetric Flow Rate | Turbine Flow Meter<br>Venturi Flow Meter<br>Orifice Flow Meter | 3<br>4<br>6 | ECCS Loop 3<br>Primary Loop 10 |
| Mass Flow Rate | Turbine Flow Meter<br>Orifice Flow Meter | 4<br>3 | Recirculation Loop 4<br>Main Steam Line 3 |
| Liquid Level | Conductivity Probe<br>Capacitance Probe | 138<br>2 | |
| Density | Gamma Densitometer | 10 | 2 Beam GD 2<br>3 Beam GD 2 |
| Momentum Flux | Drag Disk | 4 | JP Spool Piece 2<br>Break Spool Piece 4<br>Break Orifice 1 |
| Signal | ON/OFF Switch | 14 | |
| Pump Speed | Revolution Counter | 2 | |
| Electric Core Power | VA Meter | 2 | |
| TOTAL | | 693 | |

Table 3.2 Measurement List for RUN 901

1Ch.- 50Ch.

| Ch. | Item | Symbol | ID. | | Location | Fig.No. | Range | | | Unit | Accuracy |
|---|---|---|---|---|---|---|---|---|---|---|---|
| 1 | Press. | P- 1 | PA | 1 | Lower Plenum | Fig.5. 1 | 0.100 | - | 10.0 | MPa | 1.08%FS |
| 2 | Press. | P- 2 | PA | 2 | Upper Plenum | Fig.5. 1 | 0.100 | - | 10.0 | MPa | 1.08%FS |
| 3 | Press. | P- 3 | PA | 3 | Steam Dome | Fig.5. 1 | 0.100 | - | 10.0 | MPa | 1.08%FS |
| 4 | Press. | P- 4 | PA | 4 | Downcomer Bottom | Fig.5. 1 | 0.100 | - | 10.0 | MPa | 1.08%FS |
| 5 | Press. | P- 5 | PA | 5 | JP-3 Drive | Fig.5. 2 | 0.100 | - | 10.0 | MPa | 1.08%FS |
| 6 | Press. | P- 6 | PA | 6 | JP-4 Drive | Fig.5. 2 | 0.100 | - | 10.0 | MPa | 1.08%FS |
| 7 | Press. | P- 7 | PA | 7 | JP-3 Suction | Fig.5. 2 | 0.100 | - | 10.0 | MPa | 1.08%FS |
| 8 | Press. | P- 8 | PA | 8 | JP-4 Suction | Fig.5. 2 | 0.100 | - | 10.0 | MPa | 1.08%FS |
| 9 | Press. | P- 9 | PA | 9 | MRP-1 Suction | Fig.5. 3 | 0.100 | - | 10.0 | MPa | 1.08%FS |
| 10 | Press. | P-10 | PA | 10 | MRP-2 Suction | FIG.5. 3 | 0.100 | - | 10.0 | MPa | 1.08%FS |
| 11 | Press. | P-11 | PA | 11 | MRP-2 Delivery | FIG.5. 3 | 0.100 | - | 10.0 | MPa | 1.08%FS |
| 12 | Press. | P-12 | PA | 12 | Break A Upstream | FIG.5. 4 | 0.100 | - | 10.0 | MPa | 1.08%FS |
| 13 | Press. | P-13 | PA | 13 | Break A Downstream | FIG.5. 4 | 0.100 | - | 10.0 | MPa | 1.08%FS |
| 14 | Press. | P-14 | PA | 14 | Break B Upstream | FIG.5. 5 | 0.100 | - | 10.0 | MPa | 1.08%FS |
| 15 | Press. | P-15 | PA | 15 | Break B Downstream | FIG.5. 5 | 0.100 | - | 10.0 | MPa | 1.08%FS |
| 16 | Press. | P-16 | PA | 16 | Steam Line | FIG.5. 6 | 0.100 | - | 10.0 | MPa | 1.08%FS |
| 17 | Press. | P-17 | PA | 17 | JP-1,2 Outlet Spool | Not Measured | 0.100 | - | 10.0 | MPa | 1.08%FS |
| 18 | Press. | P-18 | PA | 18 | JP-3,4 Outlet Spool | Not Measured | 0.100 | - | 10.0 | MPa | 1.08%FS |
| 19 | Press. | P-19 | PA | 19 | Break A Spool Piece | FIG.5. 4 | 0.100 | - | 10.0 | MPa | 1.08%FS |
| 20 | Press. | P-30 | PA | 20 | Break B Spool Piece | FIG.5. 5 | 0.100 | - | 10.0 | MPa | 1.08%FS |
| 21 | Diff.P. | D- 1 | PD | 21 | Lower Pl.-Upper Pl. | FIG.5. 7 | -50.0 | - | 350. | kPa | 0.63%FS |
| 22 | Diff.P. | D- 2 | PD | 22 | Upper Pl.-Steam Dome | FIG.5. 8 | -10.0 | - | 90.0 | kPa | 0.63%FS |
| 23 | Diff.P. | D- 3 | PD | 23 | Lower Plenum Head | Not Measured | | | | | |
| 24 | Diff.P. | D- 4 | PD | 24 | Downcomer Head | FIG.5. 9 | 0.0 | - | 100. | kPa | 0.63%FS |
| 25 | Diff.P. | D- 5 | PD | 25 | PV Bottom-Top | FIG.5.10 | -100. | - | 900. | kPa | 0.63%FS |
| 26 | Diff.P. | D- 6 | PD | 26 | JP-1 Disch.-Suction | FIG.5.11 | -100. | - | 300. | kPa | 0.63%FS |
| 27 | Diff.P. | D- 7 | PD | 27 | JP-1 Drive -Suction | FIG.5.12 | 0.0 | - | 2.50 | MPa | 0.63%FS |
| 28 | Diff.P. | D- 8 | PD | 28 | JP-2 Disch.-Suction | FIG.5.11 | -100. | - | 300. | kPa | 0.63%FS |
| 29 | Diff.P. | D- 9 | PD | 29 | JP-2 Drive -Suction | FIG.5.12 | 0.0 | - | 2.50 | MPa | 0.63%FS |
| 30 | Diff.P. | D-10 | PD | 30 | JP-3 Disch.-Suction | FIG.5.13 | -100. | - | 300. | kPa | 0.63%FS |
| 31 | Diff.P. | D-11 | PD | 31 | JP-3 Drive -Suction | FIG.5.14 | -4.00 | - | 2.00 | MPa | 0.63%FS |
| 32 | Diff.P. | D-12 | PD | 32 | JP-4 Disch.-Suction | FIG.5.13 | -100. | - | 300. | kPa | 0.63%FS |
| 33 | Diff.P. | D-13 | PD | 33 | JP-4 Drive -Suction | FIG.5.14 | -4.00 | - | 2.00 | MPa | 0.63%FS |
| 34 | Diff.P. | D-14 | PD | 34 | MRP-1 Deliv.-Suction | FIG.5.15 | -0.100 | - | 2.50 | MPa | 0.63%FS |
| 35 | Diff.P. | D-15 | PD | 35 | MRP-2 Deliv.-Suction | FIG.5.15 | -0.100 | - | 2.50 | MPa | 0.63%FS |
| 36 | Diff.P. | D-16 | PD | 36 | DC Bottom- MRP-1 Suc. | FIG.5.16 | -50.0 | - | 50.0 | kPa | 0.63%FS |
| 37 | Diff.P. | D-17 | PD | 37 | MRP1 Deliv.-JP1 Drive | FIG.5.17 | 0.0 | - | 250. | kPa | 0.63%FS |
| 38 | Diff.P. | D-18 | PD | 38 | MRP1 Deliv.-JP2 Drive | FIG.5.17 | 0.0 | - | 250. | kPa | 0.63%FS |
| 39 | Diff.P. | D-19 | PD | 39 | DC Middle-JP1 Suction | FIG.5.18 | 0.0 | - | 250. | kPa | 0.63%FS |
| 40 | Diff.P. | D-20 | PD | 40 | DC Middle-JP2 Suction | FIG.5.18 | 0.0 | - | 250. | kPa | 0.63%FS |
| 41 | Diff.P. | D-21 | PD | 41 | JP1 Disch.-Lower Pl. | FIG.5.19 | -100. | - | 100. | kPa | 0.63%FS |
| 42 | Diff.P. | D-22 | PD | 42 | JP2 Disch.-Lower Pl. | FIG.5.19 | -100. | - | 100. | kPa | 0.63%FS |
| 43 | Diff.P. | D-23 | PD | 43 | DC Bottom- Break B | FIG.5.20 | -60.0 | - | 540. | kPa | 0.63%FS |
| 44 | Diff.P. | D-24 | PD | 44 | Break B- Break A | FIG.5.21 | 0.0 | - | 100. | kPa | 0.63%FS |
| 45 | Diff.P. | D-25 | PD | 45 | Break A- MRP2 Suction | FIG.5.22 | -500. | - | 100. | kPa | 0.63%FS |
| 46 | Diff.P. | D-26 | PD | 46 | MRP2 Deliv.-JP3 Drive | FIG.5.23 | -500. | - | 500. | kPa | 0.63%FS |
| 47 | Diff.P. | D-27 | PD | 47 | MRP2 Deliv.-JP4 Drive | FIG.5.23 | -500. | - | 500. | kPa | 0.63%FS |
| 48 | Diff.P. | D-28 | PD | 48 | DC Middle-JP3 Suction | FIG.5.24 | -250. | - | 250. | kPa | 0.63%FS |
| 49 | Diff.P. | D-29 | PD | 49 | DC Middle-JP4 Suction | FIG.5.24 | -250. | - | 250. | kPa | 0.63%FS |
| 50 | Diff.P. | D-30 | PD | 50 | JP3 Disch.-Confluence | FIG.5.25 | -100. | - | 100. | kPa | 0.63%FS |

Table 3.2 Measurement List for RUN 901 (Continued)

51Ch.- 100Ch.

| Ch. | Item | Symbol | ID. | | Location | Fig.No. | Range | | | Unit | Accuracy |
|---|---|---|---|---|---|---|---|---|---|---|---|
| 51 | Diff.P. | D-31 | PD | 51 | JP4 Disch.-Confluence | FIG.5.25 | -100. | - | 100. | kPa | 0.63%FS |
| 52 | Diff.P. | D-32 | PD | 52 | Confluence -Lower Pl. | FIG.5.26 | -50.0 | - | 50.0 | kPa | 0.63%FS |
| 53 | Diff.P. | D-33 | PD | 53 | Lower Pl.-DC Middle | FIG.5.27 | -250. | - | 250. | kPa | 0.63%FS |
| 54 | Diff.P. | D-34 | PD | 54 | Lower Pl.-DC Bottom | FIG.5.28 | -250. | - | 250. | kPa | 0.63%FS |
| 55 | Diff.P. | D-35 | PD | 55 | DC Bottom-DC Middle | FIG.5.29 | -50.0 | - | 50.0 | kPa | 0.63%FS |
| 56 | Diff.P. | D-36 | PD | 56 | DC Middle-Steam Dome | FIG.5.30 | -50.0 | - | 50.0 | kPa | 0.63%FS |
| 57 | Diff.P. | D-37 | PD | 57 | Lower Pl.Mid-Upper PL | Not Measured | | | | | |
| 58 | Diff.P. | D-38 | PD | 58 | Lower Pl.Bottom-Mid. | FIG.5.31 | 0.0 | - | 50.0 | kPa | 0.63%FS |
| 59 | Diff.P. | D-39 | PD | 59 | Upper Pl.-DC High | Not Used | -20.0 | - | 100. | kPa | 0.63%FS |
| 60 | Diff.P. | D-40 | PD | 60 | Channel Orifice A | FIG.5.32 | -50.0 | - | 50.0 | kPa | 0.63%FS |
| 61 | Diff.P. | D-41 | PD | 61 | Channel Orifice B | FIG.5.33 | -50.0 | - | 50.0 | kPa | 0.63%FS |
| 62 | Diff.P. | D-42 | PD | 62 | Channel Orifice C | FIG.5.34 | -25.0 | - | 75.0 | kPa | 0.63%FS |
| 63 | Diff.P. | D-43 | PD | 63 | Channel Orifice D | FIG.5.35 | -50.0 | - | 50.0 | kPa | 0.63%FS |
| 64 | Diff.P. | D-44 | PD | 64 | Lower Plenum Head | FIG.5.36 | -100. | - | 100. | kPa | 0.63%FS |
| 65 | Level | WL- 1 | LM | 65 | HPCS Tank | FIG.5.37 | 0.0 | - | 2.30 | m | 1.00%FS |
| 66 | Level | WL- 2 | LM | 66 | LPCS Tank | FIG.5.37 | 0.0 | - | 2.30 | m | 1.00%FS |
| 67 | Level | WL- 3 | LM | 67 | LPCI Tank | FIG.5.37 | 0.0 | - | 4.25 | m | 1.00%FS |
| 68 | Level | WL- 4 | LM | 68 | Upper Downcomer | FIG.5.38 | 3.90 | - | 6.04 | m | 1.00%FS |
| 69 | Level | WL- 5 | LM | 69 | Lower Downcomer | FIG.5.38 | 0.938 | - | 3.90 | m | 1.00%FS |
| 70 | Mass.F. | F- 1 | FM | 70 | Steam Line (Low Range) | FIG.5.39 | 0.0 | - | 1.13 | kg/s | 0.92%FS |
| 71 | Mass.F. | F- 2 | FM | 71 | Steam Line(High Range) | FIG.5.39 | 0.0 | - | 3.00 | kg/s | 0.92%FS |
| 72 | Mass.F. | F- 3 | FM | 72 | Steam Line (Mid Range) | FIG.5.39 | 0.0 | - | 1.94 | kg/s | 1.40%FS |
| 73 | Vol.F. | F- 7 | FV | 73 | HPCS (Upper Plenum) | FIG.5.40 | 0.0 | - | 0.250E-02 | m3/s | 0.79%FS |
| 74 | Vol.F. | F- 9 | FV | 74 | LPCS (Upper Plenum) | FIG.5.40 | 0.0 | - | 0.250E-02 | m3/s | 0.79%FS |
| 75 | Vol.F. | F-11 | FV | 75 | LPCI (Core Bypass) | FIG.5.40 | 0.0 | - | 0.830E-02 | m3/s | 0.79%FS |
| 76 | Vol.F. | F-15 | FV | 76 | Feedwater | FIG.5.41 | 0.0 | - | 0.100E-01 | m3/s | 0.79%FS |
| 77 | Vol.F. | F-16 | FV | 77 | PWT Flow | Not Measured | 0.0 | - | 0.420E-02 | m3/s | 0.79%FS |
| 78 | Vol.F. | F-17 | FV | 78 | JP1 Discharge | FIG.5.42 | 0.0 | - | 0.170E-01 | m3/s | 0.88%FS |
| 79 | Vol.F. | F-18 | FV | 79 | JP2 Discharge | FIG.5.42 | 0.0 | - | 0.170E-01 | m3/s | 0.88%FS |
| 80 | Vol.F. | F-19 | FV | 80 | JP3 Disch. Positive | FIG.5.43 | 0.0 | - | 0.170E-01 | m3/s | 0.92%FS |
| 81 | Vol.F. | F-20 | FV | 81 | JP3 Disch. Negative | FIG.5.44 | 0.0 | - | 0.500E-02 | m3/s | 0.92%FS |
| 82 | Vol.F. | F-21 | FV | 82 | JP4 Disch. Positive | FIG.5.43 | 0.0 | - | 0.170E-01 | m3/s | 0.92%FS |
| 83 | Vol.F. | F-22 | FV | 83 | JP4 Disch. Negative | FIG.5.44 | 0.0 | - | 0.500E-02 | m3/s | 0.92%FS |
| 84 | Mass.F. | F-23 | FM | 84 | JP1,2 Outlet Spool | Not Measured | 0.0 | - | 30.0 | kg/s | 1.40%FS |
| 85 | Mass.F. | F-24 | FM | 85 | JP3,4 Outlet Spool | Not Measured | 0.0 | - | 30.0 | kg/s | 1.40%FS |
| 86 | Mass.F. | F-25 | FM | 86 | Break A Spool Piece | Not Measured | 0.0 | - | 30.0 | kg/s | 1.40%FS |
| 87 | Mass.F. | F-26 | FM | 87 | Break B Spool Piece | Not Measured | 0.0 | - | 30.0 | kg/s | 1.40%FS |
| 88 | Vol.F. | F-27 | FV | 88 | MRP-1 | FIG.5.45 | 0.0 | - | 0.120E-01 | m3/s | 0.88%FS |
| 89 | Vol.F. | F-28 | FV | 89 | MRP-2 | FIG.5.45 | 0.0 | - | 0.120E-01 | m3/s | 0.63%FS |
| 90 | Diff.P. | D-F1 | PD | 90 | F1 Orifice | FIG.5.46 | 0.0 | - | 4.90 | kPa | 0.63%FS |
| 91 | Diff.P. | D-F2 | PD | 91 | F2 Orifice | FIG.5.47 | 0.0 | - | 34.9 | kPa | 0.63%FS |
| 92 | Diff.P. | D-F3 | PD | 92 | F3 Orifice | FIG.5.48 | 0.0 | - | 14.6 | kPa | 0.63%FS |
| 93 | Diff.P. | D-F17 | PD | 93 | F17 Venturi | FIG.5.49 | 0.0 | - | 98.1 | kPa | 0.63%FS |
| 94 | Diff.P. | D-F18 | PD | 94 | F18 Venturi | FIG.5.50 | 0.0 | - | 98.1 | kPa | 0.63%FS |
| 95 | Diff.P. | D-F19 | PD | 95 | F19 Orifice | FIG.5.51 | 0.0 | - | 147. | kPa | 0.63%FS |
| 96 | Diff.P. | D-F20 | PD | 96 | F20 Orifice | FIG.5.52 | 0.0 | - | 13.2 | kPa | 0.63%FS |
| 97 | Diff.P. | D-F21 | PD | 97 | F21 Orifice | FIG.5.53 | 0.0 | - | 147. | kPa | 0.63%FS |
| 98 | Diff.P. | D-F22 | PD | 98 | F22 Orifice | FIG.5.54 | 0.0 | - | 13.2 | kPa | 0.63%FS |
| 99 | Diff.P. | D-F27 | PD | 99 | F27 Venturi | FIG.5.55 | 0.0 | - | 200. | kPa | 0.63%FS |
| 100 | Diff.P. | D-F28 | PD | 100 | F28 Venturi | FIG.5.56 | 0.0 | - | 200. | kPa | 0.63%FS |

Table 3.2 Measurement List for RUN 901 (Continued)

101Ch.- 150Ch.

| Ch. | Item | Symbol | ID. | | Location | Fig.No. | Range | | | Unit | Accuracy |
|---|---|---|---|---|---|---|---|---|---|---|---|
| 101 | Power | W- 1 | WE | 101 | 2100 kW Power Supplier | FIG.5.57 | 0.0 | - | 0.210E+04 | kW | 1.00%FS |
| 102 | Power | W- 2 | WE | 102 | 3150 kW Power Supplier | FIG.5.57 | 0.0 | - | 0.315E+04 | kW | 1.00%FS |
| 103 | | | | | | | | | | | |
| 104 | Rev. | N- 1 | SR | 104 | MRP-1 Revolution | FIG.5.58 | 0.0 | - | 0.500E+04 | RPM | 1.08%FS |
| 105 | Rev. | N- 2 | SR | 105 | MRP-2 Revolution | FIG.5.58 | 0.0 | - | 0.500E+04 | RPM | 1.08%FS |
| 106 | Signal | S- 1 | EV | 106 | Break Signal A | FIG.5.59 | | | | | |
| 107 | Signal | S- 2 | EV | 107 | Break Signal B | FIG.5.59 | | | | | |
| 108 | Signal | S- 3 | EV | 108 | QSV Signal | FIG.5.59 | | | | | |
| 109 | Signal | S- 6 | EV | 109 | HPCS Valve | FIG.5.60 | | | | | |
| 110 | Signal | S- 7 | EV | 110 | LPCS Valve | FIG.5.60 | | | | | |
| 111 | Signal | S- 8 | EV | 111 | LPCI Valve | FIG.5.60 | | | | | |
| 112 | Signal | S- 9 | EV | 112 | Feedwater Control | FIG.5.59 | | | | | |
| 113 | Signal | S-10 | EV | 113 | MSIV Signal | FIG.5.59 | | | | | |
| 114 | Signal | S-11 | EV | 114 | Steam Line Valve | FIG.5.59 | | | | | |
| 115 | Signal | S-12 | EV | 115 | ADS Valve | FIG.5.60 | | | | | |
| 116 | Signal | S-13 | EV | 116 | MRP-1 Power OFF | FIG.5.61 | | | | | |
| 117 | Signal | S-14 | EV | 117 | MRP-2 Power OFF | FIG.5.61 | | | | | |
| 118 | Signal | RD- 1 | EV | 118 | MRP-1 Rev. Direction | FIG.5.61 | | | | | |
| 119 | Signal | RD- 2 | EV | 119 | MRP-2 Rev. Direction | FIG.5.61 | | | | | |
| 120 | Density | DF- 1 | DE | 120 | JP1,2 Outlet Beam A | FIG.5.62 | 0.0 | - | 0.100E+04 | kg/m3 | 1.00%FS |
| 121 | Density | DF- 2 | DE | 121 | JP1,2 Outlet Beam B | FIG.5.63 | 0.0 | - | 0.100E+04 | kg/m3 | 1.00%FS |
| 122 | Density | DF- 3 | DE | 122 | JP1,2 Outlet Beam C | FIG.5.64 | 0.0 | - | 0.100E+04 | kg/m3 | 1.00%FS |
| 123 | Density | DF- 4 | DE | 123 | JP3,4 Outlet Beam A | FIG.5.65 | 0.0 | - | 0.100E+04 | kg/m3 | 1.00%FS |
| 124 | Density | DF- 5 | DE | 124 | JP3,4 Outlet Beam B | FIG.5.66 | 0.0 | - | 0.100E+04 | kg/m3 | 1.00%FS |
| 125 | Density | DF- 6 | DE | 125 | JP3,4 Outlet Beam C | FIG.5.67 | 0.0 | - | 0.100E+04 | kg/m3 | 1.00%FS |
| 126 | Density | DF- 7 | DE | 126 | Break A Beam A | FIG.5.68 | 0.0 | - | 0.100E+04 | kg/m3 | 1.00%FS |
| 127 | Density | DF- 8 | DE | 127 | Break A Beam B | FIG.5.69 | 0.0 | - | 0.100E+04 | kg/m3 | 1.00%FS |
| 128 | Density | DF- 9 | DE | 128 | Break B Beam A | FIG.5.70 | 0.0 | - | 0.100E+04 | kg/m3 | 1.00%FS |
| 129 | Density | DF-10 | DE | 129 | Break B Beam B | FIG.5.71 | 0.0 | - | 0.100E+04 | kg/m3 | 1.00%FS |
| 130 | Mo.Flux | M- 1 | MF | 130 | JP1,2 Outlet Spool | Not Measured | 0.0 | - | 0.220E+05 | kg/ms2 | 1.00%FS |
| 131 | Mo.Flux | M- 2 | MF | 131 | JP3,4 Outlet Spool | Not Measured | 0.0 | - | 0.220E+05 | kg/ms2 | 1.00%FS |
| 132 | Mo.Flux | M- 3 | MF | 132 | Break A (Low Range) | FIG.5.72 | 0.0 | - | 0.220E+05 | kg/ms2 | 1.00%FS |
| 133 | Mo.Flux | M- 4 | MF | 133 | Break B (Low Range) | Not Measured | 0.0 | - | 0.220E+05 | kg/ms2 | 1.00%FS |
| 134 | Mo.Flux | M- 5 | MF | 134 | Break A (High Range) | FIG.5.73 | 0.0 | - | 0.220E+06 | kg/ms2 | 1.00%FS |
| 135 | Mo.Flux | M- 6 | MF | 135 | Break B (High Range) | FIG.5.74 | 0.0 | - | 0.220E+06 | kg/ms2 | 1.00%FS |
| 136 | Mo.Flux | M- 7 | MF | 136 | Break Orifice | Not Measured | 0.0 | - | 0.220E+05 | kg/ms2 | 1.00%FS |
| 137 | | | | | | | | | | | |
| 138 | Fluid T. | T- 1 | TE | 138 | Lower Plenum | FIG.5.75 | 273. | - | 673. | K | 0.64%FS |
| 139 | Fluid T. | T- 2 | TE | 139 | Upper Plenum | FIG.5.75 | 273. | - | 673. | K | 0.64%FS |
| 140 | Fluid T. | T- 3 | TE | 140 | Steam Dome | FIG.5.76 | 273. | - | 673. | K | 0.64%FS |
| 141 | Fluid T. | T- 4 | TE | 141 | Upper Downcomer | FIG.5.77 | 273. | - | 673. | K | 0.64%FS |
| 142 | Fluid T. | T- 5 | TE | 142 | Lower Downcomer | FIG.5.77 | 273. | - | 673. | K | 0.64%FS |
| 143 | Fluid T. | T- 6 | TE | 143 | JP-1 Drive | FIG.5.78 | 273. | - | 673. | K | 0.64%FS |
| 144 | Fluid T. | T- 7 | TE | 144 | JP-2 Drive | FIG.5.78 | 273. | - | 673. | K | 0.64%FS |
| 145 | Fluid T. | T- 8 | TE | 145 | JP-3 Drive | FIG.5.79 | 273. | - | 673. | K | 0.64%FS |
| 146 | Fluid T. | T- 9 | TE | 146 | JP-4 Drive | FIG.5.79 | 273. | - | 673. | K | 0.64%FS |
| 147 | Fluid T. | T-10 | TE | 147 | JP-1 Discharge | FIG.5.80 | 273. | - | 673. | K | 0.64%FS |
| 148 | Fluid T. | T-11 | TE | 148 | JP-2 Discharge | FIG.5.80 | 273. | - | 673. | K | 0.64%FS |
| 149 | Fluid T. | T-12 | TE | 149 | JP-3 Discharge | FIG.5.81 | 273. | - | 673. | K | 0.64%FS |
| 150 | Fluid T. | T-13 | TE | 150 | JP-4 Discharge | FIG.5.81 | 273. | - | 673. | K | 0.64%FS |

Table 3.2 Measurement List for RUN 901 (Continued)

151Ch.- 200Ch.

| Ch. | Item | Symbol | ID. | | Location | Fig.No. | Range | | | Unit | Accuracy |
|---|---|---|---|---|---|---|---|---|---|---|---|
| 151 | Fluid T. | T-14 | TE | 151 | MRP-1 Suction | FIG.5.78 | 273. | - | 673. | K | 0.64%FS |
| 152 | Fluid T. | T-15 | TE | 152 | MRP-1 Delivery | FIG.5.78 | 273. | - | 673. | K | 0.64%FS |
| 153 | Fluid T. | T-16 | TE | 153 | MRP-2 Suction | FIG.5.79 | 273. | - | 673. | K | 0.64%FS |
| 154 | Fluid T. | T-17 | TE | 154 | MRP-2 Delivery | FIG.5.79 | 273. | - | 673. | K | 0.64%FS |
| 155 | Fluid T. | T-18 | TE | 155 | Break A Upstream | FIG.5.82 | 273. | - | 673. | K | 0.64%FS |
| 156 | Fluid T. | T-19 | TE | 156 | Break B Upstream | FIG.5.82 | 273. | - | 673. | K | 0.64%FS |
| 157 | Fluid T. | T-20 | TE | 157 | RCN A Condenced Water | Not Used | 273. | - | 698. | K | 0.64%FS |
| 158 | Fluid T. | T-21 | TE | 158 | RCN B Condenced Water | Not Used | 273. | - | 698. | K | 0.64%FS |
| 159 | Fluid T. | T-22 | TE | 159 | Discharged Steam | FIG.5.76 | 273. | - | 673. | K | 0.64%FS |
| 160 | Fluid T. | T-24 | TE | 160 | JP-1,2 Outlet Spool | FIG.5.80 | 273. | - | 763. | K | 0.64%FS |
| 161 | Fluid T. | T-25 | TE | 161 | JP-3,4 Outlet Spool | FIG.5.81 | 273. | - | 763. | K | 0.64%FS |
| 162 | Fluid T. | T-26 | TE | 162 | Break A Spool Piece | FIG.5.82 | 273. | - | 763. | K | 0.64%FS |
| 163 | Fluid T. | T-37 | TE | 163 | Break B Spool Piece | FIG.5.82 | 273. | - | 763. | K | 0.64%FS |
| 164 | Fluid T. | T-38 | TE | 164 | Feedwater | FIG.5.83 | 273. | - | 673. | K | 0.64%FS |
| 165 | Slab T. | TS- 1 | TE | 165 | Core Barrel C Pos.1 | Not Measured | 273. | - | 673. | K | 0.64%FS |
| 166 | Slab T. | TS- 2 | TE | 166 | Core Barrel C Pos.2 | Not Measured | 273. | - | 673. | K | 0.64%FS |
| 167 | Slab T. | TS- 3 | TE | 167 | Core Barrel C Pos.3 | Not Measured | 273. | - | 673. | K | 0.64%FS |
| 168 | Slab T. | TS- 4 | TE | 168 | Core Barrel C Pos.4 | Not Measured | 273. | - | 673. | K | 0.64%FS |
| 169 | Slab T. | TS- 5 | TE | 169 | Core Barrel C Pos.5 | Not Measured | 273. | - | 673. | K | 0.64%FS |
| 170 | Slab T. | TS- 6 | TE | 170 | Core Barrel C Pos.6 | Not Measured | 273. | - | 673. | K | 0.64%FS |
| 171 | Slab T. | TS- 7 | TE | 171 | Core Barrel A Pos.1 | Not Measured | 273. | - | 673. | K | 0.64%FS |
| 172 | Slab T. | TS- 8 | TE | 172 | Core Barrel A Pos.2 | Not Measured | 273. | - | 673. | K | 0.64%FS |
| 173 | Slab T. | TS- 9 | TE | 173 | Core Barrel A Pos.3 | Not Measured | 273. | - | 673. | K | 0.64%FS |
| 174 | Slab T. | TS-10 | TE | 174 | Core Barrel A Pos.4 | Not Measured | 273. | - | 673. | K | 0.64%FS |
| 175 | Slab T. | TS-11 | TE | 175 | Core Barrel A Pos.5 | Not Measured | 273. | - | 673. | K | 0.64%FS |
| 176 | Slab T. | TS-12 | TE | 176 | Core Barrel A Pos.6 | Not Measured | 273. | - | 673. | K | 0.64%FS |
| 177 | Slab T. | TS-13 | TE | 177 | Filler Block C Pos.1 | Not Measured | 273. | - | 673. | K | 0.64%FS |
| 178 | Slab T. | TS-14 | TE | 178 | Filler Block C Pos.2 | Not Measured | 273. | - | 673. | K | 0.64%FS |
| 179 | Slab T. | TS-15 | TE | 179 | Filler Block C Pos.3 | Not Measured | 273. | - | 673. | K | 0.64%FS |
| 180 | Slab T. | TS-16 | TE | 180 | Filler Block C Pos.4 | Not Measured | 273. | - | 673. | K | 0.64%FS |
| 181 | Slab T. | TS-17 | TE | 181 | Filler Block C Pos.5 | Not Measured | 273. | - | 673. | K | 0.64%FS |
| 182 | Slab T. | TS-18 | TE | 182 | Filler Block C Pos.6 | Not Measured | 273. | - | 673. | K | 0.64%FS |
| 183 | Slab T. | TS-19 | TE | 183 | Filler Block A Pos.1 | Not Measured | 273. | - | 673. | K | 0.64%FS |
| 184 | Slab T. | TS-20 | TE | 184 | Filler Block A Pos.2 | Not Measured | 273. | - | 673. | K | 0.64%FS |
| 185 | Slab T. | TS-21 | TE | 185 | Filler Block A Pos.3 | Not Measured | 273. | - | 673. | K | 0.64%FS |
| 186 | Slab T. | TS-22 | TE | 186 | Filler Block A Pos.4 | Not Measured | 273. | - | 673. | K | 0.64%FS |
| 187 | Slab T. | TS-23 | TE | 187 | Filler Block A Pos.5 | Not Measured | 273. | - | 673. | K | 0.64%FS |
| 188 | Slab T. | TS-24 | TE | 188 | Filler Block A Pos.6 | Not Measured | 273. | - | 673. | K | 0.64%FS |
| 189 | Slab T. | TS-25 | TE | 189 | JP-1 Diffuser Wall | Not Measured | 273. | - | 673. | K | 0.64%FS |
| 190 | Slab T. | TS-26 | TE | 190 | JP-2 Diffuser Wall | Not Measured | 273. | - | 673. | K | 0.64%FS |
| 191 | Slab T. | TS-27 | TE | 191 | JP-3 Diffuser Wall | Not Measured | 273. | - | 673. | K | 0.64%FS |
| 192 | Slab T. | TS-28 | TE | 192 | JP-4 Diffuser Wall | Not Measured | 273. | - | 673. | K | 0.64%FS |
| 193 | Slab T. | TS-29 | TE | 193 | PV Wall Inside 1-1 | Not Measured | 273. | - | 673. | K | 0.64%FS |
| 194 | Slab T. | TS-30 | TE | 194 | PV Inner Surface 1-2 | Not Measured | 273. | - | 673. | K | 0.64%FS |
| 195 | Slab T. | TS-31 | TE | 195 | PV Inner Surface 1-3 | Not Measured | 273. | - | 673. | K | 0.64%FS |
| 196 | Slab T. | TS-32 | TE | 196 | PV Wall Inside 2 | Not Measured | 273. | - | 673. | K | 0.64%FS |
| 197 | Slab T. | TS-33 | TE | 197 | PV Wall Inside 3 | Not Measured | 273. | - | 673. | K | 0.64%FS |
| 198 | Slab T. | TS-34 | TE | 198 | PV Wall Inside 4 | Not Measured | 273. | - | 673. | K | 0.64%FS |
| 199 | Slab T. | TS-35 | TE | 199 | L.P. Inner Surface | Not Measured | 273. | - | 673. | K | 0.64%FS |
| 200 | Slab T. | TS-36 | TE | 200 | L.P. Wall Inside | Not Measured | 273. | - | 673. | K | 0.64%FS |

Table 3.2 Measurement List for RUN 901 (Continued)

201Ch.- 250Ch.

| Ch. | Item | Symbol | ID. | Location | Fig.No. | Range | Unit | Accuracy |
|---|---|---|---|---|---|---|---|---|
| 201 | Temp. | TF- 1 | TE 201 | A11 Fuel Rod Pos.1 | FIG.5.84, 132 | 273. - 0.147E+04 | K | 0.64%FS |
| 202 | Temp. | TF- 2 | TE 202 | A11 Fuel Rod Pos.2 | FIG.5.84, 133 | 273. - 0.147E+04 | K | 0.64%FS |
| 203 | Temp. | TF- 3 | TE 203 | A11 Fuel Rod Pos.3 | FIG.5.84, 134 | 273. - 0.147E+04 | K | 0.64%FS |
| 204 | Temp. | TF- 4 | TE 204 | A11 Fuel Rod Pos.4 | FIG.5.84, 135 | 273. - 0.147E+04 | K | 0.64%FS |
| 205 | Temp. | TF- 5 | TE 205 | A11 Fuel Rod Pos.5 | FIG.5.84, 136 | 273. - 0.147E+04 | K | 0.64%FS |
| 206 | Temp. | TF- 6 | TE 206 | A11 Fuel Rod Pos.6 | FIG.5.84, 137 | 273. - 0.147E+04 | K | 0.64%FS |
| 207 | Temp. | TF- 7 | TE 207 | A11 Fuel Rod Pos.7 | FIG.5.84, 138 | 273. - 0.147E+04 | K | 0.64%FS |
| 208 | Temp. | TF- 8 | TE 208 | A12 Fuel Rod Pos.1 | FIG.5.85, 132 | 273. - 0.147E+04 | K | 0.64%FS |
| 209 | Temp. | TF- 9 | TE 209 | A12 Fuel Rod Pos.2 | FIG.5.85, 133 | 273. - 0.147E+04 | K | 0.64%FS |
| 210 | Temp. | TF- 10 | TE 210 | A12 Fuel Rod Pos.3 | FIG.5.85, 134 | 273. - 0.147E+04 | K | 0.64%FS |
| 211 | Temp. | TF- 11 | TE 211 | A12 Fuel Rod Pos.4 | FIG.5.85, 135 | 273. - 0.147E+04 | K | 0.64%FS |
| 212 | Temp. | TF- 12 | TE 212 | A12 Fuel Rod Pos.5 | FIG.5.85, 136 | 273. - 0.147E+04 | K | 0.64%FS |
| 213 | Temp. | TF- 13 | TE 213 | A12 Fuel Rod Pos.6 | FIG.5.85, 137 | 273. - 0.147E+04 | K | 0.64%FS |
| 214 | Temp. | TF- 14 | TE 214 | A12 Fuel Rod Pos.7 | FIG.5.85, 138 | 273. - 0.147E+04 | K | 0.64%FS |
| 215 | Temp. | TF- 15 | TE 215 | A13 Fuel Rod Pos.1 | FIG.5.86, 132 | 273. - 0.147E+04 | K | 0.64%FS |
| 216 | Temp. | TF- 16 | TE 216 | A13 Fuel Rod Pos.2 | FIG.5.86, 133 | 273. - 0.147E+04 | K | 0.64%FS |
| 217 | Temp. | TF- 17 | TE 217 | A13 Fuel Rod Pos.3 | FIG.5.86, 134 | 273. - 0.147E+04 | K | 0.64%FS |
| 218 | Temp. | TF- 18 | TE 218 | A13 Fuel Rod Pos.4 | FIG.5.86, 135 | 273. - 0.147E+04 | K | 0.64%FS |
| 219 | Temp. | TF- 19 | TE 219 | A13 Fuel Rod Pos.5 | FIG.5.86, 136 | 273. - 0.147E+04 | K | 0.64%FS |
| 220 | Temp. | TF- 20 | TE 220 | A13 Fuel Rod Pos.6 | FIG.5.86, 137 | 273. - 0.147E+04 | K | 0.64%FS |
| 221 | Temp. | TF- 21 | TE 221 | A13 Fuel Rod Pos.7 | FIG.5.86, 138 | 273. - 0.147E+04 | K | 0.64%FS |
| 222 | Temp. | TF- 22 | TE 222 | A14 Fuel Rod Pos.1 | FIG.5.87 | 273. - 0.147E+04 | K | 0.64%FS |
| 223 | Temp. | TF- 23 | TE 223 | A14 Fuel Rod Pos.2 | FIG.5.87 | 273. - 0.147E+04 | K | 0.64%FS |
| 224 | Temp. | TF- 24 | TE 224 | A14 Fuel Rod Pos.3 | FIG.5.87 | 273. - 0.147E+04 | K | 0.64%FS |
| 225 | Temp. | TF- 25 | TE 225 | A14 Fuel Rod Pos.4 | FIG.5.87 | 273. - 0.147E+04 | K | 0.64%FS |
| 226 | Temp. | TF- 26 | TE 226 | A14 Fuel Rod Pos.5 | FIG.5.87 | 273. - 0.147E+04 | K | 0.64%FS |
| 227 | Temp. | TF- 27 | TE 227 | A14 Fuel Rod Pos.6 | FIG.5.87 | 273. - 0.147E+04 | K | 0.64%FS |
| 228 | Temp. | TF- 28 | TE 228 | A14 Fuel Rod Pos.7 | FIG.5.87 | 273. - 0.147E+04 | K | 0.64%FS |
| 229 | Temp. | TF- 29 | TE 229 | A15 Fuel Rod Pos.1 | FIG.5.88 | 273. - 0.147E+04 | K | 0.64%FS |
| 230 | Temp. | TF- 30 | TE 230 | A15 Fuel Rod Pos.4 | FIG.5.88 | 273. - 0.147E+04 | K | 0.64%FS |
| 231 | Temp. | TF- 31 | TE 231 | A17 Fuel Rod Pos.1 | FIG.5.89 | 273. - 0.147E+04 | K | 0.64%FS |
| 232 | Temp. | TF- 32 | TE 232 | A17 Fuel Rod Pos.4 | FIG.5.89 | 273. - 0.147E+04 | K | 0.64%FS |
| 233 | Temp. | TF- 33 | TE 233 | A22 Fuel Rod Pos.1 | FIG.5.90, 139 | 273. - 0.147E+04 | K | 0.64%FS |
| 234 | Temp. | TF- 34 | TE 234 | A22 Fuel Rod Pos.2 | FIG.5.90, 140 | 273. - 0.147E+04 | K | 0.64%FS |
| 235 | Temp. | TF- 35 | TE 235 | A22 Fuel Rod Pos.3 | FIG.5.90, 141 | 273. - 0.147E+04 | K | 0.64%FS |
| 236 | Temp. | TF- 36 | TE 236 | A22 Fuel Rod Pos.4 | FIG.5.90, 142 | 273. - 0.125E+04 | K | 0.64%FS |
| 237 | Temp. | TF- 37 | TE 237 | A22 Fuel Rod Pos.5 | FIG.5.90, 143 | 273. - 0.125E+04 | K | 0.64%FS |
| 238 | Temp. | TF- 38 | TE 238 | A22 Fuel Rod Pos.6 | FIG.5.90, 144 | 273. - 0.125E+04 | K | 0.64%FS |
| 239 | Temp. | TF- 39 | TE 239 | A22 Fuel Rod Pos.7 | FIG.5.90, 145 | 273. - 0.125E+04 | K | 0.64%FS |
| 240 | Temp. | TF- 40 | TE 240 | A24 Fuel Rod Pos.1 | FIG.5.91 | 273. - 0.125E+04 | K | 0.64%FS |
| 241 | Temp. | TF- 41 | TE 241 | A24 Fuel Rod Pos.2 | FIG.5.91 | 273. - 0.125E+04 | K | 0.64%FS |
| 242 | Temp. | TF- 42 | TE 242 | A24 Fuel Rod Pos.3 | FIG.5.91 | 273. - 0.125E+04 | K | 0.64%FS |
| 243 | Temp. | TF- 43 | TE 243 | A24 Fuel Rod Pos.4 | FIG.5.91 | 273. - 0.125E+04 | K | 0.64%FS |
| 244 | Temp. | TF- 44 | TE 244 | A24 Fuel Rod Pos.5 | FIG.5.91 | 273. - 0.125E+04 | K | 0.64%FS |
| 245 | Temp. | TF- 45 | TE 245 | A24 Fuel Rod Pos.6 | FIG.5.91 | 273. - 0.125E+04 | K | 0.64%FS |
| 246 | Temp. | TF- 46 | TE 246 | A24 Fuel Rod Pos.7 | FIG.5.91 | 273. - 0.125E+04 | K | 0.64%FS |
| 247 | Temp. | TF- 47 | TE 247 | A26 Fuel Rod Pos.1 | FIG.5.92 | 273. - 0.125E+04 | K | 0.64%FS |
| 248 | Temp. | TF- 48 | TE 248 | A26 Fuel Rod Pos.2 | FIG.5.92 | 273. - 0.125E+04 | K | 0.64%FS |
| 249 | Temp. | TF- 49 | TE 249 | A28 Fuel Rod Pos.1 | FIG.5.93 | 273. - 0.125E+04 | K | 0.64%FS |
| 250 | Temp. | TF- 50 | TE 250 | A28 Fuel Rod Pos.4 | FIG.5.93 | 273. - 0.125E+04 | K | 0.64%FS |

Table 3.2 Measurement List for RUN 901 (Continued)

251Ch.- 300Ch.

| Ch. | Item | Symbol | ID. | Location | Fig.No. | Range | Unit | Accuracy |
|---|---|---|---|---|---|---|---|---|
| 251 | Temp. | TF- 51 | TE 251 | A31 Fuel Rod Pos.1 | FIG.5.94 | 273. - 0.125E+04 | K | 0.64%FS |
| 252 | Temp. | TF- 52 | TE 252 | A31 Fuel Rod Pos.4 | FIG.5.94 | 273. - 0.125E+04 | K | 0.64%FS |
| 253 | Temp. | TF- 53 | TE 253 | A33 Fuel Rod Pos.1 | FIG.5.95 | 273. - 0.125E+04 | K | 0.64%FS |
| 254 | Temp. | TF- 54 | TE 254 | A33 Fuel Rod Pos.2 | FIG.5.95 | 273. - 0.125E+04 | K | 0.64%FS |
| 255 | Temp. | TF- 55 | TE 255 | A33 Fuel Rod Pos.3 | FIG.5.95 | 273. - 0.125E+04 | K | 0.64%FS |
| 256 | Temp. | TF- 56 | TE 256 | A33 Fuel Rod Pos.4 | FIG.5.95 | 273. - 0.125E+04 | K | 0.64%FS |
| 257 | Temp. | TF- 57 | TE 257 | A33 Fuel Rod Pos.5 | FIG.5.95 | 273. - 0.125E+04 | K | 0.64%FS |
| 258 | Temp. | TF- 58 | TE 258 | A33 Fuel Rod Pos.6 | FIG.5.95 | 273. - 0.125E+04 | K | 0.64%FS |
| 259 | Temp. | TF- 59 | TE 259 | A33 Fuel Rod Pos.7 | FIG.5.95 | 273. - 0.125E+04 | K | 0.64%FS |
| 260 | Temp. | TF- 60 | TE 260 | A34 Fuel Rod Pos.1 | FIG.5.96 | 273. - 0.125E+04 | K | 0.64%FS |
| 261 | Temp. | TF- 61 | TE 261 | A34 Fuel Rod Pos.2 | Failure | 273. - 0.125E+04 | K | 0.64%FS |
| 262 | Temp. | TF- 62 | TE 262 | A34 Fuel Rod Pos.3 | FIG.5.96 | 273. - 0.125E+04 | K | 0.64%FS |
| 263 | Temp. | TF- 63 | TE 263 | A34 Fuel Rod Pos.4 | FIG.5.96 | 273. - 0.125E+04 | K | 0.64%FS |
| 264 | Temp. | TF- 64 | TE 264 | A34 Fuel Rod Pos.5 | FIG.5.96 | 273. - 0.125E+04 | K | 0.64%FS |
| 265 | Temp. | TF- 65 | TE 265 | A34 Fuel Rod Pos.6 | FIG.5.96 | 273. - 0.125E+04 | K | 0.64%FS |
| 266 | Temp. | TF- 66 | TE 266 | A34 Fuel Rod Pos.7 | FIG.5.96 | 273. - 0.125E+04 | K | 0.64%FS |
| 267 | Temp. | TF- 67 | TE 267 | A37 Fuel Rod Pos.1 | FIG.5.97 | 273. - 0.125E+04 | K | 0.64%FS |
| 268 | Temp. | TF- 68 | TE 268 | A37 Fuel Rod Pos.4 | FIG.5.97 | 273. - 0.125E+04 | K | 0.64%FS |
| 269 | Temp. | TF- 69 | TE 269 | A42 Fuel Rod Pos.1 | FIG.5.98 | 273. - 0.125E+04 | K | 0.64%FS |
| 270 | Temp. | TF- 70 | TE 270 | A42 Fuel Rod Pos.4 | Failure | 273. - 0.125E+04 | K | 0.64%FS |
| 271 | Temp. | TF- 71 | TE 271 | A44 Fuel Rod Pos.1 | FIG.5.99 | 273. - 0.125E+04 | K | 0.64%FS |
| 272 | Temp. | TF- 72 | TE 272 | A44 Fuel Rod Pos.2 | FIG.5.99 | 273. - 0.125E+04 | K | 0.64%FS |
| 273 | Temp. | TF- 73 | TE 273 | A44 Fuel Rod Pos.3 | FIG.5.99 | 273. - 0.125E+04 | K | 0.64%FS |
| 274 | Temp. | TF- 74 | TE 274 | A44 Fuel Rod Pos.4 | FIG.5.99 | 273. - 0.125E+04 | K | 0.64%FS |
| 275 | Temp. | TF- 75 | TE 275 | A44 Fuel Rod Pos.5 | FIG.5.99 | 273. - 0.125E+04 | K | 0.64%FS |
| 276 | Temp. | TF- 76 | TE 276 | A44 Fuel Rod Pos.6 | FIG.5.99 | 273. - 0.125E+04 | K | 0.64%FS |
| 277 | Temp. | TF- 77 | TE 277 | A44 Fuel Rod Pos.7 | FIG.5.99 | 273. - 0.125E+04 | K | 0.64%FS |
| 278 | Temp. | TF- 78 | TE 278 | A48 Fuel Rod Pos.1 | FIG.5.100 | 273. - 0.125E+04 | K | 0.64%FS |
| 279 | Temp. | TF- 79 | TE 279 | A48 Fuel Rod Pos.4 | FIG.5.100 | 273. - 0.125E+04 | K | 0.64%FS |
| 280 | Temp. | TF- 80 | TE 280 | A51 Fuel Rod Pos.1 | FIG.5.101 | 273. - 0.125E+04 | K | 0.64%FS |
| 281 | Temp. | TF- 81 | TE 281 | A51 Fuel Rod Pos.4 | FIG.5.101 | 273. - 0.125E+04 | K | 0.64%FS |
| 282 | Temp. | TF- 82 | TE 282 | A53 Fuel Rod Pos.1 | FIG.5.102 | 273. - 0.125E+04 | K | 0.64%FS |
| 283 | Temp. | TF- 83 | TE 283 | A53 Fuel Rod Pos.4 | FIG.5.102 | 273. - 0.125E+04 | K | 0.64%FS |
| 284 | Temp. | TF- 84 | TE 284 | A57 Fuel Rod Pos.1 | FIG.5.103 | 273. - 0.125E+04 | K | 0.64%FS |
| 285 | Temp. | TF- 85 | TE 285 | A57 Fuel Rod Pos.4 | FIG.5.103 | 273. - 0.125E+04 | K | 0.64%FS |
| 286 | Temp. | TF- 86 | TE 286 | A62 Fuel Rod Pos.1 | FIG.5.104 | 273. - 0.125E+04 | K | 0.64%FS |
| 287 | Temp. | TF- 87 | TE 287 | A62 Fuel Rod Pos.4 | FIG.5.104 | 273. - 0.125E+04 | K | 0.64%FS |
| 288 | Temp. | TF- 88 | TE 288 | A66 Fuel Rod Pos.1 | FIG.5.105 | 273. - 0.125E+04 | K | 0.64%FS |
| 289 | Temp. | TF- 89 | TE 289 | A66 Fuel Rod Pos.4 | Failure | 273. - 0.125E+04 | K | 0.64%FS |
| 290 | Temp. | TF- 90 | TE 290 | A68 Fuel Rod Pos.1 | FIG.5.106 | 273. - 0.125E+04 | K | 0.64%FS |
| 291 | Temp. | TF- 91 | TE 291 | A68 Fuel Rod Pos.4 | FIG.5.106 | 273. - 0.125E+04 | K | 0.64%FS |
| 292 | Temp. | TF- 92 | TE 292 | A71 Fuel Rod Pos.1 | FIG.5.107 | 273. - 0.125E+04 | K | 0.64%FS |
| 293 | Temp. | TF- 93 | TE 293 | A71 Fuel Rod Pos.4 | Failure | 273. - 0.125E+04 | K | 0.64%FS |
| 294 | Temp. | TF- 94 | TE 294 | A73 Fuel Rod Pos.1 | FIG.5.108 | 273. - 0.125E+04 | K | 0.64%FS |
| 295 | Temp. | TF- 95 | TE 295 | A73 Fuel Rod Pos.4 | FIG.5.108 | 273. - 0.125E+04 | K | 0.64%FS |
| 296 | Temp. | TF- 96 | TE 296 | A75 Fuel Rod Pos.1 | FIG.5.109 | 273. - 0.125E+04 | K | 0.64%FS |
| 297 | Temp. | TF- 97 | TE 297 | A75 Fuel Rod Pos.4 | FIG.5.109 | 273. - 0.125E+04 | K | 0.64%FS |
| 298 | Temp. | TF- 98 | TE 298 | A77 Fuel Rod Pos.1 | FIG.5.110, 146 | 273. - 0.125E+04 | K | 0.64%FS |
| 299 | Temp. | TF- 99 | TE 299 | A77 Fuel Rod Pos.2 | FIG.5.110, 147 | 273. - 0.125E+04 | K | 0.64%FS |
| 300 | Temp. | TF-100 | TE 300 | A77 Fuel Rod Pos.3 | FIG.5.110, 148 | 273. - 0.125E+04 | K | 0.64%FS |

Table 3.2 Measurement List for RUN 901 (Continued)

301Ch.- 350Ch.

| Ch. | Item | Symbol | ID. | | Location | Fig.No. | Range | | | Unit | Accuracy |
|---|---|---|---|---|---|---|---|---|---|---|---|
| 301 | Temp. | TF-101 | TE | 301 | A77 Fuel Rod Pos.4 | FIG.5.110, 149 | 273. | - | 0.125E+04 | K | 0.64%FS |
| 302 | Temp. | TF-102 | TE | 302 | A77 Fuel Rod Pos.5 | FIG.5.110, 150 | 273. | - | 0.125E+04 | K | 0.64%FS |
| 303 | Temp. | TF-103 | TE | 303 | A77 Fuel Rod Pos.6 | FIG.5.110, 151 | 273. | - | 0.125E+04 | K | 0.64%FS |
| 304 | Temp. | TF-104 | TE | 304 | A77 Fuel Rod Pos.7 | Failure | 273. | - | 0.125E+04 | K | 0.64%FS |
| 305 | Temp. | TF-105 | TE | 305 | A82 Fuel Rod Pos.1 | FIG.5.111 | 273. | - | 0.125E+04 | K | 0.64%FS |
| 306 | Temp. | TF-106 | TE | 306 | A82 Fuel Rod Pos.4 | Failure | 273. | - | 0.125E+04 | K | 0.64%FS |
| 307 | Temp. | TF-107 | TE | 307 | A84 Fuel Rod Pos.1 | FIG.5.112 | 273. | - | 0.125E+04 | K | 0.64%FS |
| 308 | Temp. | TF-108 | TE | 308 | A84 Fuel Rod Pos.4 | FIG.5.112 | 273. | - | 0.125E+04 | K | 0.64%FS |
| 309 | Temp. | TF-109 | TE | 309 | A85 Fuel Rod Pos.1 | FIG.5.113 | 273. | - | 0.125E+04 | K | 0.64%FS |
| 310 | Temp. | TF-110 | TE | 310 | A85 Fuel Rod Pos.2 | Failure | 273. | - | 0.125E+04 | K | 0.64%FS |
| 311 | Temp. | TF-111 | TE | 311 | A85 Fuel Rod Pos.3 | Failure | 273. | - | 0.125E+04 | K | 0.64%FS |
| 312 | Temp. | TF-112 | TE | 312 | A85 Fuel Rod Pos.4 | FIG.5.113 | 273. | - | 0.125E+04 | K | 0.64%FS |
| 313 | Temp. | TF-113 | TE | 313 | A85 Fuel Rod Pos.5 | FIG.5.113 | 273. | - | 0.125E+04 | K | 0.64%FS |
| 314 | Temp. | TF-114 | TE | 314 | A85 Fuel Rod Pos.6 | FIG.5.113 | 273. | - | 0.125E+04 | K | 0.64%FS |
| 315 | Temp. | TF-115 | TE | 315 | A85 Fuel Rod Pos.7 | FIG.5.113 | 273. | - | 0.125E+04 | K | 0.64%FS |
| 316 | Temp. | TF-116 | TE | 316 | A87 Fuel Rod Pos.1 | FIG.5.114, 132 | 273. | - | 0.125E+04 | K | 0.64%FS |
| 317 | Temp. | TF-117 | TE | 317 | A87 Fuel Rod Pos.2 | Failure | 273. | - | 0.125E+04 | K | 0.64%FS |
| 318 | Temp. | TF-118 | TE | 318 | A87 Fuel Rod Pos.3 | FIG.5.114, 134 | 273. | - | 0.125E+04 | K | 0.64%FS |
| 319 | Temp. | TF-119 | TE | 319 | A87 Fuel Rod Pos.4 | FIG.5.114, 135 | 273. | - | 0.125E+04 | K | 0.64%FS |
| 320 | Temp. | TF-120 | TE | 320 | A87 Fuel Rod Pos.5 | FIG.5.114, 136 | 273. | - | 0.125E+04 | K | 0.64%FS |
| 321 | Temp. | TF-121 | TE | 321 | A87 Fuel Rod Pos.6 | FIG.5.114, 137 | 273. | - | 0.125E+04 | K | 0.64%FS |
| 322 | Temp. | TF-122 | TE | 322 | A87 Fuel Rod Pos.7 | FIG.5.114, 138 | 273. | - | 0.125E+04 | K | 0.64%FS |
| 323 | Temp. | TF-123 | TE | 323 | A88 Fuel Rod Pos.1 | FIG.5.115, 132 | 273. | - | 0.125E+04 | K | 0.64%FS |
| 324 | Temp. | TF-124 | TE | 324 | A88 Fuel Rod Pos.2 | FIG.5.115, 133 | 273. | - | 0.125E+04 | K | 0.64%FS |
| 325 | Temp. | TF-125 | TE | 325 | A88 Fuel Rod Pos.3 | FIG.5.115, 134 | 273. | - | 0.125E+04 | K | 0.64%FS |
| 326 | Temp. | TF-126 | TE | 326 | A88 Fuel Rod Pos.4 | FIG.5.115, 135 | 273. | - | 0.125E+04 | K | 0.64%FS |
| 327 | Temp. | TF-127 | TE | 327 | A88 Fuel Rod Pos.5 | FIG.5.115, 136 | 273. | - | 0.125E+04 | K | 0.64%FS |
| 328 | Temp. | TF-128 | TE | 328 | A88 Fuel Rod Pos.6 | FIG.5.115, 137 | 273. | - | 0.125E+04 | K | 0.64%FS |
| 329 | Temp. | TF-129 | TE | 329 | A88 Fuel Rod Pos.7 | FIG.5.115, 138 | 273. | - | 0.125E+04 | K | 0.64%FS |
| 330 | Temp. | TF-130 | TE | 330 | B11 Fuel Rod Pos.1 | FIG.5.116 | 273. | - | 0.125E+04 | K | 0.64%FS |
| 331 | Temp. | TF-131 | TE | 331 | B11 Fuel Rod Pos.2 | FIG.5.116 | 273. | - | 0.125E+04 | K | 0.64%FS |
| 332 | Temp. | TF-132 | TE | 332 | B11 Fuel Rod Pos.3 | FIG.5.116 | 273. | - | 0.125E+04 | K | 0.64%FS |
| 333 | Temp. | TF-133 | TE | 333 | B11 Fuel Rod Pos.4 | FIG.5.116 | 273. | - | 0.125E+04 | K | 0.64%FS |
| 334 | Temp. | TF-134 | TE | 334 | B11 Fuel Rod Pos.5 | FIG.5.116 | 273. | - | 0.125E+04 | K | 0.64%FS |
| 335 | Temp. | TF-135 | TE | 335 | B11 Fuel Rod Pos.6 | FIG.5.116 | 273. | - | 0.125E+04 | K | 0.64%FS |
| 336 | Temp. | TF-136 | TE | 336 | B11 Fuel Rod Pos.7 | FIG.5.116 | 273. | - | 0.125E+04 | K | 0.64%FS |
| 337 | Temp. | TF-137 | TE | 337 | B13 Fuel Rod Pos.4 | FIG.5.117 | 273. | - | 0.125E+04 | K | 0.64%FS |
| 338 | Temp. | TF-138 | TE | 338 | B22 Fuel Rod Pos.1 | FIG.5.118, 139 | 273. | - | 0.125E+04 | K | 0.64%FS |
| 339 | Temp. | TF-139 | TE | 339 | B22 Fuel Rod Pos.2 | FIG.5.118, 140 | 273. | - | 0.125E+04 | K | 0.64%FS |
| 340 | Temp. | TF-140 | TE | 340 | B22 Fuel Rod Pos.3 | FIG.5.118, 141 | 273. | - | 0.125E+04 | K | 0.64%FS |
| 341 | Temp. | TF-141 | TE | 341 | B22 Fuel Rod Pos.4 | Failure | 273. | - | 0.125E+04 | K | 0.64%FS |
| 342 | Temp. | TF-142 | TE | 342 | B22 Fuel Rod Pos.5 | FIG.5.118, 143 | 273. | - | 0.125E+04 | K | 0.64%FS |
| 343 | Temp. | TF-143 | TE | 343 | B22 Fuel Rod Pos.6 | FIG.5.118, 144 | 273. | - | 0.125E+04 | K | 0.64%FS |
| 344 | Temp. | TF-144 | TE | 344 | B22 Fuel Rod Pos.7 | FIG.5.118, 145 | 273. | - | 0.125E+04 | K | 0.64%FS |
| 345 | Temp. | TF-145 | TE | 345 | B31 Fuel Rod Pos.4 | FIG.5.117 | 273. | - | 0.125E+04 | K | 0.64%FS |
| 346 | Temp. | TF-146 | TE | 346 | B33 Fuel Rod Pos.4 | FIG.5.119 | 273. | - | 0.125E+04 | K | 0.64%FS |
| 347 | Temp. | TF-147 | TE | 347 | B51 Fuel Rod Pos.4 | FIG.5.120 | 273. | - | 0.125E+04 | K | 0.64%FS |
| 348 | Temp. | TF-148 | TE | 348 | B53 Fuel Rod Pos.4 | FIG.5.119 | 273. | - | 0.125E+04 | K | 0.64%FS |
| 349 | Temp. | TF-149 | TE | 349 | B66 Fuel Rod Pos.4 | FIG.5.119 | 273. | - | 0.125E+04 | K | 0.64%FS |
| 350 | Temp. | TF-150 | TE | 350 | B77 Fuel Rod Pos.1 | FIG.5.121,146 | 273. | - | 0.125E+04 | K | 0.64%FS |

Table 3.2 Measurement List for RUN 901 (Continued)

351Ch.- 400Ch.

| Ch. | Item | Symbol | ID. | Location | Fig.No. | Range | Unit | Accuracy |
|---|---|---|---|---|---|---|---|---|
| 351 | Temp. | TF-151 | TE 351 | B77 Fuel Rod Pos.2 | FIG.5.121,147 | 273. - 0.125E+04 | K | 0.64%FS |
| 352 | Temp. | TF-152 | TE 352 | B77 Fuel Rod Pos.3 | FIG.5.121,148 | 273. - 0.125E+04 | K | 0.64%FS |
| 353 | Temp. | TF-153 | TE 353 | B77 Fuel Rod Pos.4 | FIG.5.121,149 | 273. - 0.125E+04 | K | 0.64%FS |
| 354 | Temp. | TF-154 | TE 354 | B77 Fuel Rod Pos.5 | FIG.5.121,150 | 273. - 0.125E+04 | K | 0.64%FS |
| 355 | Temp. | TF-155 | TE 355 | B77 Fuel Rod Pos.6 | FIG.5.121,151 | 273. - 0.125E+04 | K | 0.64%FS |
| 356 | Temp. | TF-156 | TE 356 | B77 Fuel Rod Pos.7 | FIG.5.121,152 | 273. - 0.125E+04 | K | 0.64%FS |
| 357 | Temp. | TF-157 | TE 357 | B86 Fuel Rod Pos.4 | Failure | 273. - 0.125E+04 | K | 0.64%FS |
| 358 | Temp. | TF-158 | TE 358 | C11 Fuel Rod Pos.1 | FIG.5.122 | 273. - 0.125E+04 | K | 0.64%FS |
| 359 | Temp. | TF-159 | TE 359 | C11 Fuel Rod Pos.2 | FIG.5.122 | 273. - 0.125E+04 | K | 0.64%FS |
| 360 | Temp. | TF-160 | TE 360 | C11 Fuel Rod Pos.3 | FIG.5.122 | 273. - 0.125E+04 | K | 0.64%FS |
| 361 | Temp. | TF-161 | TE 361 | C11 Fuel Rod Pos.4 | FIG.5.122 | 273. - 0.125E+04 | K | 0.64%FS |
| 362 | Temp. | TF-162 | TE 362 | C11 Fuel Rod Pos.5 | FIG.5.122 | 273. - 0.125E+04 | K | 0.64%FS |
| 363 | Temp. | TF-163 | TE 363 | C11 Fuel Rod Pos.6 | FIG.5.122 | 273. - 0.125E+04 | K | 0.64%FS |
| 364 | Temp. | TF-164 | TE 364 | C11 Fuel Rod Pos.7 | FIG.5.122 | 273. - 0.125E+04 | K | 0.64%FS |
| 365 | Temp. | TF-165 | TE 365 | C13 Fuel Rod Pos.1 | FIG.5.123 | 273. - 0.125E+04 | K | 0.64%FS |
| 366 | Temp. | TF-166 | TE 366 | C13 Fuel Rod Pos.2 | FIG.5.123 | 273. - 0.125E+04 | K | 0.64%FS |
| 367 | Temp. | TF-167 | TE 367 | C13 Fuel Rod Pos.3 | FIG.5.123 | 273. - 0.125E+04 | K | 0.64%FS |
| 368 | Temp. | TF-168 | TE 368 | C13 Fuel Rod Pos.4 | Failure | 273. - 0.125E+04 | K | 0.64%FS |
| 369 | Temp. | TF-169 | TE 369 | C13 Fuel Rod Pos.5 | FIG.5.123 | 273. - 0.125E+04 | K | 0.64%FS |
| 370 | Temp. | TF-170 | TE 370 | C13 Fuel Rod Pos.6 | FIG.5.123 | 273. - 0.125E+04 | K | 0.64%FS |
| 371 | Temp. | TF-171 | TE 371 | C13 Fuel Rod Pos.7 | FIG.5.123 | 273. - 0.125E+04 | K | 0.64%FS |
| 372 | Temp. | TF-172 | TE 372 | C15 Fuel Rod Pos.4 | FIG.5.120 | 273. - 0.125E+04 | K | 0.64%FS |
| 373 | Temp. | TF-173 | TE 373 | C22 Fuel Rod Pos.1 | FIG.5.124, 139 | 273. - 0.125E+04 | K | 0.64%FS |
| 374 | Temp. | TF-174 | TE 374 | C22 Fuel Rod Pos.2 | FIG.5.124, 140 | 273. - 0.125E+04 | K | 0.64%FS |
| 375 | Temp. | TF-175 | TE 375 | C22 Fuel Rod Pos.3 | FIG.5.124, 141 | 273. - 0.125E+04 | K | 0.64%FS |
| 376 | Temp. | TF-176 | TE 376 | C22 Fuel Rod Pos.4 | FIG.5.124, 142 | 273. - 0.125E+04 | K | 0.64%FS |
| 377 | Temp. | TF-177 | TE 377 | C22 Fuel Rod Pos.5 | FIG.5.124, 143 | 273. - 0.125E+04 | K | 0.64%FS |
| 378 | Temp. | TF-178 | TE 378 | C22 Fuel Rod Pos.6 | FIG.5.124, 144 | 273. - 0.125E+04 | K | 0.64%FS |
| 379 | Temp. | TF-179 | TE 379 | C22 Fuel Rod Pos.7 | FIG.5.124, 145 | 273. - 0.125E+04 | K | 0.64%FS |
| 380 | Temp. | TF-180 | TE 380 | C31 Fuel Rod Pos.4 | FIG.5.125 | 273. - 0.125E+04 | K | 0.64%FS |
| 381 | Temp. | TF-181 | TE 381 | C33 Fuel Rod Pos.1 | FIG.5.126 | 273. - 0.125E+04 | K | 0.64%FS |
| 382 | Temp. | TF-182 | TE 382 | C33 Fuel Rod Pos.2 | FIG.5.126 | 273. - 0.125E+04 | K | 0.64%FS |
| 383 | Temp. | TF-183 | TE 383 | C33 Fuel Rod Pos.3 | FIG.5.126 | 273. - 0.125E+04 | K | 0.64%FS |
| 384 | Temp. | TF-184 | TE 384 | C33 Fuel Rod Pos.4 | FIG.5.126 | 273. - 0.125E+04 | K | 0.64%FS |
| 385 | Temp. | TF-185 | TE 385 | C33 Fuel Rod Pos.5 | FIG.5.126 | 273. - 0.125E+04 | K | 0.64%FS |
| 386 | Temp. | TF-186 | TE 386 | C33 Fuel Rod Pos.6 | FIG.5.126 | 273. - 0.125E+04 | K | 0.64%FS |
| 387 | Temp. | TF-187 | TE 387 | C33 Fuel Rod Pos.7 | FIG.5.126 | 273. - 0.125E+04 | K | 0.64%FS |
| 388 | Temp. | TF-188 | TE 388 | C35 Fuel Rod Pos.4 | FIG.5.127 | 273. - 0.125E+04 | K | 0.64%FS |
| 389 | Temp. | TF-189 | TE 389 | C66 Fuel Rod Pos.4 | FIG.5.127 | 273. - 0.125E+04 | K | 0.64%FS |
| 390 | Temp. | TF-190 | TE 390 | C68 Fuel Rod Pos.4 | FIG.5.125 | 273. - 0.125E+04 | K | 0.64%FS |
| 391 | Temp. | TF-191 | TE 391 | C77 Fuel Rod Pos.1 | FIG.5.128, 146 | 273. - 0.125E+04 | K | 0.64%FS |
| 392 | Temp. | TF-192 | TE 392 | C77 Fuel Rod Pos.2 | FIG.5.128, 147 | 273. - 0.125E+04 | K | 0.64%FS |
| 393 | Temp. | TF-193 | TE 393 | C77 Fuel Rod Pos.3 | FIG.5.128, 148 | 273. - 0.125E+04 | K | 0.64%FS |
| 394 | Temp. | TF-194 | TE 394 | C77 Fuel Rod Pos.4 | FIG.5.128, 149 | 273. - 0.125E+04 | K | 0.64%FS |
| 395 | Temp. | TF-195 | TE 395 | C77 Fuel Rod Pos.5 | FIG.5.128, 150 | 273. - 0.125E+04 | K | 0.64%FS |
| 396 | Temp. | TF-196 | TE 396 | C77 Fuel Rod Pos.6 | FIG.5.128, 151 | 273. - 0.125E+04 | K | 0.64%FS |
| 397 | Temp. | TF-197 | TE 397 | C77 Fuel Rod Pos.7 | FIG.5.128, 152 | 273. - 0.125E+04 | K | 0.64%FS |
| 398 | Temp. | TF-198 | TE 398 | D11 Fuel Rod Pos.4 | FIG.5.129 | 273. - 0.125E+04 | K | 0.64%FS |
| 399 | Temp. | TF-199 | TE 399 | D13 Fuel Rod Pos.4 | Failure | 273. - 0.125E+04 | K | 0.64%FS |
| 400 | Temp. | TF-200 | TE 400 | D22 Fuel Rod Pos.1 | FIG.5.130, 139 | 273. - 0.125E+04 | K | 0.64%FS |

Table 3.2 Measurement List for RUN 901 (Continued)

401Ch.- 450Ch.

| Ch. | Item | Symbol | ID. | Location | Fig.No. | Range | Unit | Accuracy |
|---|---|---|---|---|---|---|---|---|
| 401 | Temp. | TF-201 | TE 401 | D22 Fuel Rod Pos.2 | FIG.5.130, 140 | 273. - 0.125E+04 | K | 0.64%FS |
| 402 | Temp. | TF-202 | TE 402 | D22 Fuel Rod Pos.3 | FIG.5.130, 141 | 273. - 0.125E+04 | K | 0.64%FS |
| 403 | Temp. | TF-203 | TE 403 | D22 Fuel Rod Pos.4 | FIG.5.130, 142 | 273. - 0.125E+04 | K | 0.64%FS |
| 404 | Temp. | TF-204 | TE 404 | D22 Fuel Rod Pos.5 | FIG.5.130, 143 | 273. - 0.125E+04 | K | 0.64%FS |
| 405 | Temp. | TF-205 | TE 405 | D22 Fuel Rod Pos.6 | FIG.5.130, 144 | 273. - 0.125E+04 | K | 0.64%FS |
| 406 | Temp. | TF-206 | TE 406 | D22 Fuel Rod Pos.7 | FIG.5.130, 145 | 273. - 0.125E+04 | K | 0.64%FS |
| 407 | Temp. | TF-207 | TE 407 | D31 Fuel Rod Pos.4 | FIG.5.129 | 273. - 0.125E+04 | K | 0.64%FS |
| 408 | Temp. | TF-208 | TE 408 | D33 Fuel Rod Pos.4 | FIG.5.131 | 273. - 0.125E+04 | K | 0.64%FS |
| 409 | Temp. | TF-209 | TE 409 | D51 Fuel Rod Pos.4 | FIG.5.120 | 273. - 0.125E+04 | K | 0.64%FS |
| 410 | Temp. | TF-210 | TE 410 | D53 Fuel Rod Pos.4 | FIG.5.131 | 273. - 0.125E+04 | K | 0.64%FS |
| 411 | Temp. | TF-211 | TE 411 | D66 Fuel Rod Pos.4 | FIG.5.131 | 273. - 0.125E+04 | K | 0.64%FS |
| 412 | Temp. | TF-212 | TE 412 | D77 Fuel Rod Pos.4 | Failure | 273. - 0.125E+04 | K | 0.64%FS |
| 413 | Temp. | TF-213 | TE 413 | D86 Fuel Rod Pos.4 | FIG.5.129 | 273. - 0.125E+04 | K | 0.64%FS |
| 414 | Fluid T. | TW- 1 | TE 414 | A45 Tie Rod Pos.1 | FIG.5.153 | 273. - 0.125E+04 | K | 0.64%FS |
| 415 | Fluid T. | TW- 2 | TE 415 | A45 Tie Rod Pos.2 | FIG.5.153 | 273. - 0.125E+04 | K | 0.64%FS |
| 416 | Fluid T. | TW- 3 | TE 416 | A45 Tie Rod Pos.3 | FIG.5.153 | 273. - 0.125E+04 | K | 0.64%FS |
| 417 | Fluid T. | TW- 4 | TE 417 | A45 Tie Rod Pos.4 | FIG.5.153 | 273. - 0.125E+04 | K | 0.64%FS |
| 418 | Fluid T. | TW- 5 | TE 418 | A45 Tie Rod Pos.5 | FIG.5.153 | 273. - 0.125E+04 | K | 0.64%FS |
| 419 | Fluid T. | TW- 6 | TE 419 | A45 Tie Rod Pos.6 | FIG.5.153 | 273. - 0.125E+04 | K | 0.64%FS |
| 420 | Fluid T. | TW- 7 | TE 420 | A45 Tie Rod Pos.7 | FIG.5.153 | 273. - 0.125E+04 | K | 0.64%FS |
| 421 | Fluid T. | TW- 8 | TE 421 | B45 Tie Rod Pos.1 | FIG.5.154 | 273. - 0.125E+04 | K | 0.64%FS |
| 422 | Fluid T. | TW- 9 | TE 422 | B45 Tie Rod Pos.2 | FIG.5.154 | 273. - 0.125E+04 | K | 0.64%FS |
| 423 | Fluid T. | TW-10 | TE 423 | B45 Tie Rod Pos.3 | FIG.5.154 | 273. - 0.125E+04 | K | 0.64%FS |
| 424 | Fluid T. | TW-11 | TE 424 | B45 Tie Rod Pos.4 | FIG.5.154 | 273. - 0.125E+04 | K | 0.64%FS |
| 425 | Fluid T. | TW-12 | TE 425 | B45 Tie Rod Pos.5 | FIG.5.154 | 273. - 0.125E+04 | K | 0.64%FS |
| 426 | Fluid T. | TW-13 | TE 426 | B45 Tie Rod Pos.6 | FIG.5.154 | 273. - 0.125E+04 | K | 0.64%FS |
| 427 | Fluid T. | TW-14 | TE 427 | B45 Tie Rod Pos.7 | FIG.5.154 | 273. - 0.125E+04 | K | 0.64%FS |
| 428 | Fluid T. | TW-15 | TE 428 | C45 Tie Rod Pos.1 | FIG.5.155 | 273. - 0.125E+04 | K | 0.64%FS |
| 429 | Fluid T. | TW-16 | TE 429 | C45 Tie Rod Pos.2 | FIG.5.155 | 273. - 0.125E+04 | K | 0.64%FS |
| 430 | Fluid T. | TW-17 | TE 430 | C45 Tie Rod Pos.3 | FIG.5.155 | 273. - 0.125E+04 | K | 0.64%FS |
| 431 | Fluid T. | TW-18 | TE 431 | C45 Tie Rod Pos.4 | FIG.5.155 | 273. - 0.125E+04 | K | 0.64%FS |
| 432 | Fluid T. | TW-19 | TE 432 | C45 Tie Rod Pos.5 | FIG.5.155 | 273. - 0.125E+04 | K | 0.64%FS |
| 433 | Fluid T. | TW-20 | TE 433 | C45 Tie Rod Pos.6 | FIG.5.155 | 273. - 0.125E+04 | K | 0.64%FS |
| 434 | Fluid T. | TW-21 | TE 434 | C45 Tie Rod Pos.7 | FIG.5.155 | 273. - 0.125E+04 | K | 0.64%FS |
| 435 | Fluid T. | TW-22 | TE 435 | D45 Tie Rod Pos.1 | FIG.5.156 | 273. - 0.125E+04 | K | 0.64%FS |
| 436 | Fluid T. | TW-23 | TE 436 | D45 Tie Rod Pos.2 | FIG.5.156 | 273. - 0.125E+04 | K | 0.64%FS |
| 437 | Fluid T. | TW-24 | TE 437 | D45 Tie Rod Pos.3 | FIG.5.156 | 273. - 0.125E+04 | K | 0.64%FS |
| 438 | Fluid T. | TW-25 | TE 438 | D45 Tie Rod Pos.4 | FIG.5.156 | 273. - 0.125E+04 | K | 0.64%FS |
| 439 | Fluid T. | TW-26 | TE 439 | D45 Tie Rod Pos.5 | FIG.5.156 | 273. - 0.125E+04 | K | 0.64%FS |
| 440 | Fluid T. | TW-27 | TE 440 | D45 Tie Rod Pos.6 | FIG.5.156 | 273. - 0.125E+04 | K | 0.64%FS |
| 441 | Fluid T. | TW-28 | TE 441 | D45 Tie Rod Pos.7 | FIG.5.156 | 273. - 0.125E+04 | K | 0.64%FS |
| 442 | Fluid T. | TC- 1 | TE 442 | Channel Box A Inlet | FIG.5.157 | 273. - 0.125E+04 | K | 0.64%FS |
| 443 | Fluid T. | TC- 2 | TE 443 | Channel Box B Inlet | FIG.5.157 | 273. - 0.125E+04 | K | 0.64%FS |
| 444 | Fluid T. | TC- 3 | TE 444 | Channel Box C Inlet | FIG.5.157 | 273. - 0.125E+04 | K | 0.64%FS |
| 445 | Fluid T. | TC- 4 | TE 445 | Channel Box D Inlet | FIG.5.157 | 273. - 0.125E+04 | K | 0.64%FS |
| 446 | Fluid T. | TC- 5 | TE 446 | Channel Box Outlet A-1 | FIG.5.158 | 273. - 0.125E+04 | K | 0.64%FS |
| 447 | Fluid T. | TC- 6 | TE 447 | Channel Box Outlet A-2 | FIG.5.158 | 273. - 0.125E+04 | K | 0.64%FS |
| 448 | Fluid T. | TC- 7 | TE 448 | Channel Box Outlet A-3 | FIG.5.158 | 273. - 0.125E+04 | K | 0.64%FS |
| 449 | Fluid T. | TC- 8 | TE 449 | Channel Box Outlet A-4 | FIG.5.158 | 273. - 0.125E+04 | K | 0.64%FS |
| 450 | Fluid T. | TC- 9 | TE 450 | Channel Box Outlet A-6 | FIG.5.158 | 273. - 0.125E+04 | K | 0.64%FS |

Table 3.2 Measurement List for RUN 901 (Continued)

451Ch.- 500Ch.

| Ch. | Item | Symbol | ID. | Location | Fig.No. | Range | | | Unit | Accuracy |
|---|---|---|---|---|---|---|---|---|---|---|
| 451 | Fluid T. | TC-10 | TE 451 | Channel Box Outlet C-1 | FIG.5.159 | 273. | - | 0.125E+04 | K | 0.64%FS |
| 452 | Fluid T. | TC-11 | TE 452 | Channel Box Outlet C-2 | FIG.5.159 | 273. | - | 0.125E+04 | K | 0.64%FS |
| 453 | Fluid T. | TC-12 | TE 453 | Channel Box Outlet C-3 | FIG.5.159 | 273. | - | 0.125E+04 | K | 0.64%FS |
| 454 | Fluid T. | TC-13 | TE 454 | Channel Box Outlet C-4 | FIG.5.159 | 273. | - | 0.125E+04 | K | 0.64%FS |
| 455 | Fluid T. | TC-14 | TE 455 | Channel Box Outlet C-6 | FIG.5.159 | 273. | - | 0.125E+04 | K | 0.64%FS |
| 456 | Fluid T. | TG- 1 | TE 456 | Upper Tieplate A Up.1 | FIG.5.160 | 273. | - | 0.125E+04 | K | 0.64%FS |
| 457 | Fluid T. | TG- 2 | TE 457 | Upper Tieplate A Up.2 | FIG.5.160 | 273. | - | 0.125E+04 | K | 0.64%FS |
| 458 | Fluid T. | TG- 3 | TE 458 | Upper Tieplate A Up.3 | FIG.5.160 | 273. | - | 0.125E+04 | K | 0.64%FS |
| 459 | Fluid T. | TG- 4 | TE 459 | Upper Tieplate A Up.4 | FIG.5.160 | 273. | - | 0.125E+04 | K | 0.64%FS |
| 460 | Fluid T. | TG- 5 | TE 460 | Upper Tieplate A Up.5 | FIG.5.160 | 273. | - | 0.125E+04 | K | 0.64%FS |
| 461 | Fluid T. | TG- 6 | TE 461 | Upper Tieplate A Up.6 | FIG.5.161 | 273. | - | 0.125E+04 | K | 0.64%FS |
| 462 | Fluid T. | TG- 7 | TE 462 | Upper Tieplate A Up.7 | FIG.5.161 | 273. | - | 0.125E+04 | K | 0.64%FS |
| 463 | Fluid T. | TG- 8 | TE 463 | Upper Tieplate A Up.8 | FIG.5.161 | 273. | - | 0.125E+04 | K | 0.64%FS |
| 464 | Fluid T. | TG- 9 | TE 464 | Upper Tieplate A Up.9 | FIG.5.161 | 273. | - | 0.125E+04 | K | 0.64%FS |
| 465 | Fluid T. | TG-10 | TE 465 | Upper Tieplate A Up.10 | FIG.5.161 | 273. | - | 0.125E+04 | K | 0.64%FS |
| 466 | Fluid T. | TG-11 | TE 466 | Upper Tieplate A Lo.1 | Not Measured | 273. | - | 0.125E+04 | K | 0.64%FS |
| 467 | Fluid T. | TG-12 | TE 467 | Upper Tieplate A Lo.2 | Not Measured | 273. | - | 0.125E+04 | K | 0.64%FS |
| 468 | Fluid T. | TG-13 | TE 468 | Upper Tieplate A Lo.3 | Not Measured | 273. | - | 0.125E+04 | K | 0.64%FS |
| 469 | Fluid T. | TG-14 | TE 469 | Upper Tieplate A Lo.4 | Not Measured | 273. | - | 0.125E+04 | K | 0.64%FS |
| 470 | Fluid T. | TG-15 | TE 470 | Upper Tieplate A Lo.5 | Not Measured | 273. | - | 0.125E+04 | K | 0.64%FS |
| 471 | Fluid T. | TG-16 | TE 471 | Upper Tieplate A Lo.6 | Not Measured | 273. | - | 0.125E+04 | K | 0.64%FS |
| 472 | Fluid T. | TG-17 | TE 472 | Upper Tieplate A Lo.7 | Not Measured | 273. | - | 0.125E+04 | K | 0.64%FS |
| 473 | Fluid T. | TG-18 | TE 473 | Upper Tieplate A Lo.8 | Not Measured | 273. | - | 0.125E+04 | K | 0.64%FS |
| 474 | Fluid T. | TG-19 | TE 474 | Upper Tieplate A Lo.9 | Not Measured | 273. | - | 0.125E+04 | K | 0.64%FS |
| 475 | Fluid T. | TG-20 | TE 475 | Upper Tieplate A Lo.10 | Not Measured | 273. | - | 0.125E+04 | K | 0.64%FS |
| 476 | Fluid T. | TG-21 | TE 476 | Upper Tieplate C Up.1 | Not Measured | 273. | - | 0.125E+04 | K | 0.64%FS |
| 477 | Fluid T. | TG-22 | TE 477 | Upper Tieplate C Up.2 | Not Measured | 273. | - | 0.125E+04 | K | 0.64%FS |
| 478 | Fluid T. | TG-23 | TE 478 | Upper Tieplate C Up.3 | Not Measured | 273. | - | 0.125E+04 | K | 0.64%FS |
| 479 | Fluid T. | TG-24 | TE 479 | Upper Tieplate C Up.4 | Not Measured | 273. | - | 0.125E+04 | K | 0.64%FS |
| 480 | Fluid T. | TG-25 | TE 480 | Upper Tieplate C Up.5 | Not Measured | 273. | - | 0.125E+04 | K | 0.64%FS |
| 481 | Fluid T. | TG-26 | TE 481 | Upper Tieplate C Up.6 | Not Measured | 273. | - | 0.125E+04 | K | 0.64%FS |
| 482 | Fluid T. | TG-27 | TE 482 | Upper Tieplate C Up.7 | Not Measured | 273. | - | 0.125E+04 | K | 0.64%FS |
| 483 | Fluid T. | TG-28 | TE 483 | Upper Tieplate C Up.8 | Not Measured | 273. | - | 0.125E+04 | K | 0.64%FS |
| 484 | Fluid T. | TG-29 | TE 484 | Upper Tieplate C Up.9 | Not Measured | 273. | - | 0.125E+04 | K | 0.64%FS |
| 485 | Fluid T. | TG-30 | TE 485 | Upper Tieplate C Up.10 | Not Measured | 273. | - | 0.125E+04 | K | 0.64%FS |
| 486 | Fluid T. | TG-31 | TE 486 | Upper Tieplate C Lo.1 | Not Measured | 273. | - | 0.125E+04 | K | 0.64%FS |
| 487 | Fluid T. | TG-32 | TE 487 | Upper Tieplate C Lo.2 | Not Measured | 273. | - | 0.125E+04 | K | 0.64%FS |
| 488 | Fluid T. | TG-33 | TE 488 | Upper Tieplate C Lo.3 | Not Measured | 273. | - | 0.125E+04 | K | 0.64%FS |
| 489 | Fluid T. | TG-34 | TE 489 | Upper Tieplate C Lo.4 | Not Measured | 273. | - | 0.125E+04 | K | 0.64%FS |
| 490 | Fluid T. | TG-35 | TE 490 | Upper Tieplate C Lo.5 | Not Measured | 273. | - | 0.125E+04 | K | 0.64%FS |
| 491 | Fluid T. | TG-36 | TE 491 | Upper Tieplate C Lo.6 | Not Measured | 273. | - | 0.125E+04 | K | 0.64%FS |
| 492 | Fluid T. | TG-37 | TE 492 | Upper Tieplate C Lo.7 | Not Measured | 273. | - | 0.125E+04 | K | 0.64%FS |
| 493 | Fluid T. | TG-38 | TE 493 | Upper Tieplate C Lo.8 | Not Measured | 273. | - | 0.125E+04 | K | 0.64%FS |
| 494 | Fluid T. | TG-39 | TE 494 | Upper Tieplate C Lo.9 | Not Measured | 273. | - | 0.125E+04 | K | 0.64%FS |
| 495 | Fluid T. | TG-40 | TE 495 | Upper Tieplate C Lo.10 | Not Measured | 273. | - | 0.125E+04 | K | 0.64%FS |
| 496 | Slab T. | TB- 1 | TE 496 | C.B. A1 Inner ,Pos.1 | FIG.5.162, 165 | 273. | - | 0.125E+04 | K | 0.64%FS |
| 497 | Slab T. | TB- 2 | TE 497 | C.B. A1 Inner ,Pos.2 | FIG.5.162, 166 | 273. | - | 0.125E+04 | K | 0.64%FS |
| 498 | Slab T. | TB- 3 | TE 498 | C.B. A1 Inner ,Pos.3 | FIG.5.162, 167 | 273. | - | 0.125E+04 | K | 0.64%FS |
| 499 | Slab T. | TB- 4 | TE 499 | C.B. A1 Inner ,Pos.4 | FIG.5.162, 168 | 273. | - | 0.125E+04 | K | 0.64%FS |
| 500 | Slab T. | TB- 5 | TE 500 | C.B. A1 Inner ,Pos.5 | FIG.5.162, 169 | 273. | - | 0.125E+04 | K | 0.64%FS |

Table 3.2 Measurement List for RUN 901 (Continued)

501Ch.- 550Ch.

| Ch. | Item | Symbol | ID. | | Location | Fig.No. | Range | | | Unit | Accuracy |
|---|---|---|---|---|---|---|---|---|---|---|---|
| 501 | Slab T. | TB- 6 | TE | 501 | C.B. A1 Inner ,Pos.6 | FIG.5.162, 170 | 273. | - | 0.125E+04 | K | 0.64%FS |
| 502 | Slab T. | TB- 7 | TE | 502 | C.B. A1 Inner ,Pos.7 | FIG.5.162, 171 | 273. | - | 0.125E+04 | K | 0.64%FS |
| 503 | Slab T. | TB- 8 | TE | 503 | C.B. A2 Inner ,Pos.1 | FIG.5.163, 165 | 273. | - | 0.125E+04 | K | 0.64%FS |
| 504 | Slab T. | TB- 9 | TE | 504 | C.B. A2 Inner ,Pos.2 | FIG.5.163, 166 | 273. | - | 0.125E+04 | K | 0.64%FS |
| 505 | Slab T. | TB-10 | TE | 505 | C.B. A2 Inner ,Pos.3 | FIG.5.163, 167 | 273. | - | 0.125E+04 | K | 0.64%FS |
| 506 | Slab T. | TB-11 | TE | 506 | C.B. A2 Inner ,Pos.4 | FIG.5.163, 168 | 273. | - | 0.125E+04 | K | 0.64%FS |
| 507 | Slab T. | TB-12 | TE | 507 | C.B. A2 Inner ,Pos.5 | FIG.5.163, 169 | 273. | - | 0.125E+04 | K | 0.64%FS |
| 508 | Slab T. | TB-13 | TE | 508 | C.B. A2 Inner ,Pos.6 | FIG.5.163, 170 | 273. | - | 0.125E+04 | K | 0.64%FS |
| 509 | Slab T. | TB-14 | TE | 509 | C.B. A2 Inner ,Pos.7 | FIG.5.163, 171 | 273. | - | 0.125E+04 | K | 0.64%FS |
| 510 | Slab T. | TB-15 | TE | 510 | C.B. B Inner ,Pos.1 | FIG.5.164 | 273. | - | 0.125E+04 | K | 0.64%FS |
| 511 | Slab T. | TB-16 | TE | 511 | C.B. B Inner ,Pos.2 | Not Measured | 273. | - | 0.125E+04 | K | 0.64%FS |
| 512 | Slab T. | TB-17 | TE | 512 | C.B. B Inner ,Pos.3 | Not Measured | 273. | - | 0.125E+04 | K | 0.64%FS |
| 513 | Slab T. | TB-18 | TE | 513 | C.B. B Inner ,Pos.4 | Not Measured | 273. | - | 0.125E+04 | K | 0.64%FS |
| 514 | Slab T. | TB-19 | TE | 514 | C.B. B Inner ,Pos.5 | Not Measured | 273. | - | 0.125E+04 | K | 0.64%FS |
| 515 | Slab T. | TB-20 | TE | 515 | C.B. B Inner ,Pos.6 | Not Measured | 273. | - | 0.125E+04 | K | 0.64%FS |
| 516 | Slab T. | TB-21 | TE | 516 | C.B. B Inner ,Pos.7 | Not Measured | 273. | - | 0.125E+04 | K | 0.64%FS |
| 517 | Slab T. | TB-22 | TE | 517 | C.B. C Inner ,Pos.1 | Not Measured | 273. | - | 0.125E+04 | K | 0.64%FS |
| 518 | Slab T. | TB-23 | TE | 518 | C.B. C Inner ,Pos.2 | Not Measured | 273. | - | 0.125E+04 | K | 0.64%FS |
| 519 | Slab T. | TB-24 | TE | 519 | C.B. C Inner ,Pos.3 | Not Measured | 273. | - | 0.125E+04 | K | 0.64%FS |
| 520 | Slab T. | TB-25 | TE | 520 | C.B. C Inner ,Pos.4 | Not Measured | 273. | - | 0.125E+04 | K | 0.64%FS |
| 521 | Slab T. | TB-26 | TE | 521 | C.B. C Inner ,Pos.5 | Not Measured | 273. | - | 0.125E+04 | K | 0.64%FS |
| 522 | Slab T. | TB-27 | TE | 522 | C.B. C Inner ,Pos.6 | Not Measured | 273. | - | 0.125E+04 | K | 0.64%FS |
| 523 | Slab T. | TB-28 | TE | 523 | C.B. C Inner ,Pos.7 | Not Measured | 273. | - | 0.125E+04 | K | 0.64%FS |
| 524 | Slab T. | TB-29 | TE | 524 | C.B. D Inner ,Pos.1 | Not Measured | 273. | - | 0.125E+04 | K | 0.64%FS |
| 525 | Slab T. | TB-30 | TE | 525 | C.B. D Inner ,Pos.2 | Not Measured | 273. | - | 0.125E+04 | K | 0.64%FS |
| 526 | Slab T. | TB-31 | TE | 526 | C.B. D Inner ,Pos.3 | Not Measured | 273. | - | 0.125E+04 | K | 0.64%FS |
| 527 | Slab T. | TB-32 | TE | 527 | C.B. D Inner ,Pos.4 | Not Measured | 273. | - | 0.125E+04 | K | 0.64%FS |
| 528 | Slab T. | TB-33 | TE | 528 | C.B. D Inner ,Pos.5 | Not Measured | 273. | - | 0.125E+04 | K | 0.64%FS |
| 529 | Slab T. | TB-34 | TE | 529 | C.B. D Inner ,Pos.6 | Not Measured | 273. | - | 0.125E+04 | K | 0.64%FS |
| 530 | Slab T. | TB-35 | TE | 530 | C.B. D Inner ,Pos.7 | Not Measured | 273. | - | 0.125E+04 | K | 0.64%FS |
| 531 | Fluid T. | TB-36 | TE | 531 | C.B. A Outer ,Pos.1 | Not Measured | 273. | - | 0.125E+04 | K | 0.64%FS |
| 532 | Fluid T. | TB-37 | TE | 532 | C.B. A Outer ,Pos.2 | Not Measured | 273. | - | 0.125E+04 | K | 0.64%FS |
| 533 | Fluid T. | TB-38 | TE | 533 | C.B. A Outer ,Pos.3 | Not Measured | 273. | - | 0.125E+04 | K | 0.64%FS |
| 534 | Fluid T. | TB-39 | TE | 534 | C.B. A Outer ,Pos.4 | Not Measured | 273. | - | 0.125E+04 | K | 0.64%FS |
| 535 | Fluid T. | TB-40 | TE | 535 | C.B. A Outer ,Pos.5 | Not Measured | 273. | - | 0.125E+04 | K | 0.64%FS |
| 536 | Fluid T. | TB-41 | TE | 536 | C.B. A Outer ,Pos.6 | Not Measured | 273. | - | 0.125E+04 | K | 0.64%FS |
| 537 | Fluid T. | TB-42 | TE | 537 | C.B. A Outer ,Pos.7 | Not Measured | 273. | - | 0.125E+04 | K | 0.64%FS |
| 538 | Fluid T. | TB-43 | TE | 538 | C.B. C Outer ,Pos.1 | Not Measured | 273. | - | 0.125E+04 | K | 0.64%FS |
| 539 | Fluid T. | TB-44 | TE | 539 | C.B. C Outer ,Pos.2 | Not Measured | 273. | - | 0.125E+04 | K | 0.64%FS |
| 540 | Fluid T. | TB-45 | TE | 540 | C.B. C Outer ,Pos.3 | Not Measured | 273. | - | 0.125E+04 | K | 0.64%FS |
| 541 | Fluid T. | TB-46 | TE | 541 | C.B. C Outer ,Pos.4 | Not Measured | 273. | - | 0.125E+04 | K | 0.64%FS |
| 542 | Fluid T. | TB-47 | TE | 542 | C.B. C Outer ,Pos.5 | Not Measured | 273. | - | 0.125E+04 | K | 0.64%FS |
| 543 | Fluid T. | TB-48 | TE | 543 | C.B. C Outer ,Pos.6 | Not Measured | 273. | - | 0.125E+04 | K | 0.64%FS |
| 544 | Fluid T. | TB-49 | TE | 544 | C.B. C Outer ,Pos.7 | Not Measured | 273. | - | 0.125E+04 | K | 0.64%FS |
| 545 | Fluid T. | TP- 1 | TE | 545 | Lower Pl. Center 1 | Not Measured | 273. | - | 0.125E+04 | K | 0.64%FS |
| 546 | Fluid T. | TP- 2 | TE | 546 | Lower Pl. Center 2 | Not Measured | 273. | - | 0.125E+04 | K | 0.64%FS |
| 547 | Fluid T. | TP- 3 | TE | 547 | Lower Pl. Center 3 | Not Measured | 273. | - | 0.125E+04 | K | 0.64%FS |
| 548 | Fluid T. | TP- 4 | TE | 548 | Lower Pl. Center 4 | Not Measured | 273. | - | 0.125E+04 | K | 0.64%FS |
| 549 | Fluid T. | TP- 5 | TE | 549 | Lower Pl. Center 5 | Not Measured | 273. | - | 0.125E+04 | K | 0.64%FS |
| 550 | Fluid T. | TP- 6 | TE | 550 | Lower Pl. Center 7 | Not Measured | 273. | - | 0.125E+04 | K | 0.64%FS |

Table 3.2 Measurement List for RUN 901 (Continued)

551Ch.- 600Ch.

| Ch. | Item | Symbol | ID. | | Location | Fig.No. | Range | | | Unit | Accuracy |
|---|---|---|---|---|---|---|---|---|---|---|---|
| 551 | Slab T. | TP- 7 | TE | 551 | Lower Pl. North 1 | Not Measured | 273. | - | 0.125E+04 | K | 0.64%FS |
| 552 | Slab T. | TP- 8 | TE | 552 | Lower Pl. North 2 | Not Measured | 273. | - | 673. | K | 0.64%FS |
| 553 | Slab T. | TP- 9 | TE | 553 | Lower Pl. North 4 | Not Measured | 273. | - | 673. | K | 0.64%FS |
| 554 | Slab T. | TP-10 | TE | 554 | Lower Pl. North 6 | Not Measured | 273. | - | 673. | K | 0.64%FS |
| 555 | Slab T. | TP-11 | TE | 555 | Lower Pl. South 1 | Not Measured | 273. | - | 673. | K | 0.64%FS |
| 556 | Slab T. | TP-12 | TE | 556 | Lower Pl. South 2 | Not Measured | 273. | - | 673. | K | 0.64%FS |
| 557 | Slab T. | TP-13 | TE | 557 | Lower Pl. South 4 | Not Measured | 273. | - | 673. | K | 0.64%FS |
| 558 | Slab T. | TP-14 | TE | 558 | Lower Pl. South 6 | Not Measured | 273. | - | 673. | K | 0.64%FS |
| 559 | Level | LB- 1 | LM | 559 | C.B.Liquid Level A1-1 | FIG.5.172 | | | | | |
| 560 | Level | LB- 2 | LM | 560 | C.B.Liquid Level A1-2 | FIG.5.172 | | | | | |
| 561 | Level | LB- 3 | LM | 561 | C.B.Liquid Level A1-3 | FIG.5.172 | | | | | |
| 562 | Level | LB- 4 | LM | 562 | C.B.Liquid Level A1-4 | Failure | | | | | |
| 563 | Level | LB- 5 | LM | 563 | C.B.Liquid Level A1-5 | FIG.5.172 | | | | | |
| 564 | Level | LB- 6 | LM | 564 | C.B.Liquid Level A1-6 | FIG.5.172 | | | | | |
| 565 | Level | LB- 7 | LM | 565 | C.B.Liquid Level A1-7 | FIG.5.172 | | | | | |
| 566 | Level | LB- 8 | LM | 566 | C.B.Liquid Level A2-1 | FIG.5.173 | | | | | |
| 567 | Level | LB- 9 | LM | 567 | C.B.Liquid Level A2-2 | FIG.5.173 | | | | | |
| 568 | Level | LB-10 | LM | 568 | C.B.Liquid Level A2-3 | FIG.5.173 | | | | | |
| 569 | Level | LB-11 | LM | 569 | C.B.Liquid Level A2-4 | FIG.5.173 | | | | | |
| 570 | Level | LB-12 | LM | 570 | C.B.Liquid Level A2-5 | Failure | | | | | |
| 571 | Level | LB-13 | LM | 571 | C.B.Liquid Level A2-6 | FIG.5.173 | | | | | |
| 572 | Level | LB-14 | LM | 572 | C.B.Liquid Level A2-7 | FIG.5.173 | | | | | |
| 573 | Level | LB-15 | LM | 573 | C.B.Liquid Level B-1 | FIG.5.174 | | | | | |
| 574 | Level | LB-16 | LM | 574 | C.B.Liquid Level B-2 | FIG.5.174 | | | | | |
| 575 | Level | LB-17 | LM | 575 | C.B.Liquid Level B-3 | FIG.5.174 | | | | | |
| 576 | Level | LB-18 | LM | 576 | C.B.Liquid Level B-4 | FIG.5.174 | | | | | |
| 577 | Level | LB-19 | LM | 577 | C.B.Liquid Level B-5 | FIG.5.174 | | | | | |
| 578 | Level | LB-20 | LM | 578 | C.B.Liquid Level B-6 | FIG.5.174 | | | | | |
| 579 | Level | LB-21 | LM | 579 | C.B.Liquid Level B-7 | FIG.5.174 | | | | | |
| 580 | Level | LB-22 | LM | 580 | C.B.Liquid Level C-1 | FIG.5.175 | | | | | |
| 581 | Level | LB-23 | LM | 581 | C.B.Liquid Level C-2 | FIG.5.175 | | | | | |
| 582 | Level | LB-24 | LM | 582 | C.B.Liquid Level C-3 | FIG.5.175 | | | | | |
| 583 | Level | LB-25 | LM | 583 | C.B.Liquid Level C-4 | FIG.5.175 | | | | | |
| 584 | Level | LB-26 | LM | 584 | C.B.Liquid Level C-5 | FIG.5.175 | | | | | |
| 585 | Level | LB-27 | LM | 585 | C.B.Liquid Level C-6 | FIG.5.175 | | | | | |
| 586 | Level | LB-28 | LM | 586 | C.B.Liquid Level C-7 | FIG.5.175 | | | | | |
| 587 | Level | LB-29 | LM | 587 | C.B.Liquid Level D-1 | FIG.5.176 | | | | | |
| 588 | Level | LB-30 | LM | 588 | C.B.Liquid Level D-2 | FIG.5.176 | | | | | |
| 589 | Level | LB-31 | LM | 589 | C.B.Liquid Level D-3 | FIG.5.176 | | | | | |
| 590 | Level | LB-32 | LM | 590 | C.B.Liquid Level D-4 | FIG.5.176 | | | | | |
| 591 | Level | LB-33 | LM | 591 | C.B.Liquid Level D-5 | Failure | | | | | |
| 592 | Level | LB-34 | LM | 592 | C.B.Liquid Level D-6 | FIG.5.176 | | | | | |
| 593 | Level | LB-35 | LM | 593 | C.B.Liquid Level D-7 | FIG.5.176 | | | | | |
| 594 | Level | LL- 1 | LM | 594 | Ch.Box Outlet A1-5 | Failure | | | | | |
| 595 | Level | LL- 2 | LM | 595 | Ch.Box Outlet A1-6 | Failure | | | | | |
| 596 | Level | LL- 3 | LM | 596 | Ch.Box Outlet A1-7 | FIG.5.177 | | | | | |
| 597 | Level | LL- 4 | LM | 597 | Ch.Box Outlet A2-5 | Failure | | | | | |
| 598 | Level | LL- 5 | LM | 598 | Ch.Box Outlet A2-6 | FIG.5.178 | | | | | |
| 599 | Level | LL- 6 | LM | 599 | Ch.Box Outlet A2-7 | FIG.5.178 | | | | | |
| 600 | Level | LL- 7 | LM | 600 | Ch.Box Outlet A-1 | Failure | | | | | |

Table 3.2 Measurement List for RUN 901 (Continued)

601Ch.- 650Ch.

| Ch. | Item | Symbol | ID. | | Location | Fig.No. | Range | Unit | Accuracy |
|---|---|---|---|---|---|---|---|---|---|
| 601 | Level | LL- 8 | LM | 601 | Ch.Box Outlet A-2 | FIG.5.179 | | | |
| 602 | Level | LL- 9 | LM | 602 | Ch.Box Outlet A-3 | FIG.5.179 | | | |
| 603 | Level | LL-10 | LM | 603 | Ch.Box Outlet A-4 | FIG.5.179 | | | |
| 604 | Level | LL-11 | LM | 604 | Ch.Box Outlet A-6 | Not Measured | | | |
| 605 | Level | LL-12 | LM | 605 | Ch.Box Outlet C1-5 | Not Measured | | | |
| 606 | Level | LL-13 | LM | 606 | Ch.Box Outlet C1-6 | Not Measured | | | |
| 607 | Level | LL-14 | LM | 607 | Ch.Box Outlet C1-7 | Not Measured | | | |
| 608 | Level | LL-15 | LM | 608 | Ch.Box Outlet C2-5 | Not Measured | | | |
| 609 | Level | LL-16 | LM | 609 | Ch.Box Outlet C2-6 | Not Measured | | | |
| 610 | Level | LL-17 | LM | 610 | Ch.Box Outlet C2-7 | Not Measured | | | |
| 611 | Level | LL-18 | LM | 611 | Ch.Box Outlet C-1 | Not Measured | | | |
| 612 | Level | LL-19 | LM | 612 | Ch.Box Outlet C-2 | Not Measured | | | |
| 613 | Level | LL-20 | LM | 613 | Ch.Box Outlet C-3 | Not Measured | | | |
| 614 | Level | LL-21 | LM | 614 | Ch.Box Outlet C-4 | Not Measured | | | |
| 615 | Level | LL-22 | LM | 615 | Ch.Box Outlet C-6 | Not Measured | | | |
| 616 | Level | LL-23 | LM | 616 | Ch.Box Inlet A-1 | FIG.5.180 | | | |
| 617 | Level | LL-24 | LM | 617 | Ch.Box Inlet A-2 | FIG.5.180 | | | |
| 618 | Level | LL-25 | LM | 618 | Ch.Box Inlet B-1 | FIG.5.181 | | | |
| 619 | Level | LL-26 | LM | 619 | Ch.Box Inlet B-2 | FIG.5.181 | | | |
| 620 | Level | LL-27 | LM | 620 | Ch.Box Inlet C-1 | FIG.5.182 | | | |
| 621 | Level | LL-28 | LM | 621 | Ch.Box Inlet C-2 | FIG.5.182 | | | |
| 622 | Level | LL-29 | LM | 622 | Ch.Box Inlet D-1 | FIG.5.183 | | | |
| 623 | Level | LL-30 | LM | 623 | Ch.Box Inlet D-2 | FIG.5.183 | | | |
| 624 | Level | LL-31 | LM | 624 | Lower Pl. North 1 | FIG.5.184 | | | |
| 625 | Level | LL-32 | LM | 625 | Lower Pl. North 2 | FIG.5.184 | | | |
| 626 | Level | LL-33 | LM | 626 | Lower Pl. North 3 | Not Measured | | | |
| 627 | Level | LL-34 | LM | 627 | Lower Pl. North 4 | Not Measured | | | |
| 628 | Level | LL-35 | LM | 628 | Lower Pl. North 5 | Not Measured | | | |
| 629 | Level | LL-36 | LM | 629 | Lower Pl. North 6 | Not Measured | | | |
| 630 | Level | LL-37 | LM | 630 | Lower Pl. South 1 | Not Measured | | | |
| 631 | Level | LL-38 | LM | 631 | Lower Pl. South 2 | Not Measured | | | |
| 632 | Level | LL-39 | LM | 632 | Lower Pl. South 3 | Not Measured | | | |
| 633 | Level | LL-40 | LM | 633 | Lower Pl. South 4 | Not Measured | | | |
| 634 | Level | LL-41 | LM | 634 | Lower Pl. South 5 | Not Measured | | | |
| 635 | Level | LL-42 | LM | 635 | Lower Pl. South 6 | Not Measured | | | |
| 636 | Level | LL-43 | LM | 636 | Guide Tube North 0 | Not Measured | | | |
| 637 | Level | LL-44 | LM | 637 | Guide Tube North 1 | Not Measured | | | |
| 638 | Level | LL-45 | LM | 638 | Guide Tube North 3 | Not Measured | | | |
| 639 | Level | LL-46 | LM | 639 | Guide Tube North 6 | Not Measured | | | |
| 640 | Level | LL-47 | LM | 640 | Guide Tube South 0 | Not Measured | | | |
| 641 | Level | LL-48 | LM | 641 | Guide Tube South 1 | Not Measured | | | |
| 642 | Level | LL-49 | LM | 642 | Guide Tube South 3 | Not Measured | | | |
| 643 | Level | LL-50 | LM | 643 | Guide Tube South 6 | Not Measured | | | |
| 644 | Level | L- 1 | LM | 644 | Downcomer D-Side 1 | Fig.5.185 | | | |
| 645 | Level | L- 2 | LM | 645 | Downcomer D-Side 2 | Fig.5.185 | | | |
| 646 | Level | L- 3 | LM | 646 | Downcomer D-Side 3 | Fig.5.185 | | | |
| 647 | Level | L- 4 | LM | 647 | Downcomer D-Side 4 | Fig.5.185 | | | |
| 648 | Level | L- 5 | LM | 648 | Downcomer D-Side 5 | Fig.5.185 | | | |
| 649 | Level | L- 6 | LM | 649 | Downcomer B-Side 1 | Fig.5.186 | | | |
| 650 | Level | L- 7 | LM | 650 | Downcomer B-Side 2 | Fig.5.186 | | | |

Table 3.2 Measurement List for RUN 901 (Continued)

651Ch.- 700Ch.

| Ch. | Item | Symbol | ID. | | Location | Fig.No. | Range | | | Unit | Accuracy |
|---|---|---|---|---|---|---|---|---|---|---|---|
| 651 | Level | L- 8 | LM | 651 | Downcomer B-Side 3 | Fig.5.186 | | | | | |
| 652 | Level | L- 9 | LM | 652 | Downcomer B-Side 4 | Fig.5.186 | | | | | |
| 653 | Level | L-10 | LM | 653 | Downcomer B-Side 5 | Fig.5.186 | | | | | |
| 654 | Void | VF- 1 | VD | 654 | A54 Tie Rod Pos.1 | Not Measured | 0.0 | - | 1.00 | | |
| 655 | Void | VF- 2 | VD | 655 | A54 Tie Rod Pos.2 | Not Measured | 0.0 | - | 1.00 | | |
| 656 | Void | VF- 3 | VD | 656 | A54 Tie Rod Pos.3 | Not Measured | 0.0 | - | 1.00 | | |
| 657 | Void | VF- 4 | VD | 657 | A54 Tie Rod Pos.4 | Not Measured | 0.0 | - | 1.00 | | |
| 658 | Void | VF- 5 | VD | 658 | A54 Tie Rod Pos.5 | Not Measured | 0.0 | - | 1.00 | | |
| 659 | Void | VF- 6 | VD | 659 | A54 Tie Rod Pos.6 | Not Measured | 0.0 | - | 1.00 | | |
| 660 | Void | VF- 7 | VD | 660 | A54 Tie Rod Pos.7 | Not Measured | 0.0 | - | 1.00 | | |
| 661 | Void | VF- 8 | VD | 661 | B54 Tie Rod Pos.1 | Not Measured | 0.0 | - | 1.00 | | |
| 662 | Void | VF- 9 | VD | 662 | B54 Tie Rod Pos.2 | Not Measured | 0.0 | - | 1.00 | | |
| 663 | Void | VF-10 | VD | 663 | B54 Tie Rod Pos.3 | Not Measured | 0.0 | - | 1.00 | | |
| 664 | Void | VF-11 | VD | 664 | B54 Tie Rod Pos.4 | Not Measured | 0.0 | - | 1.00 | | |
| 665 | Void | VF-12 | VD | 665 | B54 Tie Rod Pos.5 | Not Measured | 0.0 | - | 1.00 | | |
| 666 | Void | VF-13 | VD | 666 | B54 Tie Rod Pos.6 | Not Measured | 0.0 | - | 1.00 | | |
| 667 | Void | VF-14 | VD | 667 | B54 Tie Rod Pos.7 | Not Measured | 0.0 | - | 1.00 | | |
| 668 | Void | VF-15 | VD | 668 | C54 Tie Rod Pos.1 | Not Measured | 0.0 | - | 1.00 | | |
| 669 | Void | VF-16 | VD | 669 | C54 Tie Rod Pos.2 | Not Measured | 0.0 | - | 1.00 | | |
| 670 | Void | VF-17 | VD | 670 | C54 Tie Rod Pos.3 | Not Measured | 0.0 | - | 1.00 | | |
| 671 | Void | VF-18 | VD | 671 | C54 Tie Rod Pos.4 | Not Measured | 0.0 | - | 1.00 | | |
| 672 | Void | VF-19 | VD | 672 | C54 Tie Rod Pos.5 | Not Measured | 0.0 | - | 1.00 | | |
| 673 | Void | VF-20 | VD | 673 | C54 Tie Rod Pos.6 | Not Measured | 0.0 | - | 1.00 | | |
| 674 | Void | VF-21 | VD | 674 | C54 Tie Rod Pos.7 | Not Measured | 0.0 | - | 1.00 | | |
| 675 | Void | VF-22 | VD | 675 | D54 Tie Rod Pos.7 | Not Measured | 0.0 | - | 1.00 | | |
| 676 | Void | VF-23 | VD | 676 | D54 Tie Rod Pos.7 | Not Measured | 0.0 | - | 1.00 | | |
| 677 | Void | VF-24 | VD | 677 | D54 Tie Rod Pos.7 | Not Measured | 0.0 | - | 1.00 | | |
| 678 | Void | VF-25 | VD | 678 | D54 Tie Rod Pos.7 | Not Measured | 0.0 | - | 1.00 | | |
| 679 | Void | VF-26 | VD | 679 | D54 Tie Rod Pos.7 | Not Measured | 0.0 | - | 1.00 | | |
| 680 | Void | VF-27 | VD | 680 | D54 Tie Rod Pos.7 | Not Measured | 0.0 | - | 1.00 | | |
| 681 | Void | VF-28 | VD | 681 | D54 Tie Rod Pos.7 | Not Measured | 0.0 | - | 1.00 | | |
| 682 | Void | VE- 1 | VD | 682 | Channel A Outlet 1 | Not Measured | 0.0 | - | 1.00 | | |
| 683 | Void | VE- 2 | VD | 683 | Channel A Outlet 2 | Not Measured | 0.0 | - | 1.00 | | |
| 684 | Void | VE- 3 | VD | 684 | Channel A Outlet 3 | Not Measured | 0.0 | - | 1.00 | | |
| 685 | Void | VE- 4 | VD | 685 | Channel B Outlet 1 | Not Measured | 0.0 | - | 1.00 | | |
| 686 | Void | VE- 5 | VD | 686 | Channel B Outlet 2 | Not Measured | 0.0 | - | 1.00 | | |
| 687 | Void | VE- 6 | VD | 687 | Channel B Outlet 3 | Not Measured | 0.0 | - | 1.00 | | |
| 688 | Void | VE- 7 | VD | 688 | Channel C Outlet 1 | Not Measured | 0.0 | - | 1.00 | | |
| 689 | Void | VE- 8 | VD | 689 | Channel C Outlet 2 | Not Measured | 0.0 | - | 1.00 | | |
| 690 | Void | VE- 9 | VD | 690 | Channel C Outlet 3 | Not Measured | 0.0 | - | 1.00 | | |
| 691 | Void | VE-10 | VD | 691 | Channel D Outlet 1 | Not Measured | 0.0 | - | 1.00 | | |
| 692 | Void | VE-11 | VD | 692 | Channel D Outlet 2 | Not Measured | 0.0 | - | 1.00 | | |
| 693 | Void | VE-12 | VD | 693 | Channel D Outlet 3 | Not Measured | 0.0 | - | 1.00 | | |
| 694 | Void | VE-13 | VD | 694 | Lower Plenum Bottom 1 | Not Measured | 0.0 | - | 1.00 | | |
| 695 | Void | VE-14 | VD | 695 | Lower Plenum Bottom 2 | Not Measured | 0.0 | - | 1.00 | | |
| 696 | Void | VE-15 | VD | 696 | Lower Plenum Bottom 3 | Not Measured | 0.0 | - | 1.00 | | |
| 697 | Void | VP- 1 | VD | 697 | Lower Plenum Inlet | Not Measured | 0.0 | - | 1.00 | | |
| 698 | Void | VP- 2 | VD | 698 | Lower Plenum Inlet | Not Measured | 0.0 | - | 1.00 | | |

Table 3.3 Core Instrumentation Map

| Item | Pos. / DL / Rod NO. | Core Outlet | Pos.1 | Pos.2 | Pos.3 | Pos.4 | Pos.5 | Pos.6 | Pos.7 | Core Inlet |
|---|---|---|---|---|---|---|---|---|---|---|
| | | 3660 | 3417 | 3114.5 | 2879.5 | 2527 | 2174.5 | 1939.5 | 1637 | 1454 |
| Surface Temp. | A11 | | TF 1 | TF 2 | TF 3 | TF 4 | TF 5 | TF 6 | TF 7 | |
| | A12 | | TF 8 | TF 9 | TF 10 | TF 11 | TF 12 | TF 13 | TF 14 | |
| | A13 | | TF 15 | TF 16 | TF 17 | TF 18 | TF 19 | TF 20 | TF 21 | |
| | A14 | | TF 22 | TF 23 | TF 24 | TF 25 | TF 26 | TF 27 | TF 28 | |
| | A15 | | TF 29 | | | TF 30 | | | | |
| | A17 | | TF 31 | | | TF 32 | | | | |
| | A22 | | TF 33 | TF 34 | TF 35 | TF 36 | TF 37 | TF 38 | TF 39 | |
| | A23 | | TF 40 | TF 41 | TF 42 | TF 43 | TF 44 | TF 45 | TF 46 | |
| | A24 | | TF 47 | TF 48 | TF 49 | TF 50 | TF.51 | TF 52 | TF 53 | |
| | A26 | | TF 54 | | | TF 55 | | | | |
| | A28 | | TF 56 | | | TF 57 | | | | |
| | A31 | | TF 58 | | | TF 59 | | | | |
| | A33 | | TF 60 | TF 61 | TF 62 | TF 63 | TF 64 | TF 65 | TF 66 | |
| | A34 | | TF 67 | TF 68 | TF 69 | TF 70 | TF 71 | TF 72 | TF 73 | |
| | A35 | | TF 74 | | | TF 75 | | | | |
| | A37 | | TF 76 | | | TF 77 | | | | |
| | A42 | | TF 78 | | | TF 79 | | | | |
| Fluid Temp. | A44 | TC 1 | TF180 | TF181 | TF182 | TF183 | TF184 | TF185 | TF186 | TC 2 |
| Surface Temp. | A45 | | TF 80 | | | TF 81 | | | | |
| | A46 | | TF 82 | | | TF 83 | | | | |
| | A48 | | TF 84 | | | TF 85 | | | | |
| | A51 | | TF 86 | | | TF 87 | | | | |
| | A53 | | TF 88 | | | TF 89 | | | | |
| | A54 | | TF 90 | | | | | | | |
| | A57 | | TF 91 | | | TF 92 | | | | |
| | A62 | | TF 93 | | | TF 94 | | | | |
| | A64 | | TF 95 | | | TF 96 | | | | |
| | A66 | | TF 97 | | | TF 98 | | | | |
| | A68 | | TF 99 | | | TF100 | | | | |
| | A71 | | TF101 | | | TF102 | | | | |
| | A73 | | TF103 | | | TF104 | | | | |
| | A75 | | TF105 | | | TF106 | | | | |
| | A77 | | TF107 | | | TF108 | | | | |

Table 3.3 Core Instrumentation Map (Continued)

| Item | Pos. / DL / Rod NO. | Core Outlet | Pos.1 | Pos.2 | Pos.3 | Pos.4 | Pos.5 | Pos.6 | Pos.7 | Core Inlet |
|---|---|---|---|---|---|---|---|---|---|---|
| | | 3660 | 3417 | 3114.5 | 2879.5 | 2527 | 2174.5 | 1939.5 | 1637 | 1454 |
| Surface Temp. | A82 | | TF109 | | | TF110 | | | | |
| | A84 | | TF111 | | | TF112 | | | | |
| | A86 | | TF113 | | | TF114 | | | | |
| | A88 | | TF115 | | | TF116 | | | | |
| | B11 | | | | | TF117 | | | | |
| | B13 | | | | | TF118 | | | | |
| | B15 | | TF119 | TF120 | TF121 | TF122 | TF123 | TF124 | TF125 | |
| | B31 | | | | | TF126 | | | | |
| | B33 | | | | | TF127 | | | | |
| | B35 | | | | | TF128 | | | | |
| Fluid Temp. | B44 | TC 3 | TF187 | TF188 | TF189 | TF190 | TF191 | TF192 | TF193 | TC 4 |
| Surface Temp. | B51 | | | | | TF129 | | | | |
| | B53 | | | | | TF130 | | | | |
| | B85 | | TF131 | TF132 | TF133 | TF134 | TF135 | TF136 | TF137 | |
| | C11 | | | | | TF138 | | | | |
| | C13 | | | | | TF139 | | | | |
| | C15 | | | | | TF140 | | | | |
| | C31 | | | | | TF141 | | | | |
| | C33 | | TF142 | TF143 | TF144 | TF145 | TF146 | TF147 | TF148 | |
| | C35 | | | | | TF149 | | | | |
| Fluid Temp. | C44 | TC 5 | TF194 | TF195 | TF196 | TF197 | TF198 | TF199 | TF200 | TC 6 |
| Surface Temp. | C51 | | | | | TF150 | | | | |
| | C53 | | | | | TF151 | | | | |
| | C77 | | TF152 | TF153 | TF154 | TF155 | TF156 | TF157 | TF158 | |
| | D11 | | | | | TF159 | | | | |
| | D13 | | | | | TF160 | | | | |
| | D27 | | TF161 | TF162 | TF163 | TF164 | TF165 | TF166 | TF167 | |
| | D31 | | | | | TF168 | | | | |
| | D33 | | | | | TF169 | | | | |
| | D35 | | | | | TF170 | | | | |
| Fluid Temp. | D44 | TC 7 | TF201 | TF202 | TF203 | TF204 | TF205 | TF206 | TF207 | TC 8 |
| Surface Temp. | D51 | | | | | TF171 | | | | |
| | D53 | | | | | TF172 | | | | |
| | D88 | | TF173 | TF174 | TF175 | TF176 | TF177 | TF178 | TF179 | |

Table 3.3 Core Instrumentation Map (Continued)

| Item | Pos. / DL / Rod NO. | Core Outlet | Pos.1 | Pos.2 | Pos.3 | Pos.4 | Pos.5 | Pos.6 | Pos.7 | Core Inlet |
|---|---|---|---|---|---|---|---|---|---|---|
| | | 3660 | 3417 | 3114.5 | 2879.5 | 2527 | 2174.5 | 1939.5 | 1673 | 1454 |
| Void | A55 | | VF 1 | VF 2 | VF 3 | VF 4 | VF 5 | VF 6 | VF 7 | |
| | B55 | | VF 8 | VF 9 | VF 10 | VF 11 | VF 12 | VF 13 | VF 14 | |
| | C55 | | VF 15 | VF 16 | VF 17 | VF 18 | VF 19 | VF 20 | VF 21 | |
| | D55 | | VF 22 | VF 23 | VF 24 | VF 25 | VF 26 | VF 27 | VF 28 | |
| Channel Box Surface Temp. | A1* | | TB 1 | TB 2 | TB 3 | TB 4 | TB 5 | TB 6 | TB 7 | |
| | A2* | | TB 8 | TB 9 | TB 10 | TB 11 | TB 12 | TB 13 | TB 14 | |
| | B* | | TB 15 | TB 16 | TB 17 | TB 18 | TB 19 | TB 20 | TB 21 | |
| | C* | | TB 22 | TB 23 | TB 24 | TB 25 | TB 26 | TB 27 | TB 28 | |
| | D* | | TB 29 | TB 30 | TB 31 | TB 32 | TB 33 | TB 34 | TB 35 | |
| Liquid Level in the Channel Box | A1* | | LB 1 | LB 2 | LB 3 | LB 4 | LB 5 | LB 6 | LB 7 | |
| | A2* | | LB 8 | LB 9 | LB 10 | LB 11 | LB 12 | LB 13 | LB 14 | |
| | B* | | LB 15 | LB 16 | LB 17 | LB 18 | LB 19 | LB 20 | LB 21 | |
| | C* | | LB 22 | LB 23 | LB 24 | LB 25 | LB 26 | LB 27 | LB 28 | |
| | D* | | LB 29 | LB 30 | LB 31 | LB 32 | LB 33 | LB 34 | LB 35 | |

Table 4.1 Test Conditions of RUN 901

| Parameter | | Specified Value | Measured Value |
|---|---|---|---|
| Break Conditions | | | |
| Location | | Recirculation pump suction | Recirculation pump suction |
| Type | | Double-ended | Double-ended |
| Break Nozzle Diameter | (mm) | 26.2/26.2 | 26.2/26.2 |
| Initial System Conditions | | | |
| Steam Dome Pressure | (MPa) | 7.35 | 7.29 |
| Lower Plenum Temperature | ( K ) | ---- | 552.0 |
| Lower Plenum Subcooling | ( K ) | ---- | 10.5 |
| Core Inlet Flow Rate | (kg/s) | 16.0 | 16.0 |
| Broken Loop Flow Rate | ($m^3$/s) | ---- | ---- |
| Intact Loop Flow Rate | ($m^3$/s) | ---- | ---- |
| Core Outlet Quality | ( % ) | ---- | 13.9 |
| Power Level | (kW) | (1400+3000) | (1250+2795) |
| Maximum Linear Heat Rate | (kW/m) | | |
| of Channel A | | 18.5 | 16.5 |
| of Channel B, C and D | | 13.2 | 12.3 |
| Power Curve | | Fig. 2.10 | Fig. 2.34 |
| Water Level in PV | ( m ) | 5.00 | 5.00 |
| Fuel Assembly | | No.4 | No.4 |
| Feedwater Conditions | | | |
| Temperature | ( K ) | 489 | 489 |
| Flow Rate | (kg/s) | Steady state value 2.388 | Fig. 2.21 |
| Initiation of line closure | (s) | 2.0 | 2.0 (completely close at 3.7 s) |

Table 4.1 Test Conditions of RUN 901 (Continued)

| Parameter | | Specified Value | Measured Value |
|---|---|---|---|
| Steam Discharge Conditions | | | |
| Steady State Line | | | |
| Flow Rate | (kg/s) | Steady State Value (2.388) | 2.00 |
| Transient Line | | | |
| Flow Rate | (kg/s) | ---- | Fig. 2.20 |
| Orifice Diameter | ( mm ) | 16.8 | 16.8 |
| Initiation of line closure | | | |
| at Water Level | ( m ) | 4.76* | 4.3 (7.5 s after break and completely closed at 9.4 s) |
| with Time Lag | ( s ) | 3 | |
| ECCS Conditions | | | |
| HPCS | | | |
| Injection Location | | Upper Plenum | Upper Plenum |
| Initiation | | | |
| at Water Level | ( m ) | 4.76 | |
| with Time Lag | ( s ) | 27 | 28.3 (31.5s after break at 5.21 MPa in PV) |
| Coolant Temperature | ( K ) | 313 | 313 |
| Injection Flow Rate | ($m^3/s$) | $6.17 \times 10^{-4}$ at 6.5 MPa | Fig. 2.22 |
| Injection Duration | ( s ) | 1500 | Fig. 2.22 |
| LPCS | | | |
| Injection Location | | Upper Plenum | Upper Plenum |
| Initiated | | | |
| at Water Level | ( m ) | 4.25 ** | |
| with Time Lag | ( s ) | 40 | |
| and at Pressure in PV | (MPa) | 2.16 | 2.23 (65.6 s after break) |
| Coolant Temperature | ( K ) | 313 | 313 |
| Injection Flow Rate | ($m^3/s$) | $1.13 \times 10^{-3}$ | Fig. 2.22 |
| Injection Duration | ( s ) | 1500 | Fig. 2.22 |

* L2 level
** L1 level

Table 4.1 Test Conditions of RUN 901 (Continued)

| Parameter | | Specified Value | Measured Value |
|---|---|---|---|
| ECCS Conditions (Continued) | | | |
| LPCI | | | |
| Injection Location | | Upper Plenum and Core Bypass | Upper Plenum and Core Bypass |
| Initiated | | | |
| at Water Level | ( m ) | 4.25 | |
| with Time Lag | ( s ) | 4 | |
| and at Pressure in PV | (MPa) | 1.57 | 1.61 (90.9s after break) |
| Coolant Temperature | ( K ) | 313 | 313 |
| Injection Flow Rate | ($m^3/s$) | $3.5 \times 10^{-3}$ | Fig. 2.23 |
| Injection Duration | ( s ) | 1500 | Fig. 2.23 |
| ADS Conditions | | | |
| Initiation | | | |
| at Water Level | ( m ) | 4.25 | |
| with Time Lag | ( s ) | 120 | 120.3 (127.7 s after break, 0.79 MPa in PV) |
| Valve Closing Time | ( s ) | No closure | No closure |
| Flow Rate | ($m^3/s$) | ---- | Fig. 2.20 |
| Orifice Diameter | ( mm ) | 15.5 | 15.5 |

Table 4.2 Characteristics of Steam Discharge Line Valves

| Valve | Close to Open (sec) | Open to Close (sec) |
|---|---|---|
| AV165 | 0.1 | 1.5 |
| AV168 | - | 0.1 |
| AV169 | 0.3 | 2.0 |

| Orifice | Diameter (mm) | Area ($mm^2$) |
|---|---|---|
| OR3 | Not Used | - |
| OR4 | 15.5 | 188.7 |
| OR5 | 16.8 | 221.7 |

Table 4.3 Control Sequence for Steam Discharge Line Valves in RUN 901

| Time | t < 0 | Break (t=0) | L2 + 3s | L1 + 120s |
|---|---|---|---|---|
| AV* 168 | Open | Close | Close | Close |
| CV 130 | Control to maintain steady state pressure | | | |
| AV 165 | Close | Open | Close | Close |
| AV 169 | Close | Close | Close | Open |

* AV ; Air Actuation Valve (Auto)
CV ; Control Valve (Manual)

Table 5.1 Sequence of Events in RUN 901

| Time after break (s) | Events |
|---|---|
| 0.0 | Break |
| | Initiate core power control |
| | Terminate intact loop recirculation pump power (simple coastdown) |
| | Terminate broken loop recirculation pump power (simple coastdown) |
| 1.2 | Initiation of feedwater line valve closure |
| 3.2 | Liquid level in downcomer decreased to L2 level |
| 4.0 | Closure of feedwater line |
| 7.0 | Initiation of core power curve reduction |
| 7.4 | Initiation of steam discharge line valve closure |
| | Liquid level in downcomer decreased to L1 level |
| 9.2 | Closure of steam discharge line |
| 9.5 | Liquid level in downcomer decreased to jet pump suction nozzle |
| 12.0 | Liquid level in downcomer decreased to recirculation pump suction line |
| 17.0 | Initiation of lower plenum flashing |
| 31.5 | HPCS initiation (at system pressure 5.21 MPa) |
| 64.8 | Feedwater line flashing |
| 65.6 | LPCS initiation (at system pressure 2.23 MPa) |
| 90.9 | LPCI initiation (at system pressure 1.61 MPa) |
| 127.3 | Quench of the whole core |
| 128.2 | ADS initiation (at system pressure 0.79 MPa) |
| 490 | End of data acquisition |

Table 5.2 Maximum Cladding Temperature Distribution in the Core

| | Pos.1 | Pos.2 | Pos.3 | Pos.4 | Pos.5 | Pos.6 | Pos.7 |
|---|---|---|---|---|---|---|---|
| A-11 rod | TE 201 | TE 202 | TE 203 | TE 204 | TE 205 | TE 206 | TE 207 |
| PCT (K) | 653.5 | 779.9 | 736.3 | 569.1 | 568.6 | 567.1 | 566.5 |
| Time (s) | 19.2 | 18.3 | 18.0 | 0.0 | 0.0 | 0.0 | 0.0 |
| A-12 rod | TE 208 | TE 209 | TE 210 | TE 211 | TE 212 | TE 213 | TE 214 |
| PCT (K) | 639.1 | 670.3 | 583.9 | 566.7 | 566.0 | 563.4 | 562.1 |
| Time (s) | 18.0 | 15.3 | 83.4 | 0.0 | 0.0 | 0.0 | 0.0 |
| A-13 rod | TE 215 | TE 216 | TE 217 | TE 218 | TE 219 | TE 220 | TE 221 |
| PCT (K) | 622.3 | 642.7 | 587.5 | 569.7 | 566.7 | 566.2 | 563.4 |
| Time (s) | 18.6 | 94.8 | 85.2 | 0.0 | 0.0 | 0.0 | 0.0 |
| A-14 rod | TE 222 | TE 223 | TE 224 | TE 225 | TE 226 | TE 227 | TE 228 |
| PCT (K) | 627.1 | 673.9 | 591.1 | 565.1 | 564.3 | 564.9 | 561.9 |
| Time (s) | 18.3 | 18.3 | 18.0 | 0.0 | 0.0 | 0.0 | 0.0 |
| A-15 rod | TE 229 | | | TE 230 | | | |
| PCT (K) | 627.1 | | | 561.3 | | | |
| Time (s) | 18.9 | | | 0.0 | | | |
| A-17 rod | TE 231 | | | TE 232 | | | |
| PCT (K) | 636.0 | | | 565.7 | | | |
| Time (s) | 18.9 | | | 0.0 | | | |
| A-22 rod | TE 233 | TE 234 | TE 235 | TE 236 | TE 237 | TE 238 | TE 239 |
| PCT (K) | 629.2 | 672.7 | 594.7 | 568.1 | 567.5 | 566.8 | 563.3 |
| Time (s) | 18.9 | 18.3 | 10.8 | 0.0 | 0.0 | 0.0 | 0.0 |
| A-24 rod | TE 240 | TE 241 | TE 242 | TE 243 | TE 244 | TE 245 | TE 246 |
| PCT (K) | 628.6 | 679.9 | 609.5 | 565.8 | 567.4 | 563.9 | 562.4 |
| Time (s) | 18.0 | 18.3 | 10.8 | 0.0 | 0.0 | 0.0 | 0.0 |
| A-26 rod | TE 247 | | | TE 248 | | | |
| PCT (K) | 627.6 | | | 566.4 | | | |
| Time (s) | 18.3 | | | 0.0 | | | |
| A-28 rod | TE 249 | | | TE 250 | | | |
| PCT (K) | 649.5 | | | 566.8 | | | |
| Time (s) | 18.3 | | | 0.0 | | | |
| A-31 rod | TE 251 | | | TE 252 | | | |
| PCT (K) | 645.7 | | | 563.8 | | | |
| Time (s) | 18.9 | | | 0.0 | | | |
| A-33 rod | TE 253 | TE 254 | TE 255 | TE 256 | TE 257 | TE 258 | TE 259 |
| PCT (K) | 617.1 | 664.7 | 588.4 | 563.6 | 561.5 | 563.5 | 561.1 |
| Time (s) | 18.9 | 18.3 | 17.7 | 0.0 | 0.0 | 0.0 | 0.0 |
| A-34 rod | TE 260 | TE 261 | TE 262 | TE 263 | TE 264 | TE 265 | TE 266 |
| PCT (K) | 613.3 | ------ | 591.3 | 563.5 | 565.6 | 564.4 | 561.3 |
| Time (s) | 18.3 | ------ | 10.8 | 0.0 | 0.0 | 0.0 | 0.0 |
| A-37 rod | TE 267 | | | TE 268 | | | |
| PCT (K) | 630.5 | | | 564.5 | | | |
| Time (s) | 18.6 | | | 0.0 | | | |
| A-42 rod | TE 269 | | | TE 270 | | | |
| PCT (K) | 624.8 | | | ------ | | | |
| Time (s) | 18.9 | | | ------ | | | |
| A-44 rod | TE 271 | TE 272 | TE 273 | TE 274 | TE 275 | TE 276 | TE 277 |
| PCT (K) | 633.3 | 671.4 | 597.0 | 561.7 | 563.3 | 564.4 | 560.5 |
| Time (s) | 18.6 | 18.6 | 10.5 | 0.0 | 0.0 | 0.0 | 0.0 |

Table 5.2 Maximum Cladding Temperature Distribution in the Core (Continued)

| | Pos.1 | Pos.2 | Pos.3 | Pos.4 | Pos.5 | Pos.6 | Pos.7 |
|---|---|---|---|---|---|---|---|
| A-48 rod | TE 278 | | | TE 279 | | | |
| PCT (K) | 632.4 | | | 565.3 | | | |
| Time (s) | 18.6 | | | 0.0 | | | |
| A-51 rod | TE 280 | | | TE 281 | | | |
| PCT (K) | 641.9 | | | 565.5 | | | |
| Time (s) | 18.6 | | | 0.0 | | | |
| A-53 rod | TE 282 | | | TE 283 | | | |
| PCT (K) | 616.2 | | | 564.1 | | | |
| Time (s) | 17.4 | | | 0.0 | | | |
| A-57 rod | TE 284 | | | TE 285 | | | |
| PCT (K) | 619.0 | | | 561.9 | | | |
| Time (s) | 18.3 | | | 0.0 | | | |
| A-62 rod | TE 286 | | | TE 287 | | | |
| PCT (K) | 622.9 | | | 565.8 | | | |
| Time (s) | 18.6 | | | 0.0 | | | |
| A-66 rod | TE 288 | | | TE 289 | | | |
| PCT (K) | 613.3 | | | ------ | | | |
| Time (s) | 18.3 | | | ------ | | | |
| A-68 rod | TE 290 | | | TE 291 | | | |
| PCT (K) | 647.6 | | | 564.1 | | | |
| Time (s) | 18.6 | | | 0.0 | | | |
| A-71 rod | TE 292 | | | TE 293 | | | |
| PCT (K) | 658.1 | | | ------ | | | |
| Time (s) | 18.9 | | | ------ | | | |
| A-73 rod | TE 294 | | | TE 295 | | | |
| PCT (K) | 631.4 | | | 564.3 | | | |
| Time (s) | 18.6 | | | 0.0 | | | |
| A-75 rod | TE 296 | | | TE 297 | | | |
| PCT (K) | 623.8 | | | 566.4 | | | |
| Time (s) | 18.9 | | | 0.0 | | | |
| A-77 rod | TE 298 | TE 299 | TE 300 | TE 301 | TE 302 | TE 303 | TE 304 |
| PCT (K) | 627.6 | 685.6 | 620.0 | 561.2 | 562.8 | 561.9 | ------ |
| Time (s) | 18.3 | 18.3 | 10.8 | 0.0 | 0.0 | 0.0 | ------ |
| A-82 rod | TE 305 | | | TE 306 | | | |
| PCT (K) | 663.8 | | | ------ | | | |
| Time (s) | 18.6 | | | ------ | | | |
| A-84 rod | TE 307 | | | TE 308 | | | |
| PCT (K) | 647.6 | | | 565.9 | | | |
| Time (s) | 18.6 | | | 0.0 | | | |
| A-85 rod | TE 309 | TE 310 | TE 311 | TE 312 | TE 313 | TE 314 | TE 315 |
| PCT (K) | 638.1 | ------ | ------ | 565.7 | 563.8 | 564.5 | 563.3 |
| Time (s) | 18.9 | ------ | ------ | 0.0 | 0.0 | 0.0 | 0.0 |
| A-87 rod | TE 316 | TE 317 | TE 318 | TE 319 | TE 320 | TE 321 | TE 322 |
| PCT (K) | 663.8 | ------ | 641.9 | 563.4 | 563.6 | 563.5 | 560.5 |
| Time (s) | 18.6 | ------ | 10.8 | 0.0 | 0.0 | 0.0 | 0.0 |
| A-88 rod | TE 323 | TE 324 | TE 325 | TE 326 | TE 327 | TE 328 | TE 329 |
| PCT (K) | 665.7 | 767.5 | 734.6 | 567.4 | 566.8 | 564.0 | 562.6 |
| Time (s) | 18.6 | 18.0 | 17.7 | 0.0 | 0.0 | 0.0 | 0.0 |

Table 5.2 Maximum Cladding Temperature Distribution in the Core (Continued)

| | Pos.1 | Pos.2 | Pos.3 | Pos.4 | Pos.5 | Pos.6 | Pos.7 |
|---|---|---|---|---|---|---|---|
| B-11 rod | TE 330 | TE 331 | TE 332 | TE 333 | TE 334 | TE 335 | TE 336 |
| PCT (K) | 613.3 | 667.6 | 647.6 | 562.6 | 562.1 | 562.3 | 561.9 |
| Time (s) | 18.9 | 18.3 | 87.6 | 0.0 | 0.0 | 0.0 | 0.0 |
| B-13 rod | | | | TE 337 | | | |
| PCT (K) | | | | 563.9 | | | |
| Time (s) | | | | 0.0 | | | |
| B-22 rod | TE 338 | TE 339 | TE 340 | TE 341 | TE 342 | TE 343 | TE 344 |
| PCT (K) | 606.6 | 654.3 | 630.5 | ------ | 562.4 | 560.9 | 559.9 |
| Time (s) | 18.6 | 18.6 | 87.0 | ------ | 0.0 | 0.0 | 0.0 |
| B-31 rod | | | | TE 345 | | | |
| PCT (K) | | | | 564.8 | | | |
| Time (s) | | | | 0.0 | | | |
| B-33 rod | | | | TE 346 | | | |
| PCT (K) | | | | 565.1 | | | |
| Time (s) | | | | 0.0 | | | |
| B-51 rod | | | | TE 347 | | | |
| PCT (K) | | | | 562.2 | | | |
| Time (s) | | | | 0.0 | | | |
| B-53 rod | | | | TE 348 | | | |
| PCT (K) | | | | 563.8 | | | |
| Time (s) | | | | 0.0 | | | |
| B-66 rod | | | | TE 349 | | | |
| PCT (K) | | | | 561.5 | | | |
| Time (s) | | | | 0.0 | | | |
| B-77 rod | TE 350 | TE 351 | TE 352 | TE 353 | TE 354 | TE 355 | TE 356 |
| PCT (K) | 609.5 | 652.4 | 600.8 | 563.6 | 564.8 | 562.9 | 561.7 |
| Time (s) | 18.6 | 18.3 | 12.3 | 0.0 | 0.0 | 0.0 | 0.0 |
| B-86 rod | | | | TE 357 | | | |
| PCT (K) | | | | ------ | | | |
| Time (s) | | | | ------ | | | |
| C-11 rod | TE 358 | TE 359 | TE 360 | TE 361 | TE 362 | TE 363 | TE 364 |
| PCT (K) | 574.9 | 662.8 | 648.6 | 564.2 | 564.4 | 563.2 | 562.4 |
| Time (s) | 15.3 | 18.6 | 13.5 | 0.0 | 0.0 | 0.0 | 0.0 |
| C-13 rod | TE 365 | TE 366 | TE 367 | TE 368 | TE 369 | TE 370 | TE 371 |
| PCT (K) | 611.4 | 649.5 | 654.3 | ------ | 564.1 | 562.1 | 561.2 |
| Time (s) | 18.6 | 18.3 | 87.3 | ------ | 0.0 | 0.0 | 0.0 |
| C-15 rod | | | | TE 372 | | | |
| PCT (K) | | | | 564.5 | | | |
| Time (s) | | | | 0.0 | | | |
| C-22 rod | TE 373 | TE 374 | TE 375 | TE 376 | TE 377 | TE 378 | TE 379 |
| PCT (K) | 605.6 | 647.6 | 648.6 | 565.9 | 565.1 | 566.6 | 560.9 |
| Time (s) | 18.3 | 18.3 | 88.8 | 0.0 | 0.0 | 0.0 | 0.0 |
| C-31 rod | | | | TE 380 | | | |
| PCT (K) | | | | 563.9 | | | |
| Time (s) | | | | 0.0 | | | |
| C-33 rod | TE 381 | TE 382 | TE 383 | TE 384 | TE 385 | TE 386 | TE 387 |
| PCT (K) | 596.1 | 636.2 | 620.0 | 562.7 | 562.5 | 562.6 | 559.6 |
| Time (s) | 18.3 | 18.3 | 87.9 | 0.0 | 0.0 | 0.0 | 0.0 |

Table 5.2 Maximum Cladding Temperature Distribution in the Core (Continued)

| | Pos.1 | Pos.2 | Pos.3 | Pos.4 | Pos.5 | Pos.6 | Pos.7 |
|---|---|---|---|---|---|---|---|
| C-35 rod | | | | TE 388 | | | |
| PCT (K) | | | | 564.5 | | | |
| Time (s) | | | | 0.0 | | | |
| C-66 rod | | | | TE 389 | | | |
| PCT (K) | | | | 564.5 | | | |
| Time (s) | | | | 0.0 | | | |
| C-68 rod | | | | TE 390 | | | |
| PCT (K) | | | | 565.6 | | | |
| Time (s) | | | | 0.0 | | | |
| C-77 rod | TE 391 | TE 392 | TE 393 | TE 394 | TE 395 | TE 396 | TE 397 |
| PCT (K) | 608.5 | 649.5 | 620.9 | 564.5 | 564.6 | 562.5 | 561.6 |
| Time (s) | 18.6 | 18.3 | 13.2 | 0.0 | 0.0 | 0.0 | 0.0 |
| D-11 rod | | | | TE 398 | | | |
| PCT (K) | | | | 562.7 | | | |
| Time (s) | | | | 0.0 | | | |
| D-13 rod | | | | TE 399 | | | |
| PCT (K) | | | | ------ | | | |
| Time (s) | | | | ------ | | | |
| D-22 rod | TE 400 | TE 401 | TE 402 | TE 403 | TE 404 | TE 405 | TE 406 |
| PCT (K) | 606.6 | 651.4 | 628.6 | 563.8 | 562.4 | 563.7 | 561.7 |
| Time (s) | 18.6 | 18.3 | 93.3 | 0.0 | 0.0 | 0.0 | 0.0 |
| D-31 rod | | | | TE 407 | | | |
| PCT (K) | | | | 565.1 | | | |
| Time (s) | | | | 0.0 | | | |
| D-33 rod | | | | TE 408 | | | |
| PCT (K) | | | | 563.2 | | | |
| Time (s) | | | | 0.0 | | | |
| D-51 rod | | | | TE 409 | | | |
| PCT (K) | | | | 565.1 | | | |
| Time (s) | | | | 0.0 | | | |
| D-53 rod | | | | TE 410 | | | |
| PCT (K) | | | | 563.9 | | | |
| Time (s) | | | | 0.0 | | | |
| D-66 rod | | | | TE 411 | | | |
| PCT (K) | | | | 564.8 | | | |
| Time (s) | | | | 0.0 | | | |
| D-77 rod | | | | TE 412 | | | |
| PCT (K) | | | | ------ | | | |
| Time (s) | | | | ------ | | | |
| D-86 rod | | | | TE 413 | | | |
| PCT (K) | | | | 564.8 | | | |
| Time (s) | | | | 0.0 | | | |

Table 5.2 Maximum Cladding Temperature Distribution in the Core (Continued)

** Order of PCT **

| | | | | | | |
|---|---|---|---|---|---|---|
| No. 1 | A-11 rod | Pos. 2 | PCT = | 779.9 (K) | Time = | 18.3 (s) |
| No. 2 | A-88 rod | Pos. 2 | PCT = | 767.5 (K) | Time = | 18.0 (s) |
| No. 3 | A-11 rod | Pos. 3 | PCT = | 736.3 (K) | Time = | 18.0 (s) |
| No. 4 | A-88 rod | Pos. 3 | PCT = | 734.6 (K) | Time = | 17.7 (s) |
| No. 5 | A-77 rod | Pos. 2 | PCT = | 685.6 (K) | Time = | 18.3 (s) |
| No. 6 | A-24 rod | Pos. 2 | PCT = | 679.9 (K) | Time = | 18.3 (s) |
| No. 7 | A-14 rod | Pos. 2 | PCT = | 673.9 (K) | Time = | 18.3 (s) |
| No. 8 | A-22 rod | Pos. 2 | PCT = | 672.7 (K) | Time = | 18.3 (s) |
| No. 9 | A-44 rod | Pos. 2 | PCT = | 671.4 (K) | Time = | 18.6 (s) |
| No.10 | A-12 rod | Pos. 2 | PCT = | 670.3 (K) | Time = | 15.3 (s) |

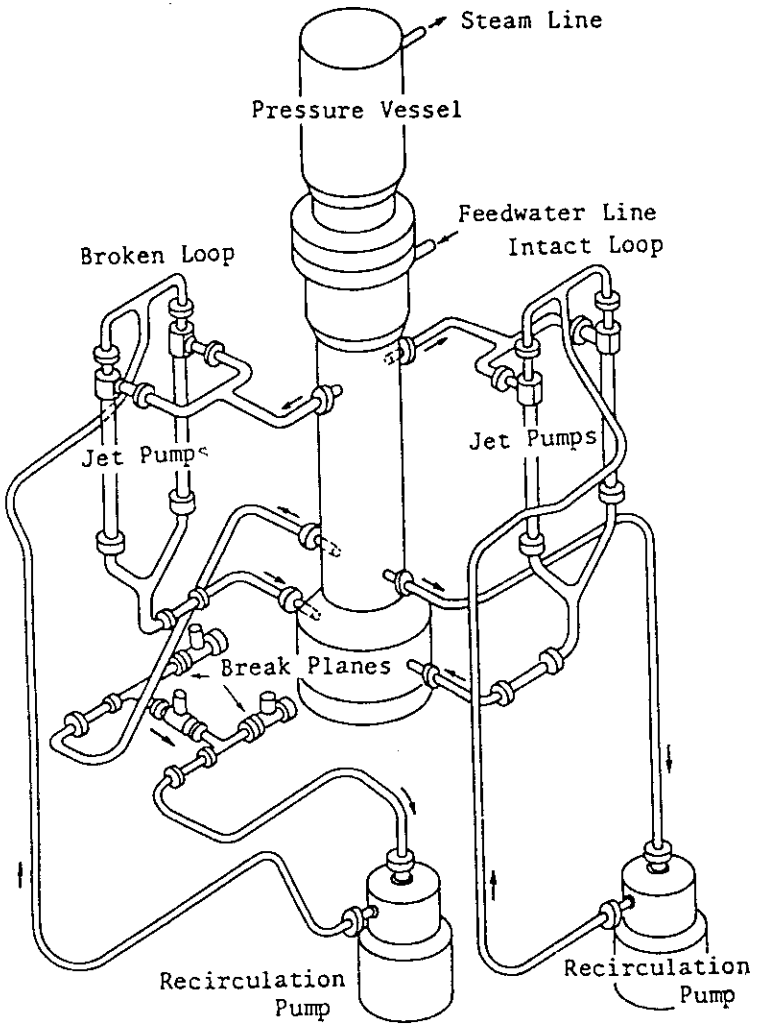


Fig. 2.1 Schematic Diagram of ROSA-III Test Facility

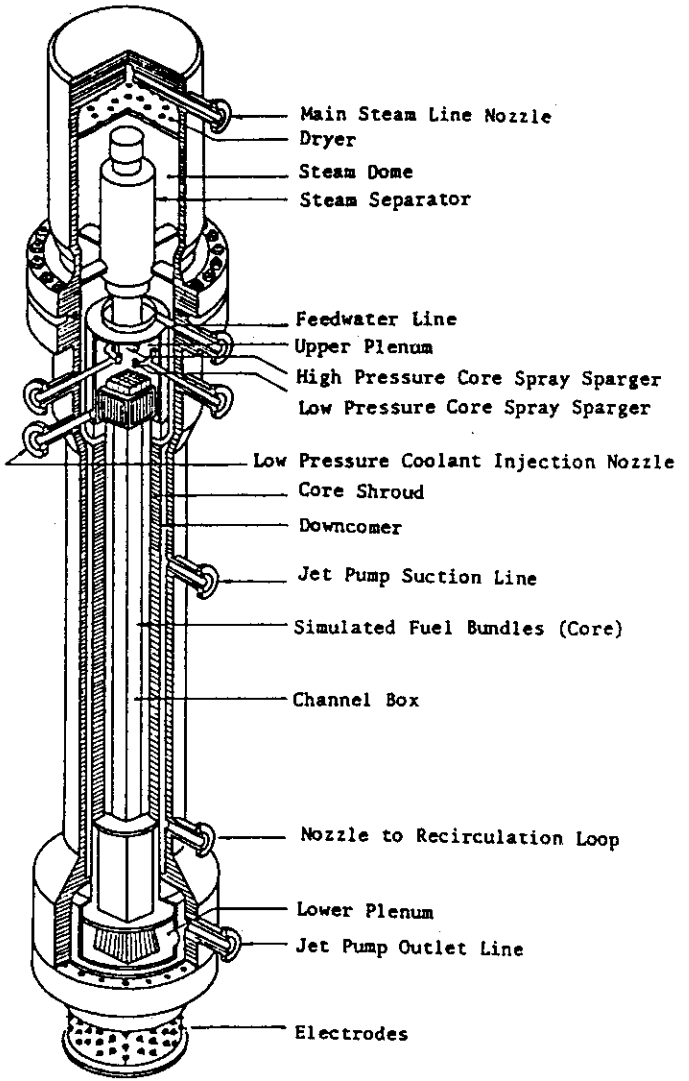


Fig. 2.2 Internal Structure of Pressure Vessel of ROSA-III

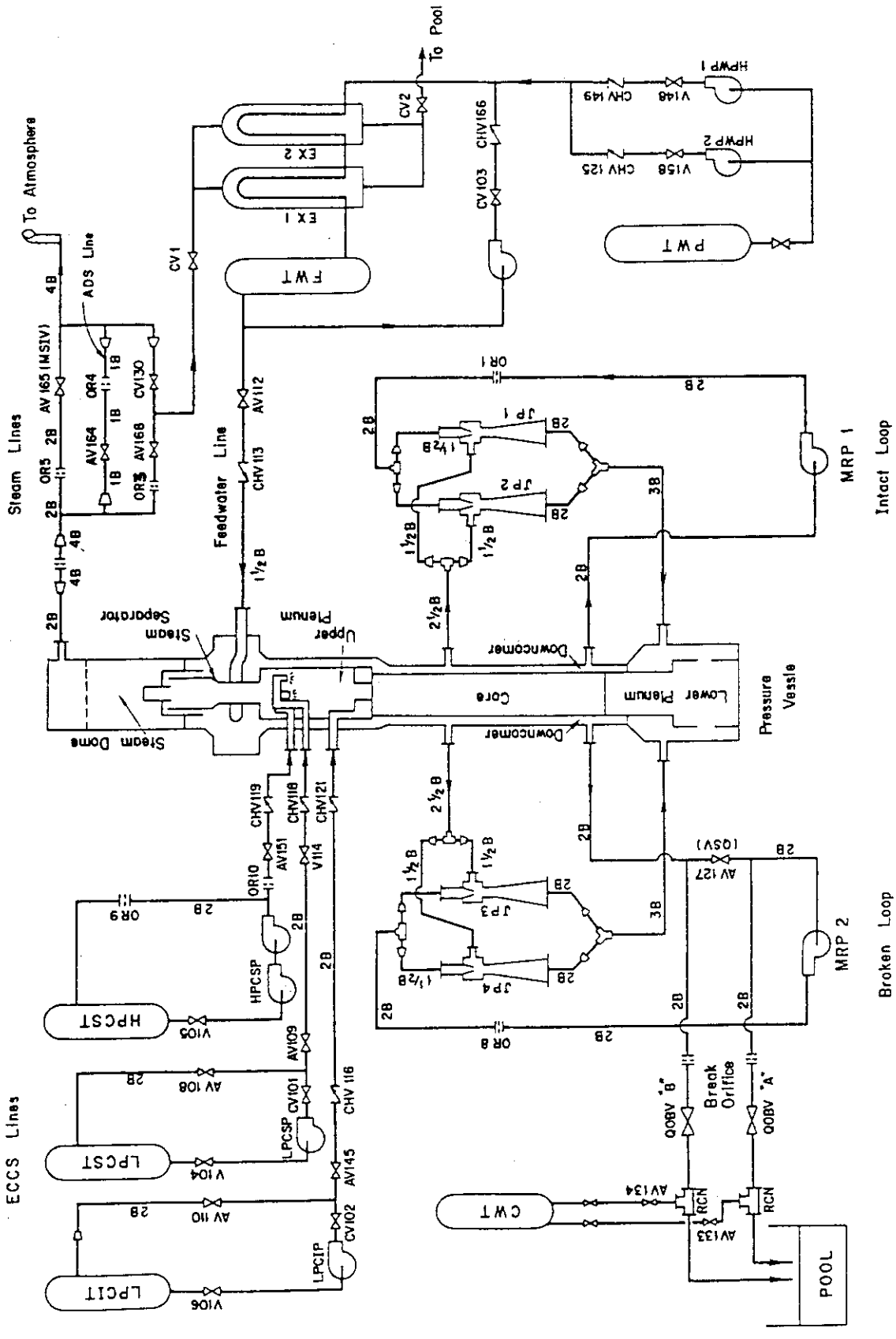


Fig. 2.3 ROSA-III Piping Schematic

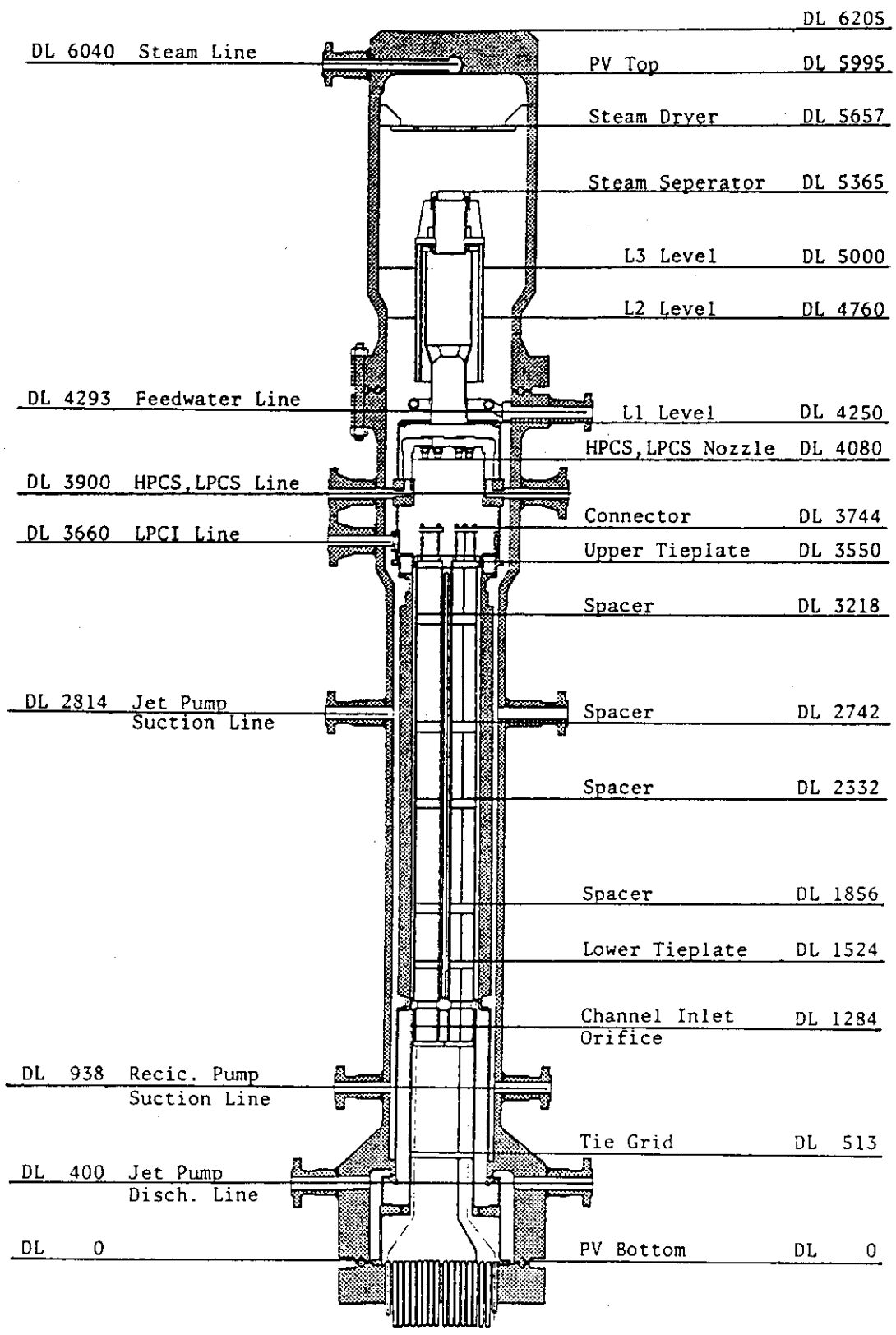


Fig. 2.4 Pressure Vessel Internals Arrangement

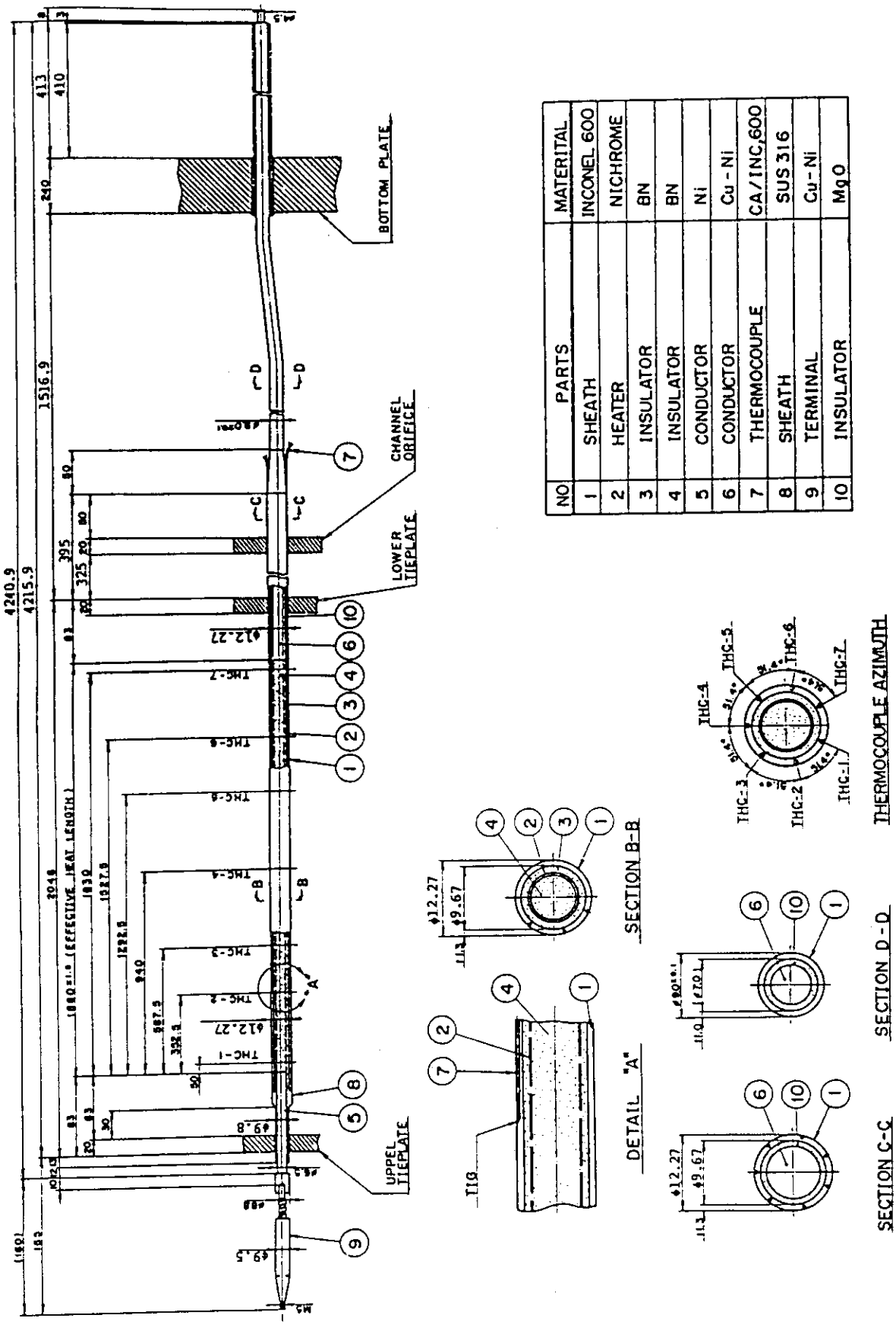


| NO | PARTS | MATERITAL |
|---|---|---|
| 1 | SHEATH | INCONEL 600 |
| 2 | HEATER | NICHROME |
| 3 | INSULATOR | BN |
| 4 | INSULATOR | BN |
| 5 | CONDUCTOR | Ni |
| 6 | CONDUCTOR | Cu－Ni |
| 7 | THERMOCOUPLE | CA/INC,600 |
| 8 | SHEATH | SUS 316 |
| 9 | TERMINAL | Cu－Ni |
| 10 | INSULATOR | MgO |

Fig. 2.5 Simulated Fuel Rod of ROSA-III

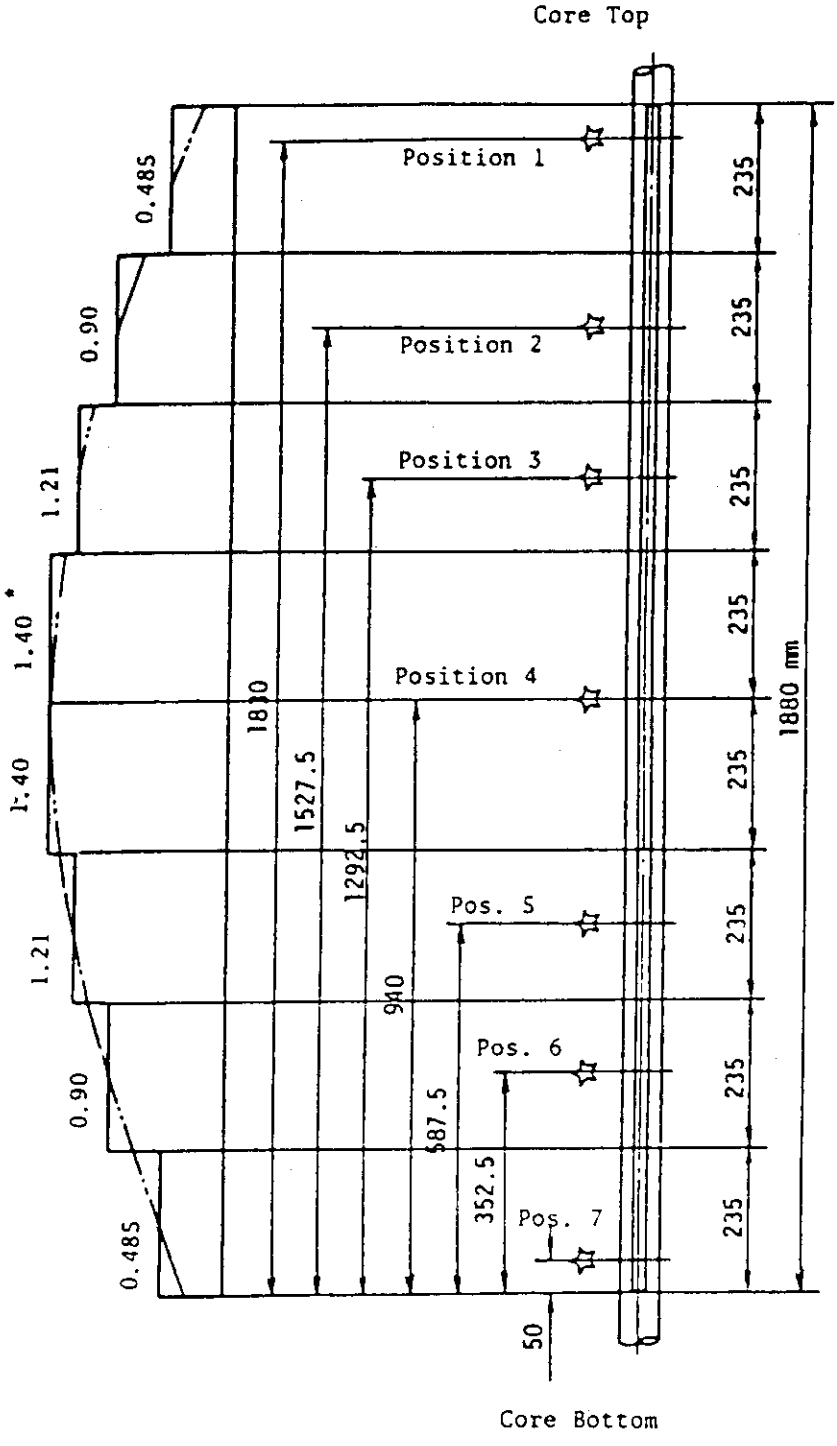


Fig.2.6 Axial Power Distribution of Heater Rod

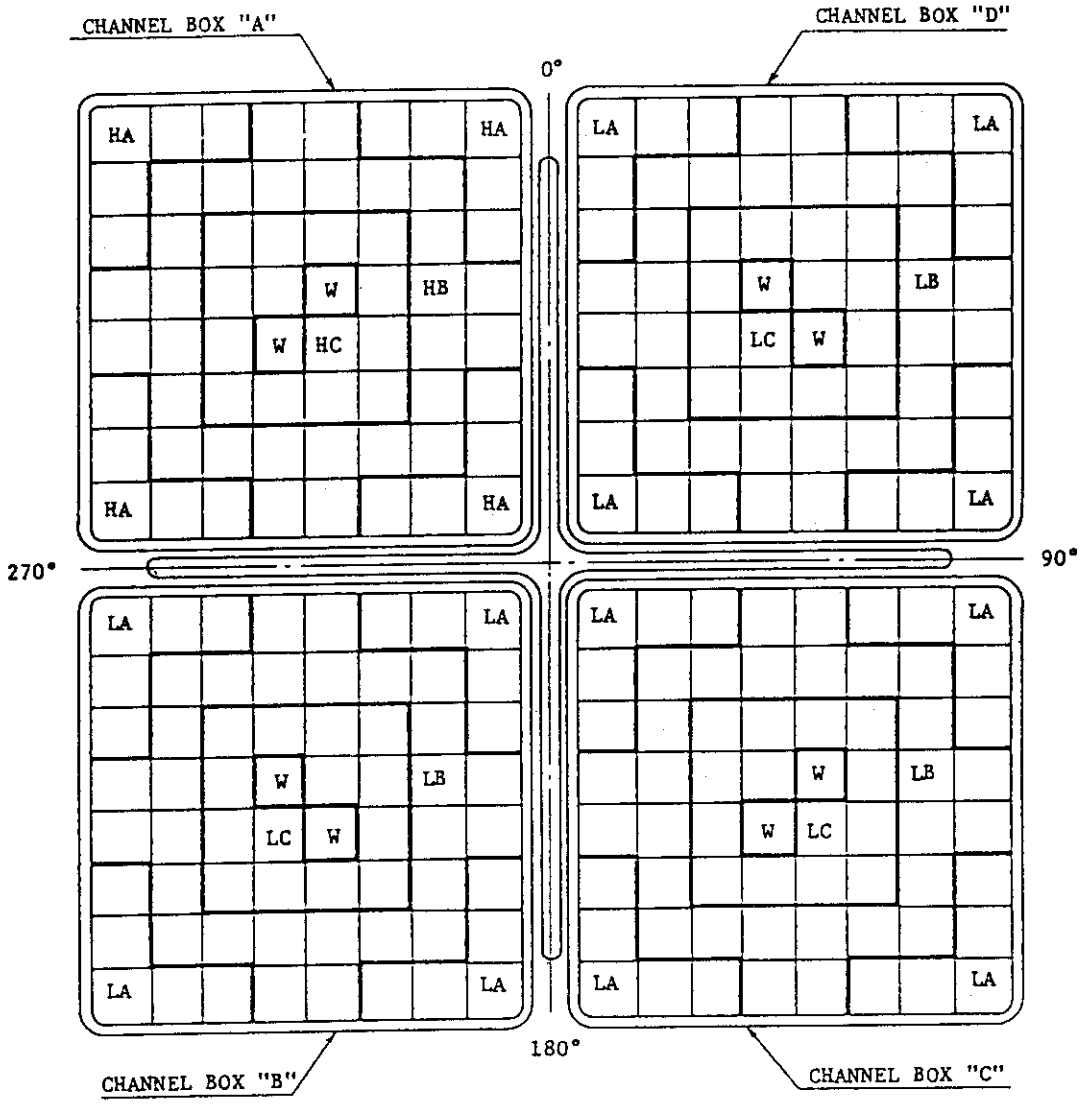


| Region | HA | HB | HC | LA | LB | LC | W |
|---|---|---|---|---|---|---|---|
| Lenear Heat Rate (kW/m) | 18.5 | 16.81 | 14.41 | 13.21 | 12.01 | 10.29 | 0.0 |
| Local peaking factor | 1.1 | 1.0 | 0.875 | 1.1 | 1.0 | 0.875 | 0.0 |
| No. of Rods | 20 | 28 | 14 | 60 | 84 | 42 | 8 |

* note : Radial peaking factor is 1.4

Fig. 2.7 Radial Power Distribution of Core

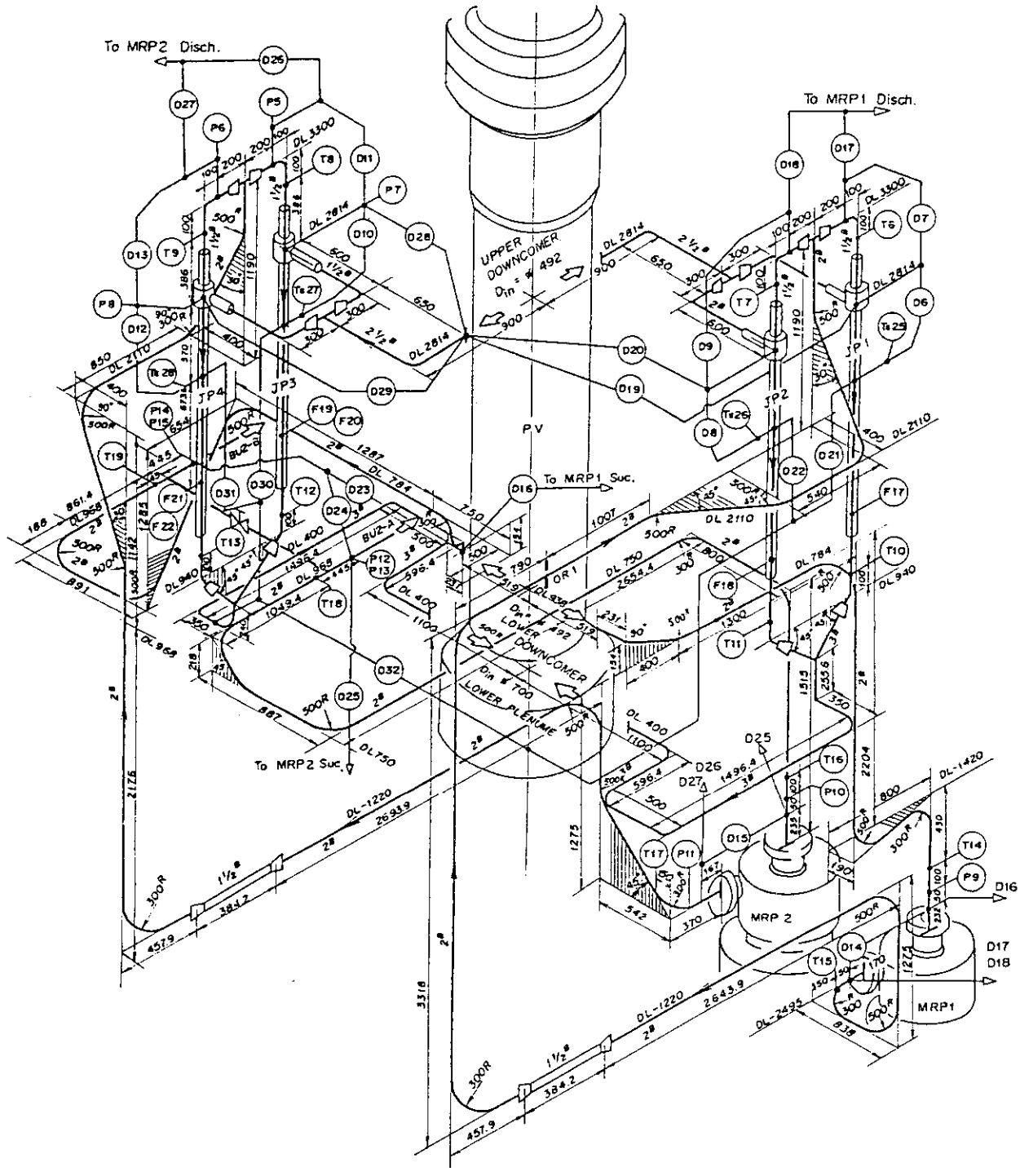


Fig. 2.8 Piping Layout of Recirculation Loops and Jet Pumps

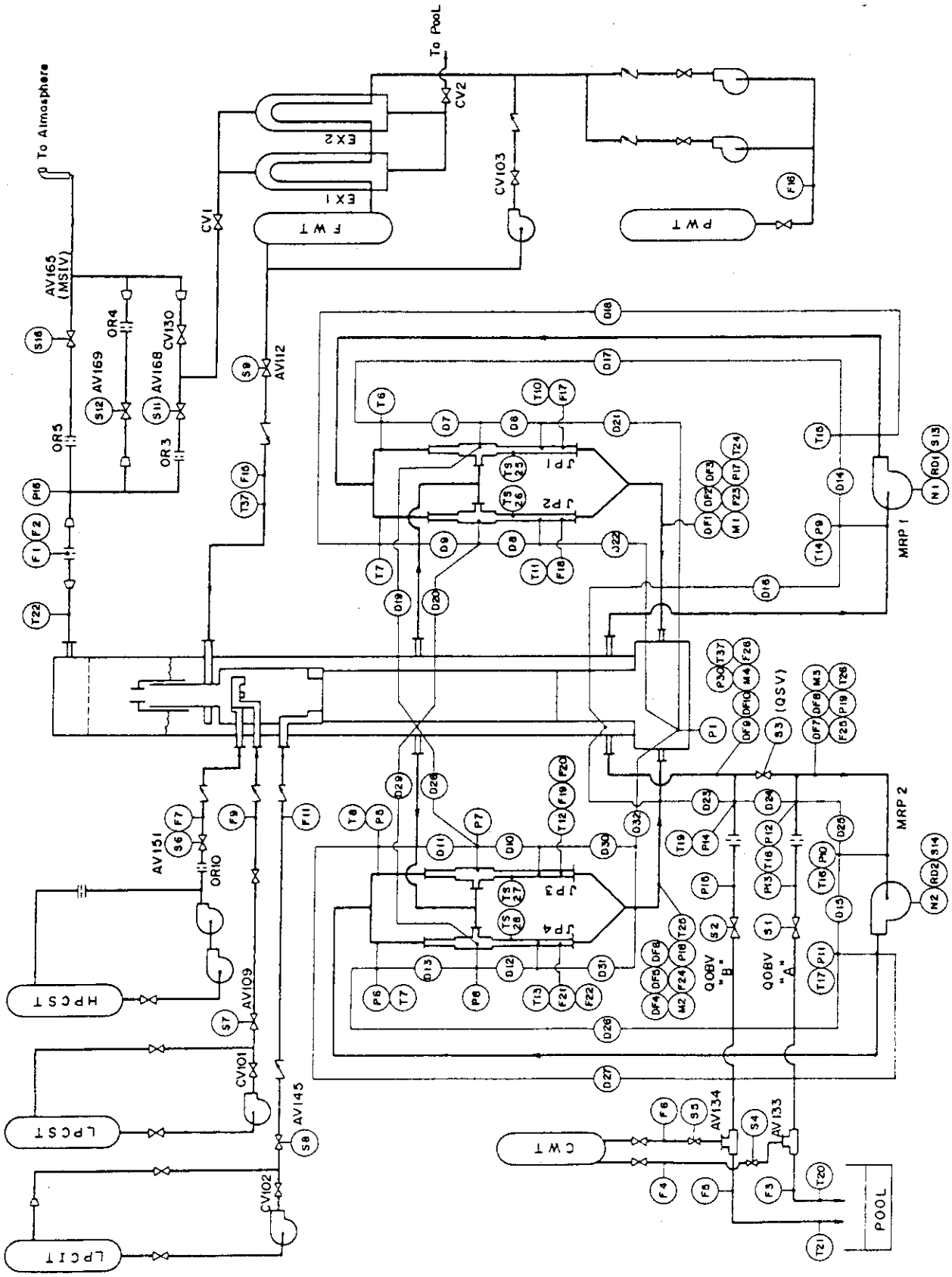


Fig. 3.1 Instrumentation Location of ROSA-III Test Facility

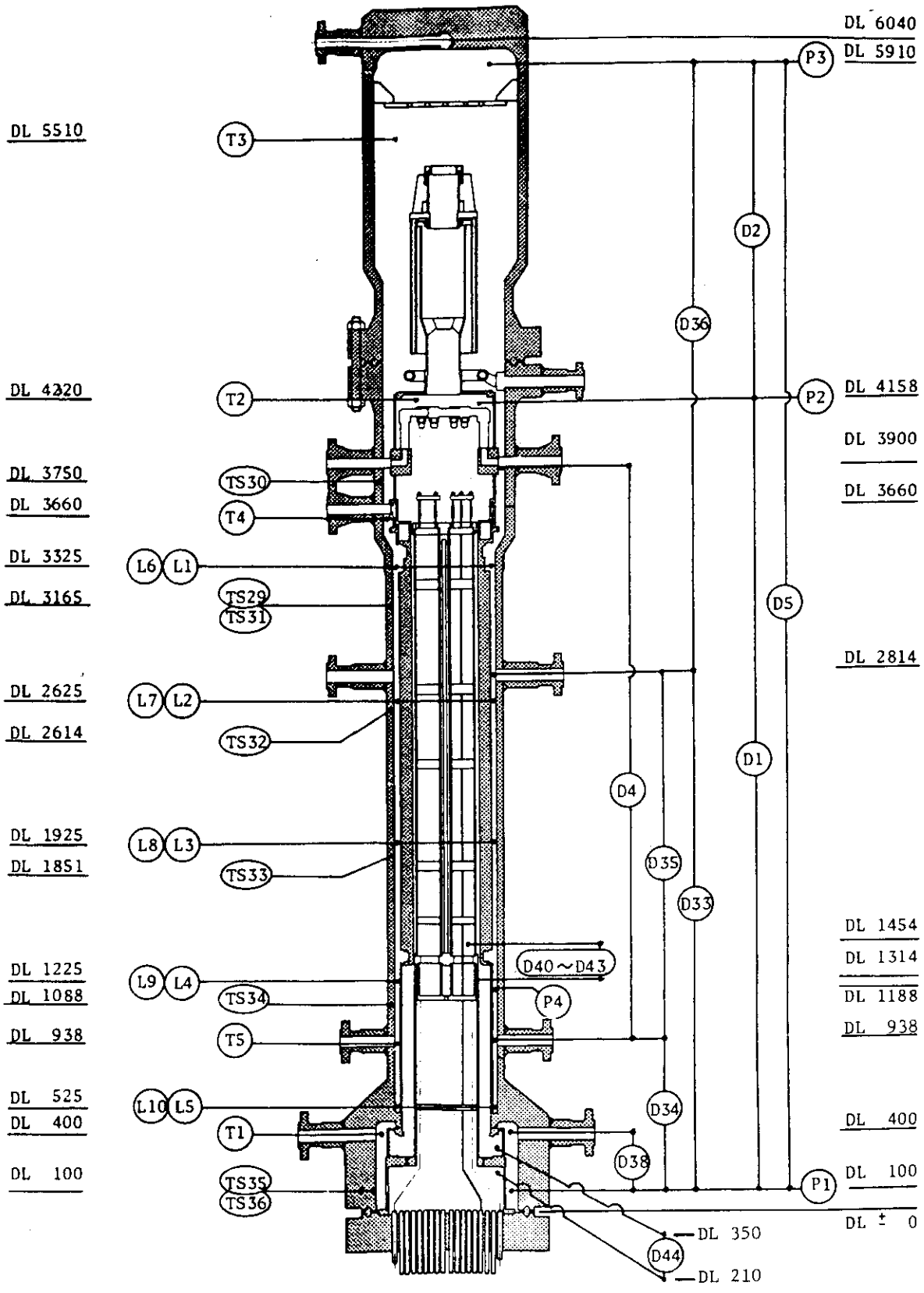


Fig. 3.2 Instrumentation Location in Pressure Vessel

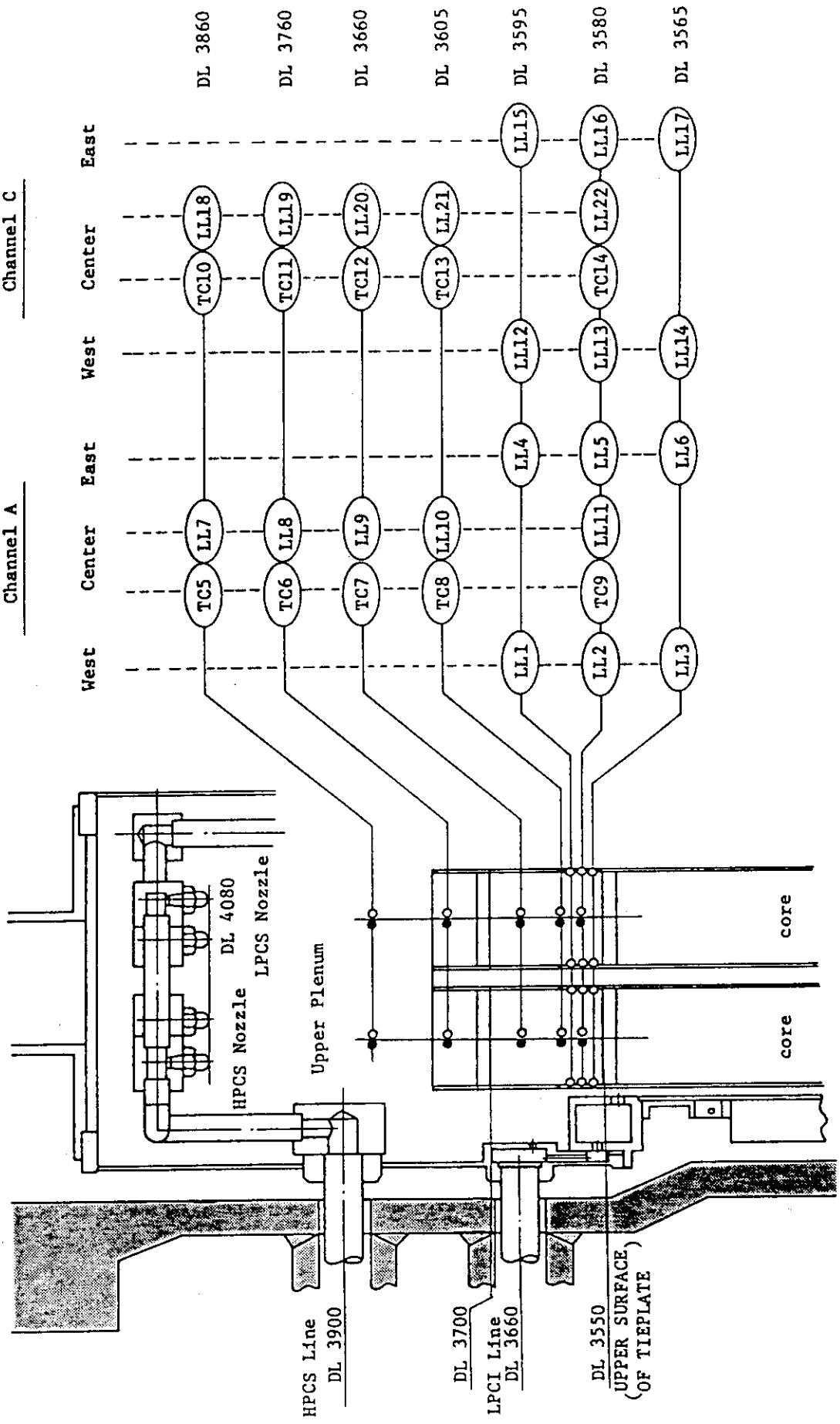


Fig. 3.3 Upper Plenum Instrumentation

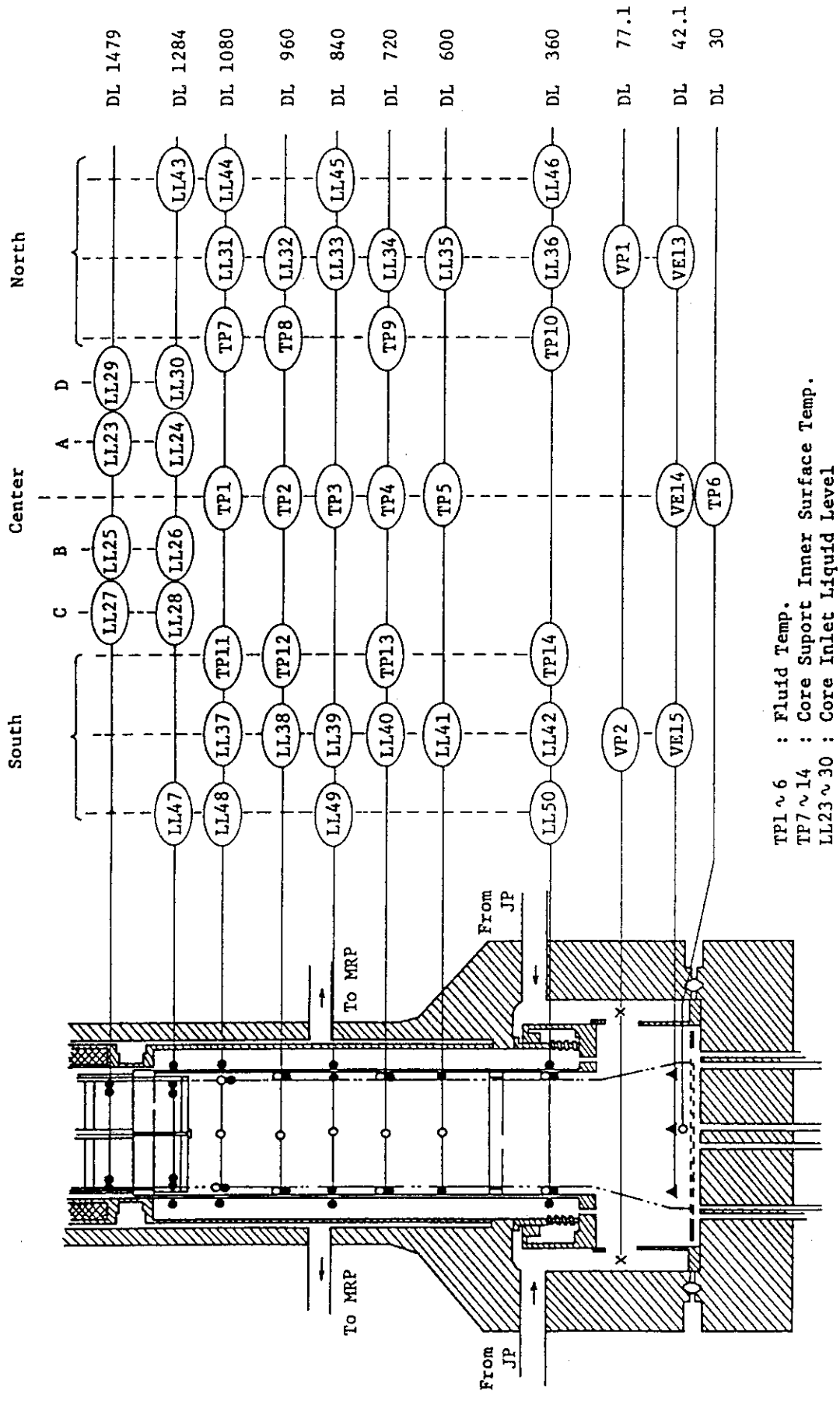


Fig. 3.4 Lower Plenum Instrumentation

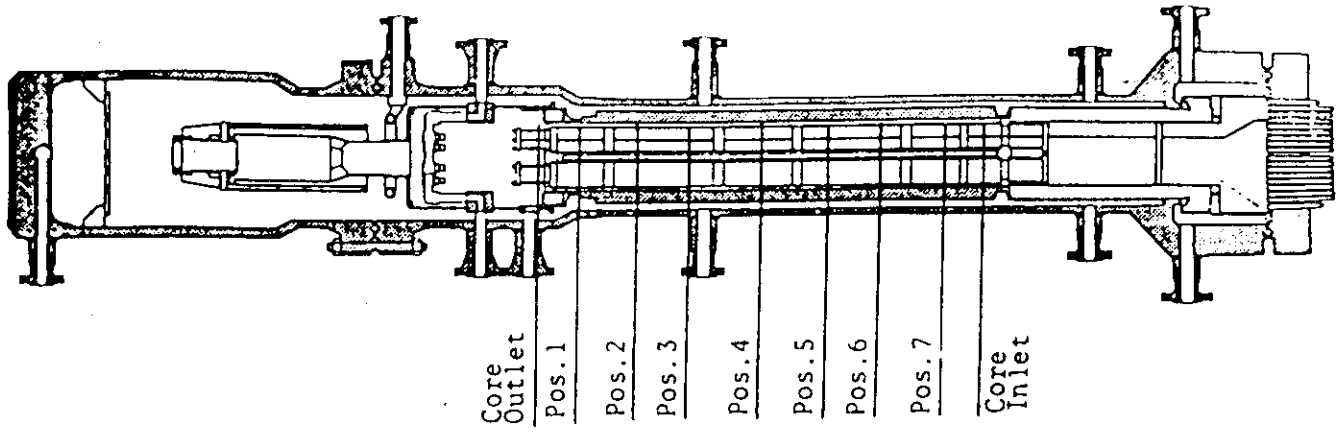


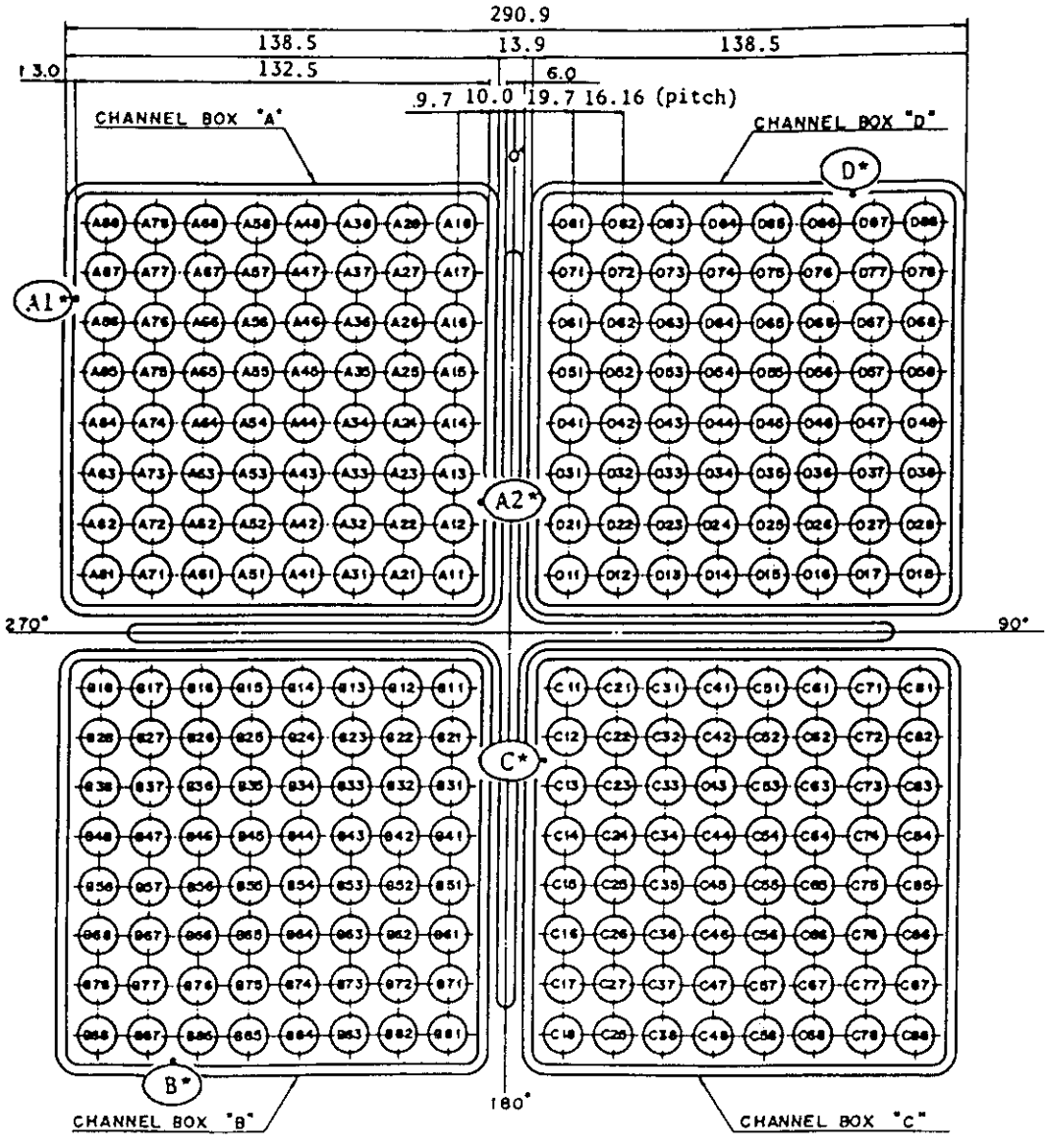


Heater rod O.D. is 12.27mm

A54,B54,C54 and D54 are water rod simulators with void probes, O.D.= 15.01mm

A45,B45,C45 and D45 are water rod simulators with thermocouples, O.D.= 15.01mm

Fig. 3.5 Core Instrumentation (cf. Table 3.3)

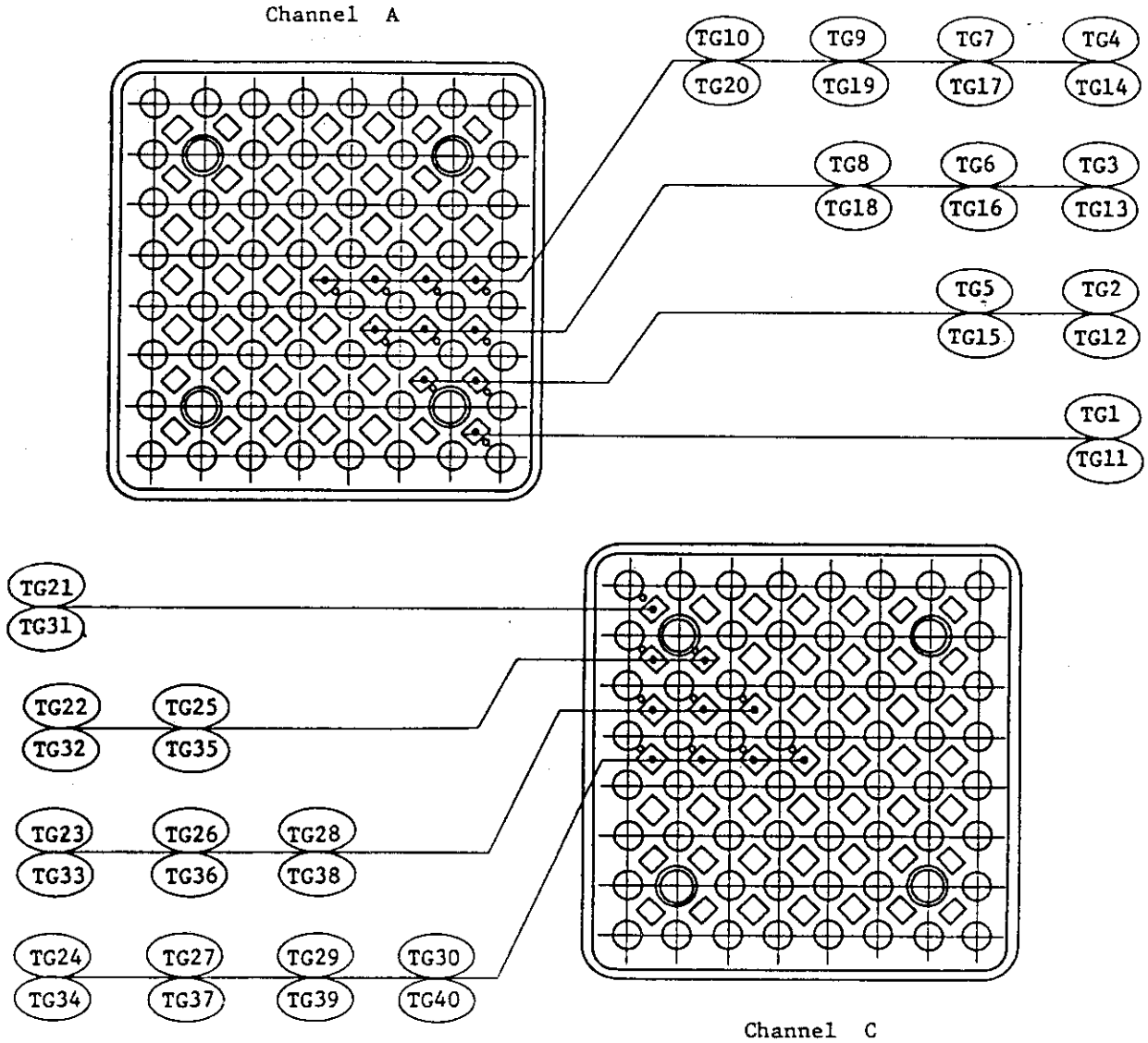


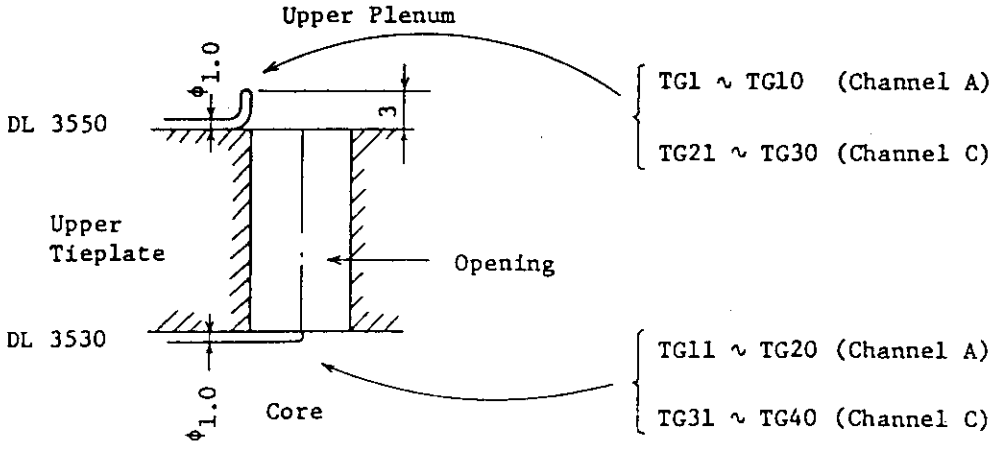


Fig. 3.6 Upper Tieplate Instrumentation

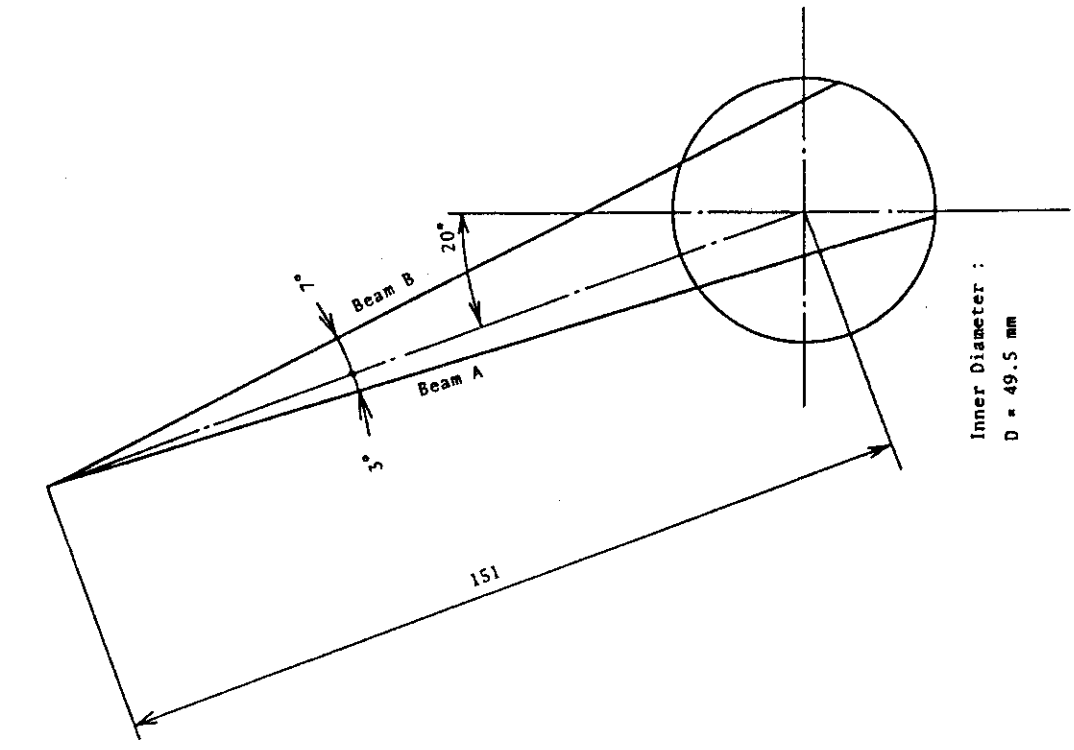


Fig. 3.8 Beam Directions of Two-Beam Gamma Densitometer

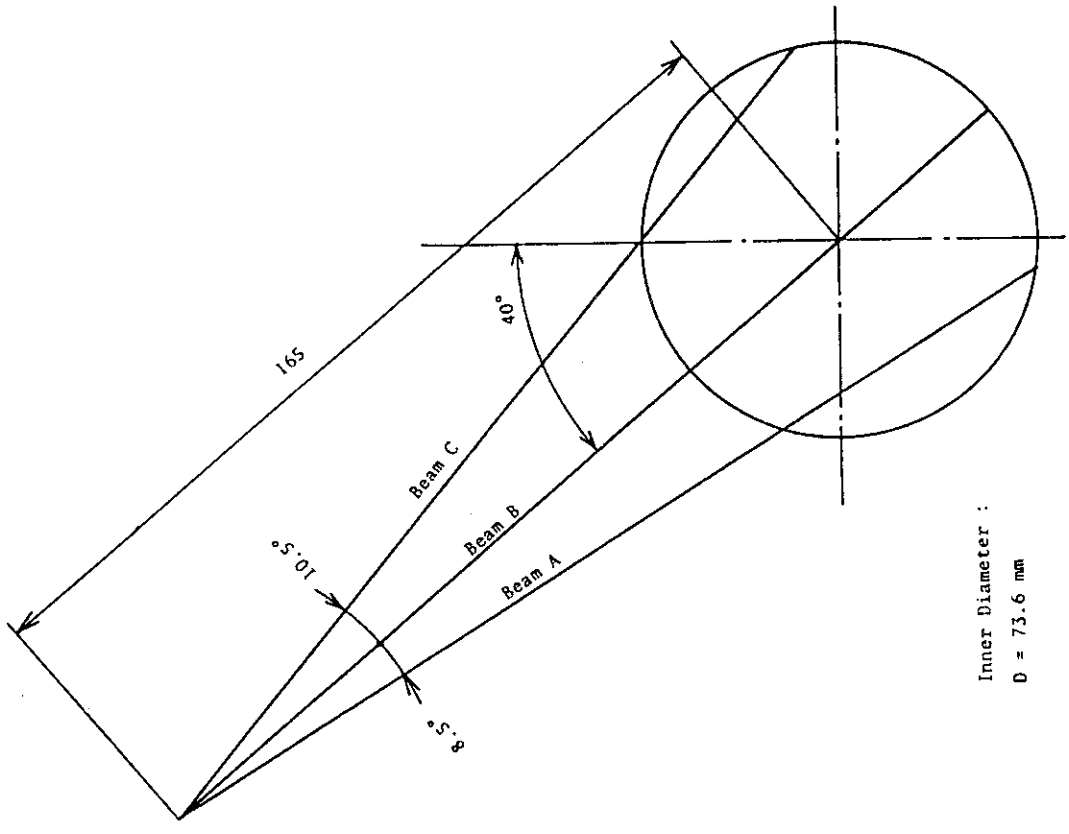


Fig. 3.7 Beam Directions of Three-Beam Gamma Densitometer

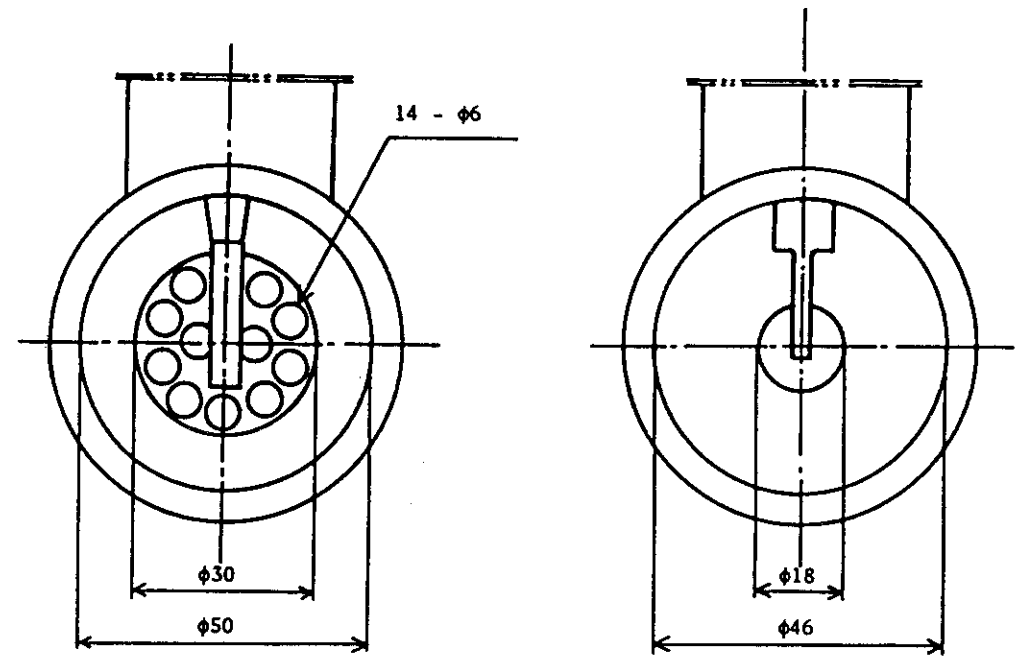


(a) High Range Drag Disc　　(b) Low Range Drag Disc

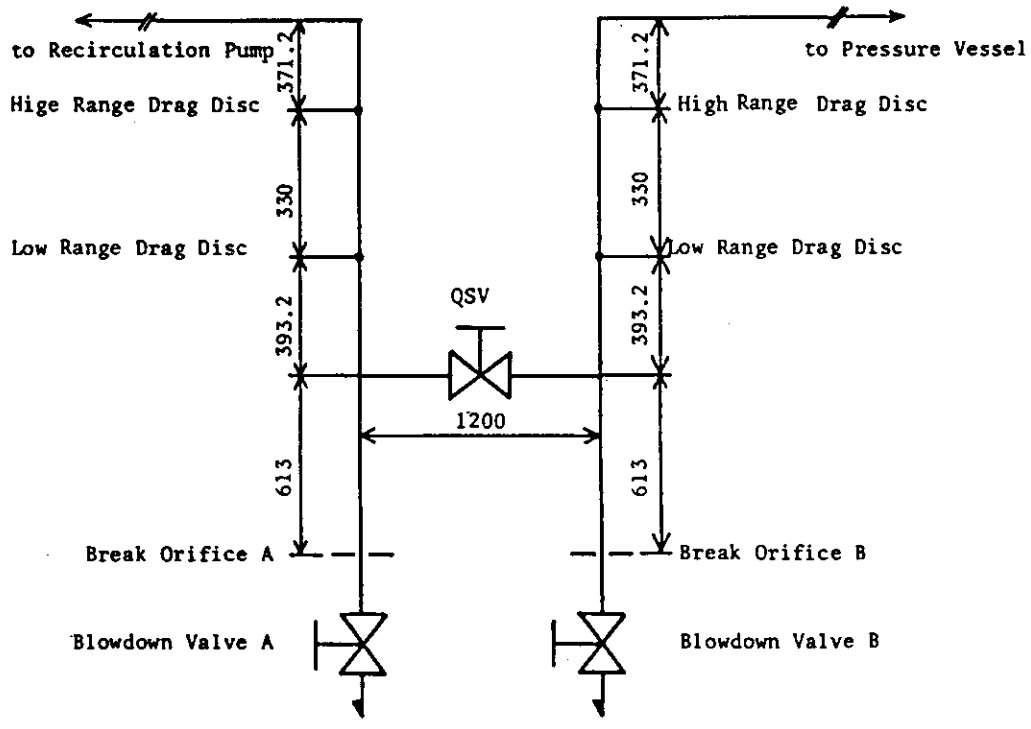


(c) Location of Drag Discs

Fig. 3.9　Arrangement and Location of Drag Disks

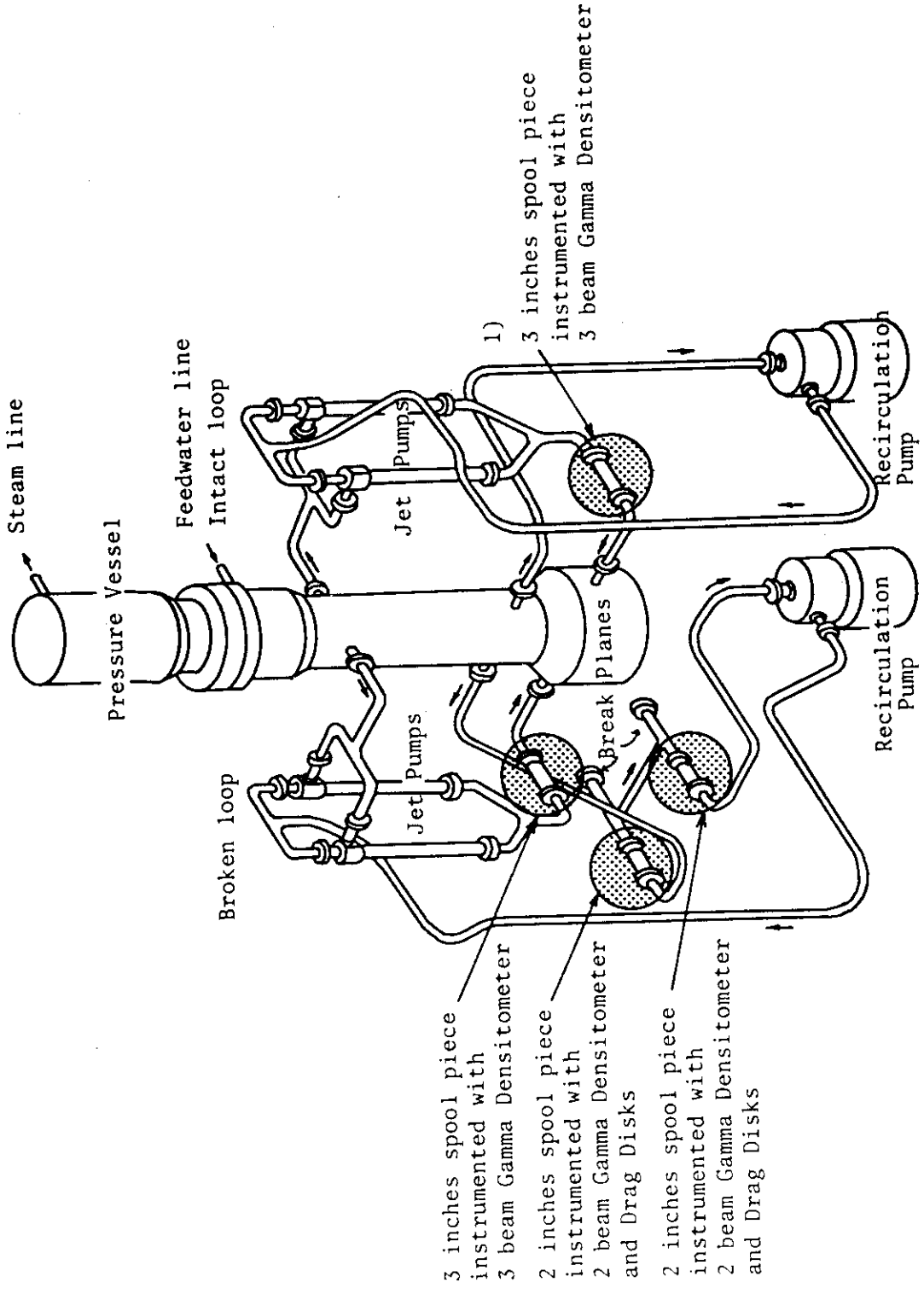


Fig. 3.10 Location of Two-Phase Flow Measurement Spool Pieces

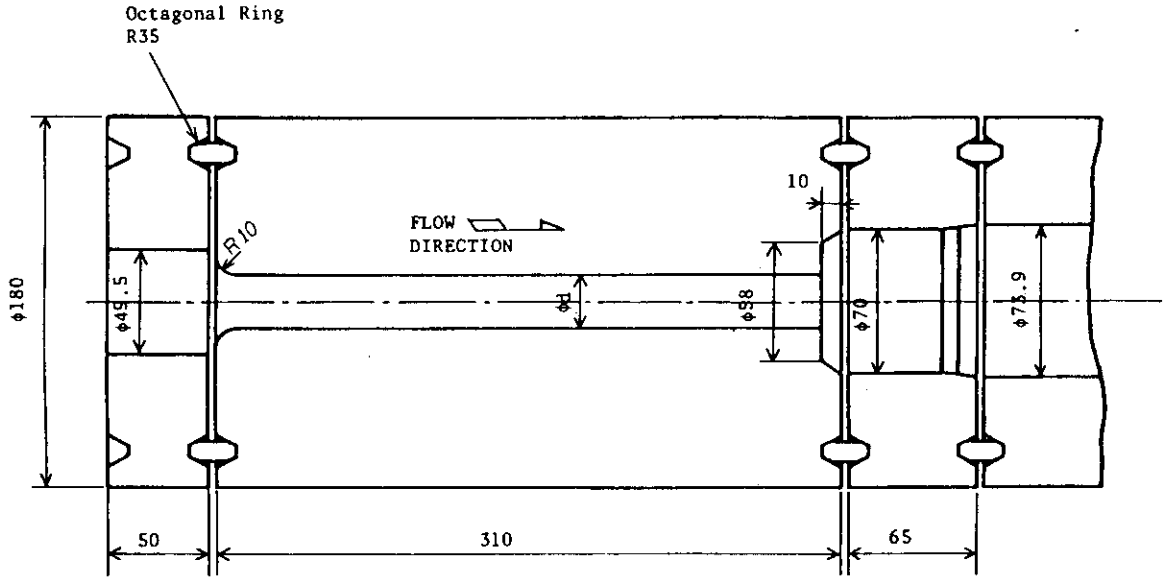


Material SUS304
Dimension in mm

| Break area ratio (%) | d (mm) |
|---|---|
| 100 | 26.2 |

Fig. 4.1 Break Nozzle Details

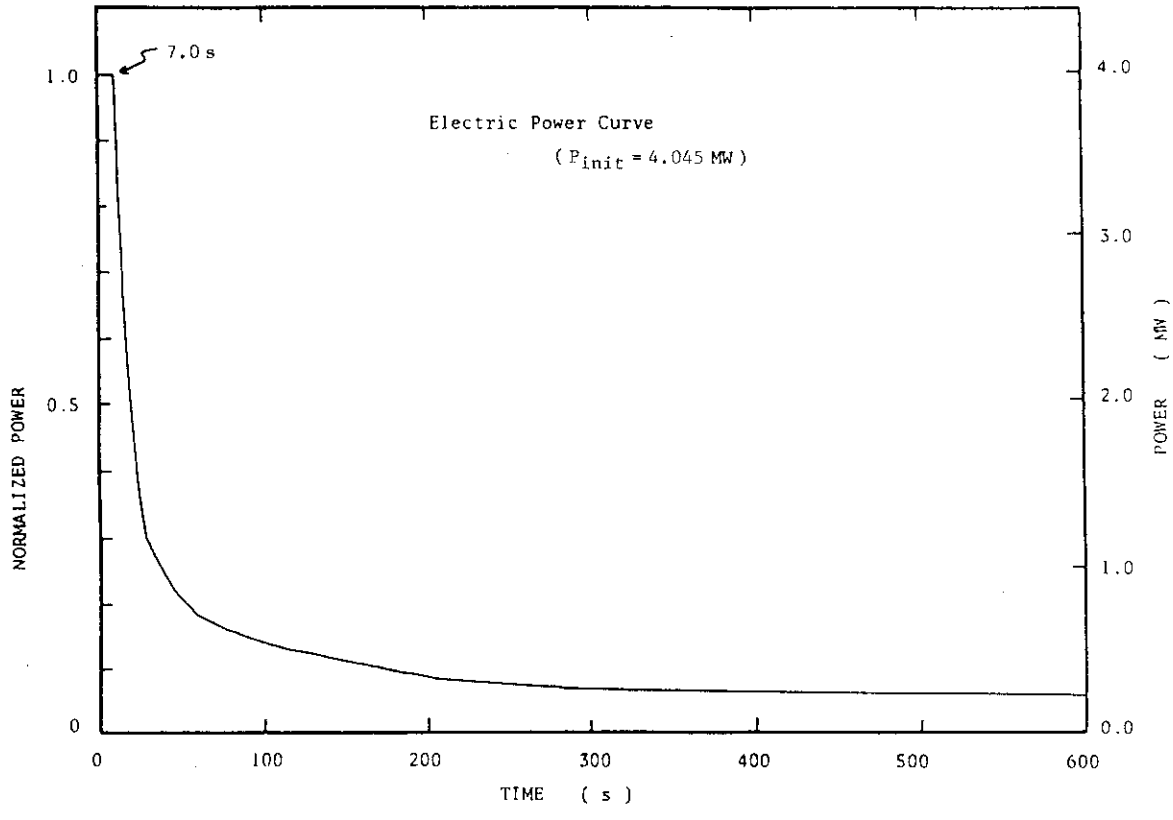


Fig. 4.2 Normalized Power Transient for ROSA-III Test

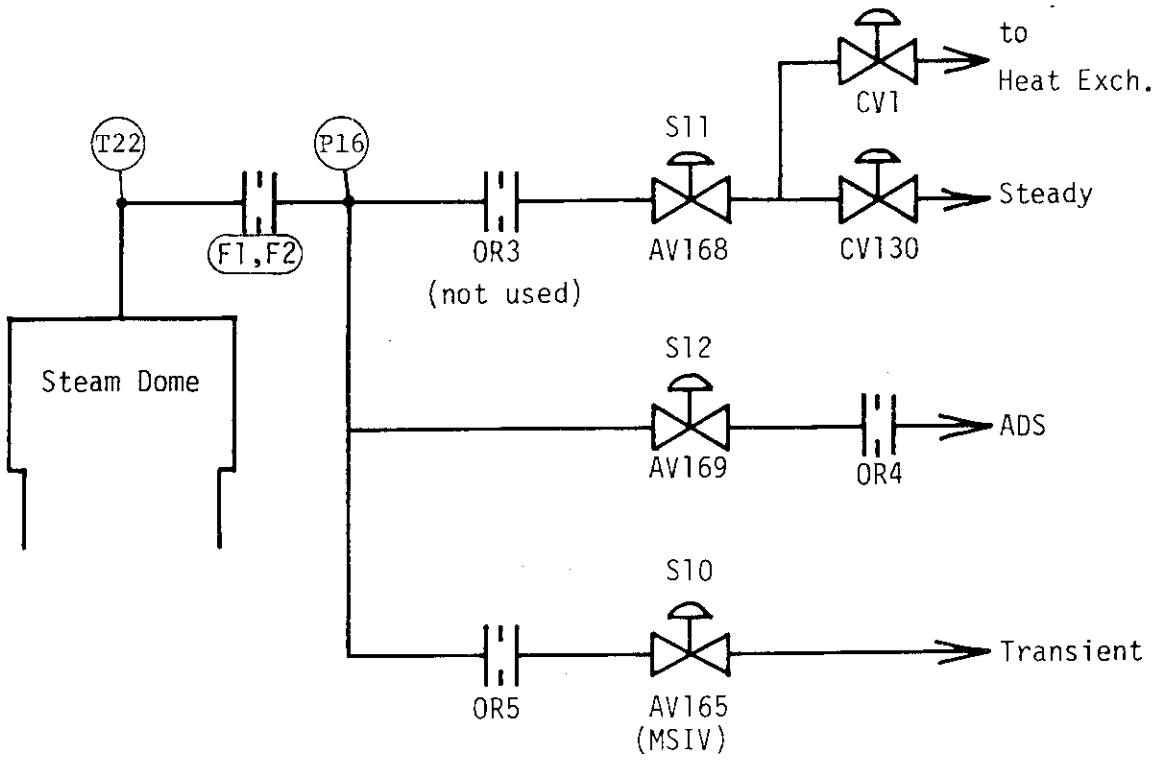


Fig. 4.3 Main Steam Line Schematic

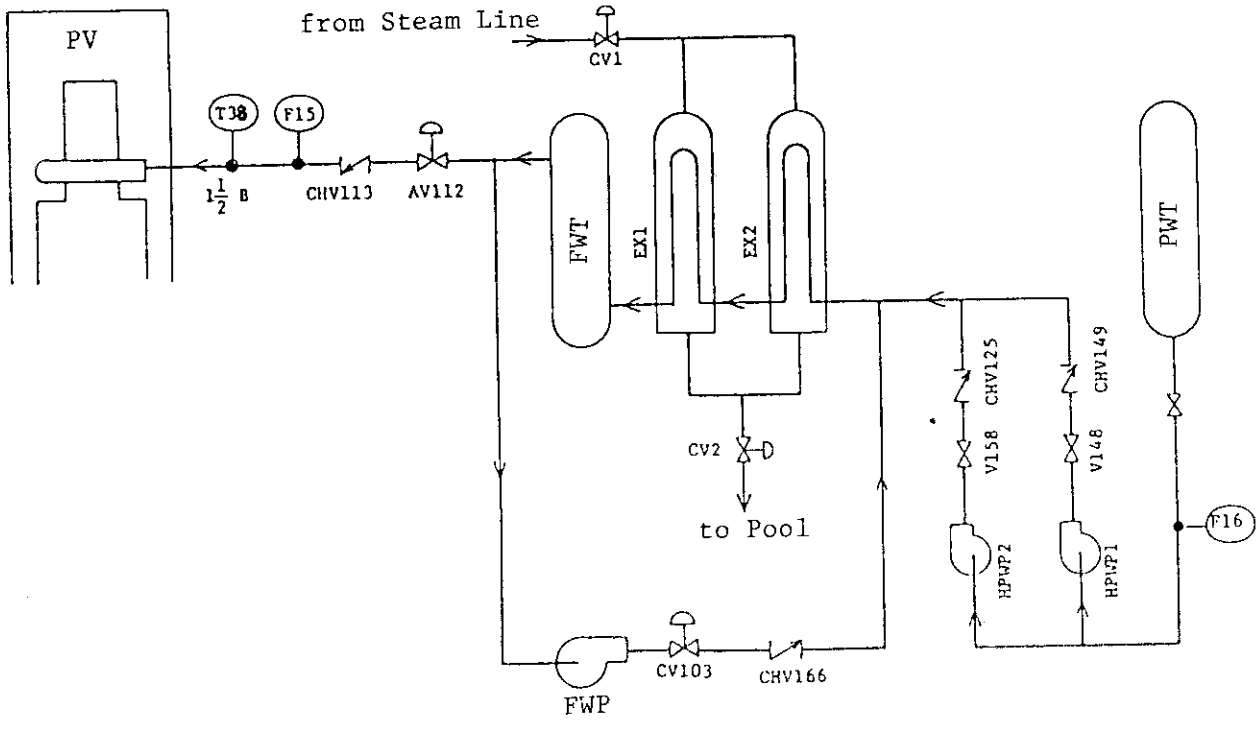


Fig. 4.4 Feedwater Line Schematic

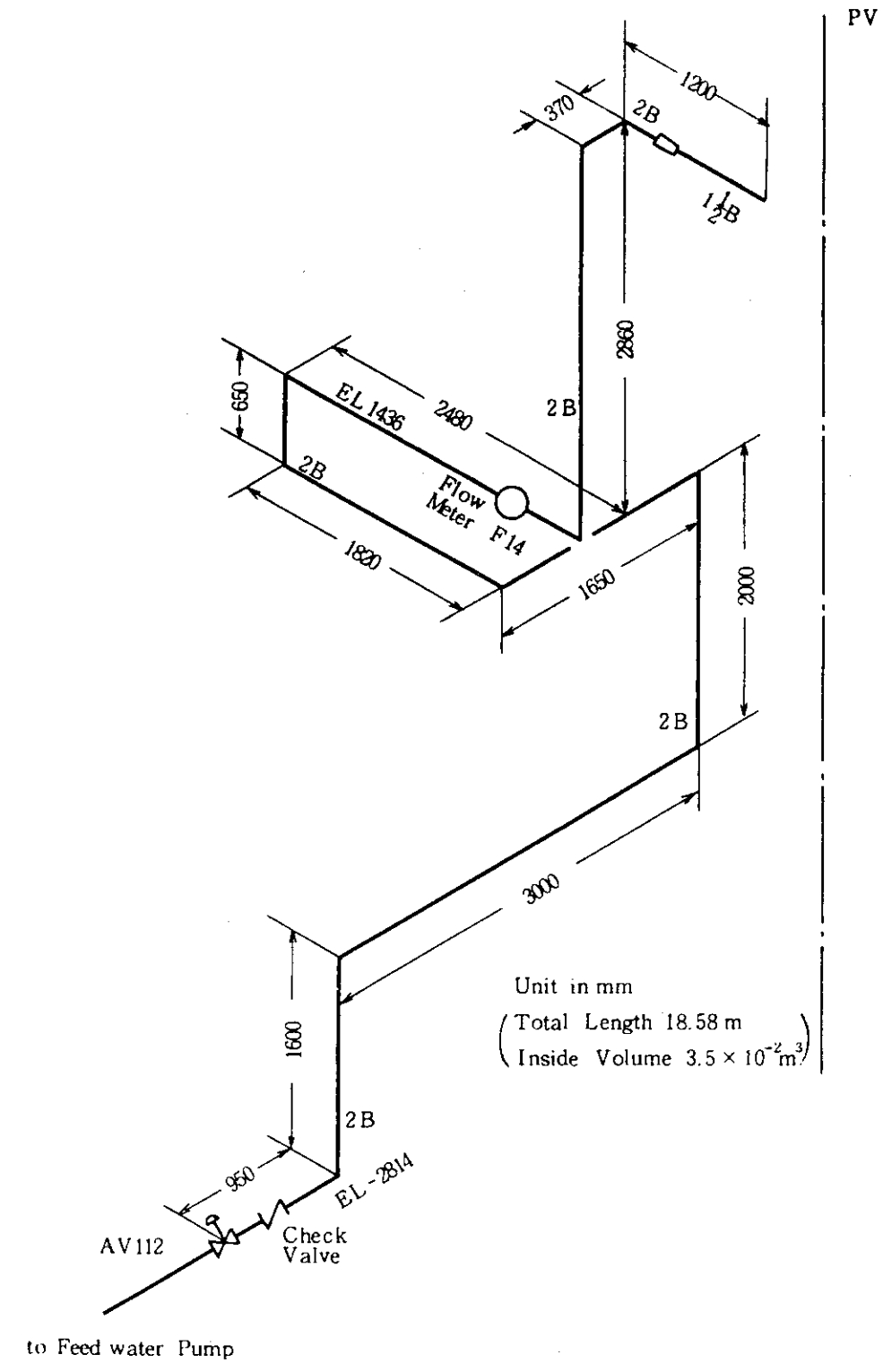


Fig. 4.5　Feedwater Line between Valve AV-112 and Pressure Vessel

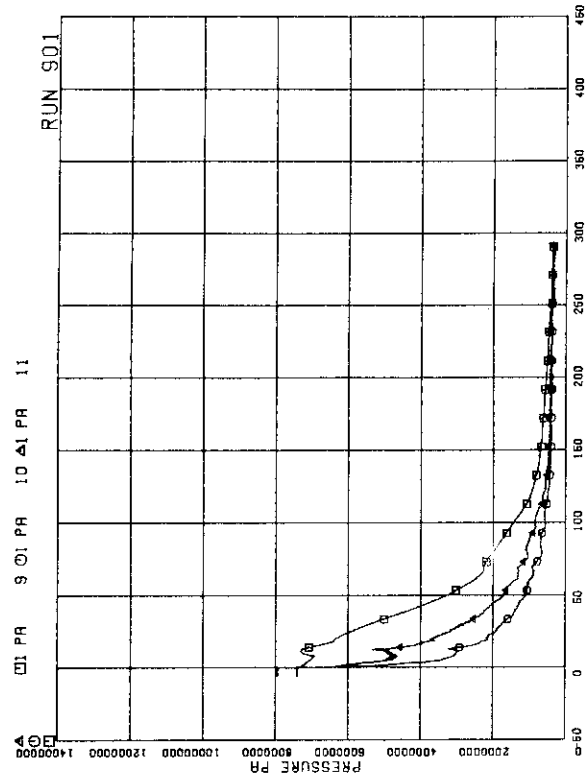


FIG.5. 3 PRESSURE NEAR MRP (MAIN RECIRCULATION PUMP)

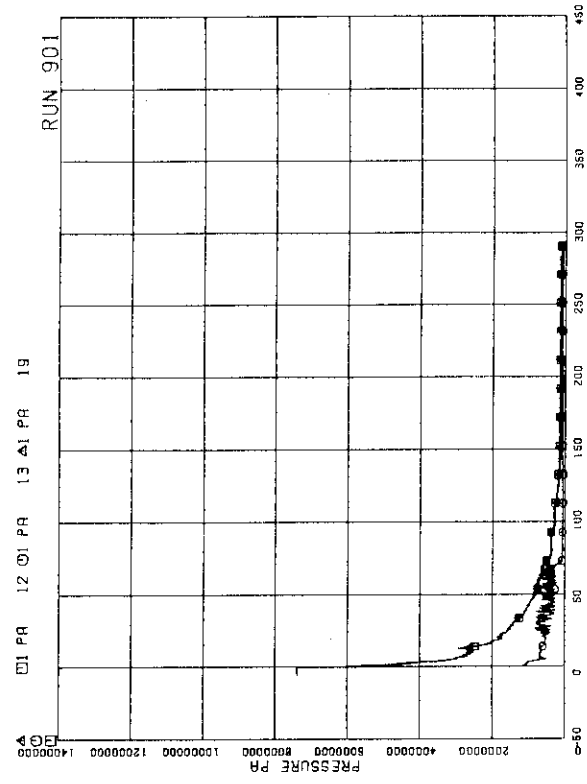


FIG.5. 4 PRESSURE AT MRP SIDE OF BREAK

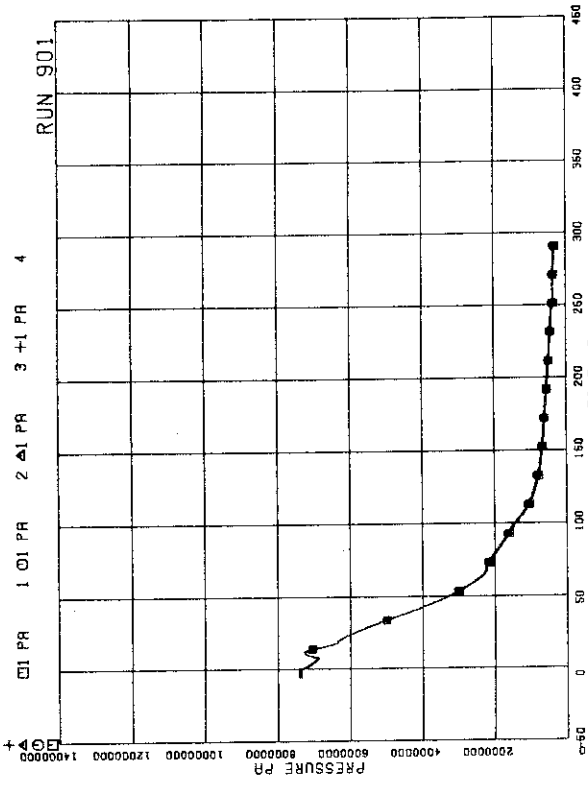


FIG.5. 1 PRESSURE IN PV (PRESSURE VESSEL)

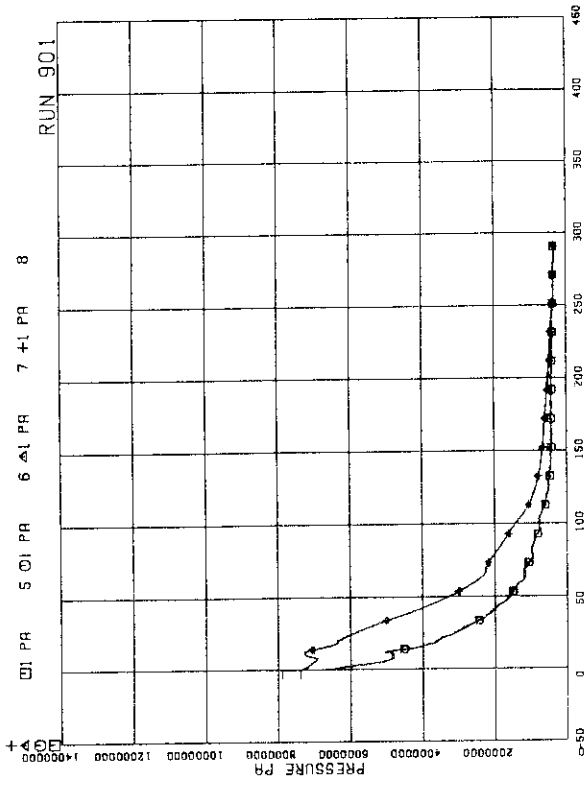


FIG.5. 2 PRESSURE IN BROKEN LOOP JP (JET PUMP)

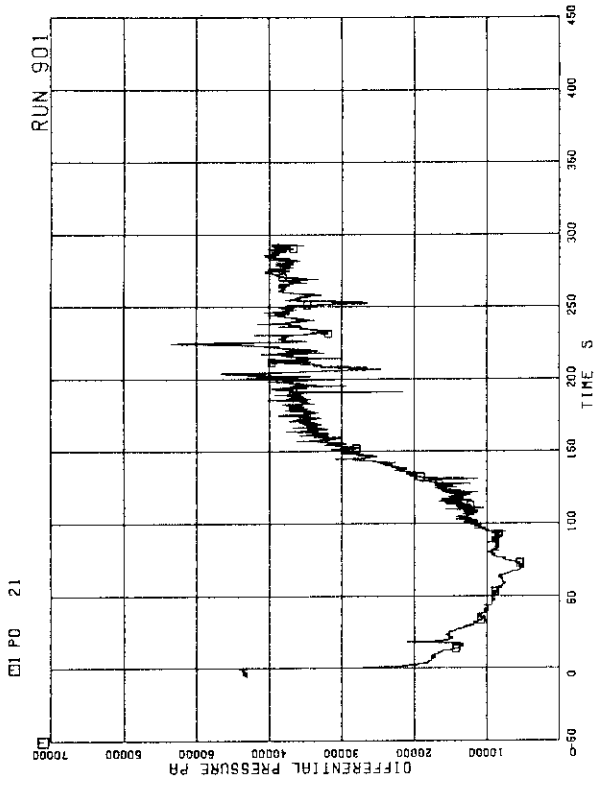


FIG.5. 7 DIFFERENTIAL PRESSURE BETWEEN LOWER PLENUM AND UPPER PLENUM

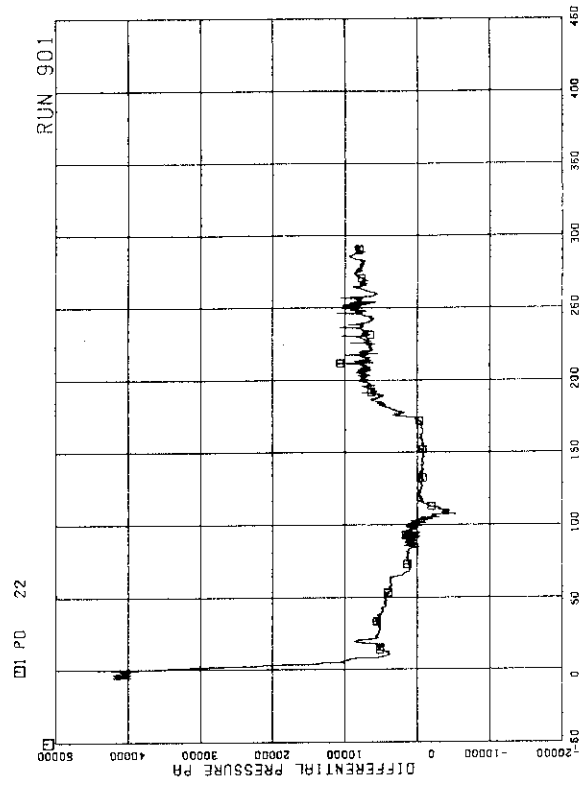


FIG.5. 8 DIFFERENTIAL PRESSURE BETWEEN UPPER PLENUM AND STEAM DOME

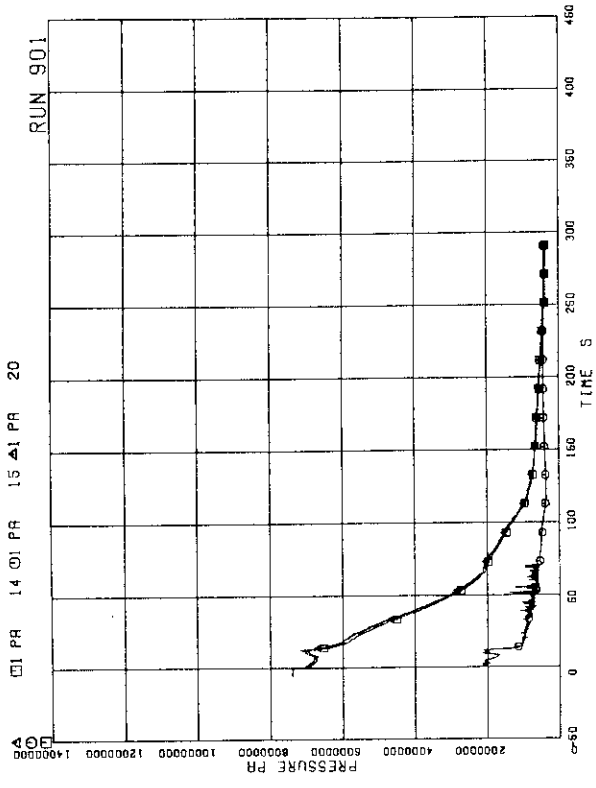


FIG.5. 5 PRESSURE AT PV SIDE OF BREAK

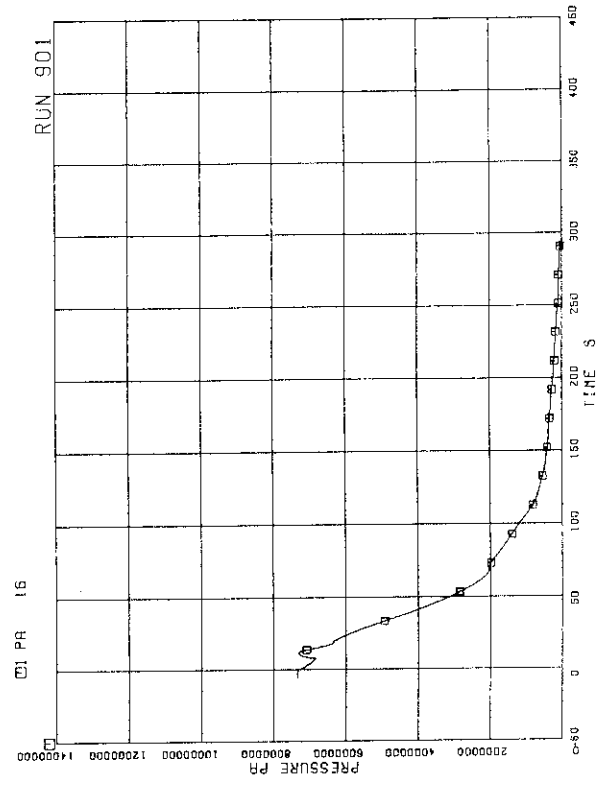


FIG.5. 6 PRESSURE IN MSL (MAIN STEAM LINE)

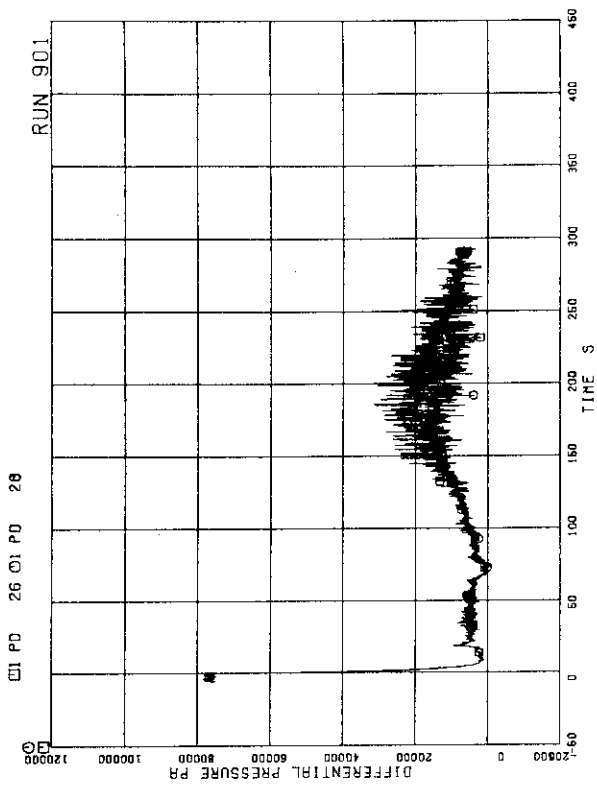


FIG.5. 11 DIFFERENTIAL PRESSURE BETWEEN JP-1.2 DISCHARGE AND SUCTION

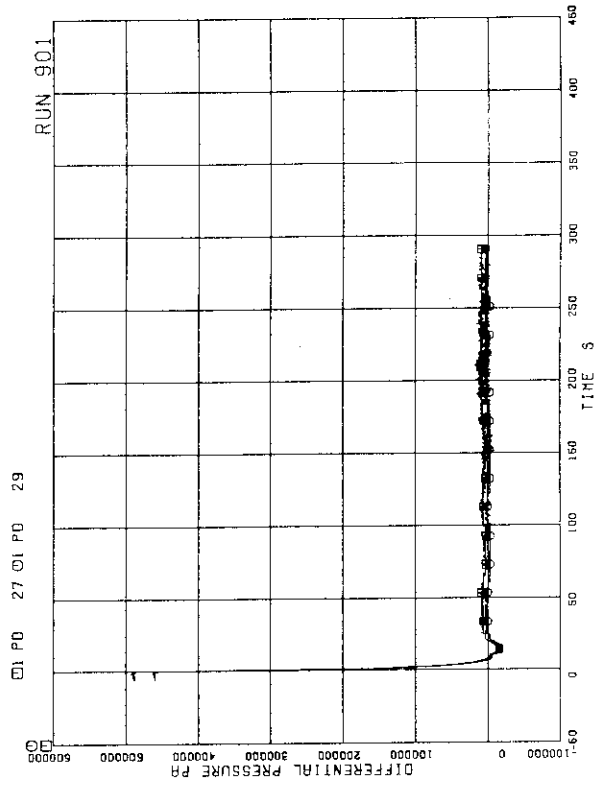


FIG.5. 12 DIFFERENTIAL PRESSURE BETWEEN JP-1.2 DRIVE AND SUCTION

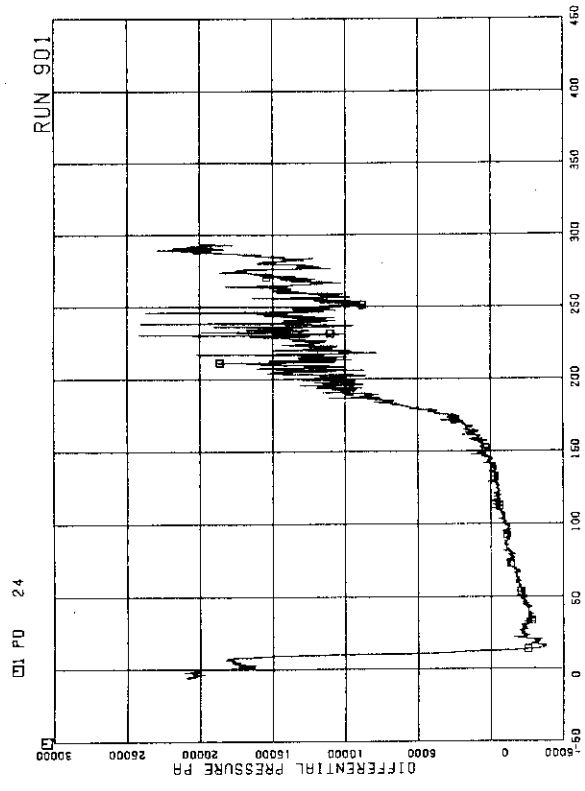


FIG.5. 9 DC (DOWNCOMER) HEAD

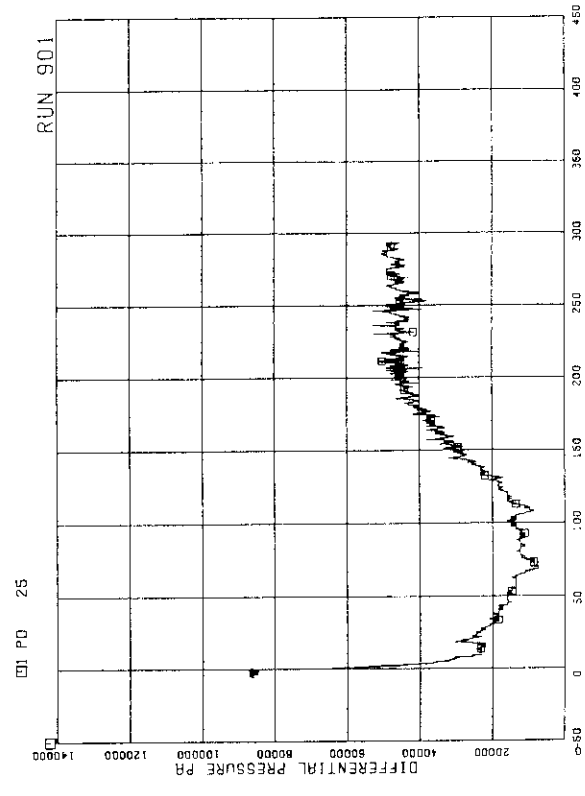


FIG.5. 10 DIFFERENTIAL PRESSURE BETWEEN PV BOTTOM AND TOP

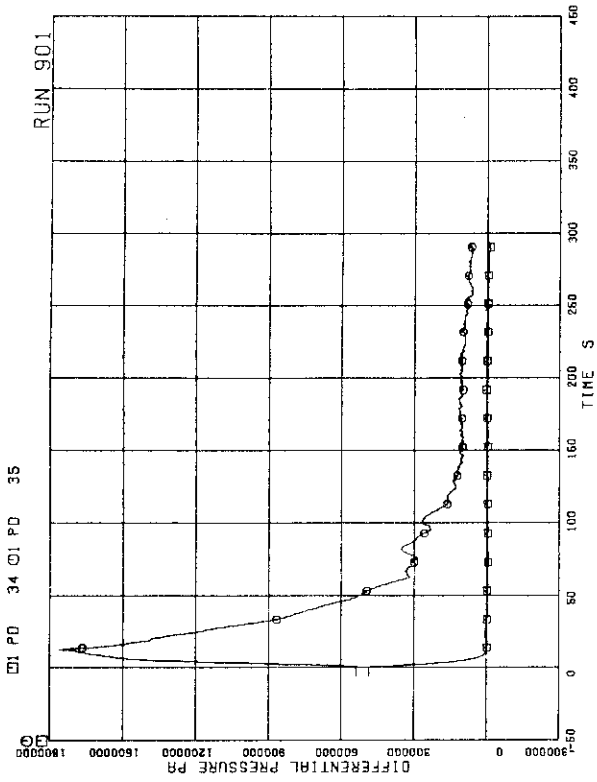


FIG.5. 15 DIFFERENTIAL PRESSURE BETWEEN MRP DELIVERY AND SUCTION

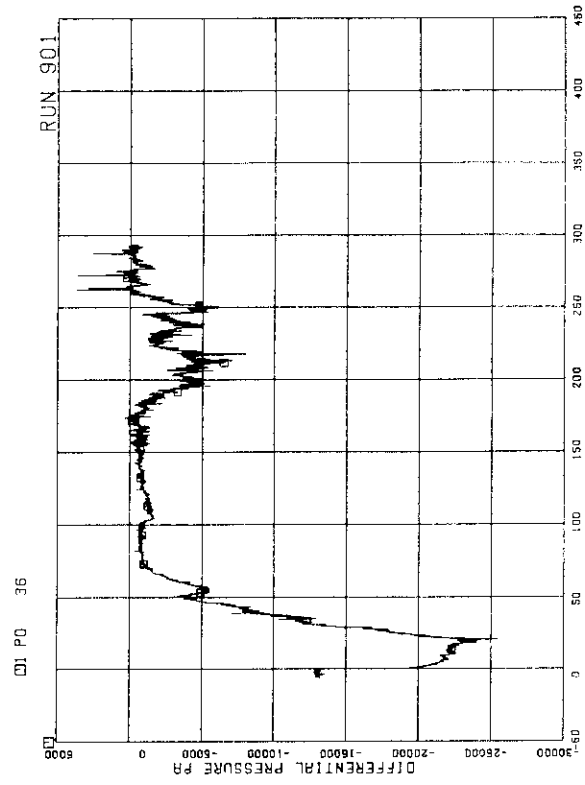


FIG.5. 16 DIFFERENTIAL PRESSURE BETWEEN DOWNCOMER BOTTOM AND MRP1 SUCTION

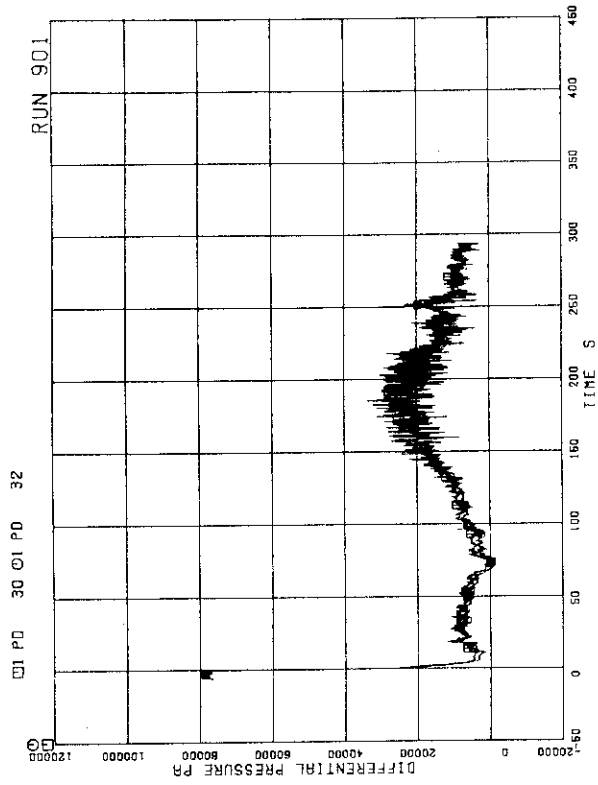


FIG.5. 13 DIFFERENTIAL PRESSURE BETWEEN JP-3,4 DISCHARGE AND SUCTION

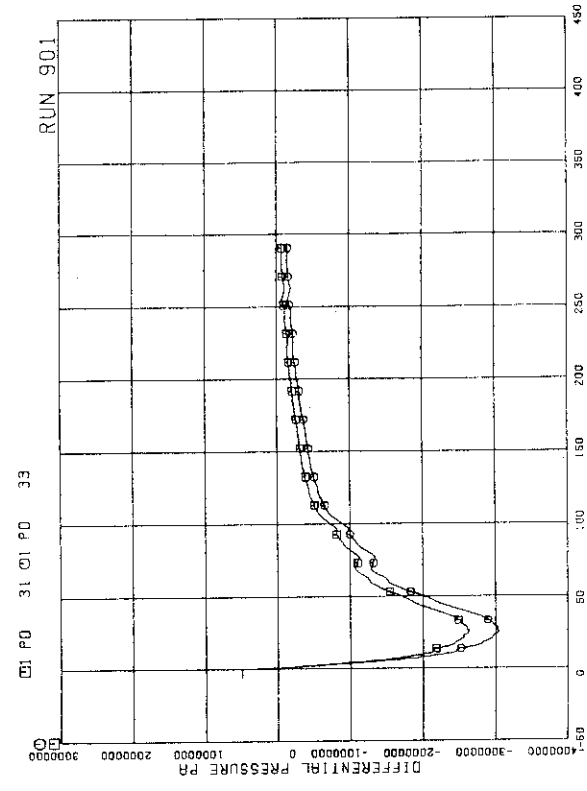


FIG.5. 14 DIFFERENTIAL PRESSURE BETWEEN JP-3,4 DRIVE AND SUCTION

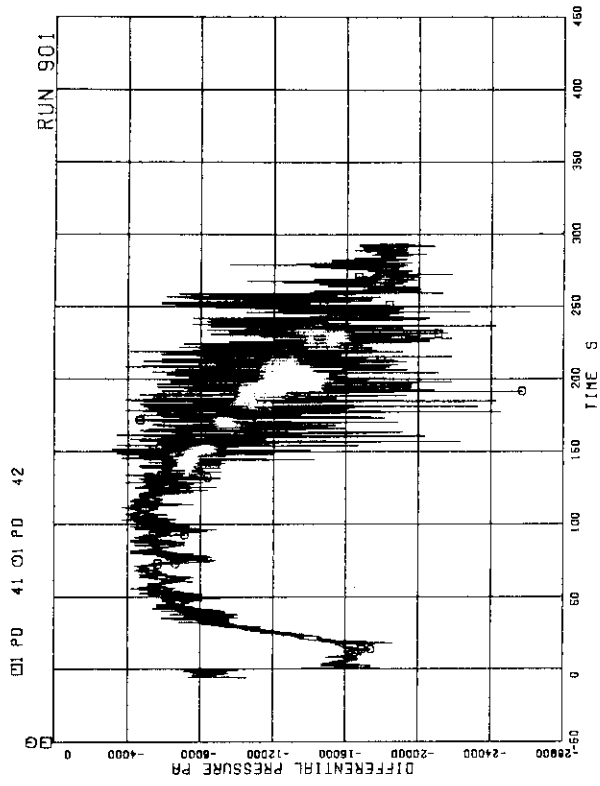


FIG.5. 19 DIFFERENTIAL PRESSURE BETWEEN JP-1.2 DISCHARGE AND LOWER PLENUM

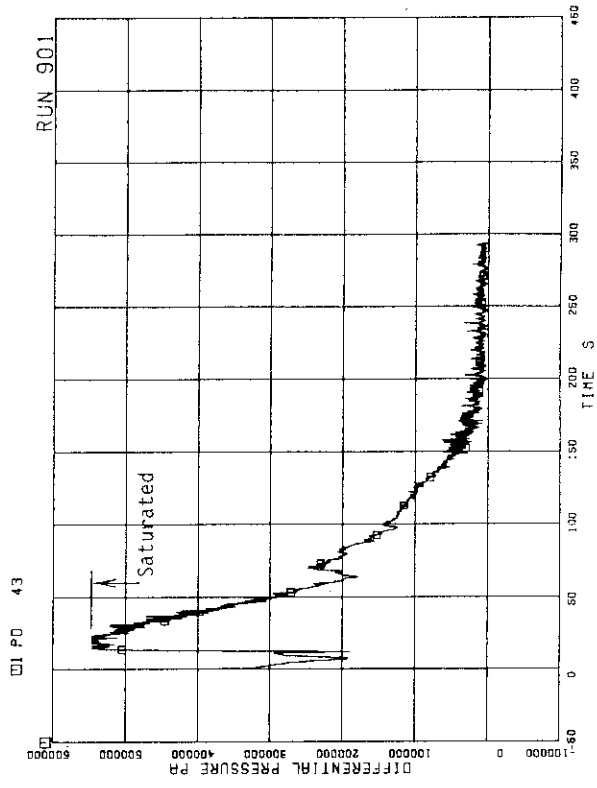


FIG.5. 20 DIFFERENTIAL PRESSURE BETWEEN DOWNCOMER BOTTOM AND BREAK B

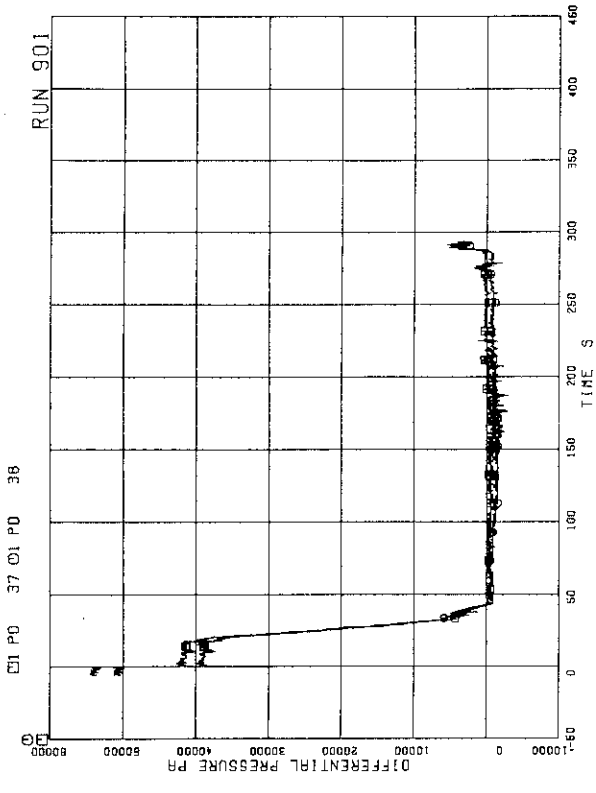


FIG.5. 17 DIFFERENTIAL PRESSURE BETWEEN MRP DELIVERY AND JP-1.2 SUCTION

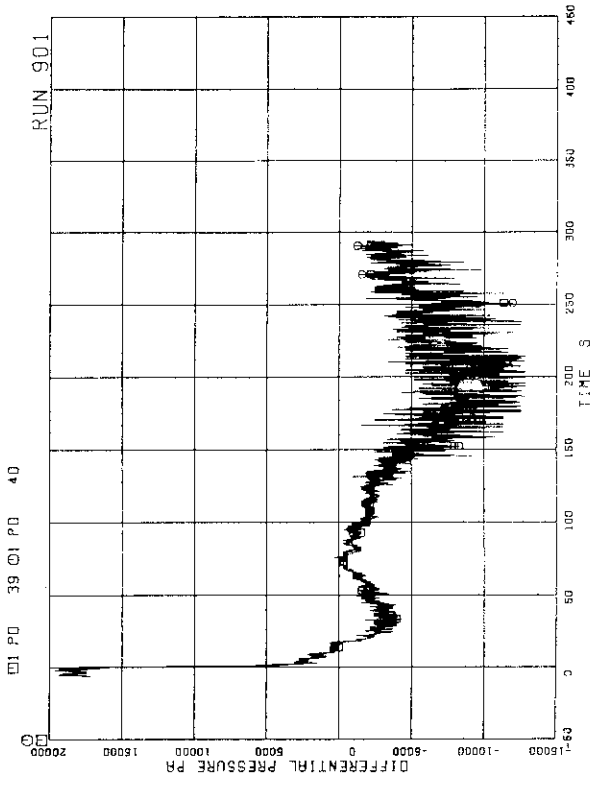


FIG.5. 18 DIFFERENTIAL PRESSURE BETWEEN DOWNCOMER MIDDLE AND JP-1.2 SUCTION

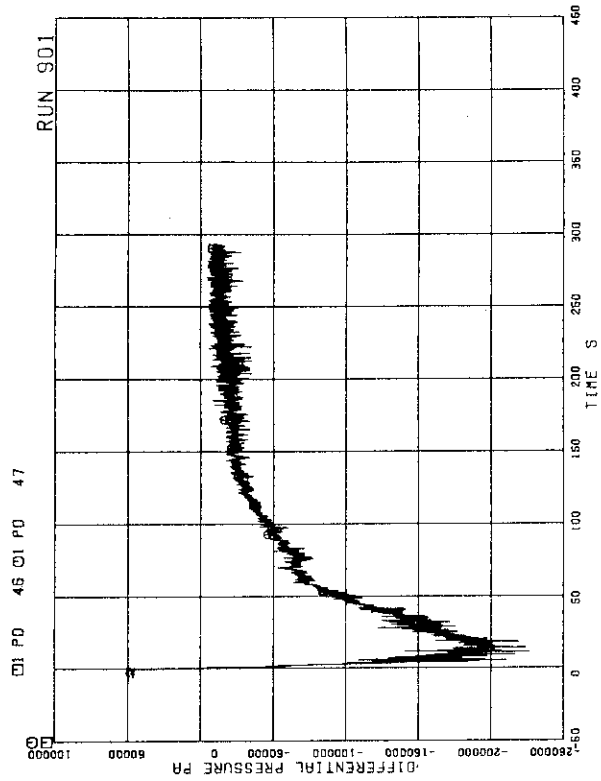


FIG.5. 21 DIFFERENTIAL PRESSURE BETWEEN BREAKS A AND B




FIG.5. 23 DIFFERENTIAL PRESSURE BETWEEN MRP DELIVERY AND JP-3,4 DRIVE

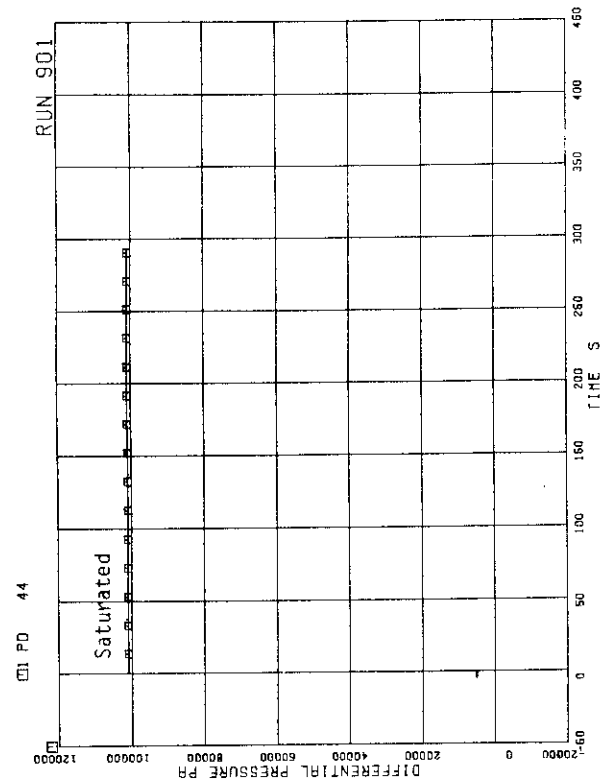


FIG.5. 22 DIFFERENTIAL PRESSURE BETWEEN BREAK A AND MRP2 SUCTION




FIG.5. 24 DIFFERENTIAL PRESSURE BETWEEN DOWNCOMER MIDDLE AND JP-3,4 SUCTION

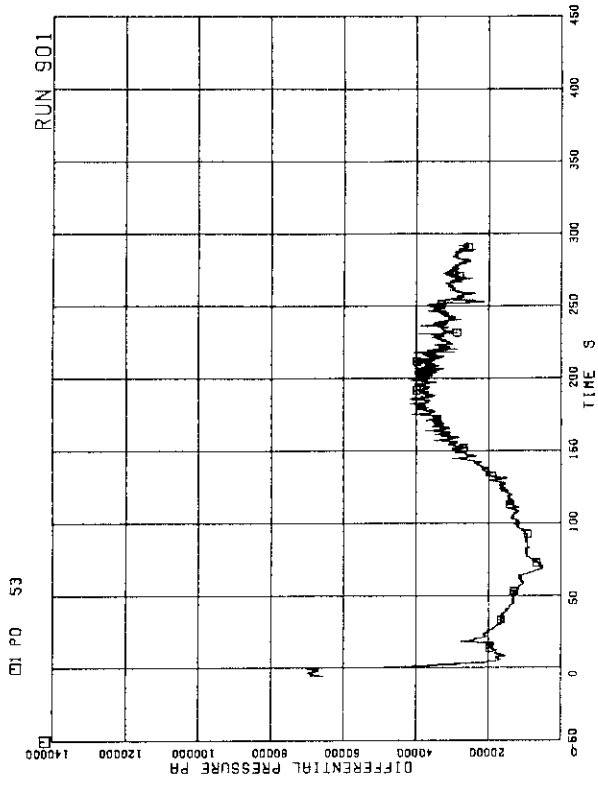


FIG.5. 27 DIFFERENTIAL PRESSURE BETWEEN LOWER PLENUM AND DOWNCOMER MIDDLE

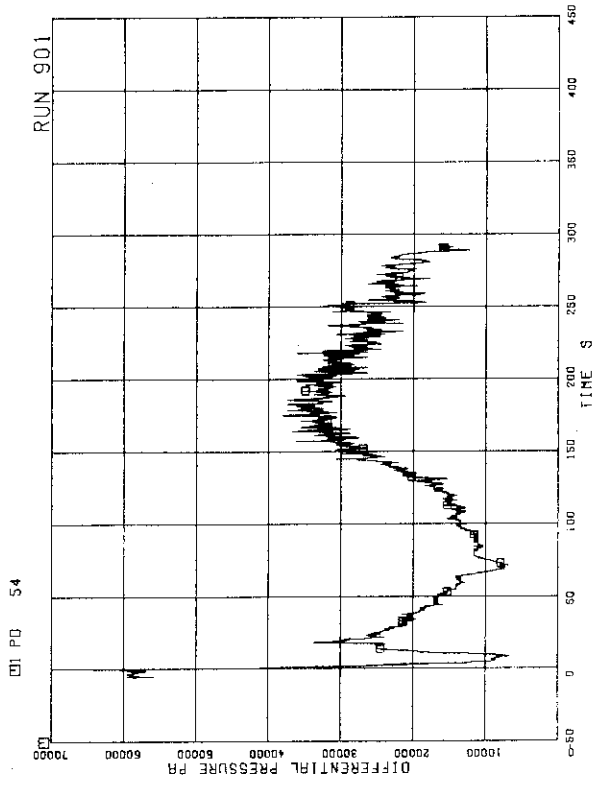


FIG.5. 28 DIFFERENTIAL PRESSURE BETWEEN LOWER PLENUM AND DOWNCOMER BOTTOM

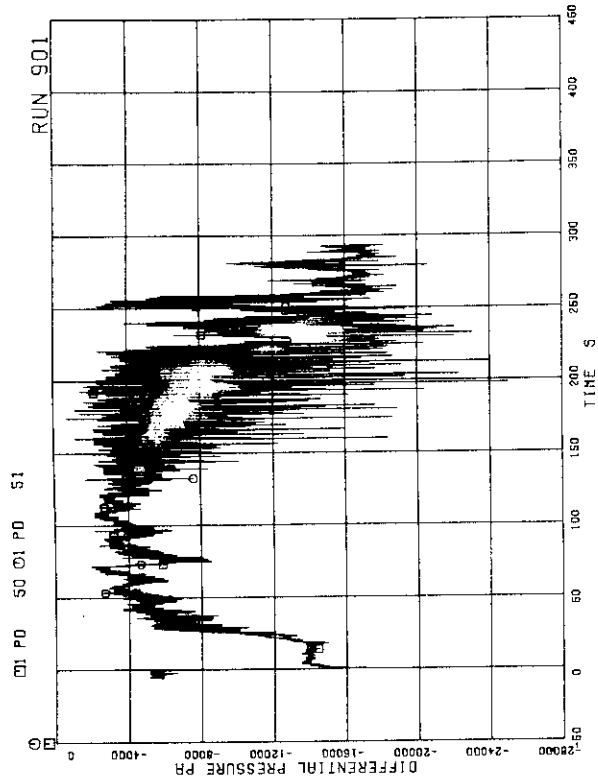


FIG.5. 25 DIFFERENTIAL PRESSURE BETWEEN JP-3,4 DISCHARGE AND CONFLURNCE

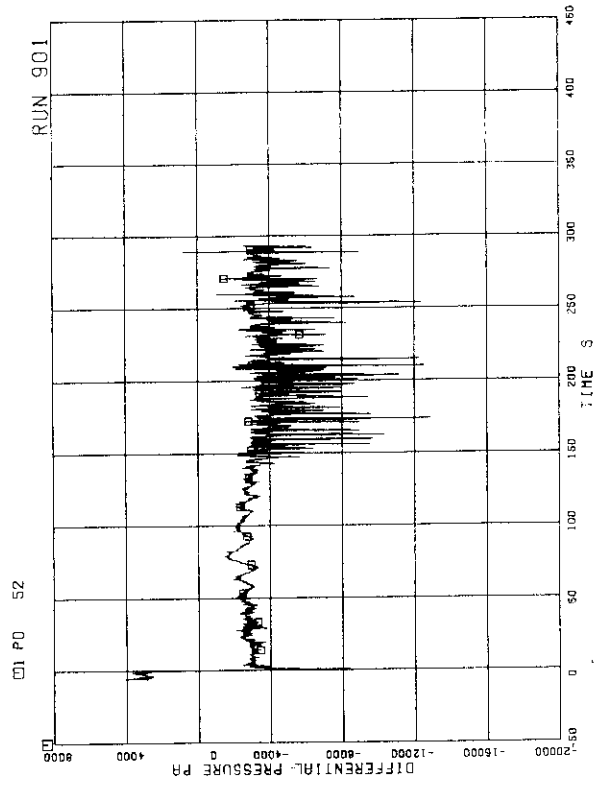


FIG.5. 26 DIFFERENTIAL PRESSURE BETWEEN JP-3,4 CONFLUENCE IN BROKEN LOOP AND LP

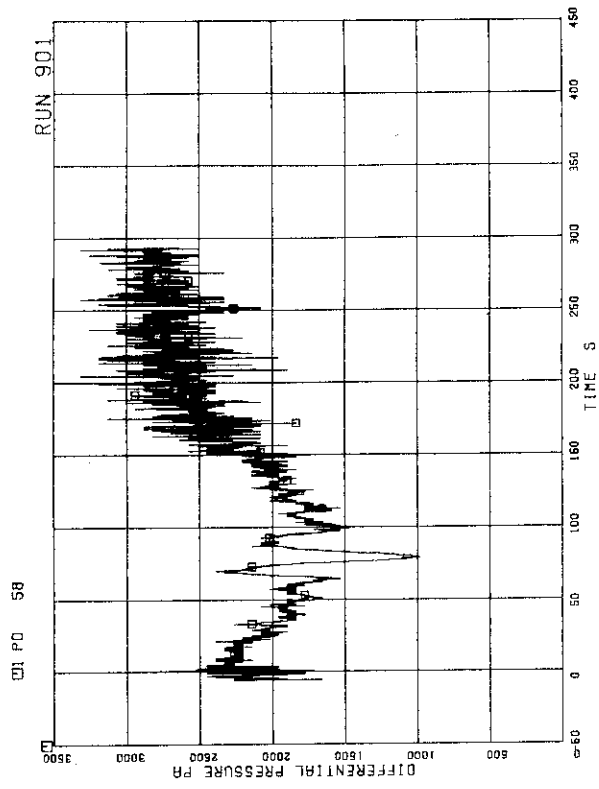


FIG.5. 31 DIFFERENTIAL PRESSURE BETWEEN LP BOTTOM AND LP MIDDLE

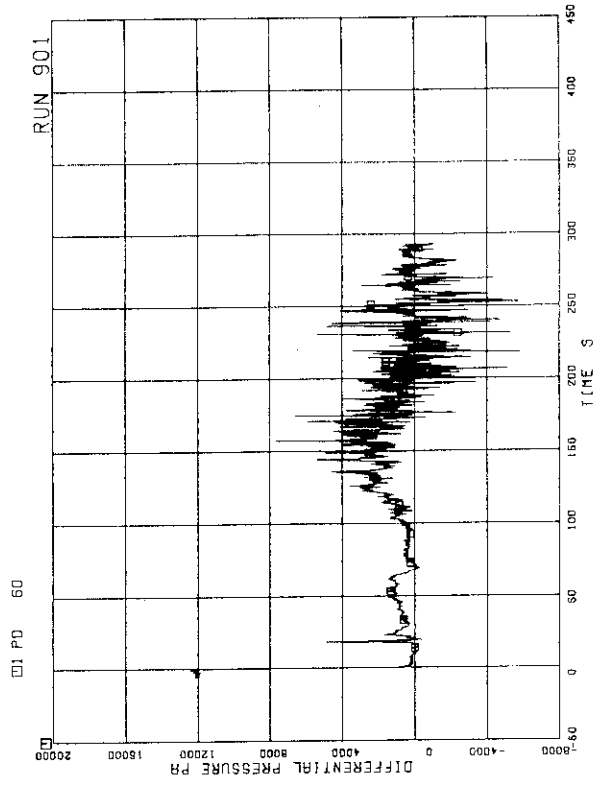


FIG.5. 32 DIFFERENTIAL PRESSURE ACROSS CHANNEL INLET ORIFICE 9

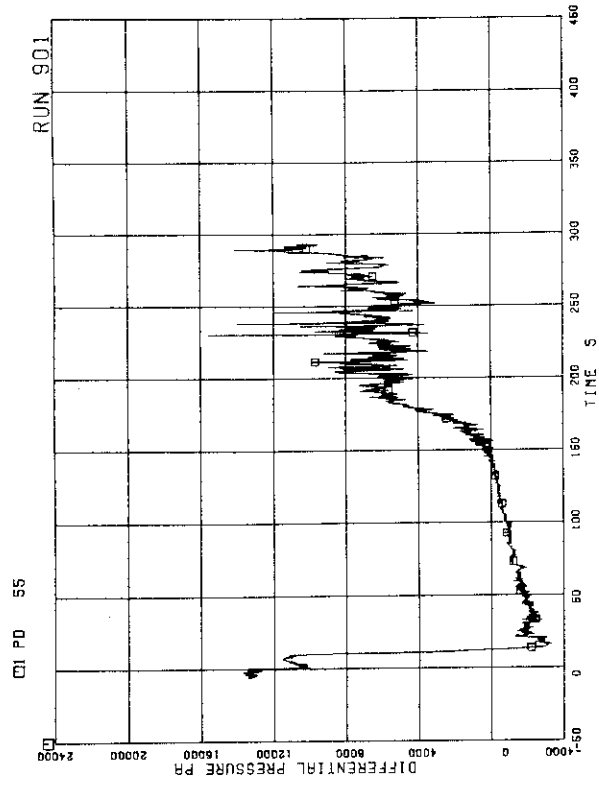


FIG.5. 29 DIFFERENTIAL PRESSURE BETWEEN DOWNCOMER BOTTOM AND DOWNCOMER MIDDLE

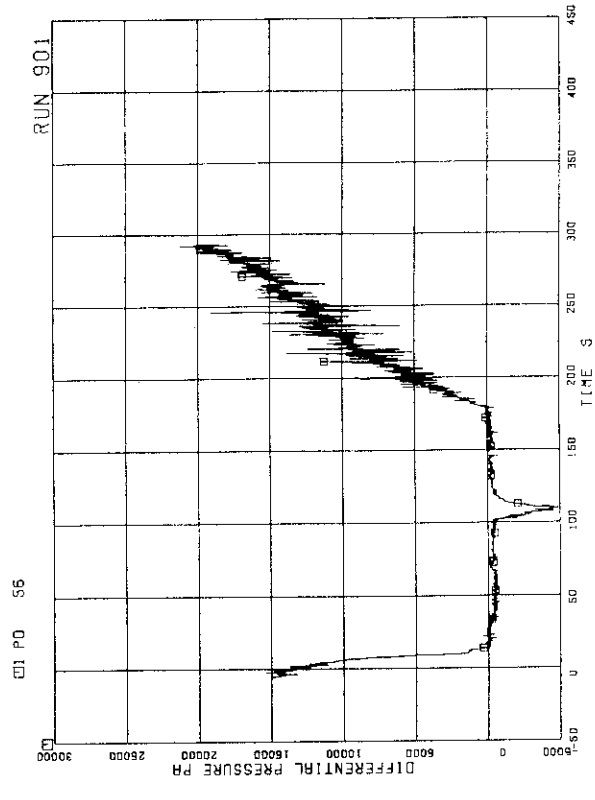


FIG.5. 30 DIFFERENTIAL PRESSURE BETWEEN DOWNCOMER MIDDLE AND STEAM DOME

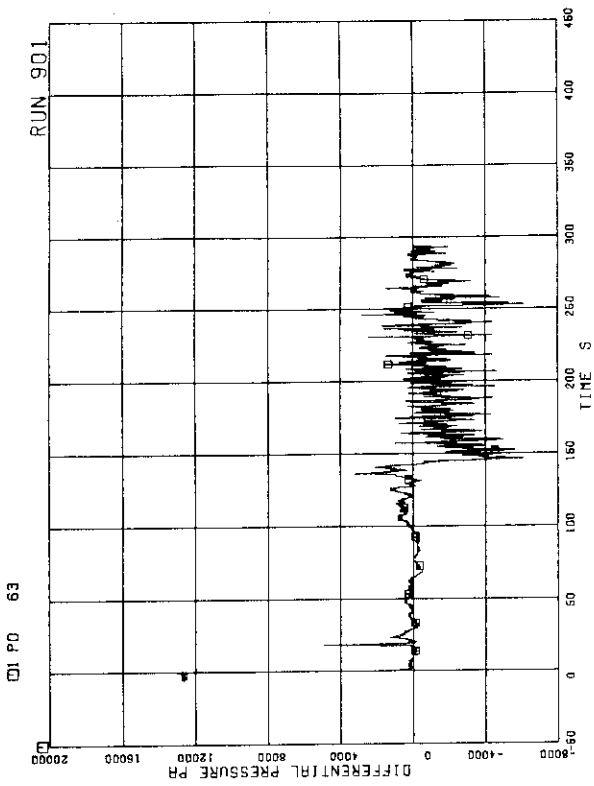


FIG.5. 35 DIFFERENTIAL PRESSURE ACROSS CHANNEL INLET ORIFICE D

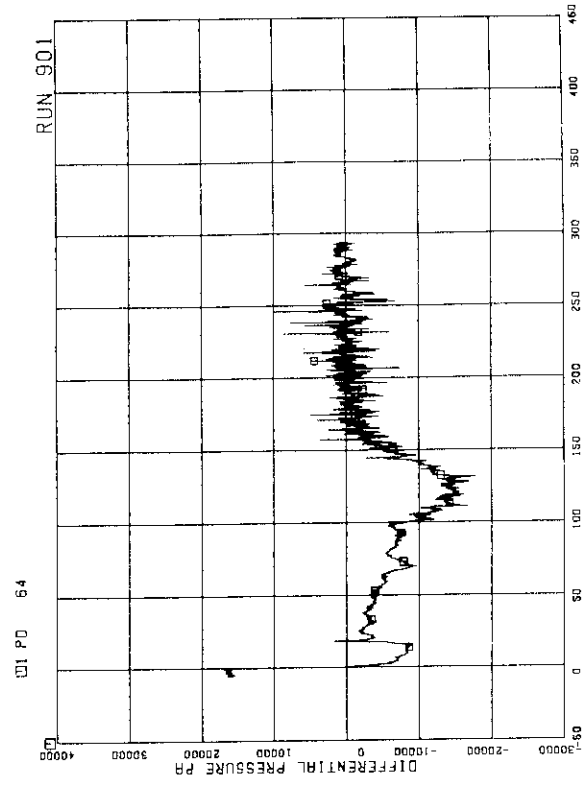


FIG.5. 36 DIFFERENTIAL PRESSURE ACROSS BYPASS HOLE

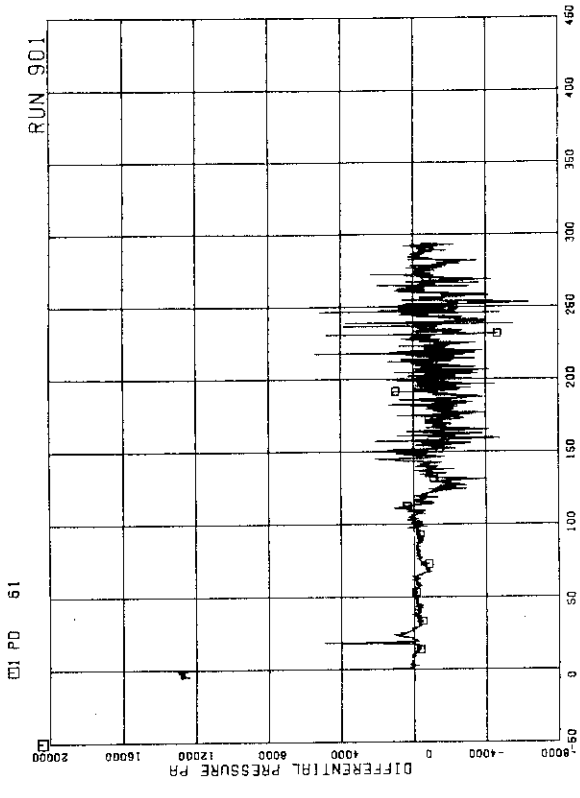


FIG.5. 33 DIFFERENTIAL PRESSURE ACROSS CHANNEL INLET ORIFICE B

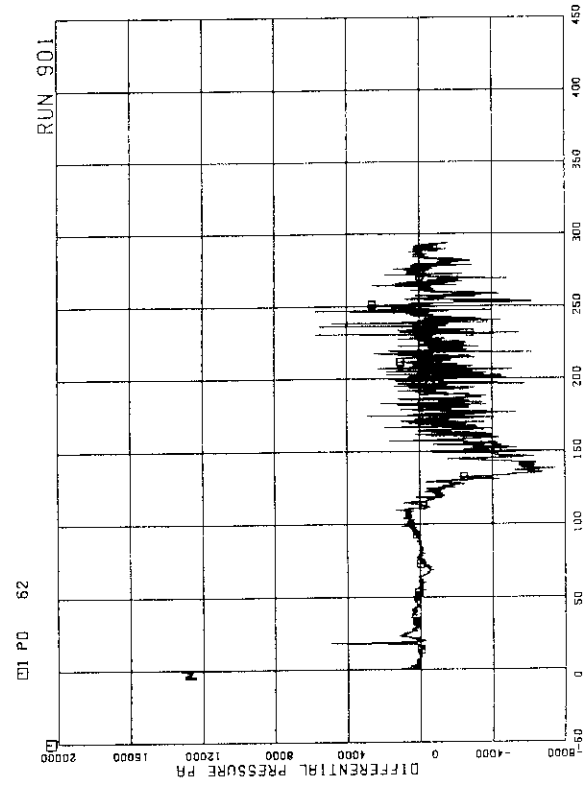


FIG.5. 34 DIFFERENTIAL PRESSURE ACROSS CHANNEL INLET ORIFICE C

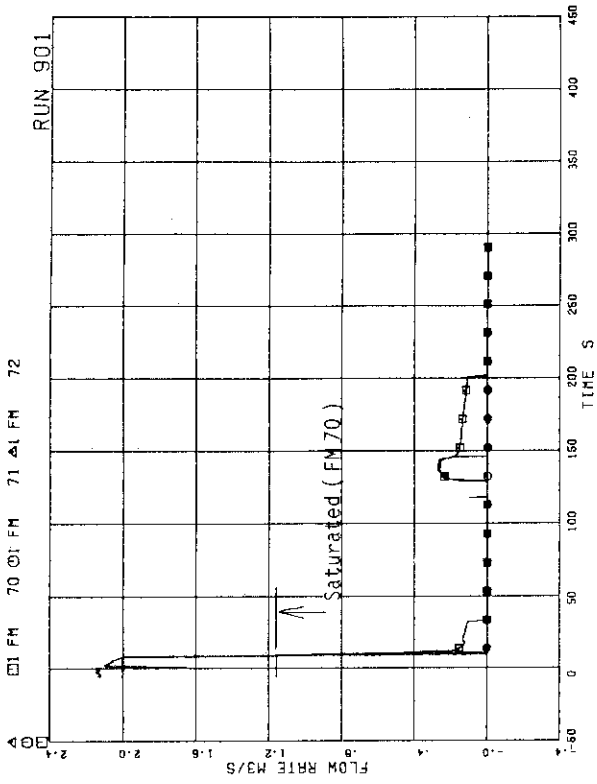


FIG.5. 39 MASS FLOW RATE IN MSL

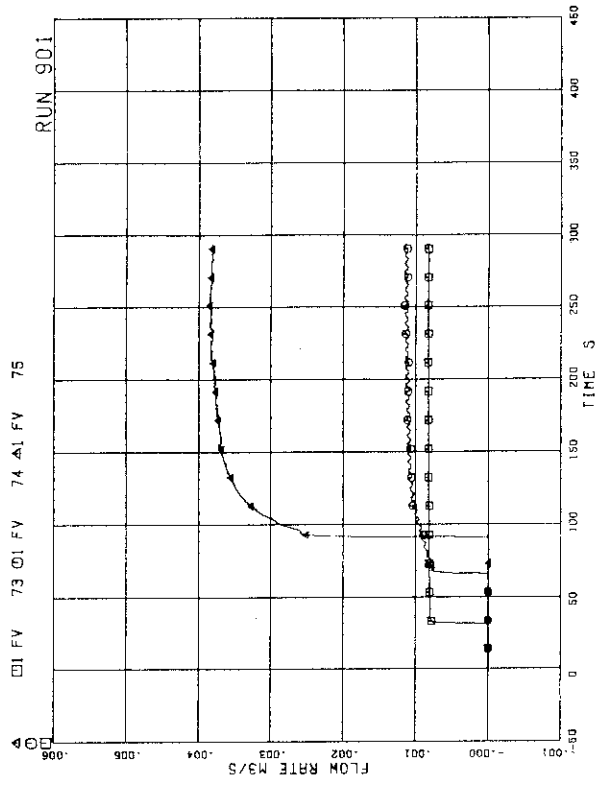


FIG.5. 40 ECC INJECTION FLOW RATE

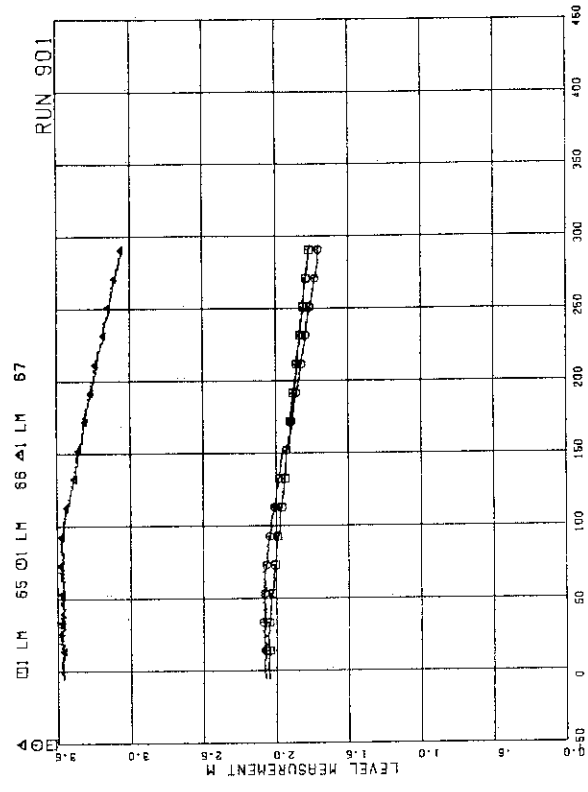


FIG.5. 37 LIQUID LEVELS IN ECCS TANKS

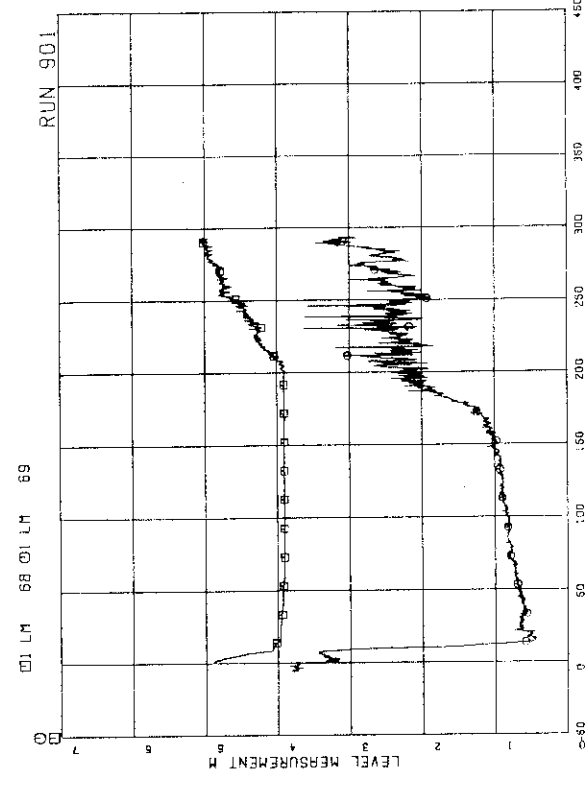


FIG.5. 38 LIQUID LEVELS IN DOWNCOMER

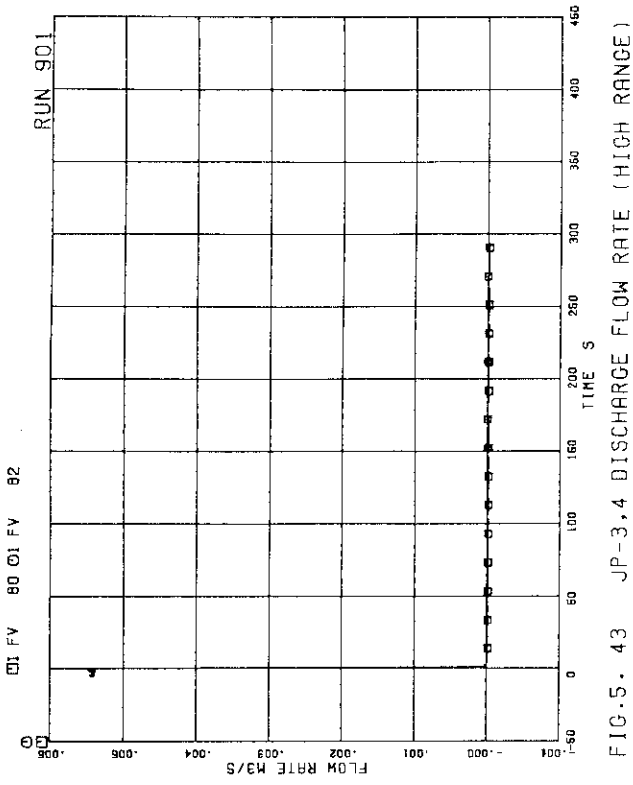


FIG.5. 43 JP-3,4 DISCHARGE FLOW RATE (HIGH RANGE)

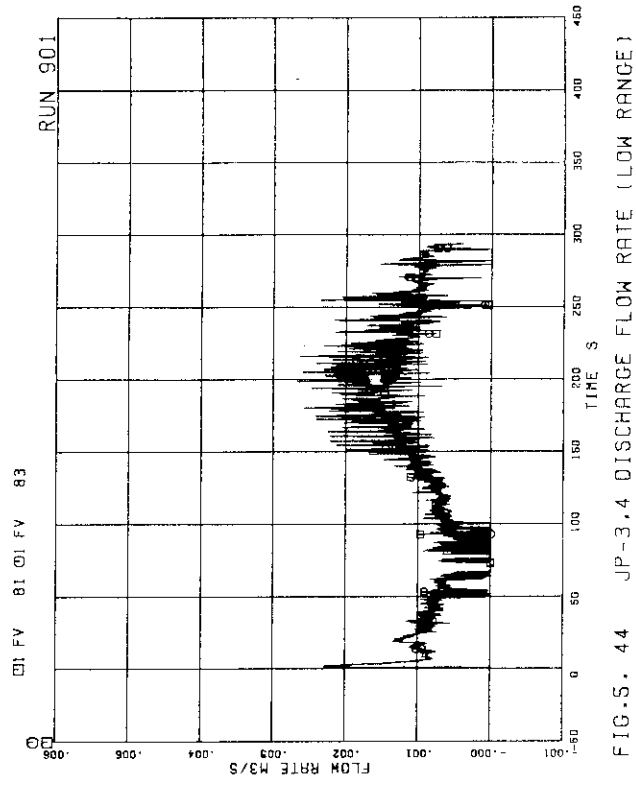


FIG.5. 44 JP-3,4 DISCHARGE FLOW RATE (LOW RANGE)

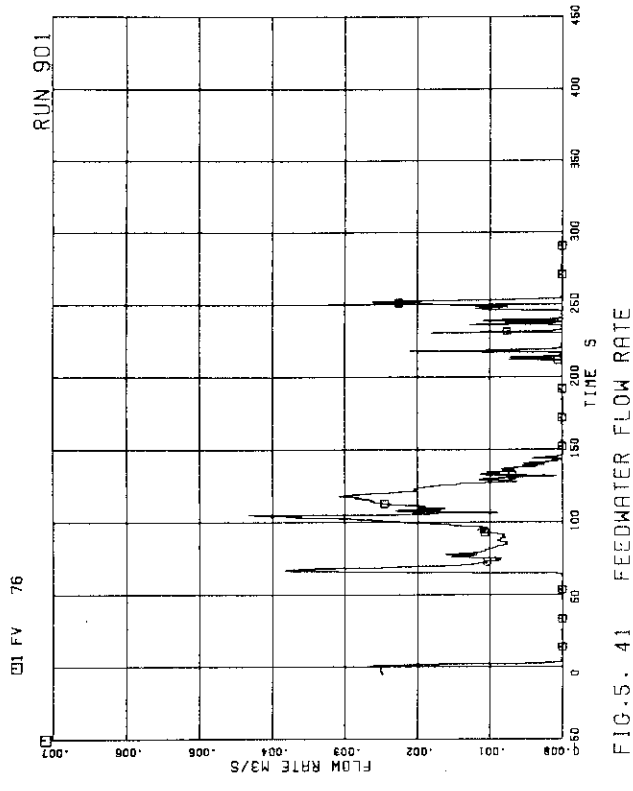


FIG.5. 41 FEEDWATER FLOW RATE

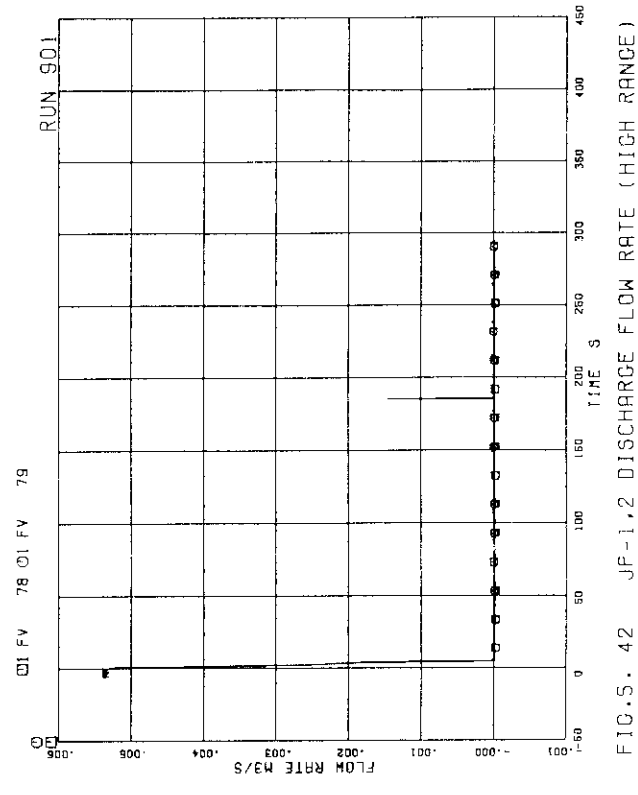


FIG.5. 42 JF-1,2 DISCHARGE FLOW RATE (HIGH RANGE)

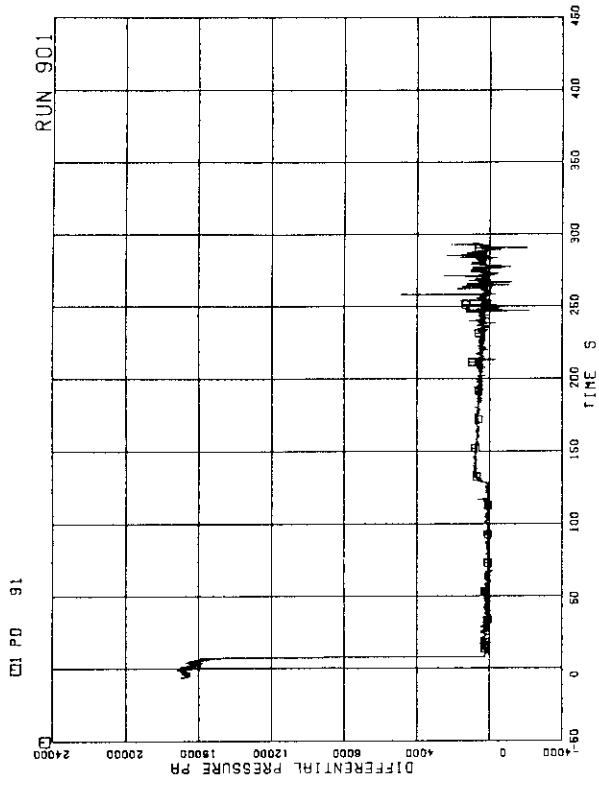


FIG.5. 47 DIFFERENTIAL PRESSURE ACROSS ORIFICE FLOWMETER F-2

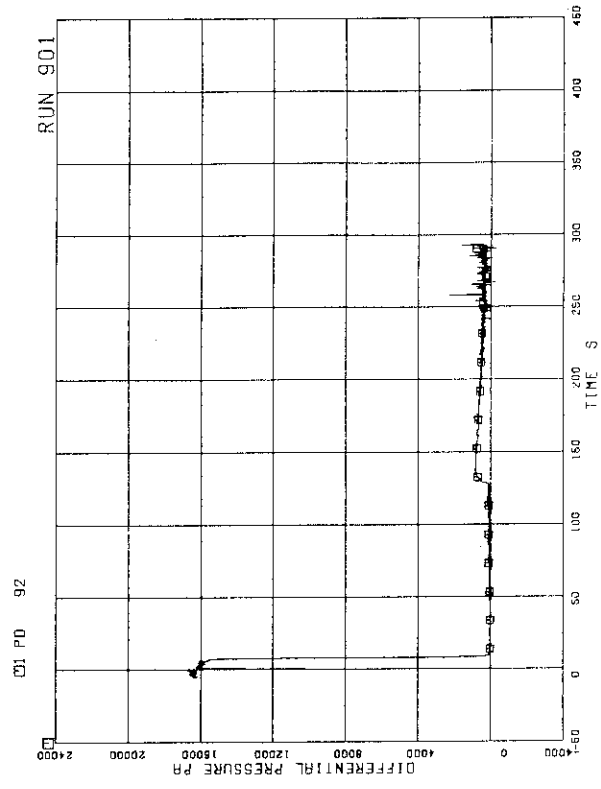


FIG.5. 48 DIFFERENTIAL PRESSURE ACROSS ORIFICE FLOWMETER F-3

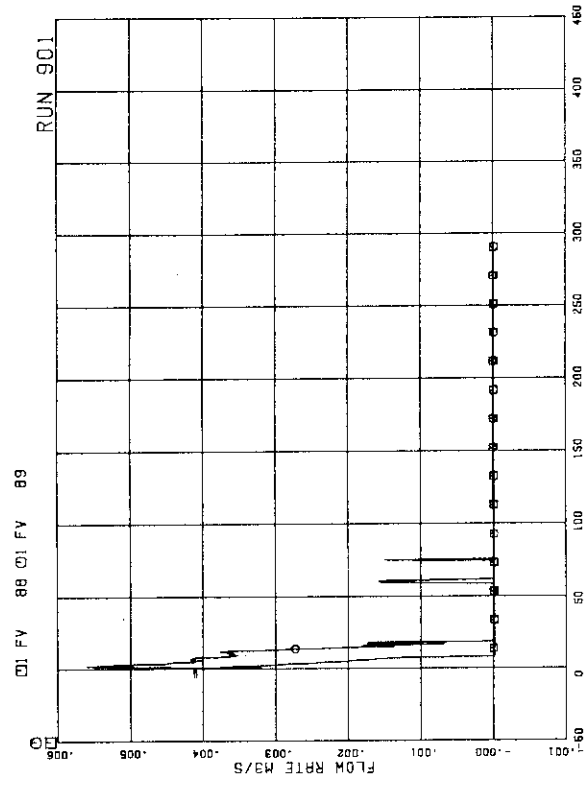


FIG.5. 45 MRP DISCHARGE FLOW RATE

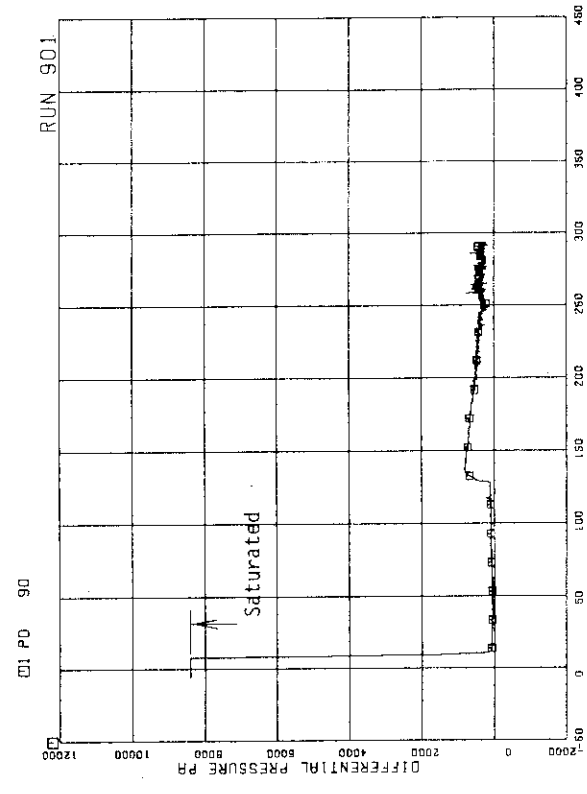


FIG.5. 46 DIFFERENTIAL PRESSURE ACROSS ORIFICE FLOWMETER F-1

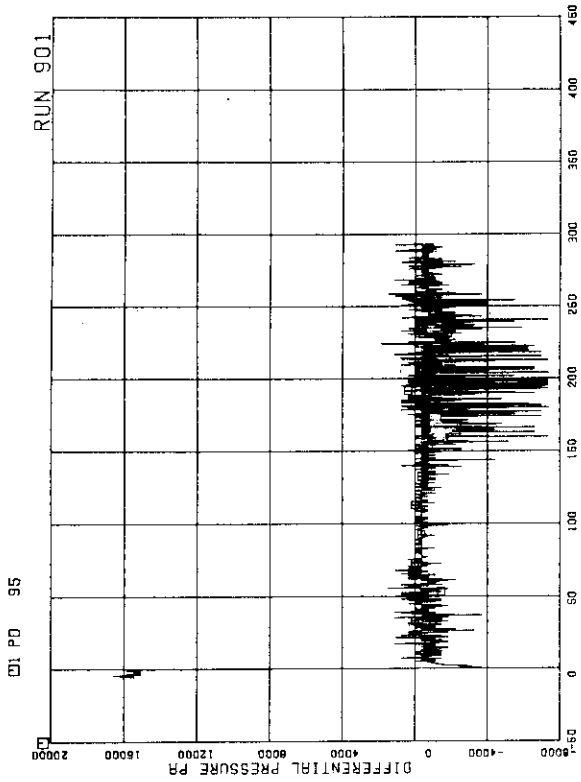


FIG.5. 51 DIFFERENTIAL PRESSURE ACROSS ORIFICE FLOWMETER F-19

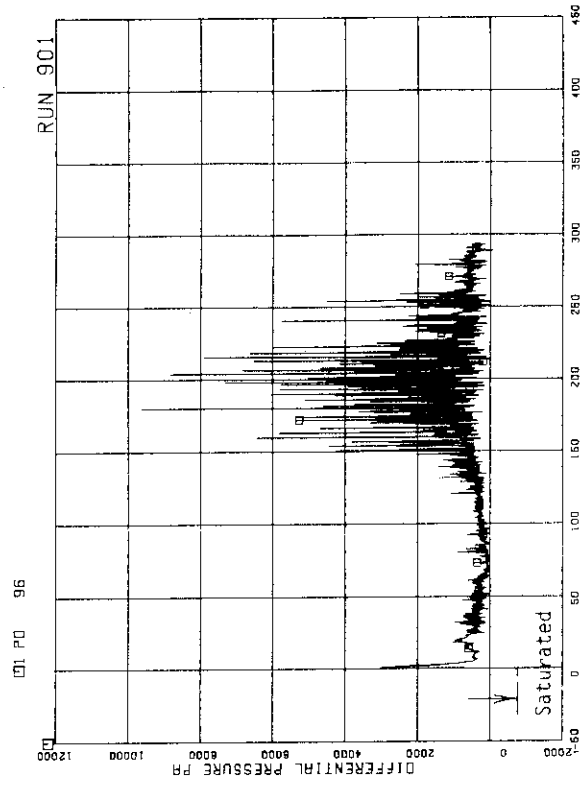


FIG.5. 52 DIFFERENTIAL PRESSURE ACROSS ORIFICE FLOWMETER F-20

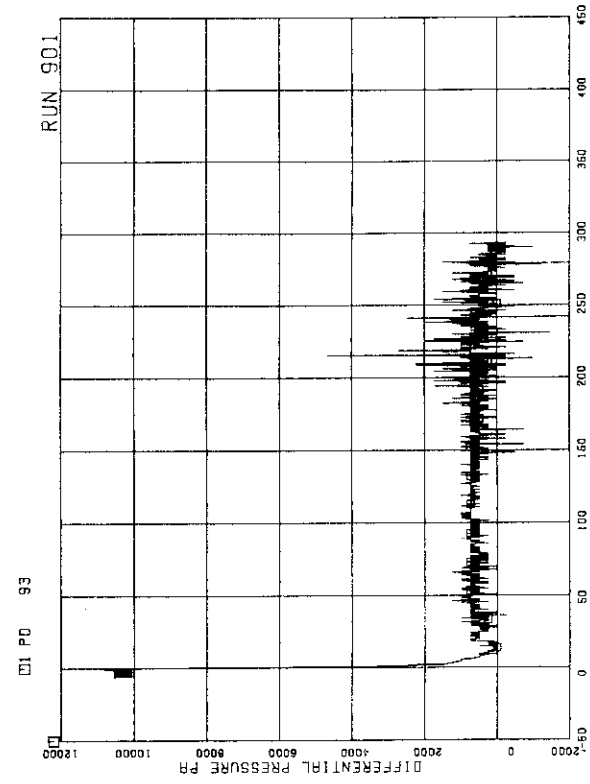


FIG.5. 49 DIFFERENTIAL PRESSURE ACROSS VENTURI FLOWMETER F-17

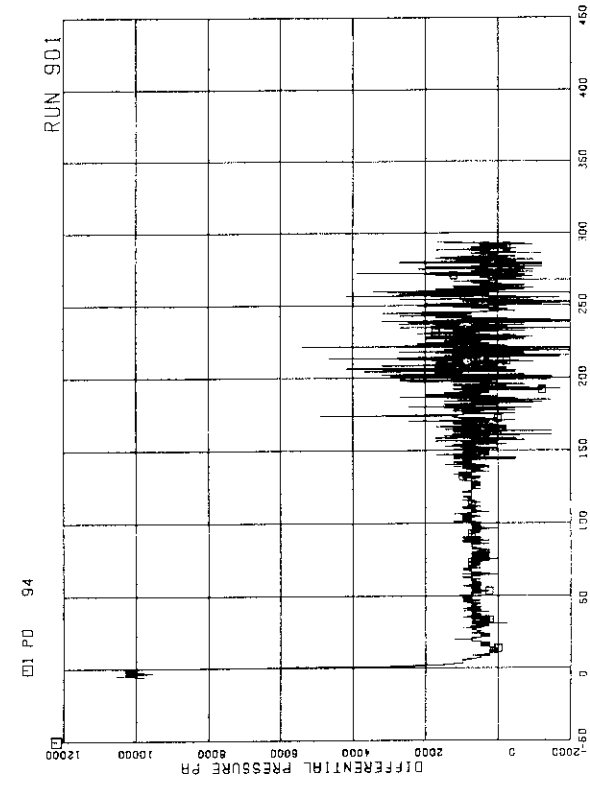


FIG.5. 50 DIFFERENTIAL PRESSURE ACROSS VENTURI FLOWMETER F-18

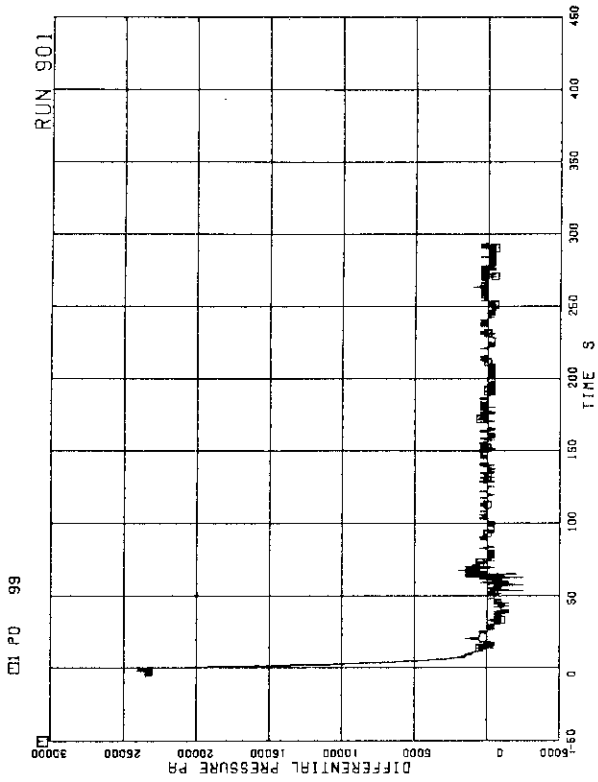


FIG.5. 55 DIFFERENTIAL PRESSURE ACROSS VENTURI FLOWMETER F-27

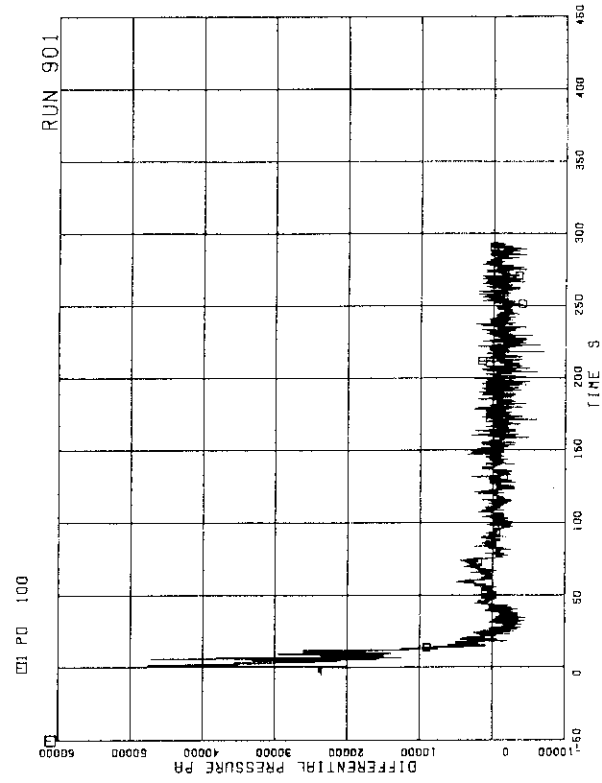


FIG.5. 56 DIFFERENTIAL PRESSURE ACROSS VENTURI FLOWMETER F-28

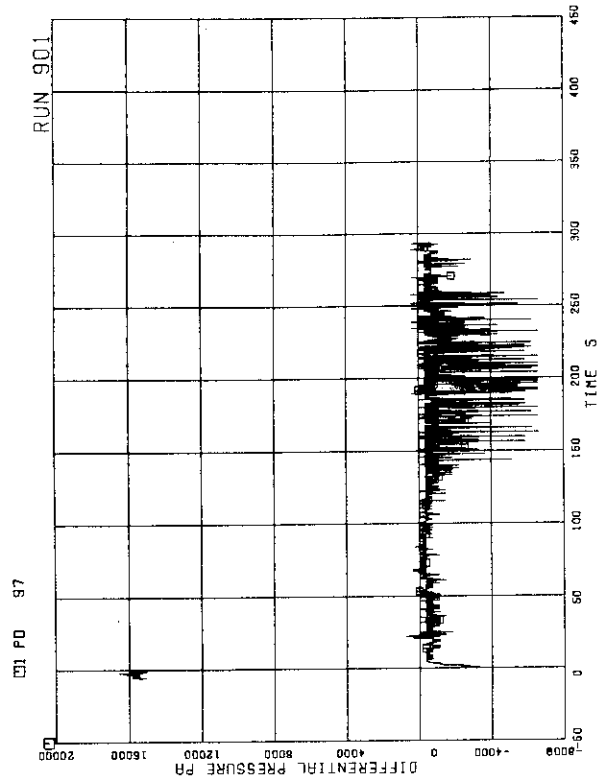


FIG.5. 53 DIFFERENTIAL PRESSURE ACROSS ORIFICE FLOWMETER F-21

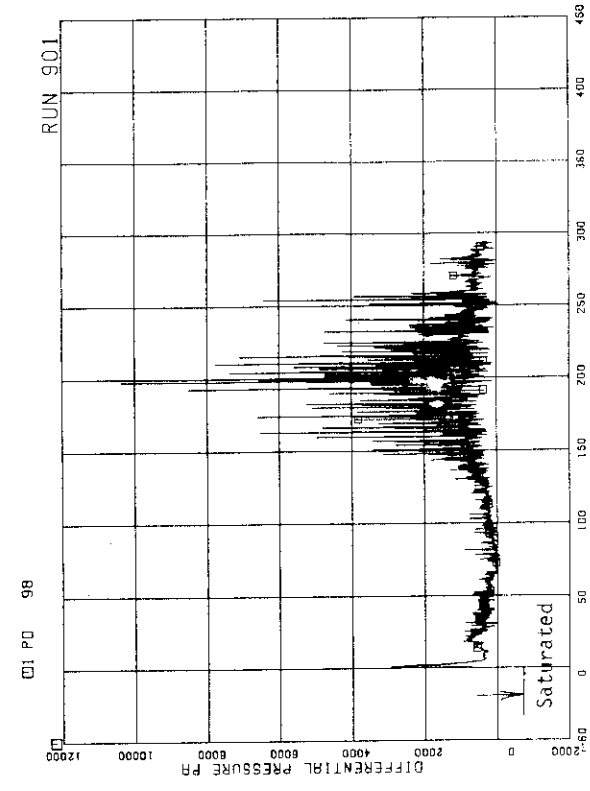


FIG.5. 54 DIFFERENTIAL PRESSURE ACROSS ORIFICE FLOWMETER F-22

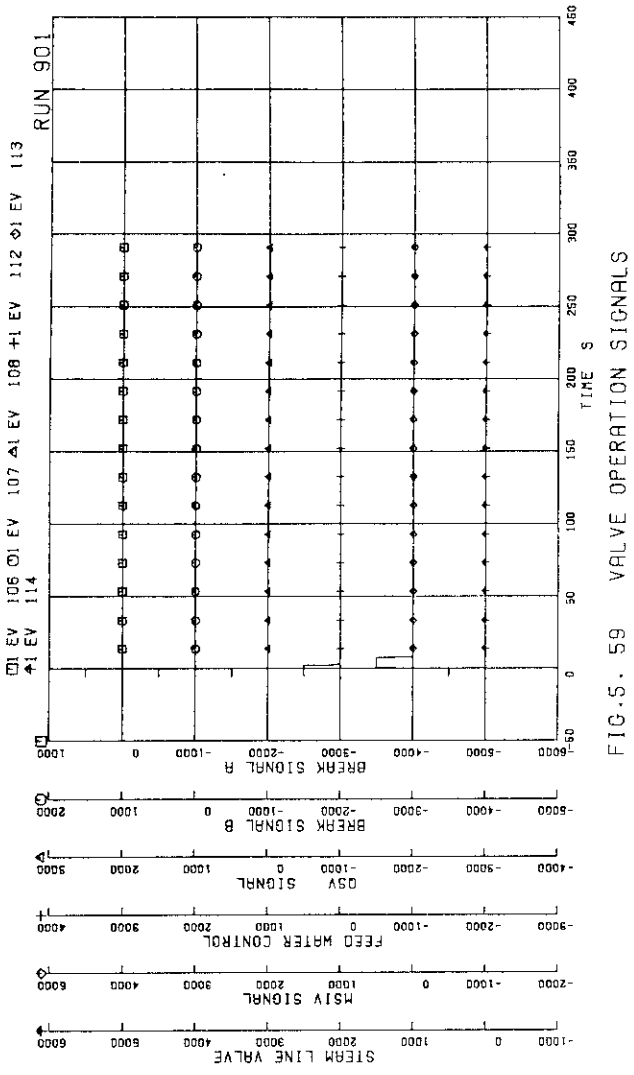


FIG.5. 59 VALVE OPERATION SIGNALS

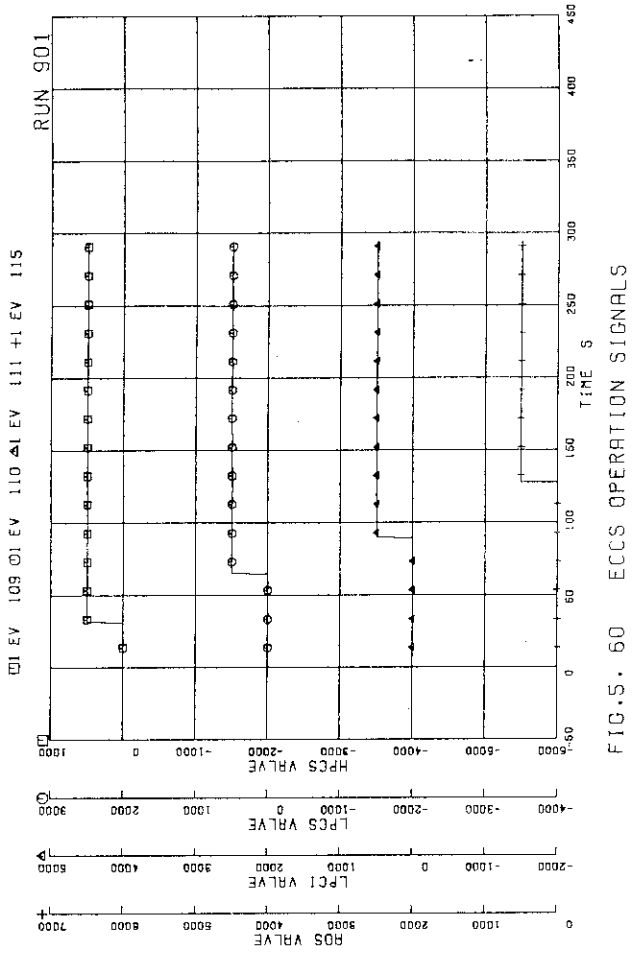


FIG.5. 60 ECCS OPERATION SIGNALS

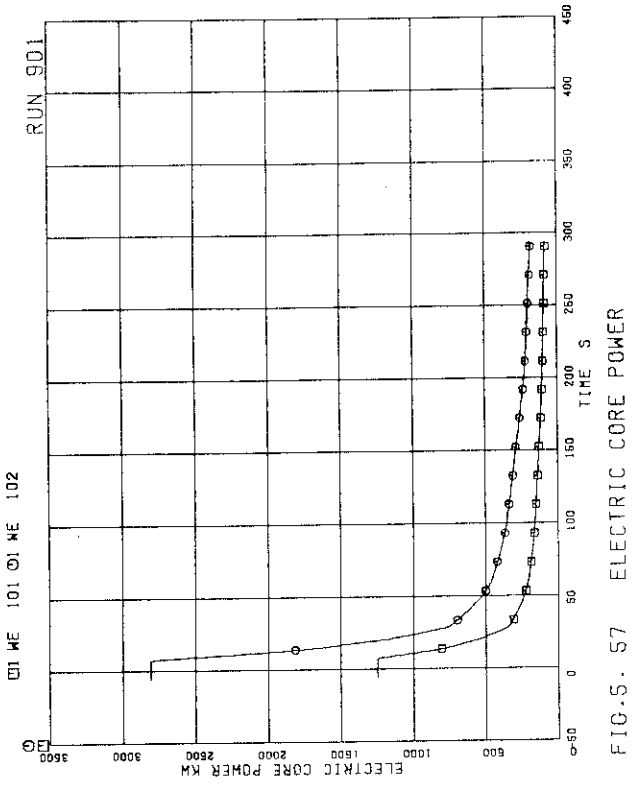


FIG.5. 57 ELECTRIC CORE POWER

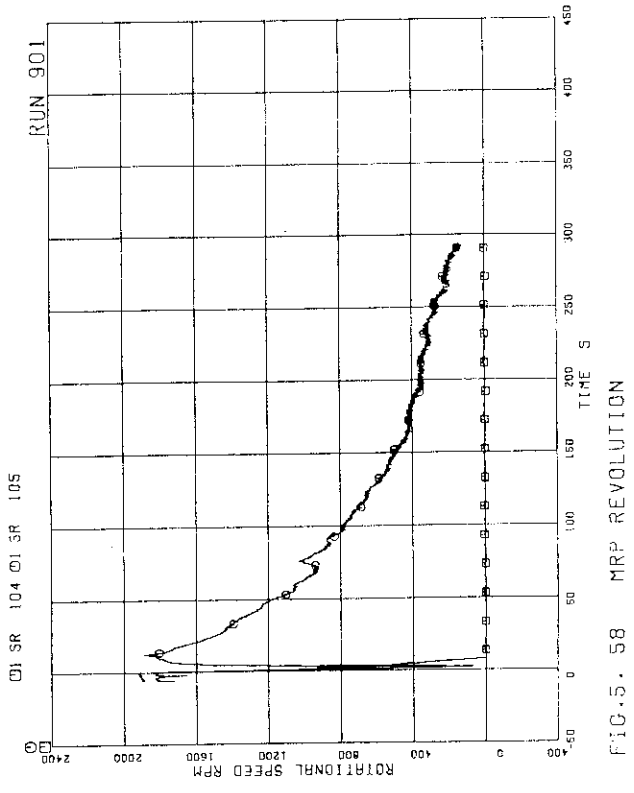


FIG.5. 58 MRP REVOLUTION

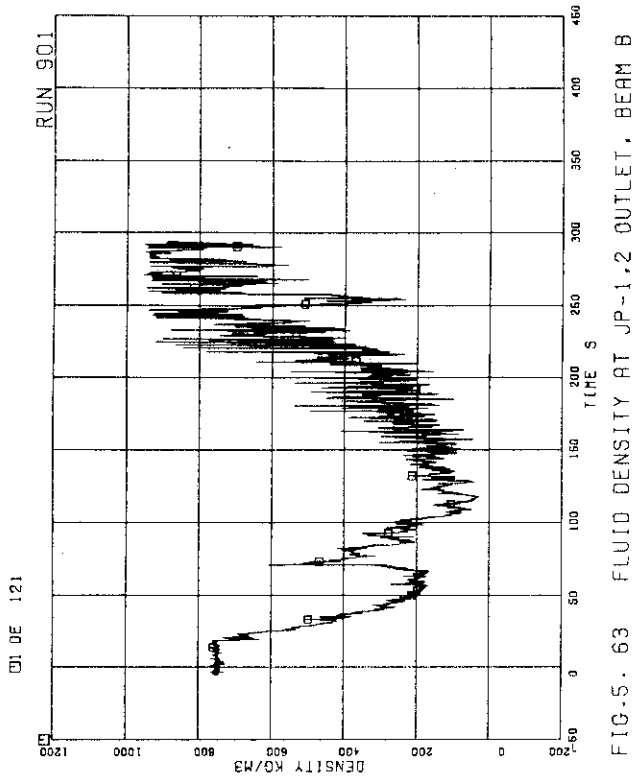


FIG.5. 63 FLUID DENSITY AT JP-1,2 OUTLET, BEAM B

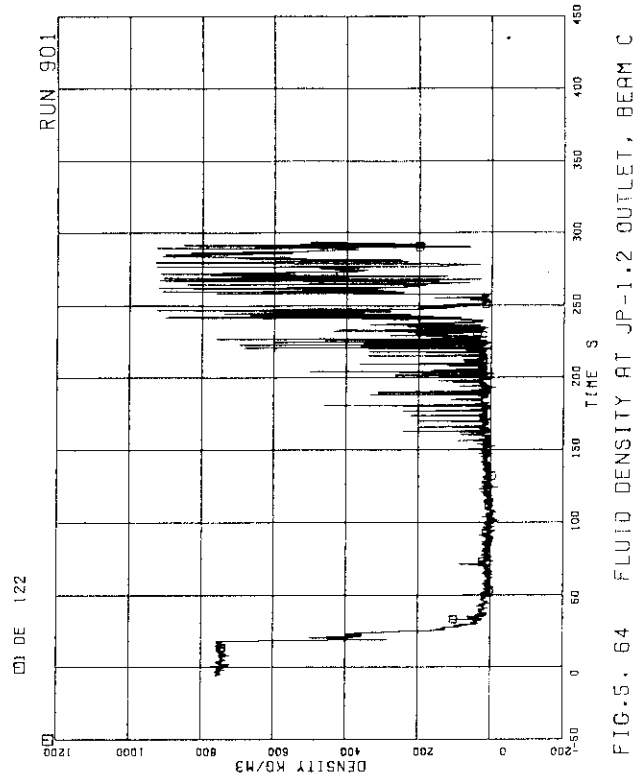


FIG.5. 64 FLUID DENSITY AT JP-1.2 OUTLET, BEAM C

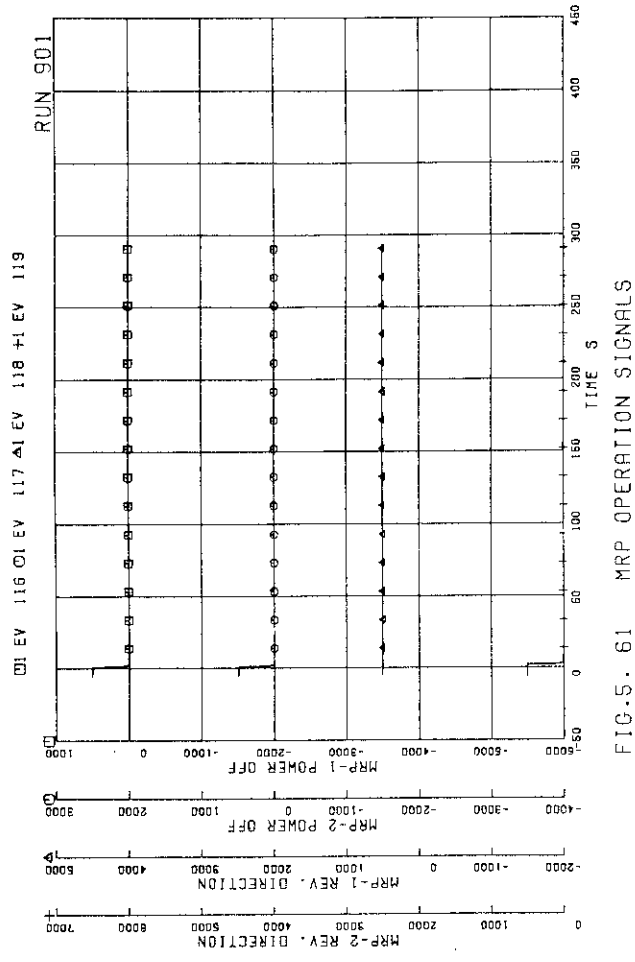


FIG.5. 61 MRP OPERATION SIGNALS

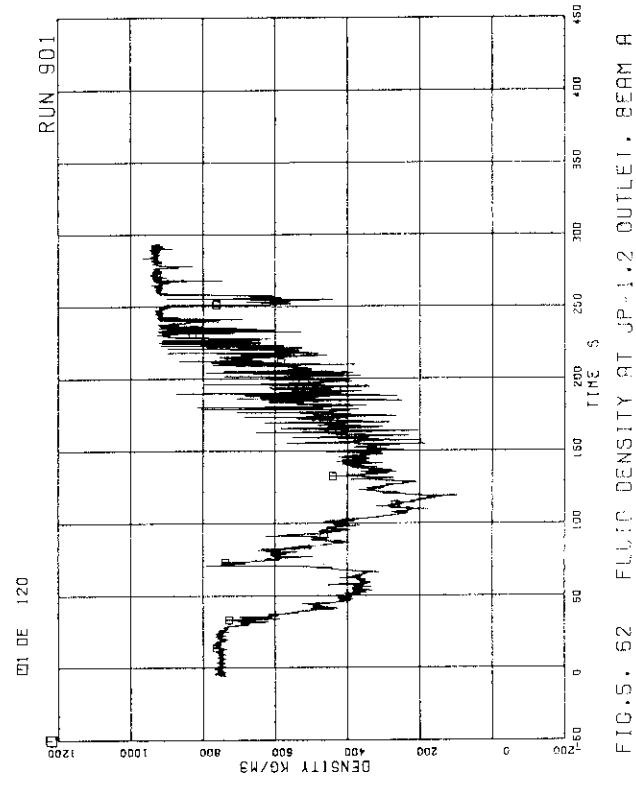


FIG.5. 62 FLUID DENSITY AT JP-1.2 OUTLET, BEAM A

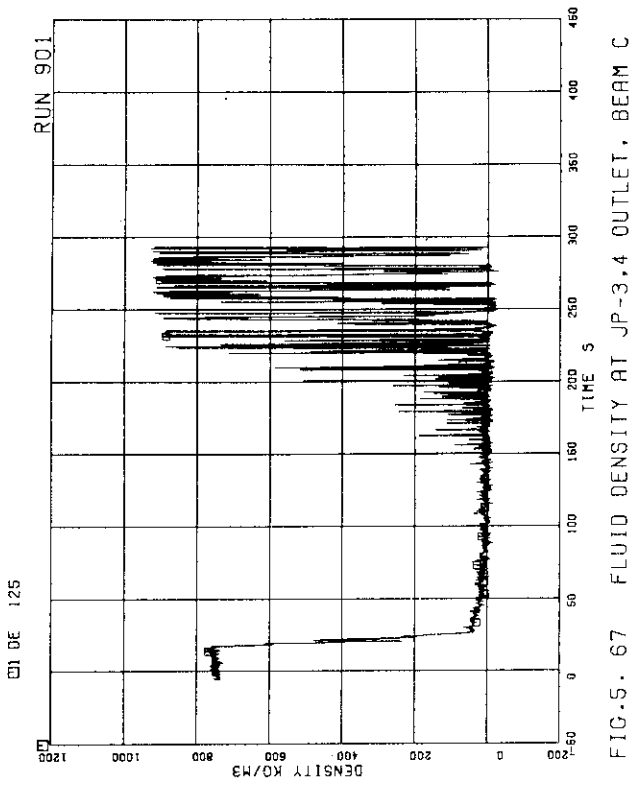


FIG.5. 67 FLUID DENSITY AT JP-3,4 OUTLET, BEAM C

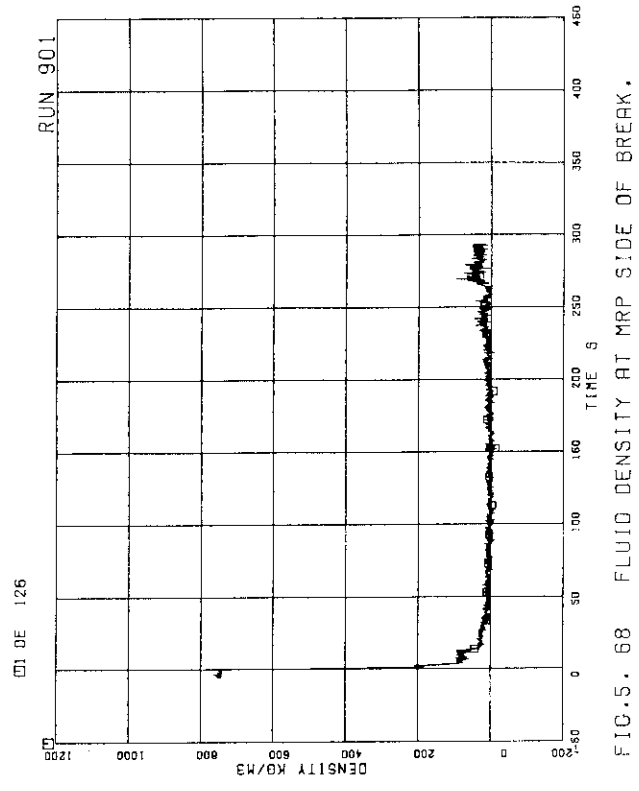


FIG.5. 68 FLUID DENSITY AT MRP SIDE OF BREAK, BEAM A

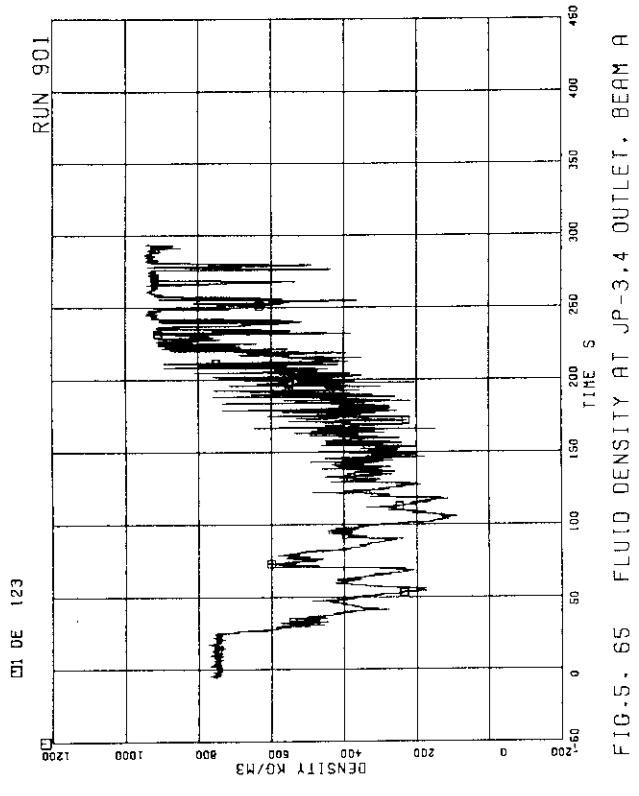


FIG.5. 65 FLUID DENSITY AT JP-3,4 OUTLET, BEAM A

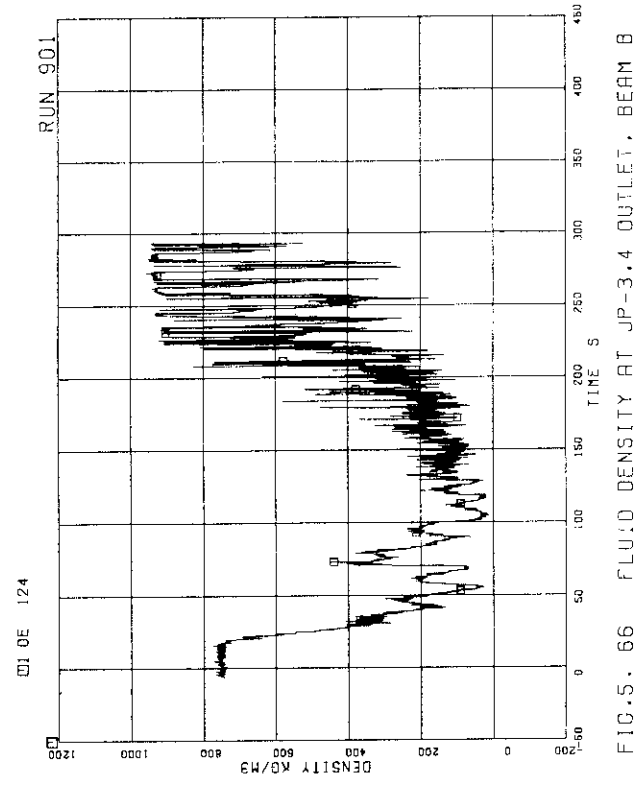


FIG.5. 66 FLUID DENSITY AT JP-3,4 OUTLET, BEAM B

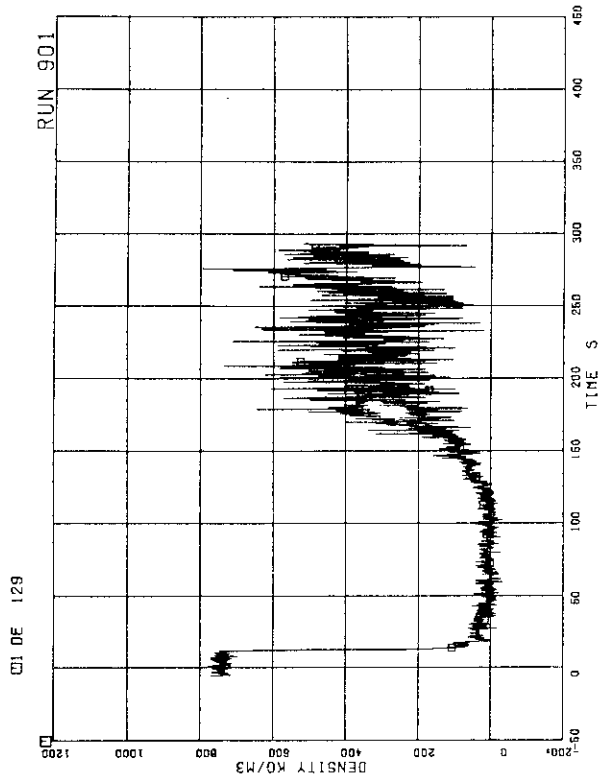


FIG.5. 71 FLUID DENSITY AT PV SIDE OF BREAK, BEAM B

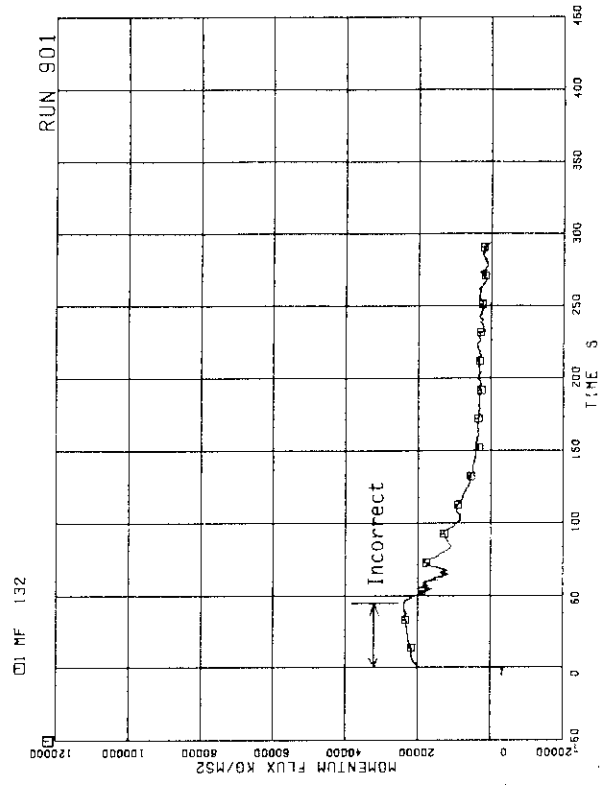


FIG.5. 72 MOMENTUM FLUX AT BREAK A SPOOL PIECE (LOW RANGE)

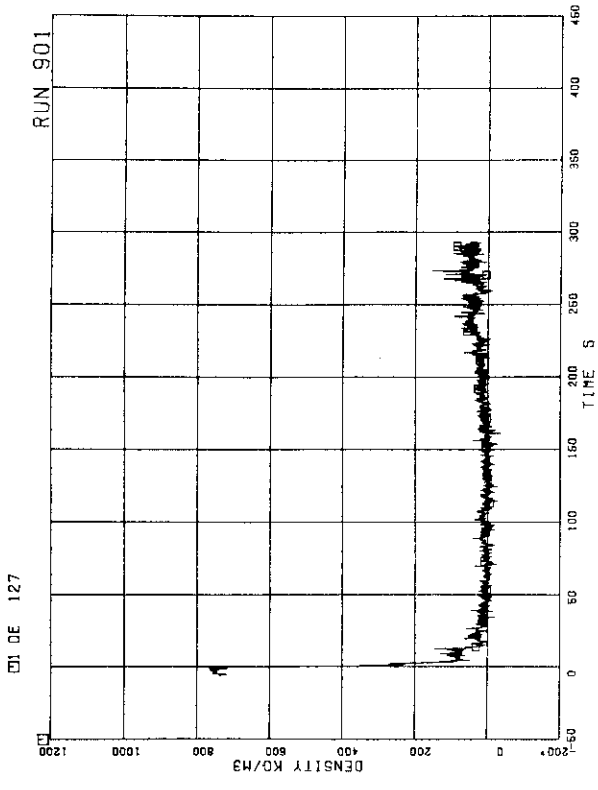


FIG.5. 69 FLUID DENSITY AT MRP SIDE OF BREAK, BEAM B

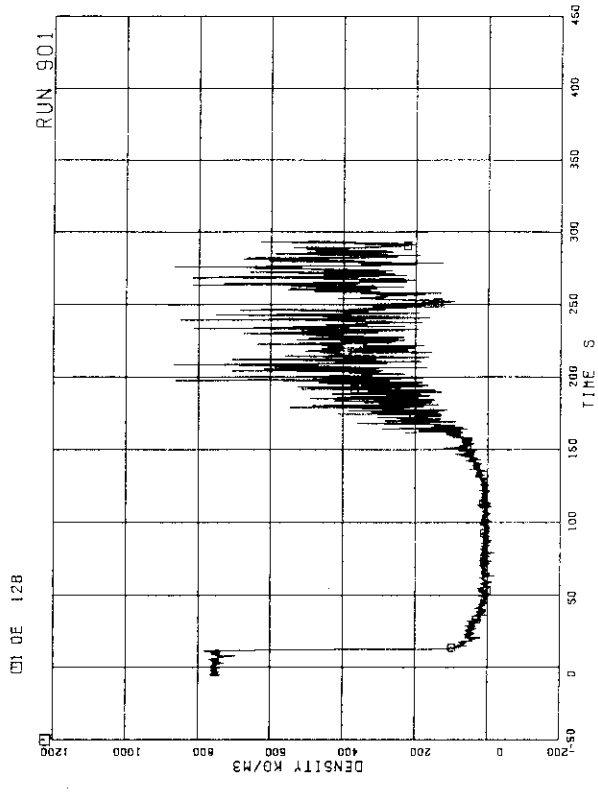


FIG.5. 70 FLUID DENSITY AT PV SIDE OF BREAK, BEAM A

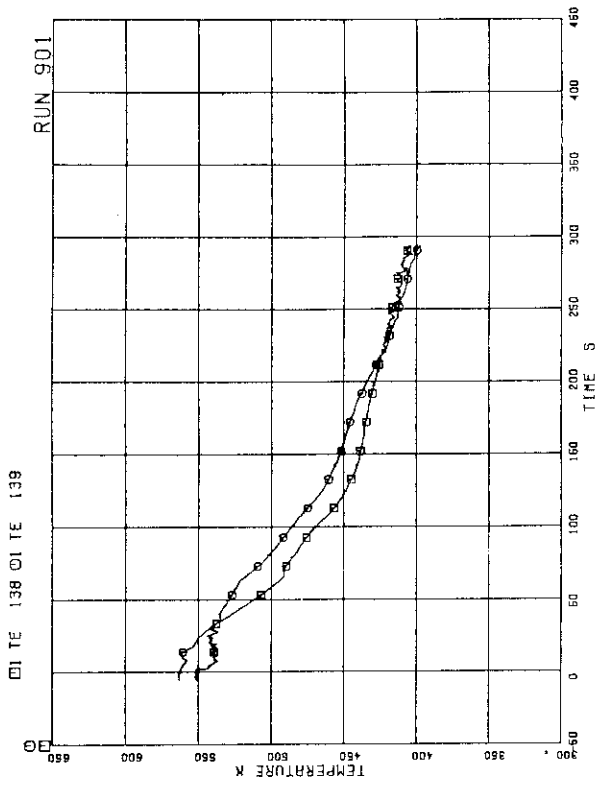


FIG.5. 75 FLUID TEMPERATURES IN LOWER PLENUM AND UPPER PLENUM

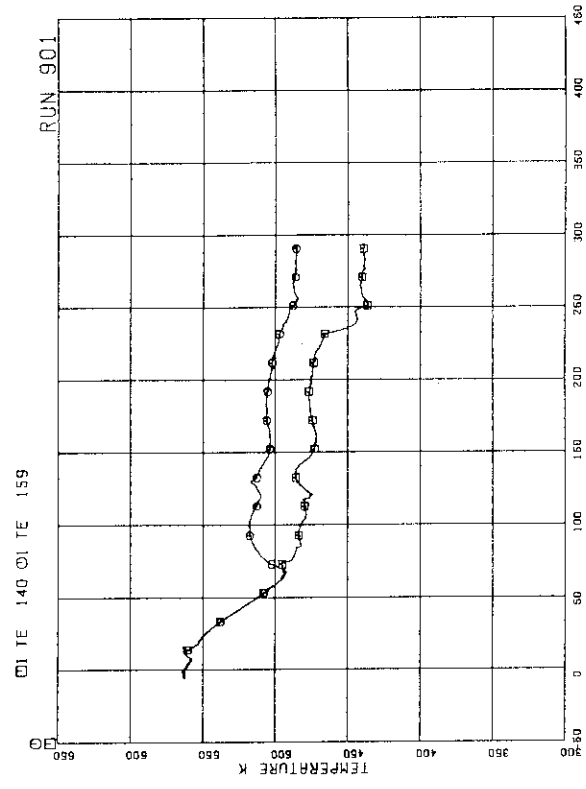


FIG.5. 76 FLUID TEMPERATURES IN STEAM DOME AND MSL

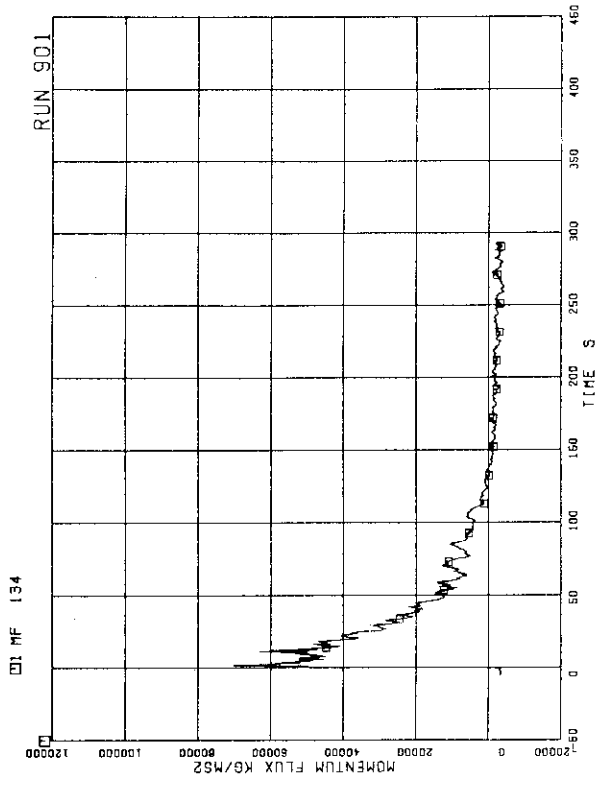


FIG.5. 73 MOMENTUM FLUX AT BREAK A SPOOL PIECE (HIGH RANGE)

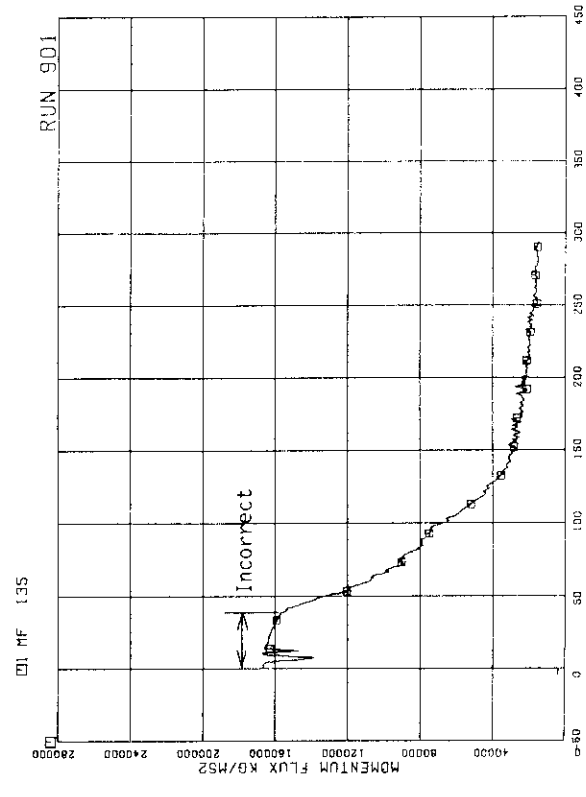


FIG.5. 74 MOMENTUM FLUX AT BREAK B SPOOL PIECE (HIGH RANGE)

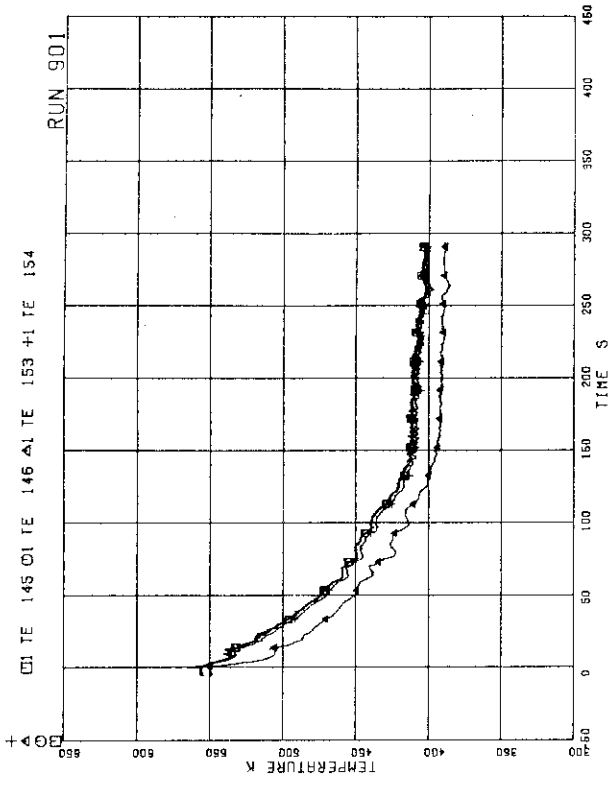


FIG.5. 79 FLUID TEMPERATURES IN BROKEN RECIRCULATION LOOP

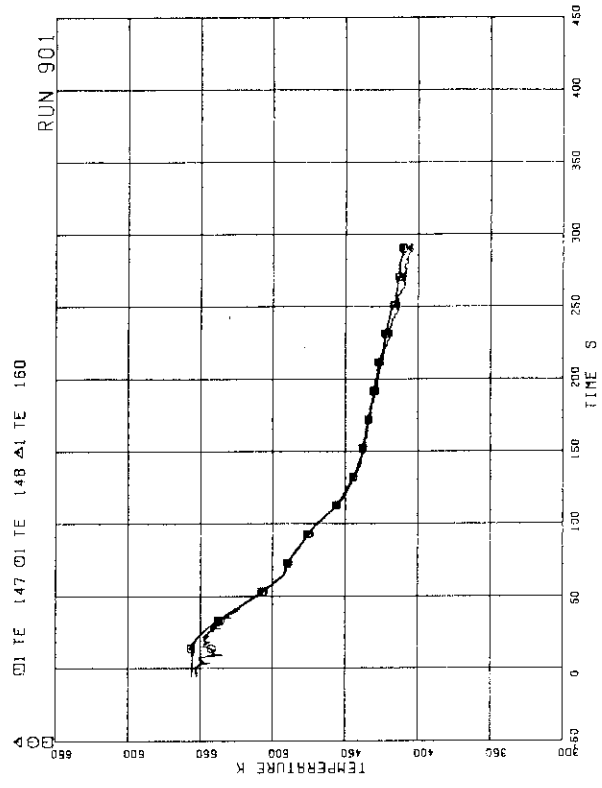


FIG.5. 80 FLUID TEMPERATURES AT CP-1.2 OUTLET

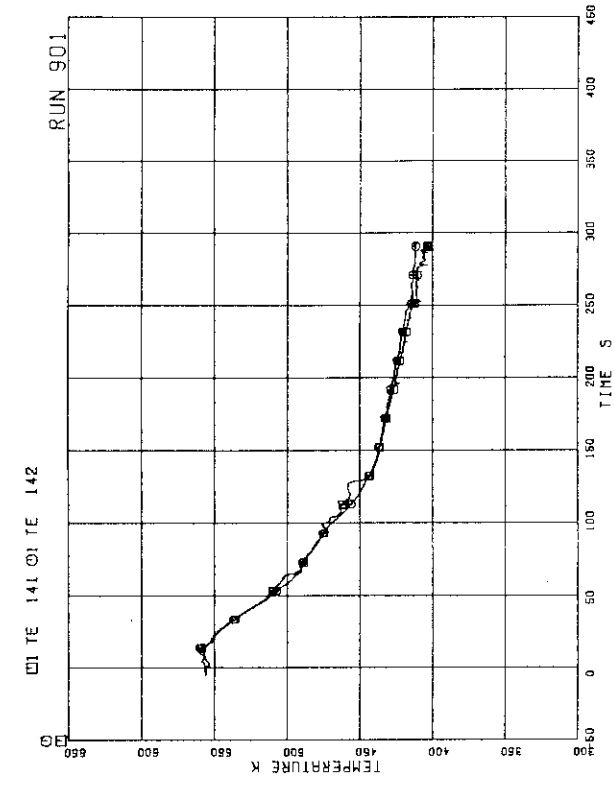


FIG.5. 77 FLUID TEMPERATURES IN DOWNCOMER

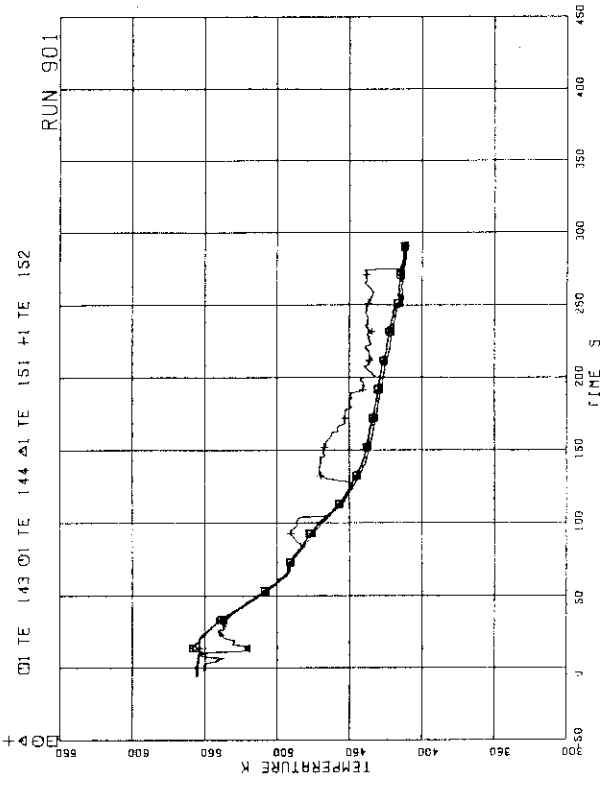


FIG.5. 78 FLUID TEMPERATURES IN INTACT RECIRCULATION LOOP

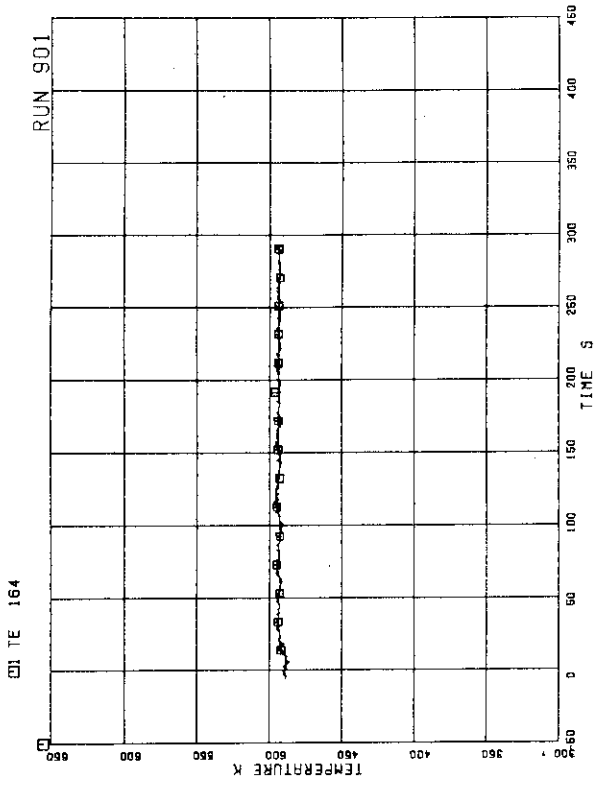


FIG.5. 83 FEEDWATER TEMPERATURE

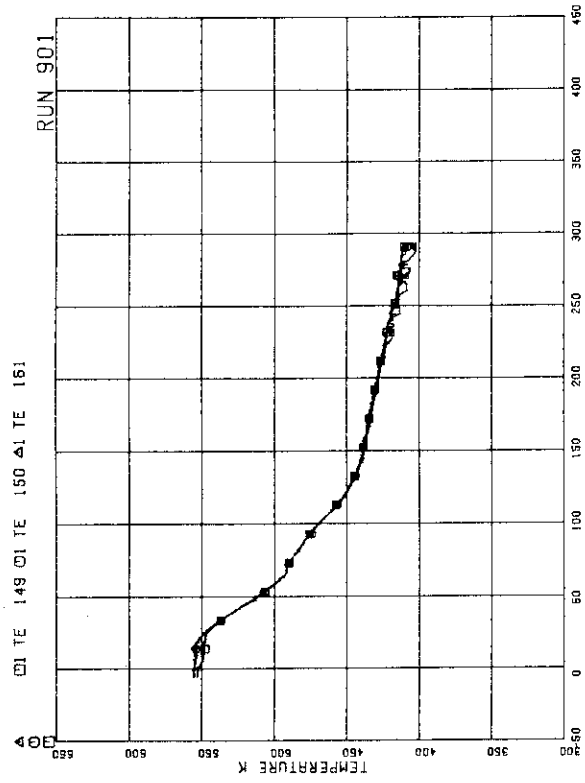


FIG.5. 81 FLUID TEMPERATURES AT JP-3,4 OUTLET

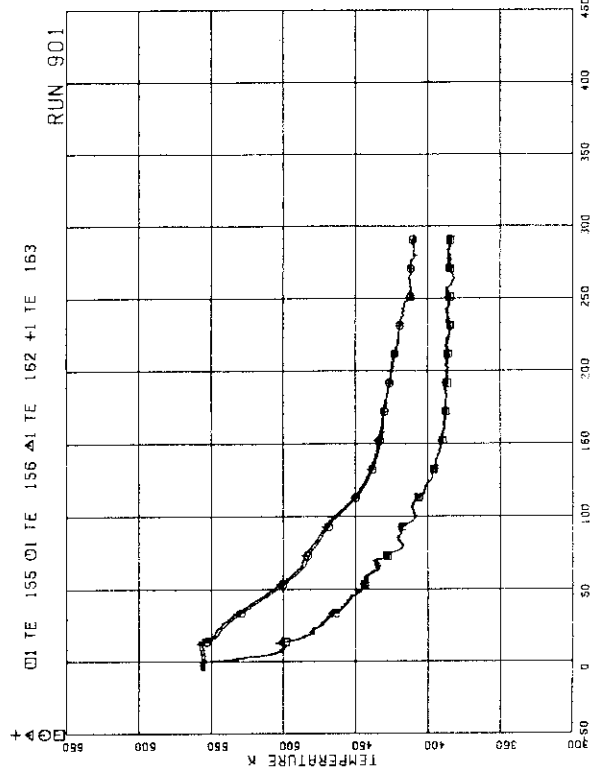


FIG.5. 82 FLUID TEMPERATURES NEAR BREAKS A AND B

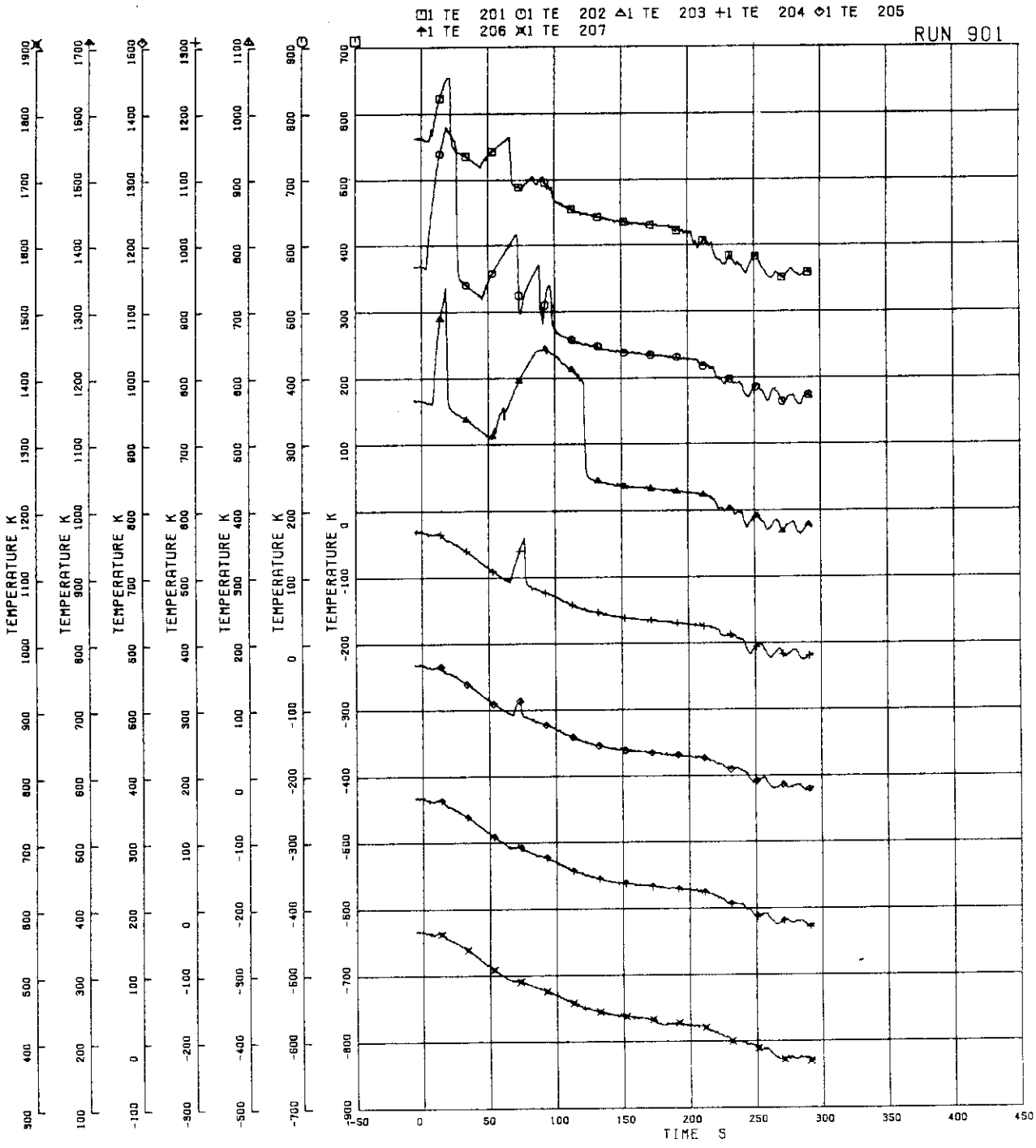


FIG.5. 84 SURFACE TEMPERATURES OF FUEL ROD A11

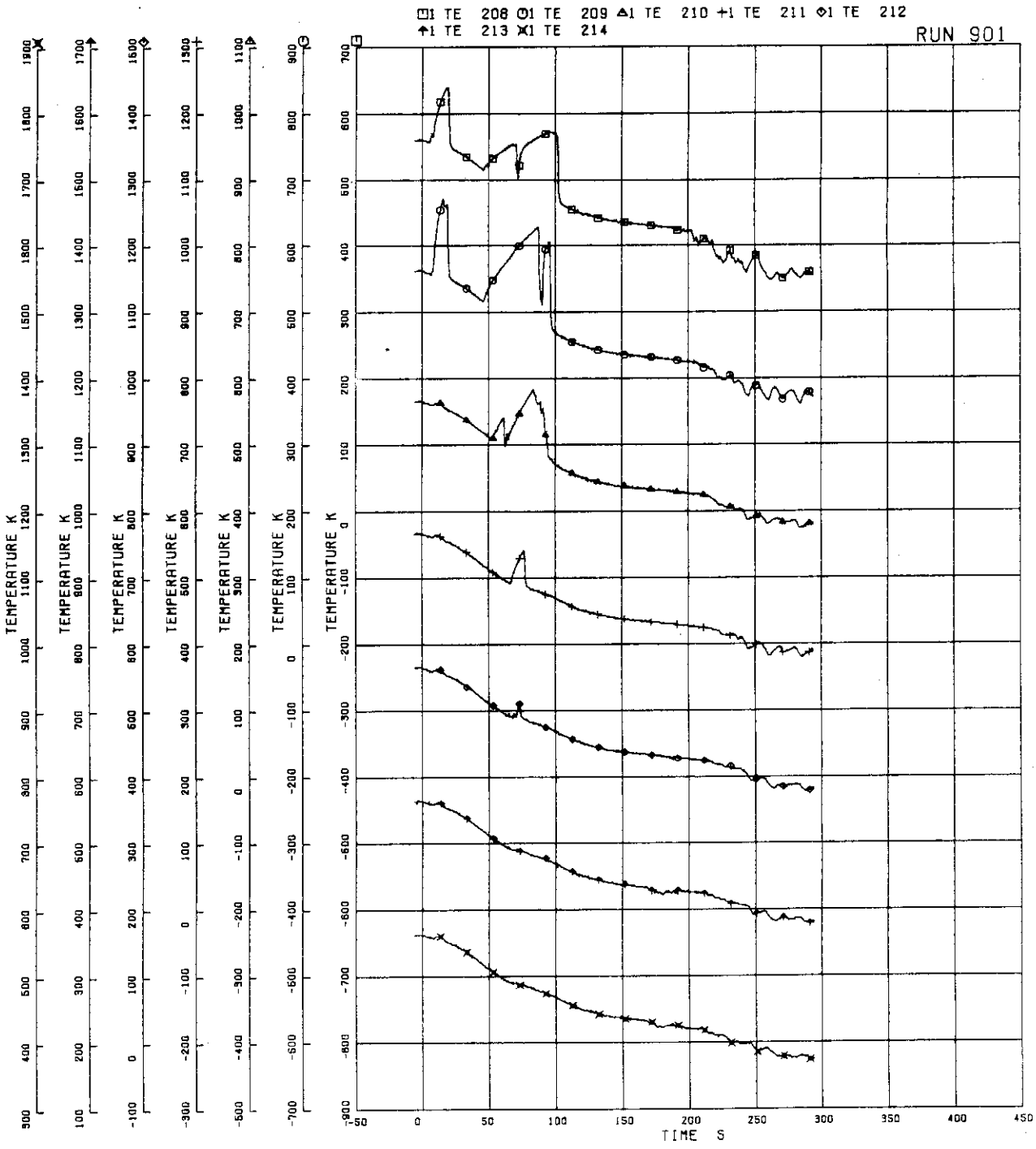


FIG.5. 85 SURFACE TEMPERATURES OF FUEL ROD A12

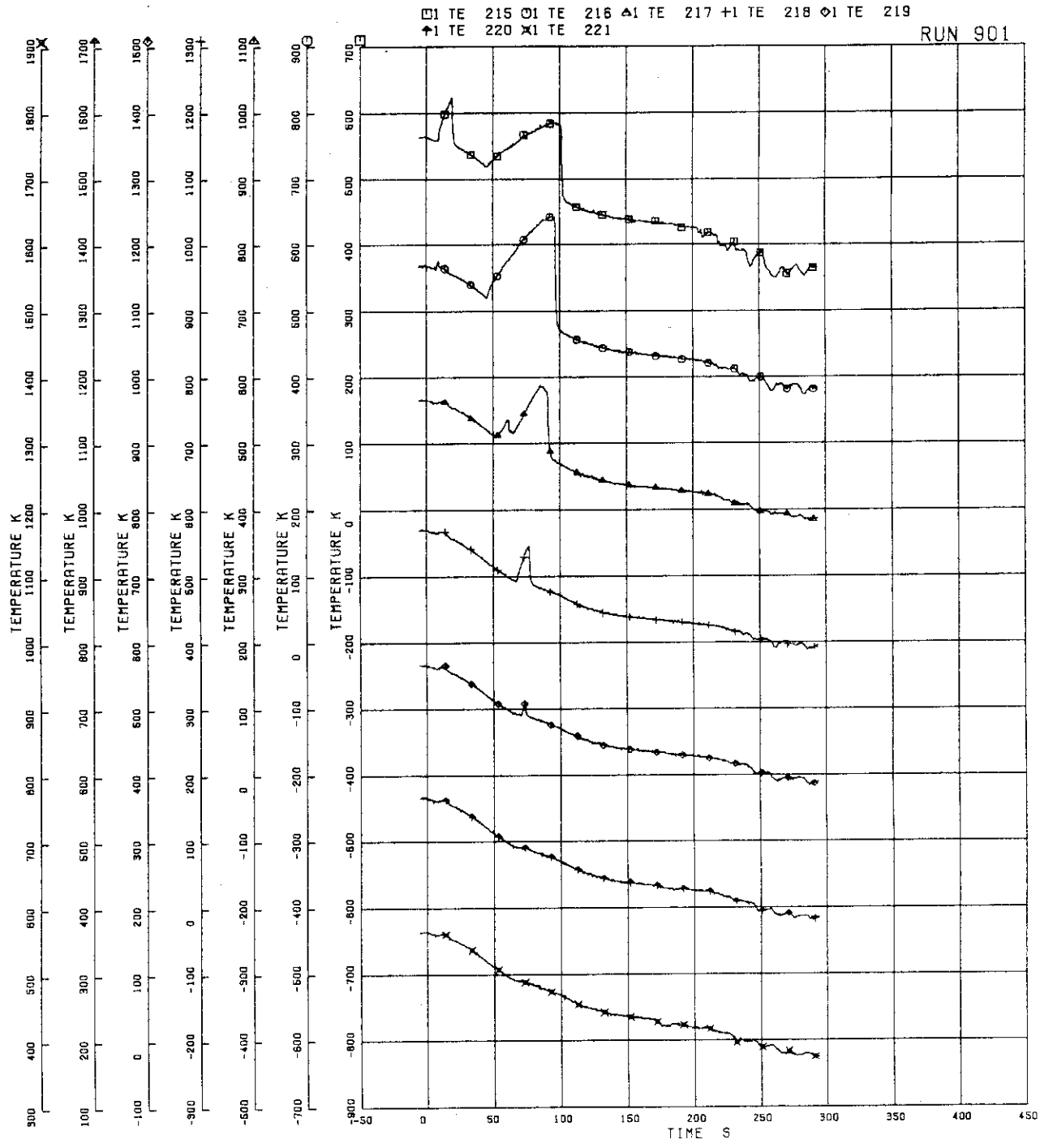


FIG.5. 86 SURFACE TEMPERATURES OF FUEL ROD A13

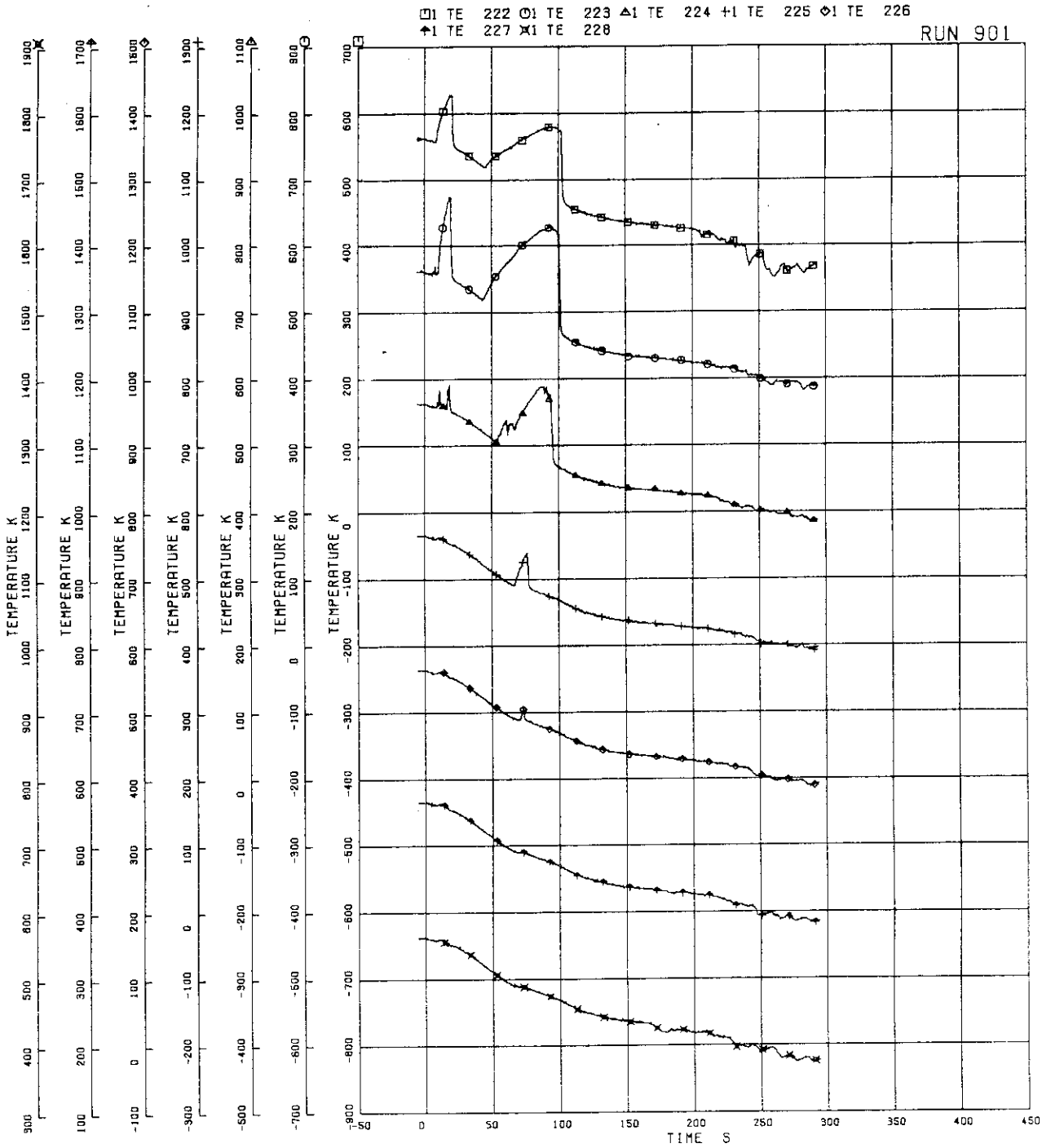


FIG.5. 87 SURFACE TEMPERATURES OF FUEL ROD A14

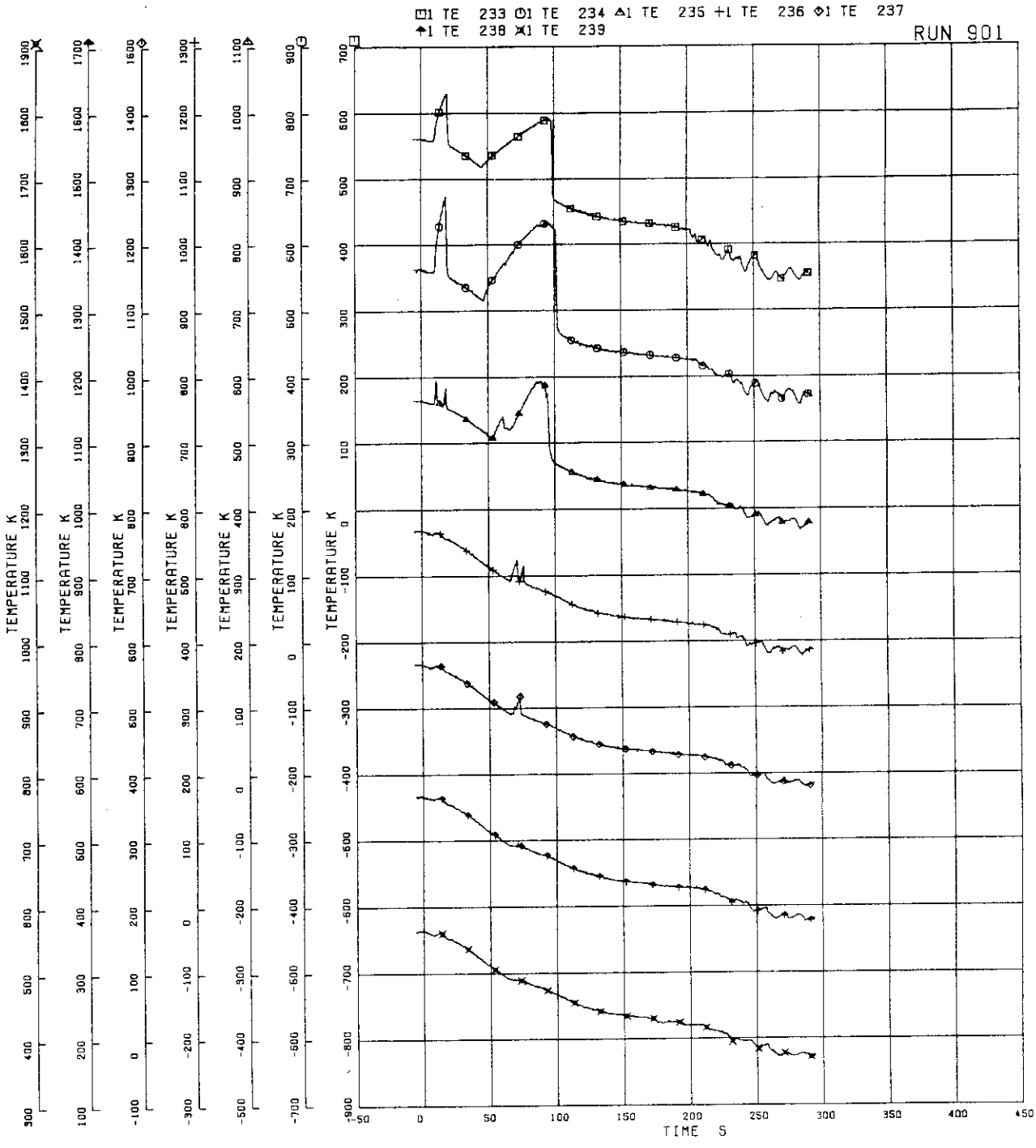


FIG.5. 88 SURFACE TEMPERATURES OF FUEL ROD A22

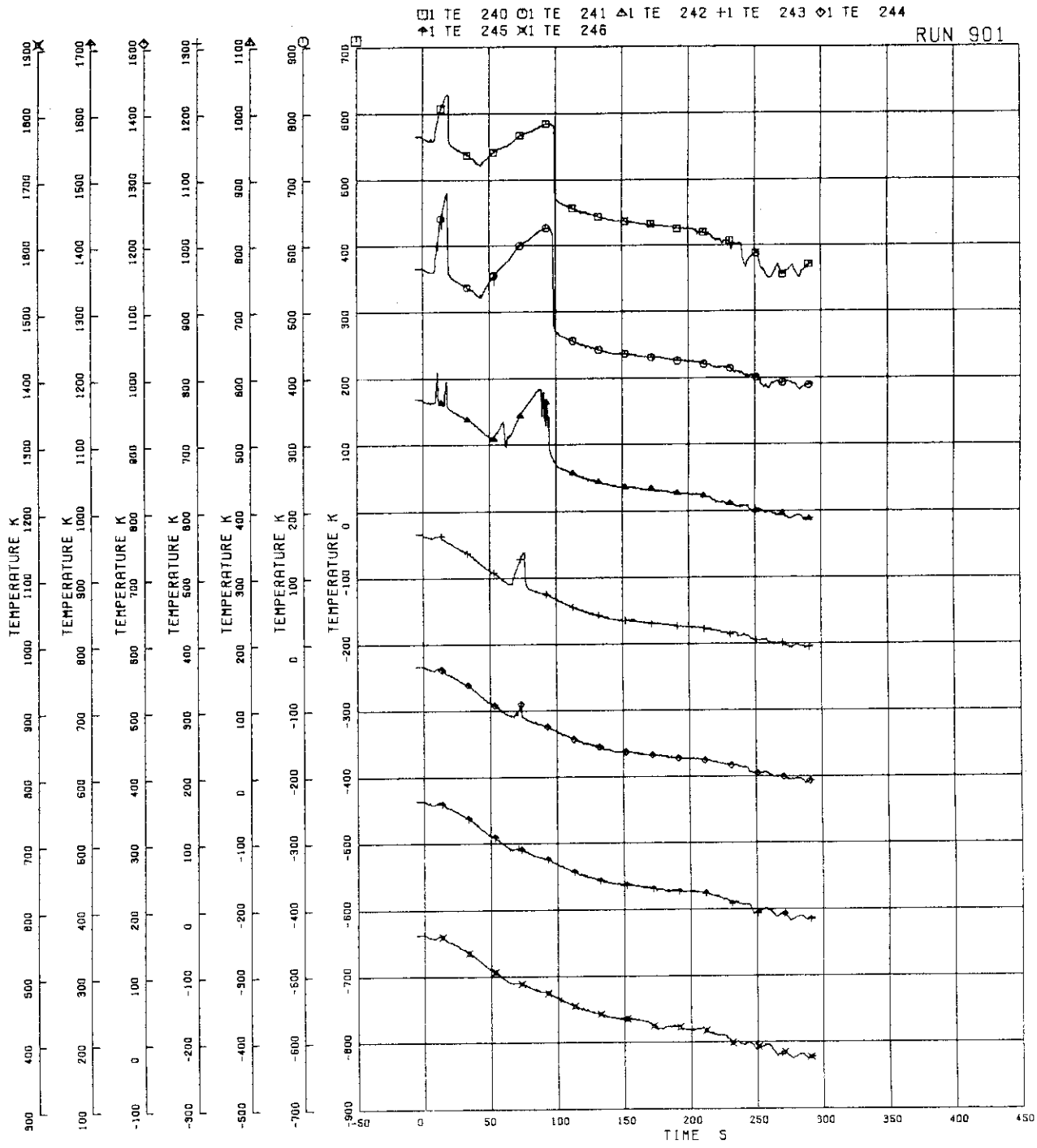


FIG.5. 89 SURFACE TEMPERATURES OF FUEL ROD A24

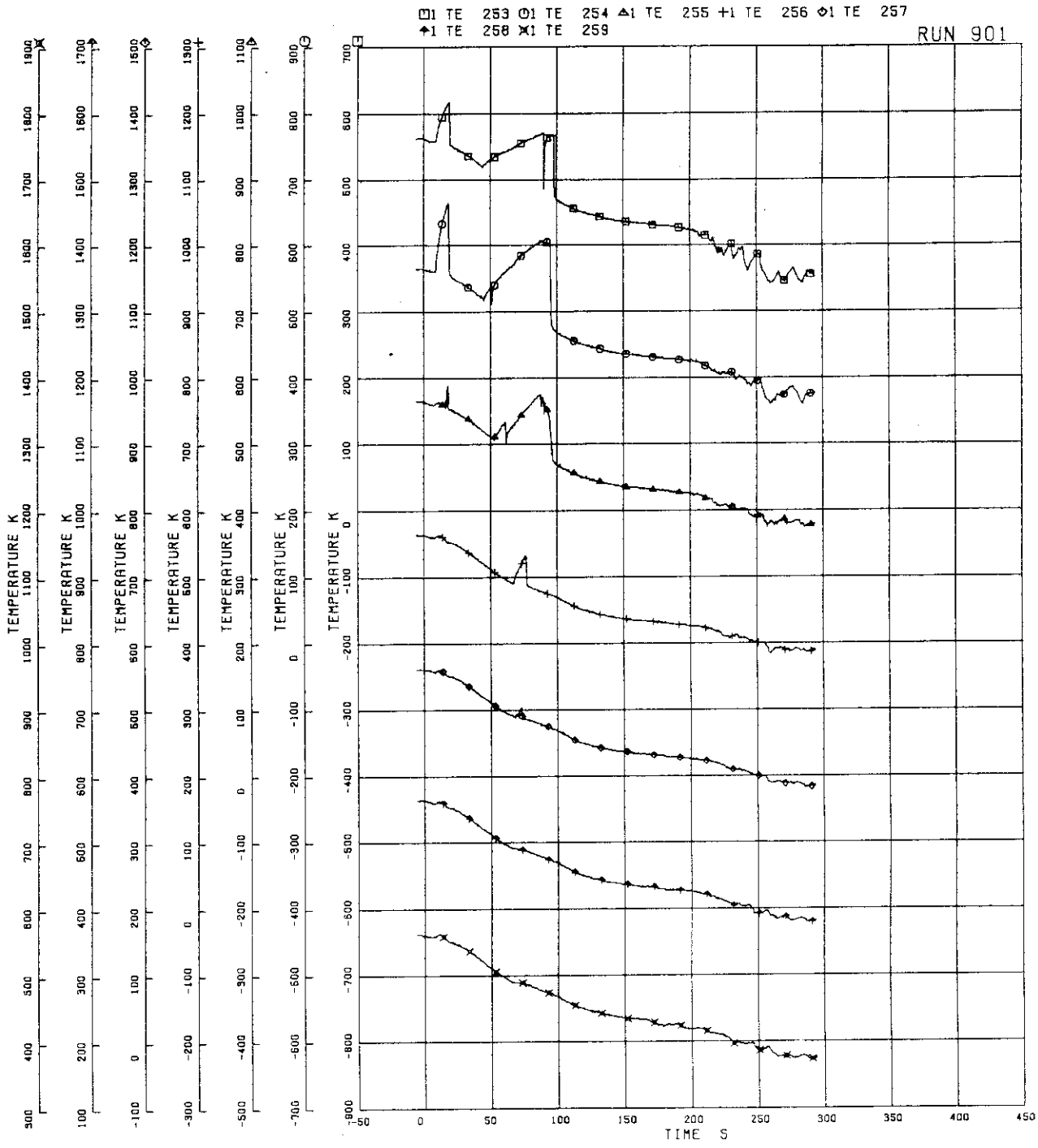


FIG.5. 90 SURFACE TEMPERATURES OF FUEL ROD A33

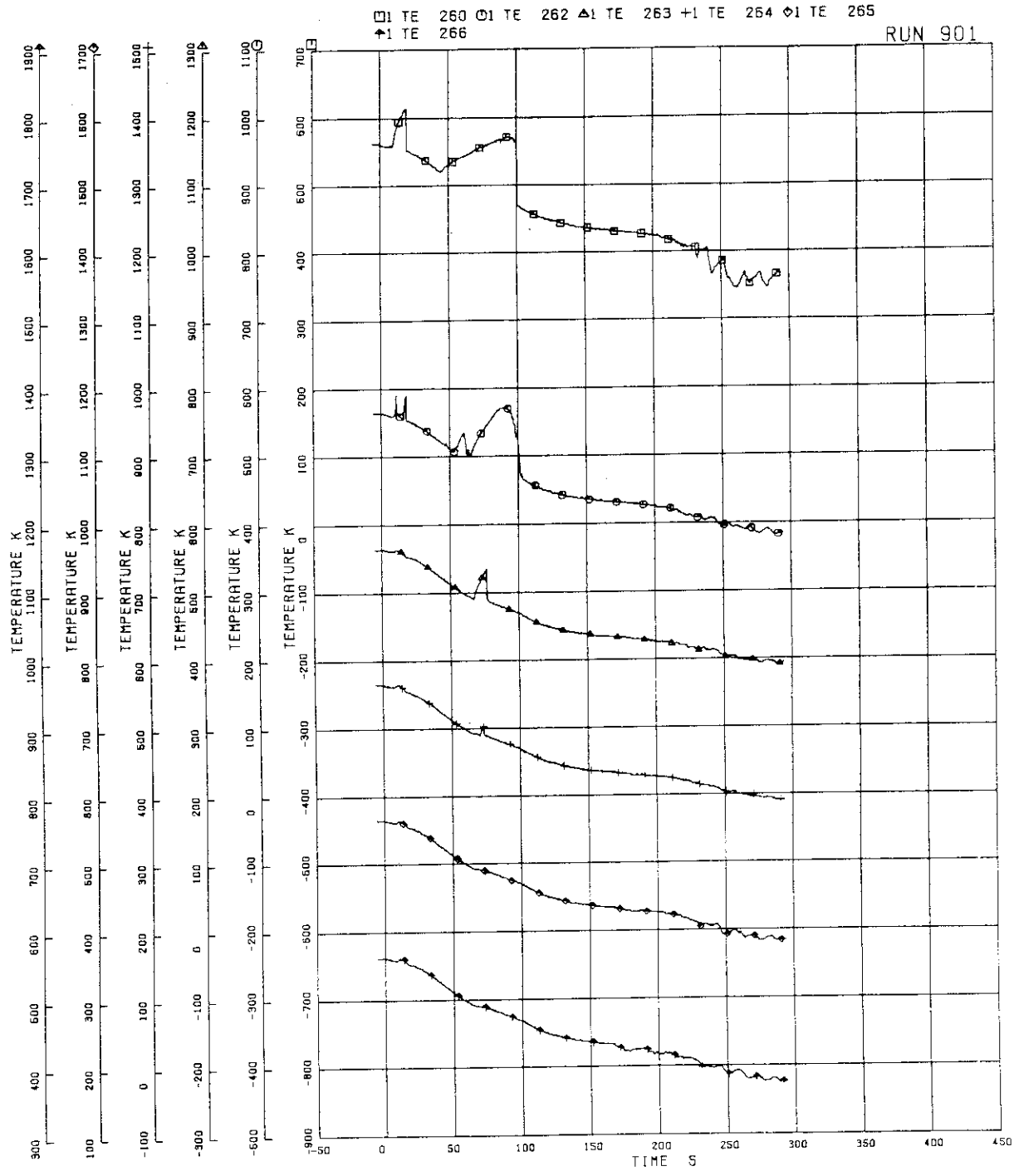


FIG.5. 91 SURFACE TEMPERATURES OF FUEL ROD A34

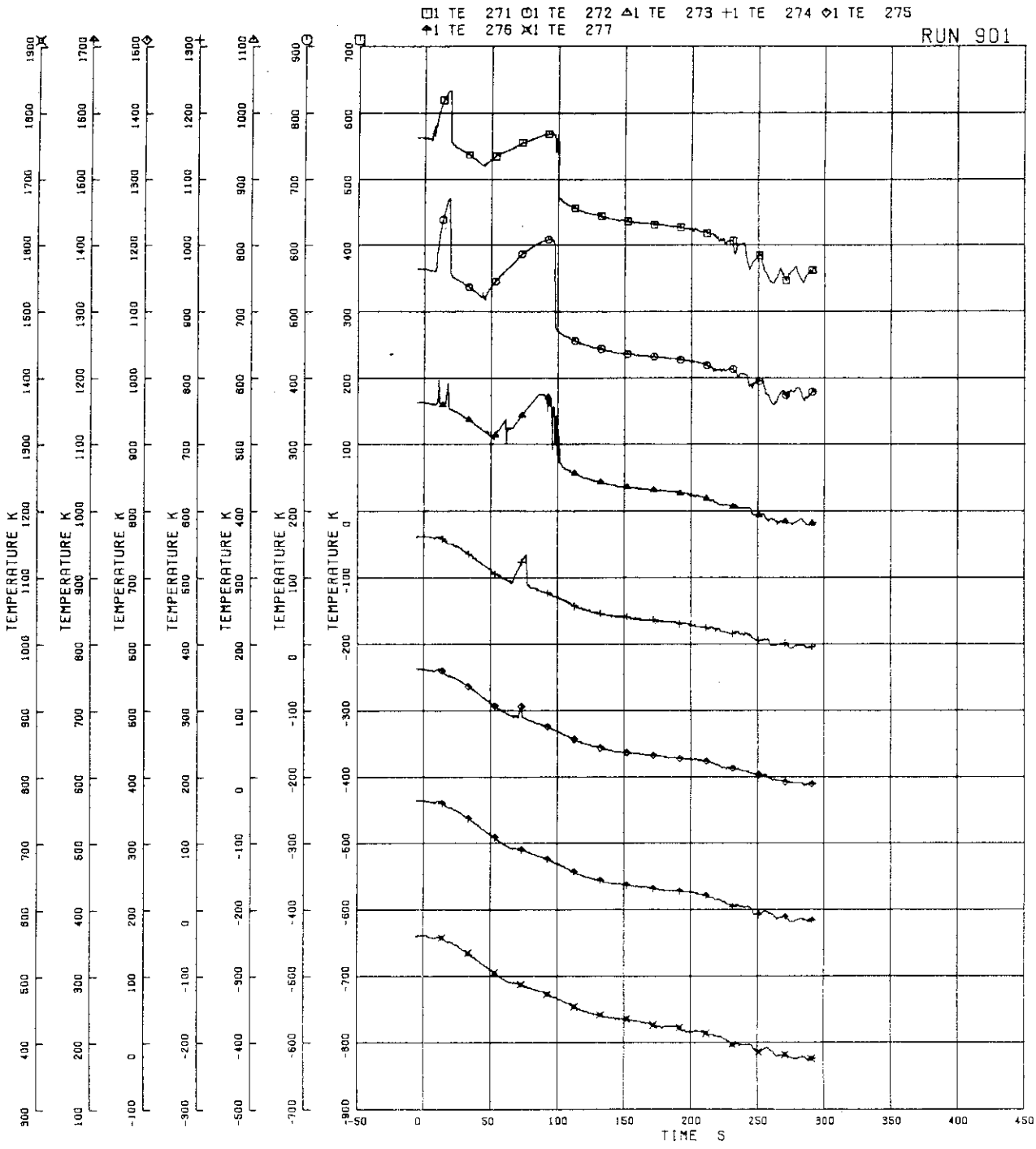


FIG.5. 92 SURFACE TEMPERATURES OF FUEL ROD A44

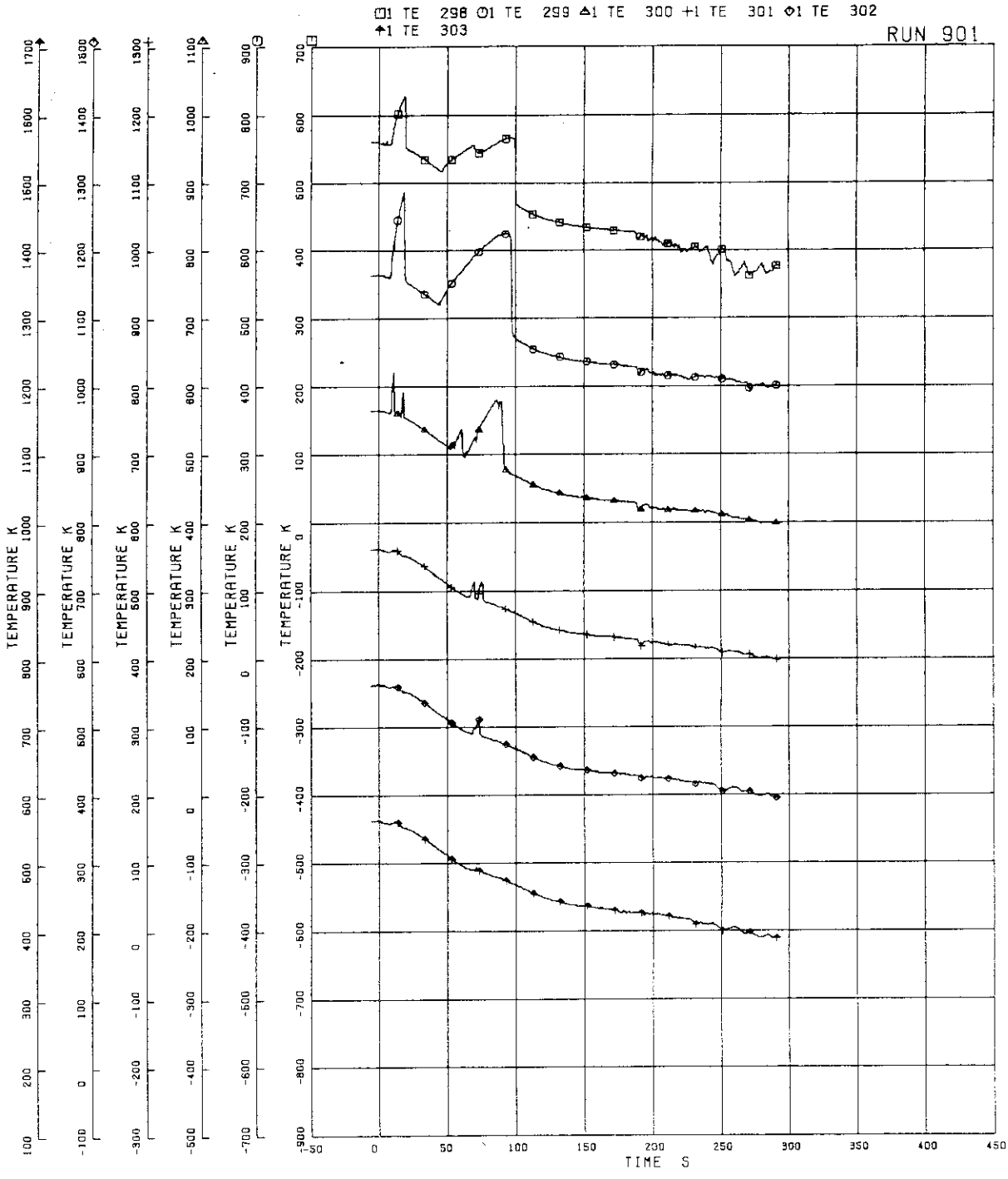


FIG.5. 93 SURFACE TEMPERATURES OF FUEL ROD A77

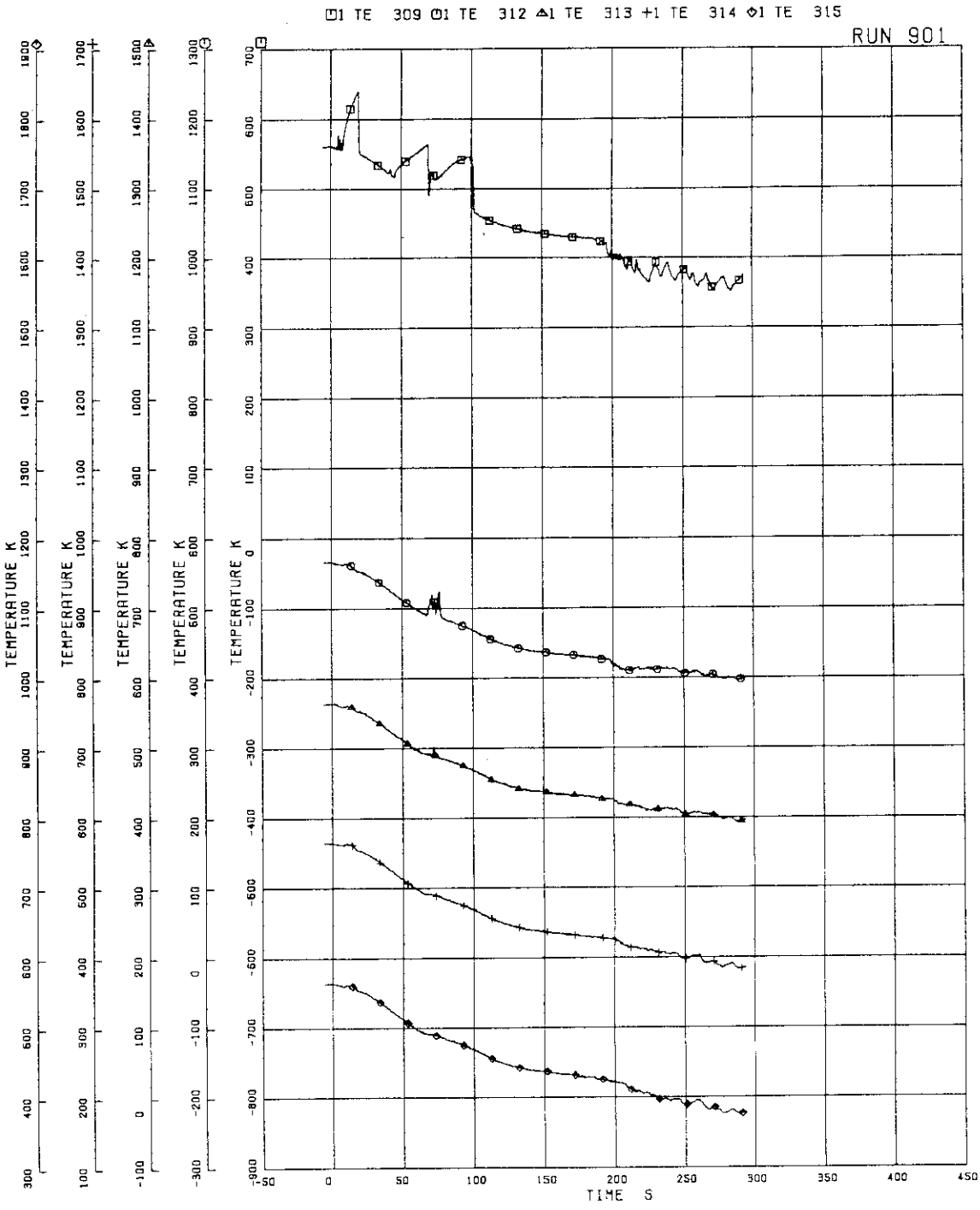


FIG.5. 94 SURFACE TEMPERATURES OF FUEL ROD A85

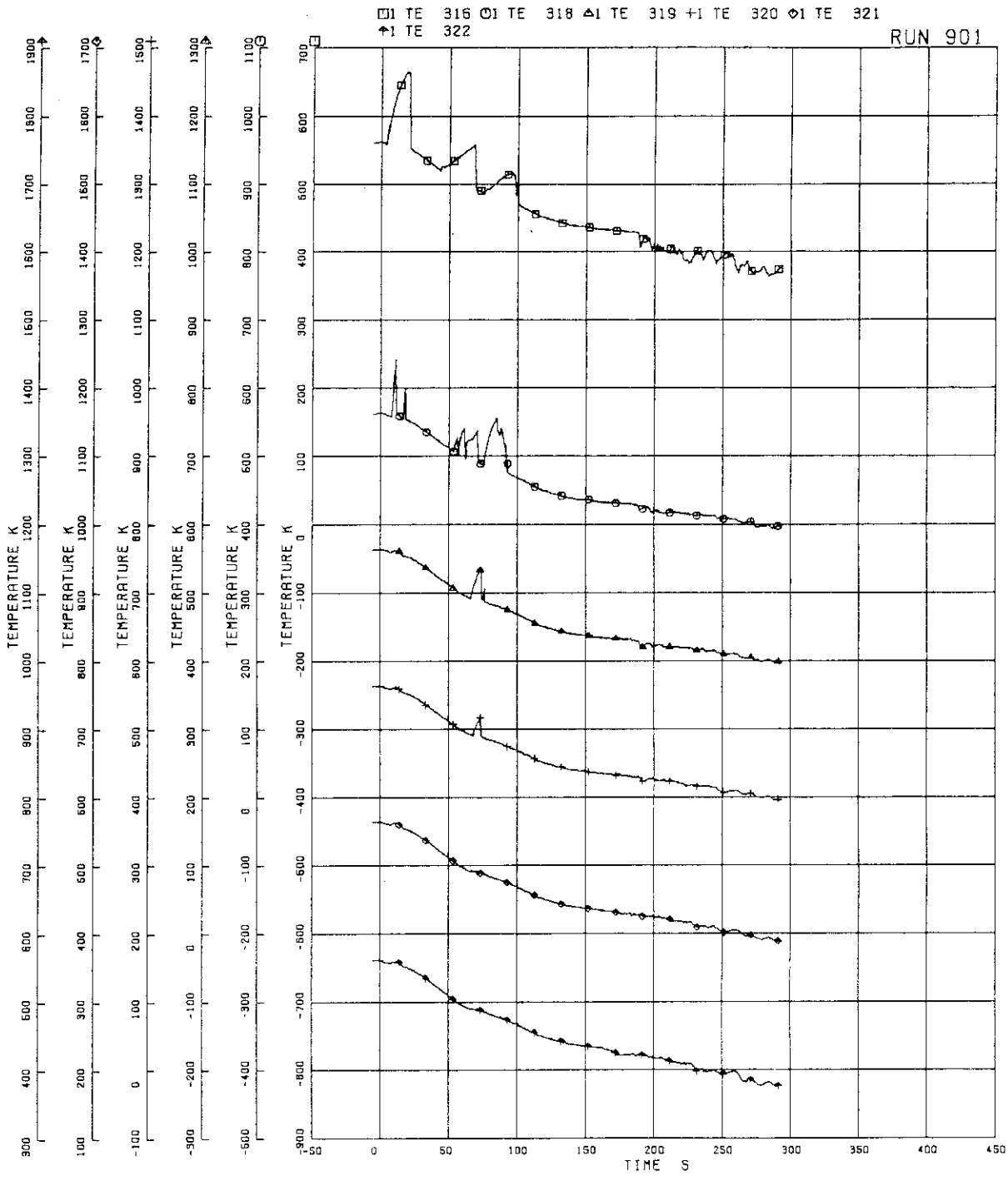


FIG.5. 95 SURFACE TEMPERATURES OF FUEL ROD A87

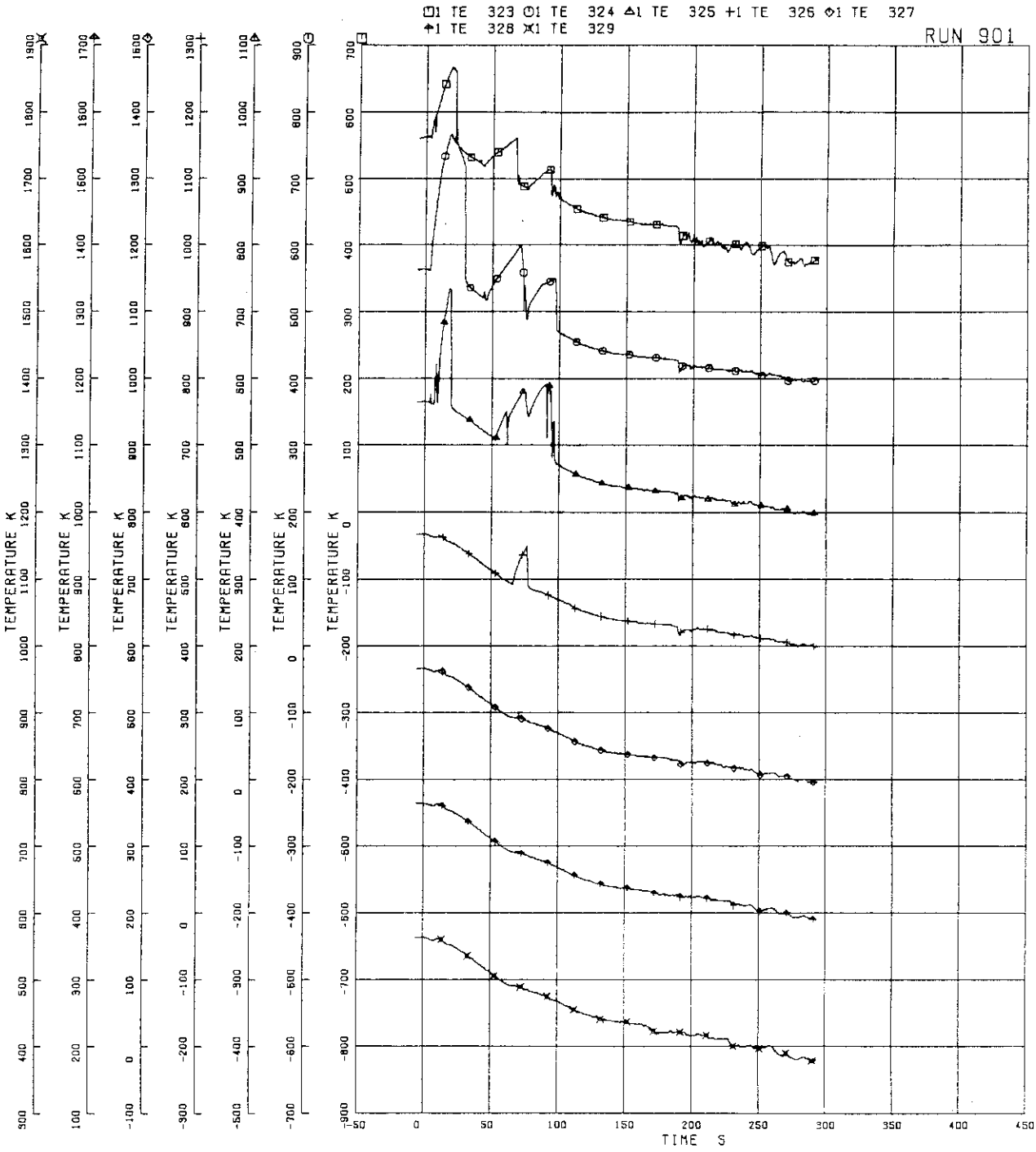


FIG.5. 96 SURFACE TEMPERATURES OF FUEL ROD A88

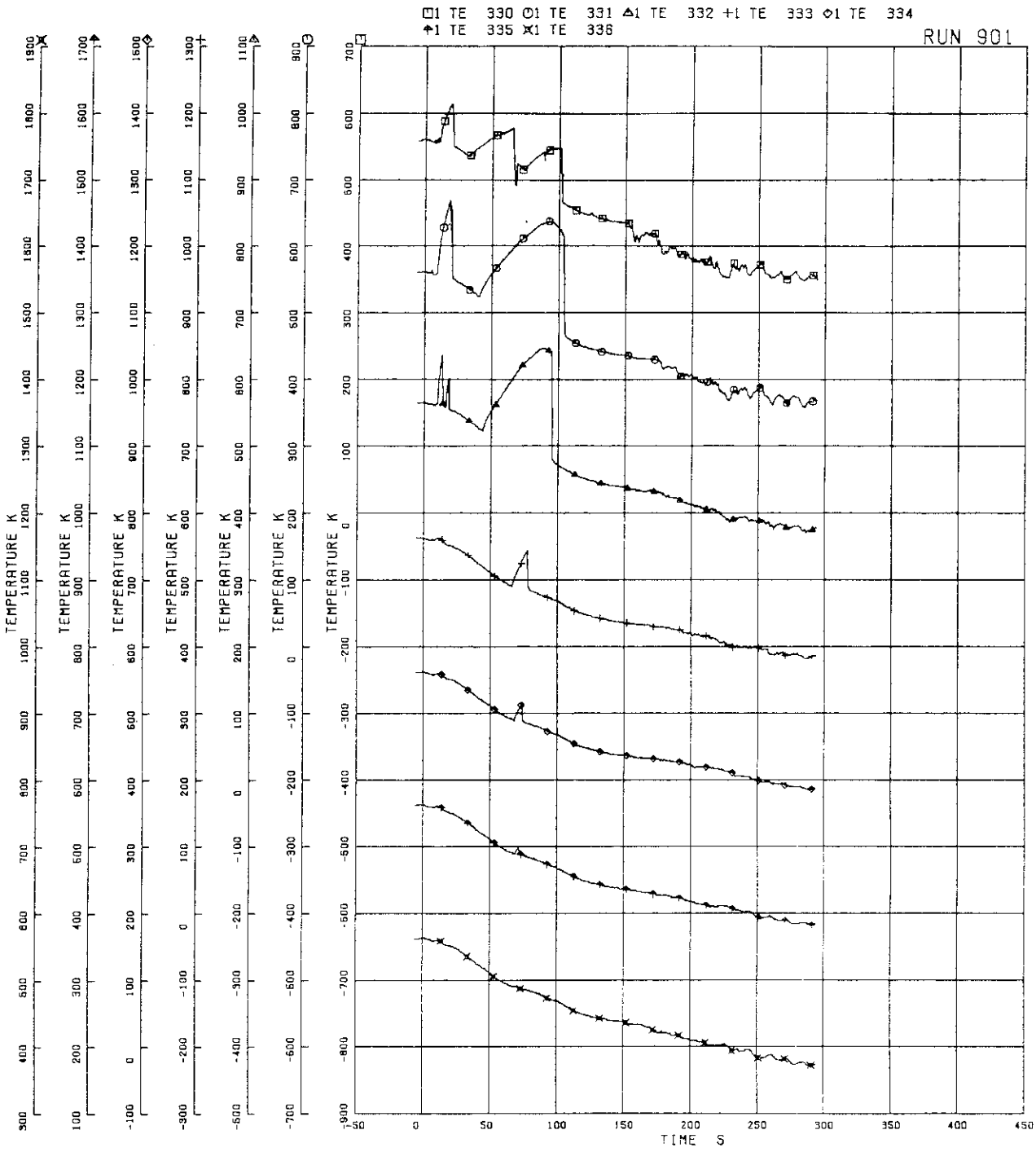


FIG.5. 97 SURFACE TEMPERATURES OF FUEL ROD B11

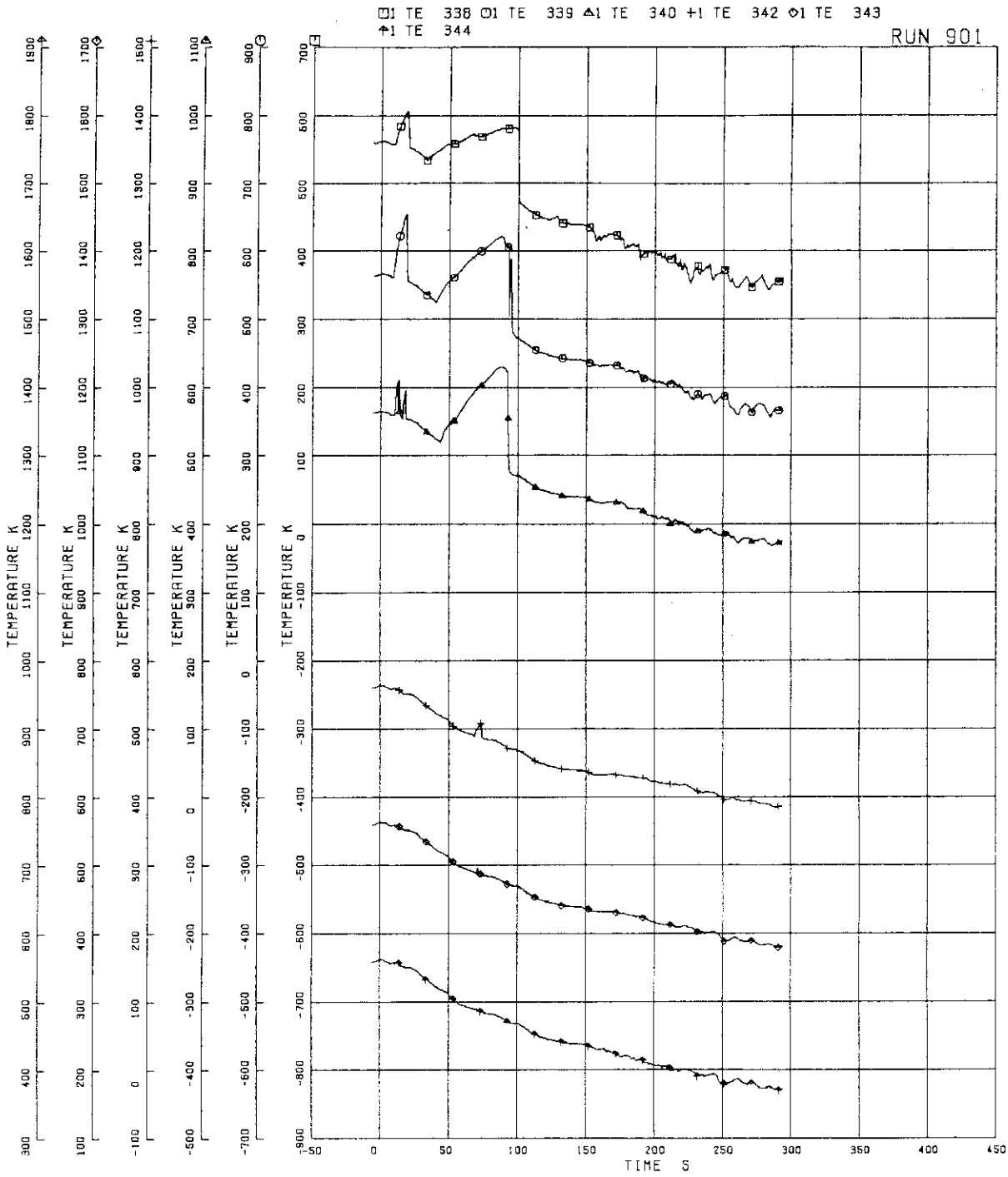


FIG.5. 98 SURFACE TEMPERATURES OF FUEL ROD B22

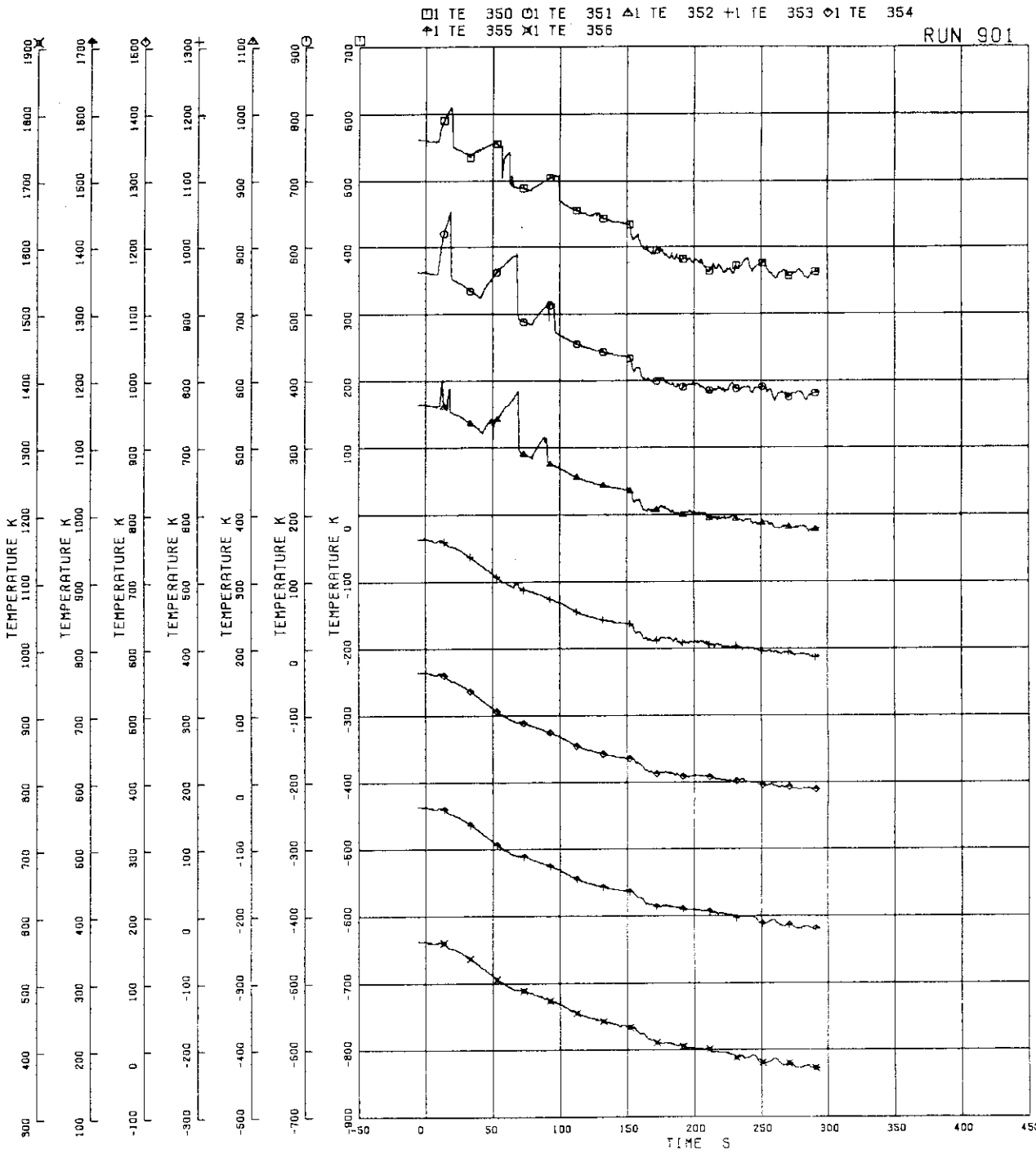


FIG.5. 99 SURFACE TEMPERATURES OF FUEL ROD B77

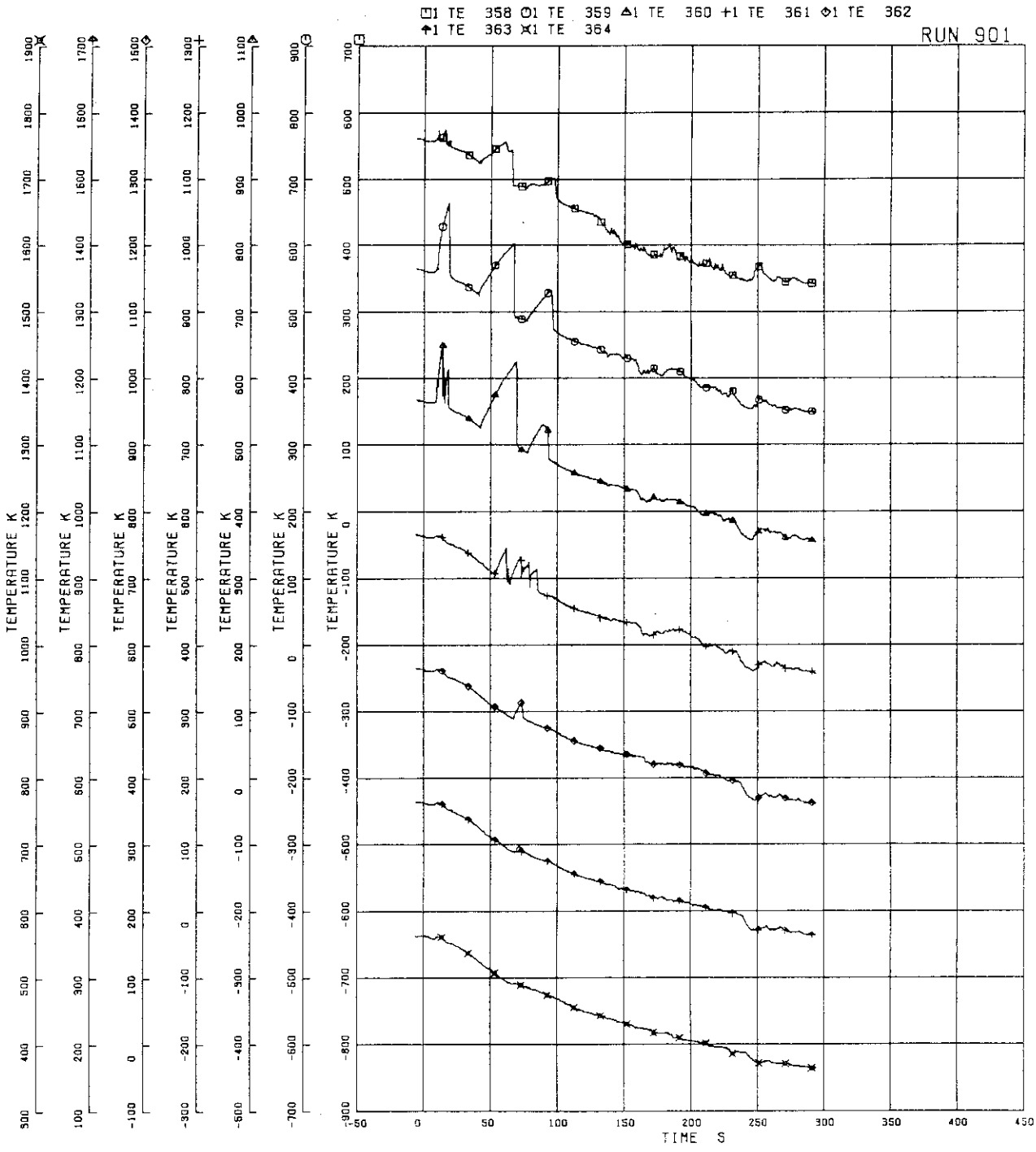


FIG.5.100 SURFACE TEMPERATURES OF FUEL ROD C11

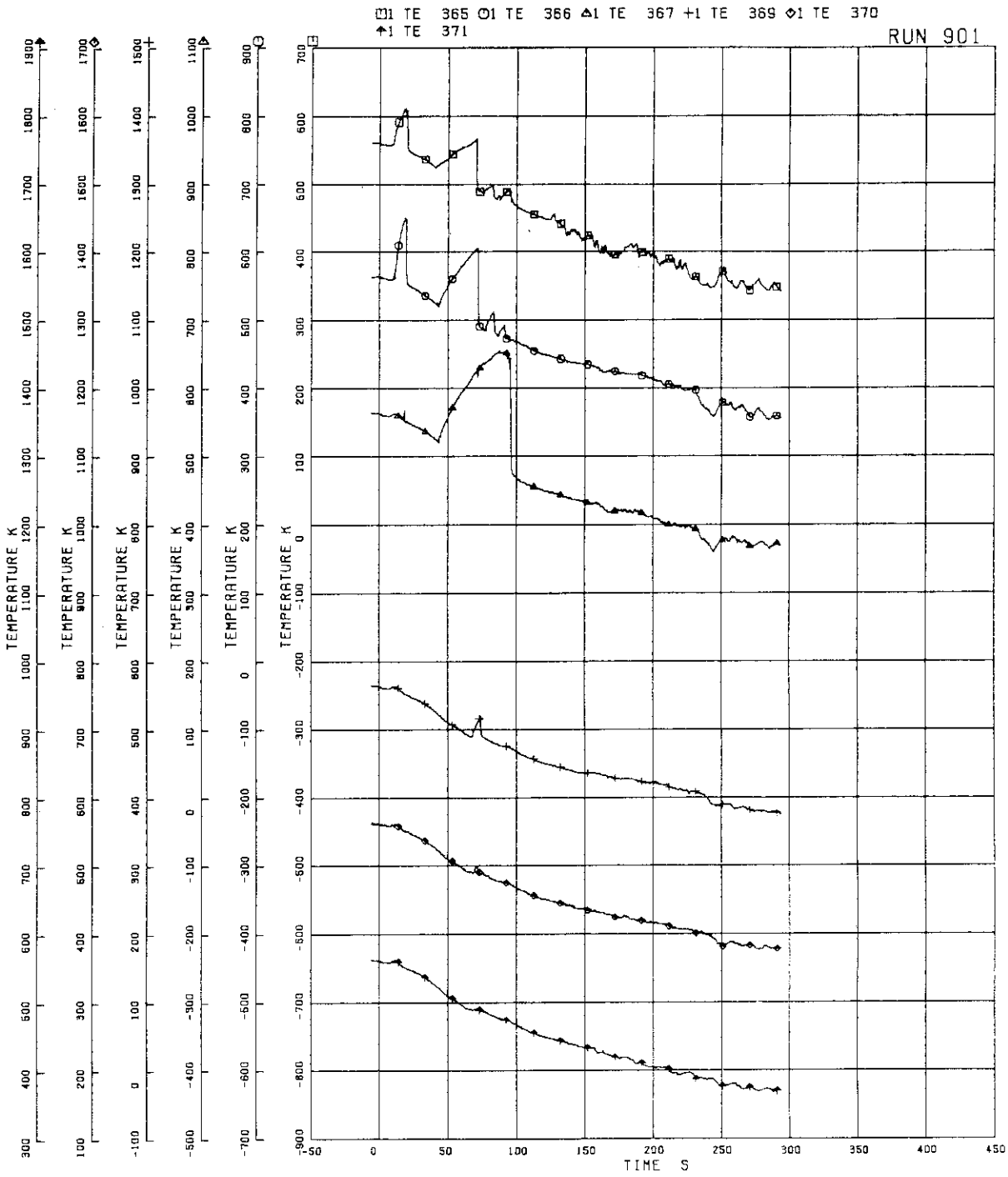


FIG.5.101 SURFACE TEMPERATURES OF FUEL ROD C13

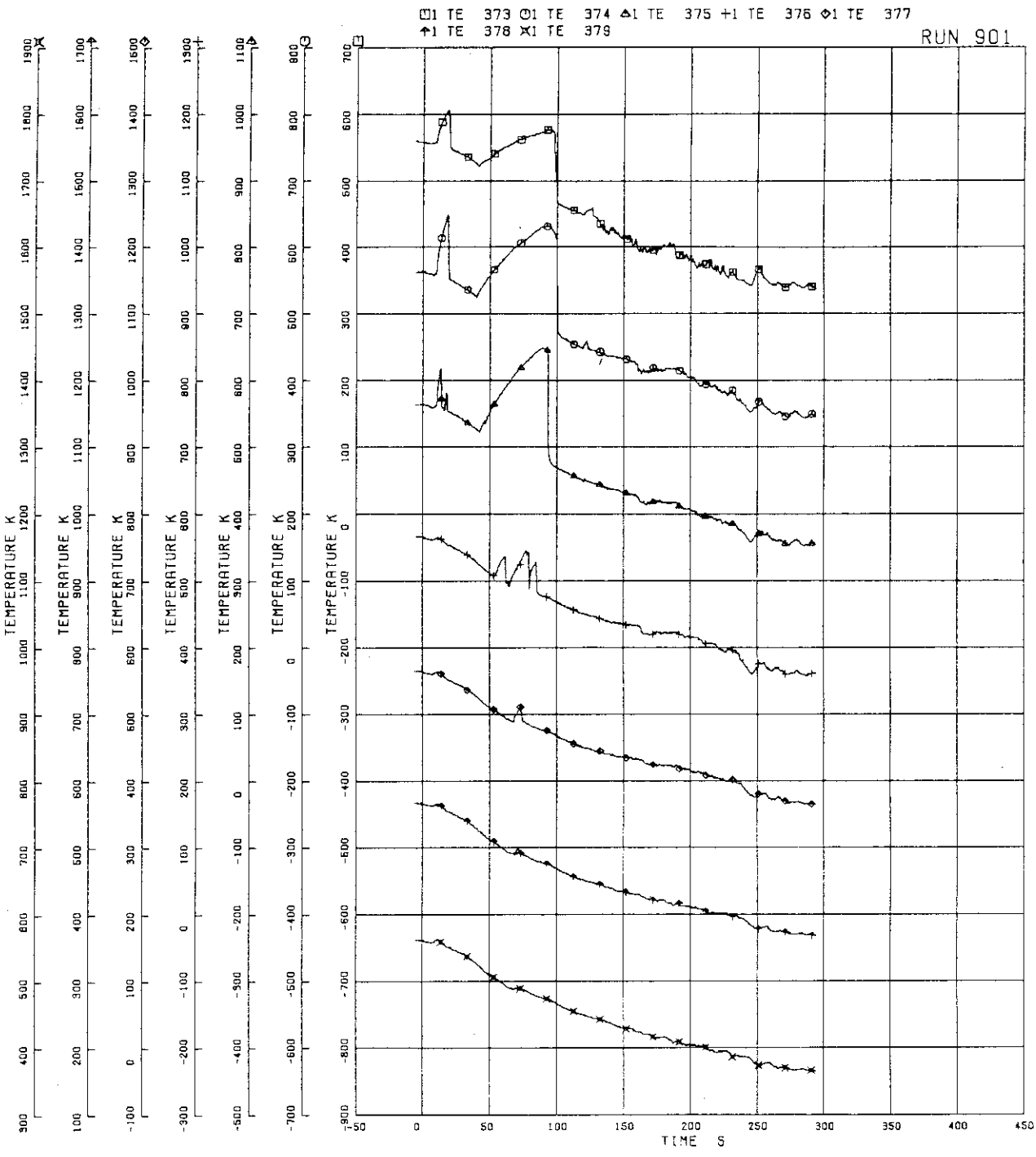


FIG.5.102 SURFACE TEMPERATURES OF FUEL ROD C22

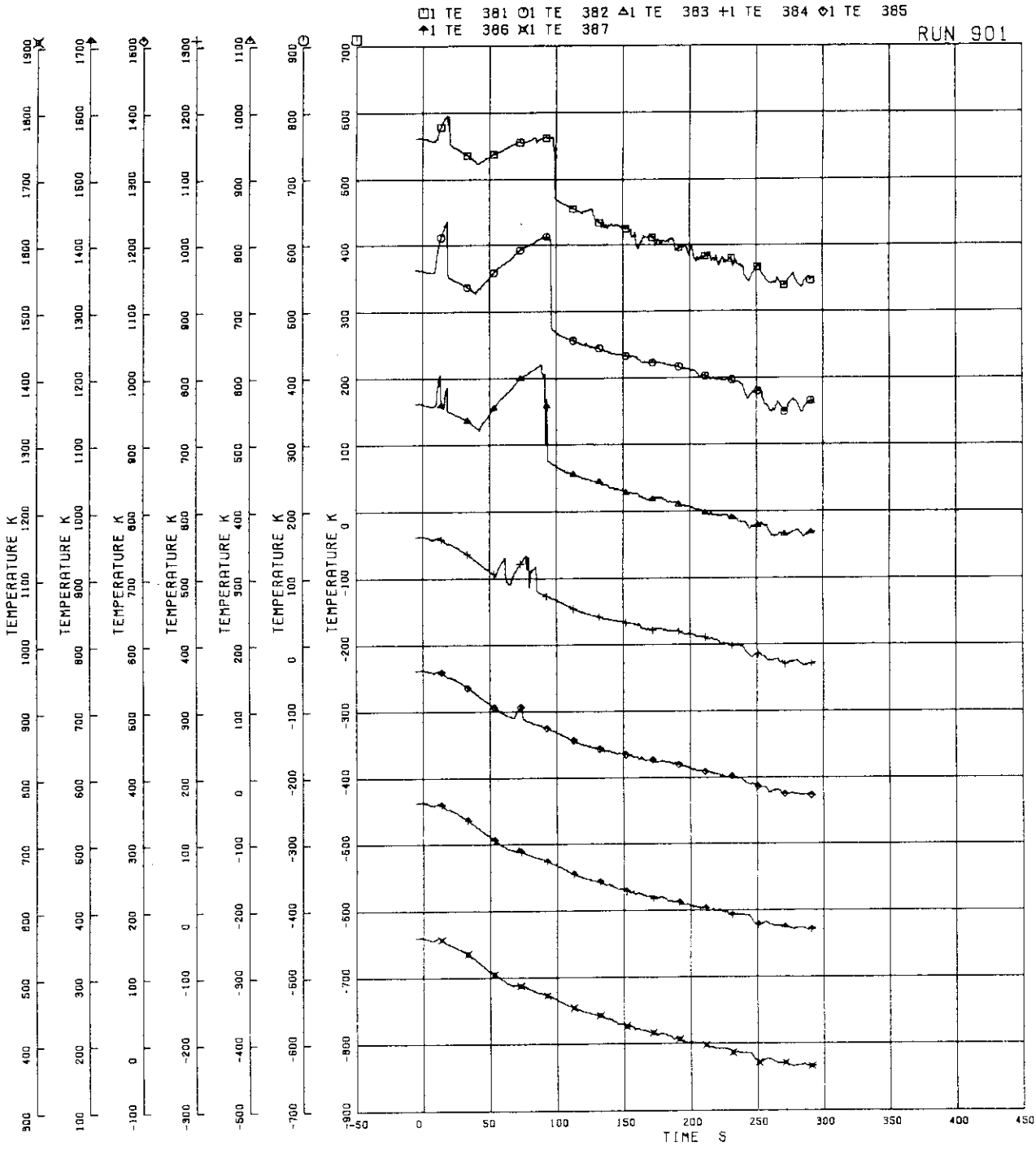


FIG.5.103 SURFACE TEMPERATURES OF FUEL ROD C33

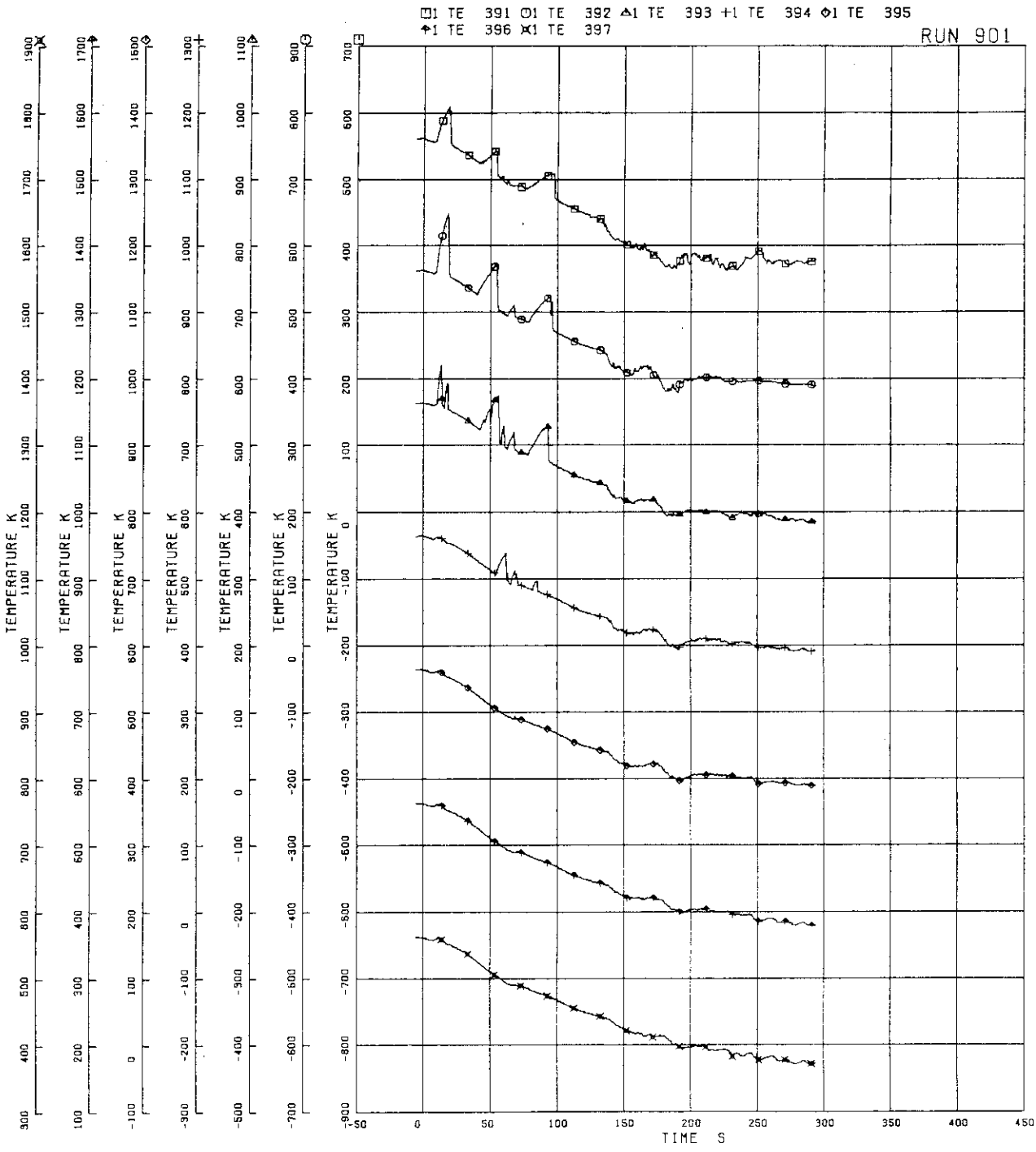


FIG.5.104 SURFACE TEMPERATURES OF FUEL ROD C77

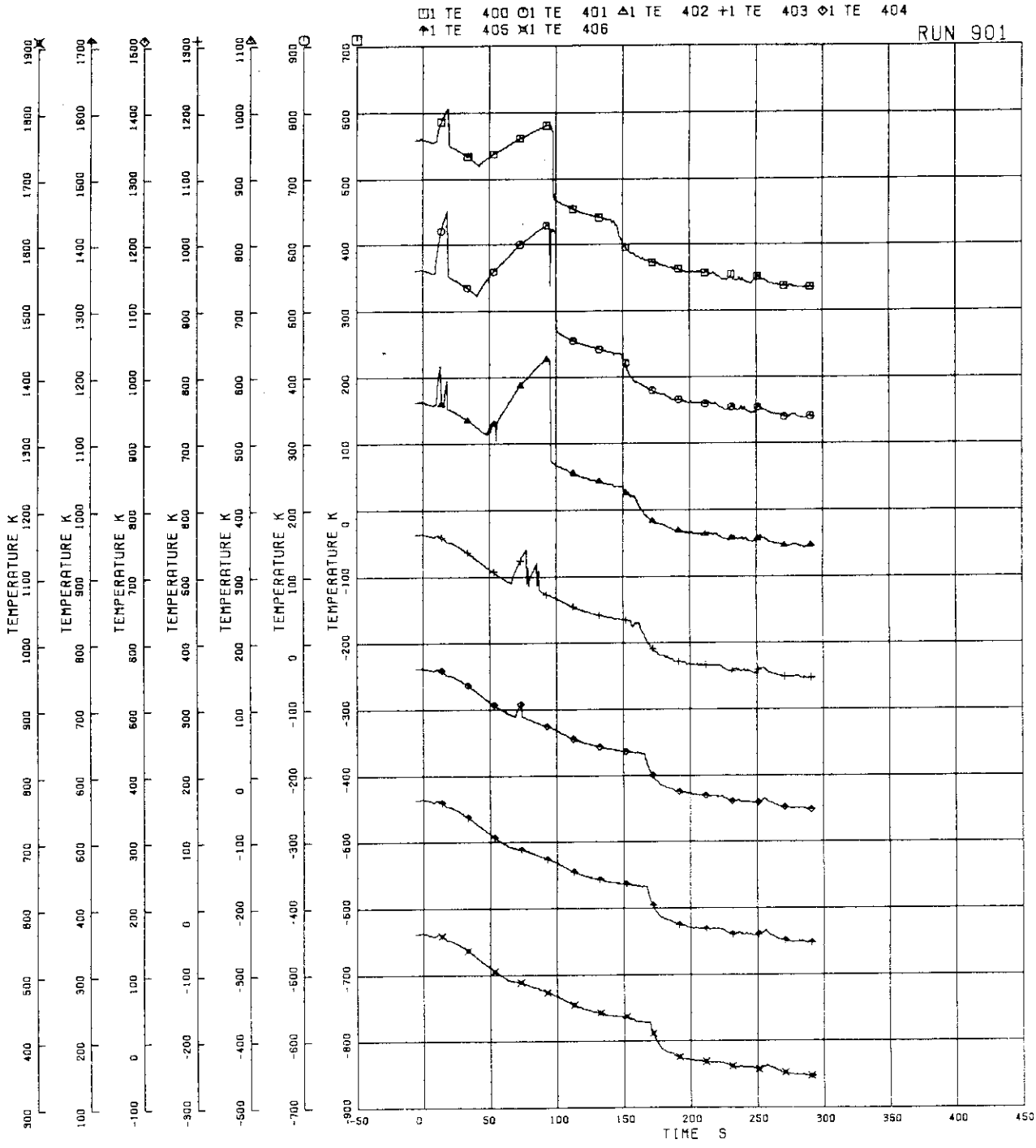


FIG.5.105 SURFACE TEMPERATURES OF FUEL ROD D22

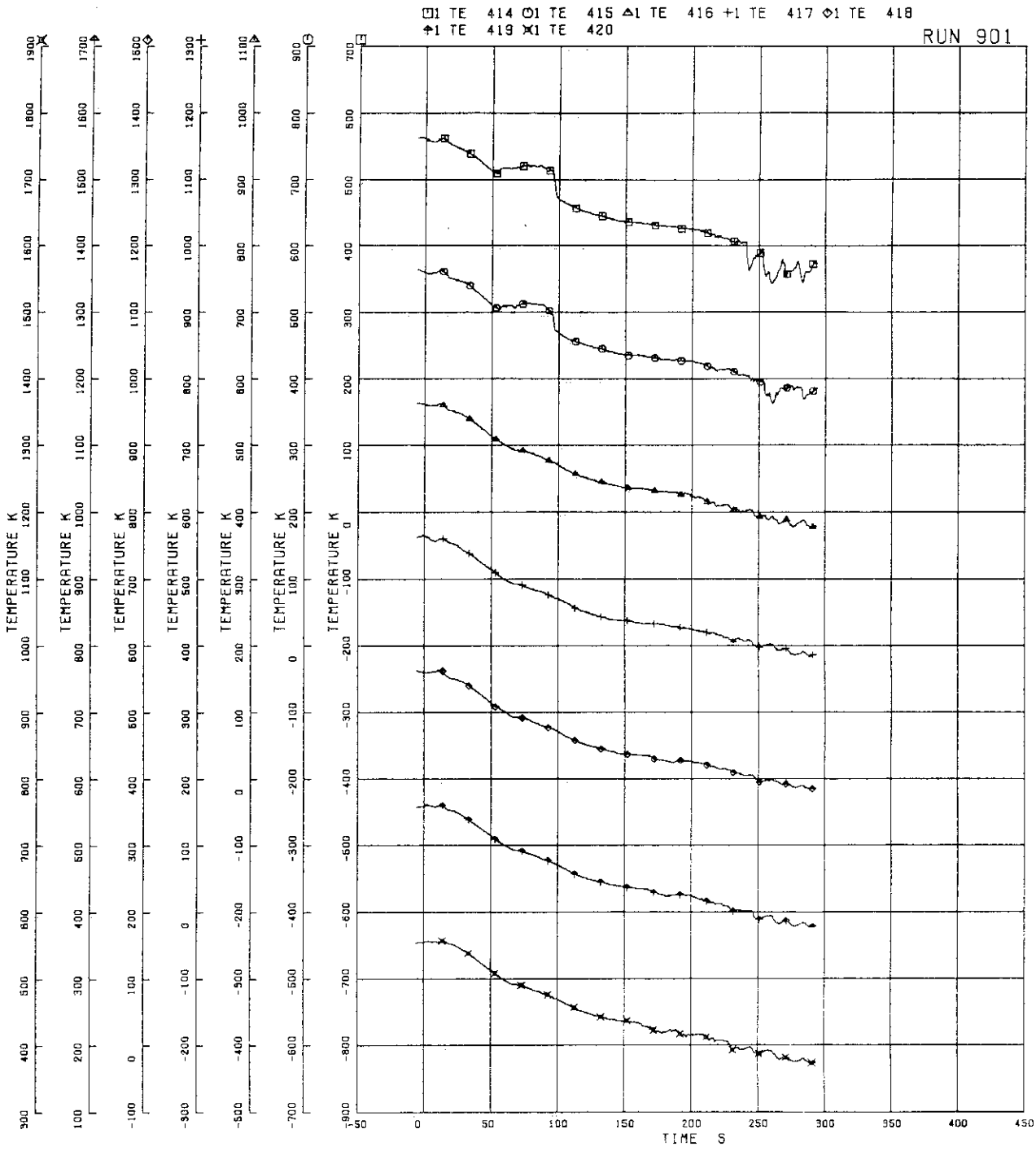


FIG.5.106 SURFACE TEMPERATURES OF WATER ROD SIMULATOR A45

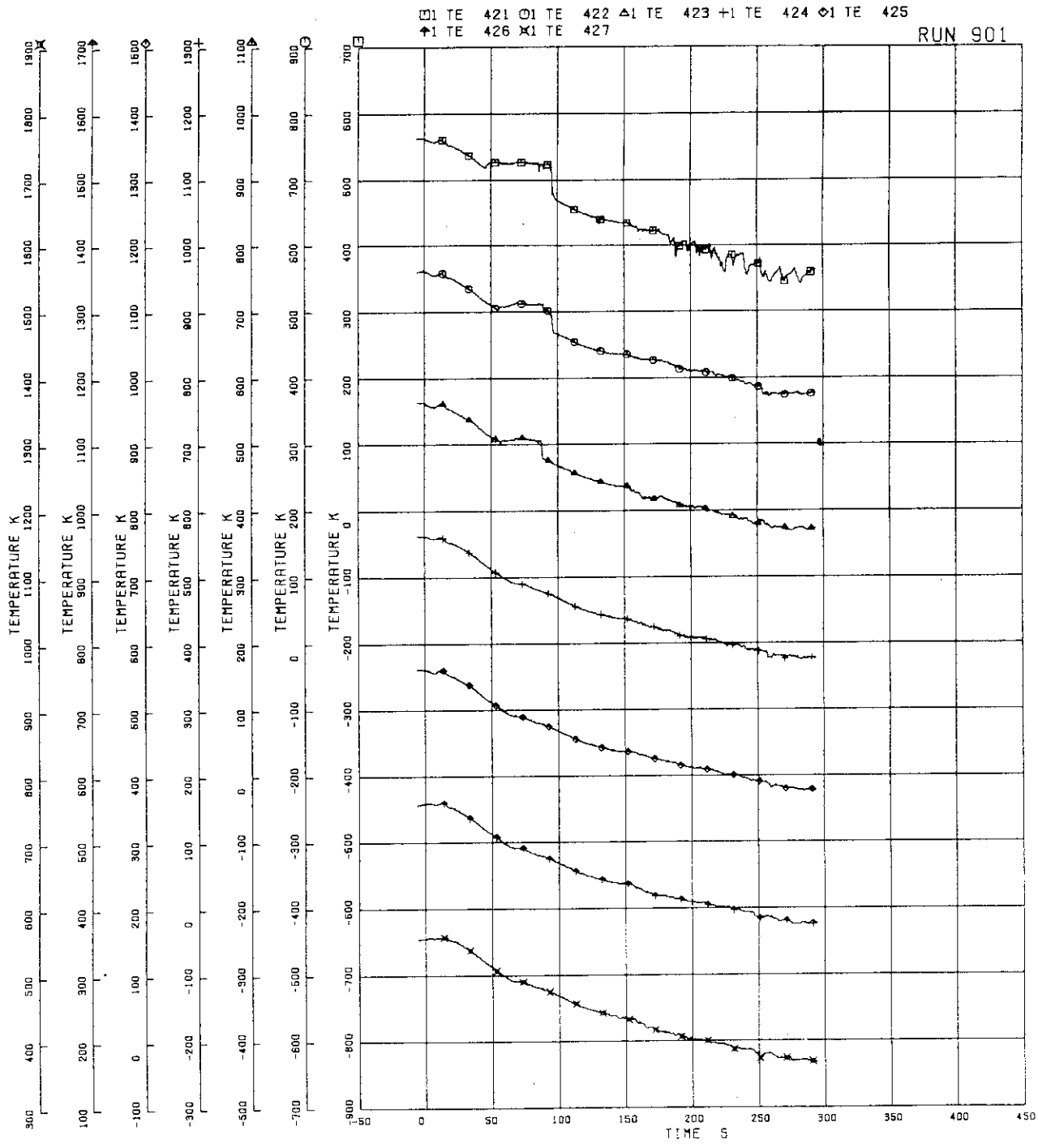


FIG.5.107 SURFACE TEMPERATURES OF WATER ROD SIMULATOR B45

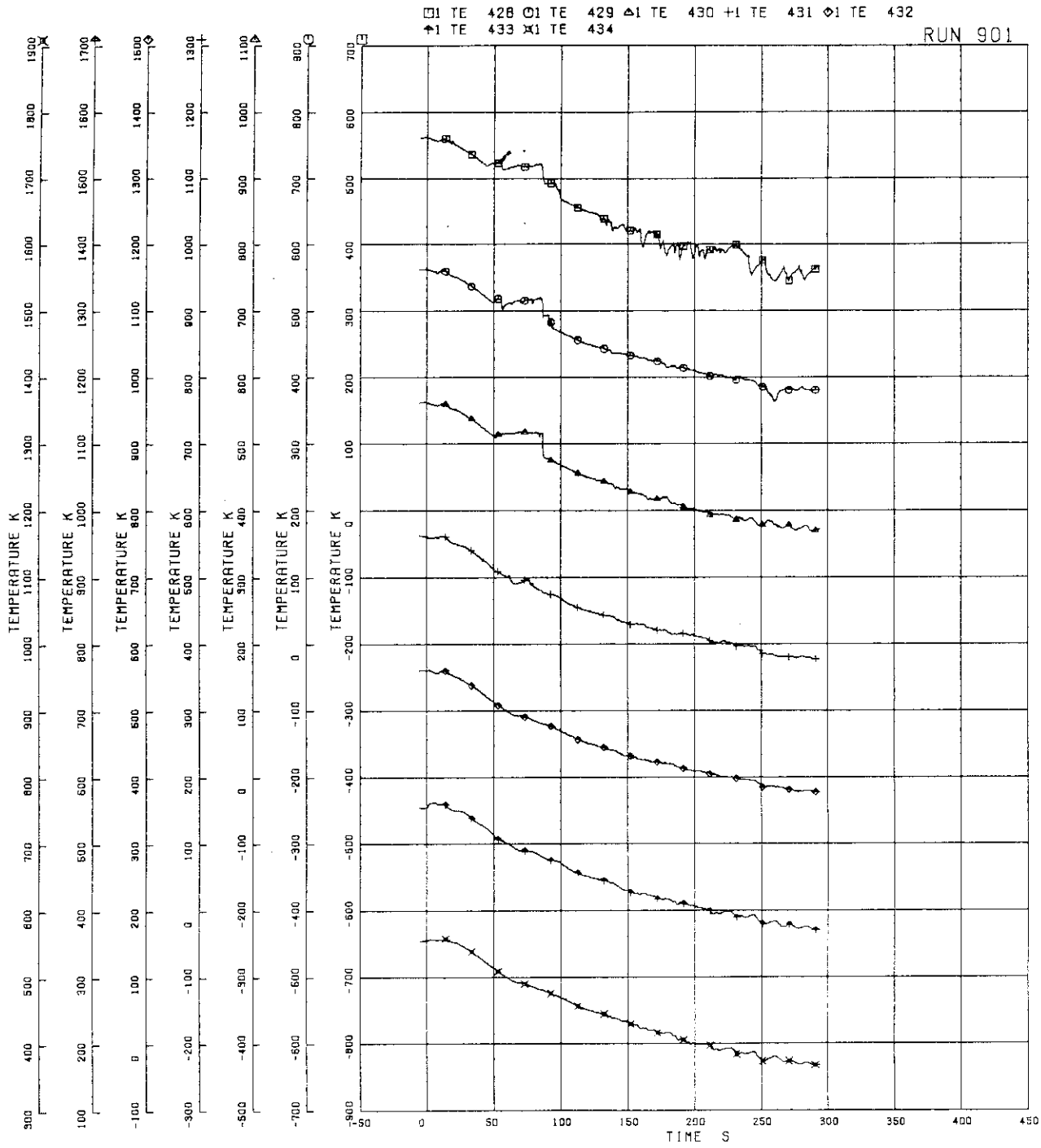


FIG.5.108 SURFACE TEMPERATURES OF WATER ROD SIMULATOR C45

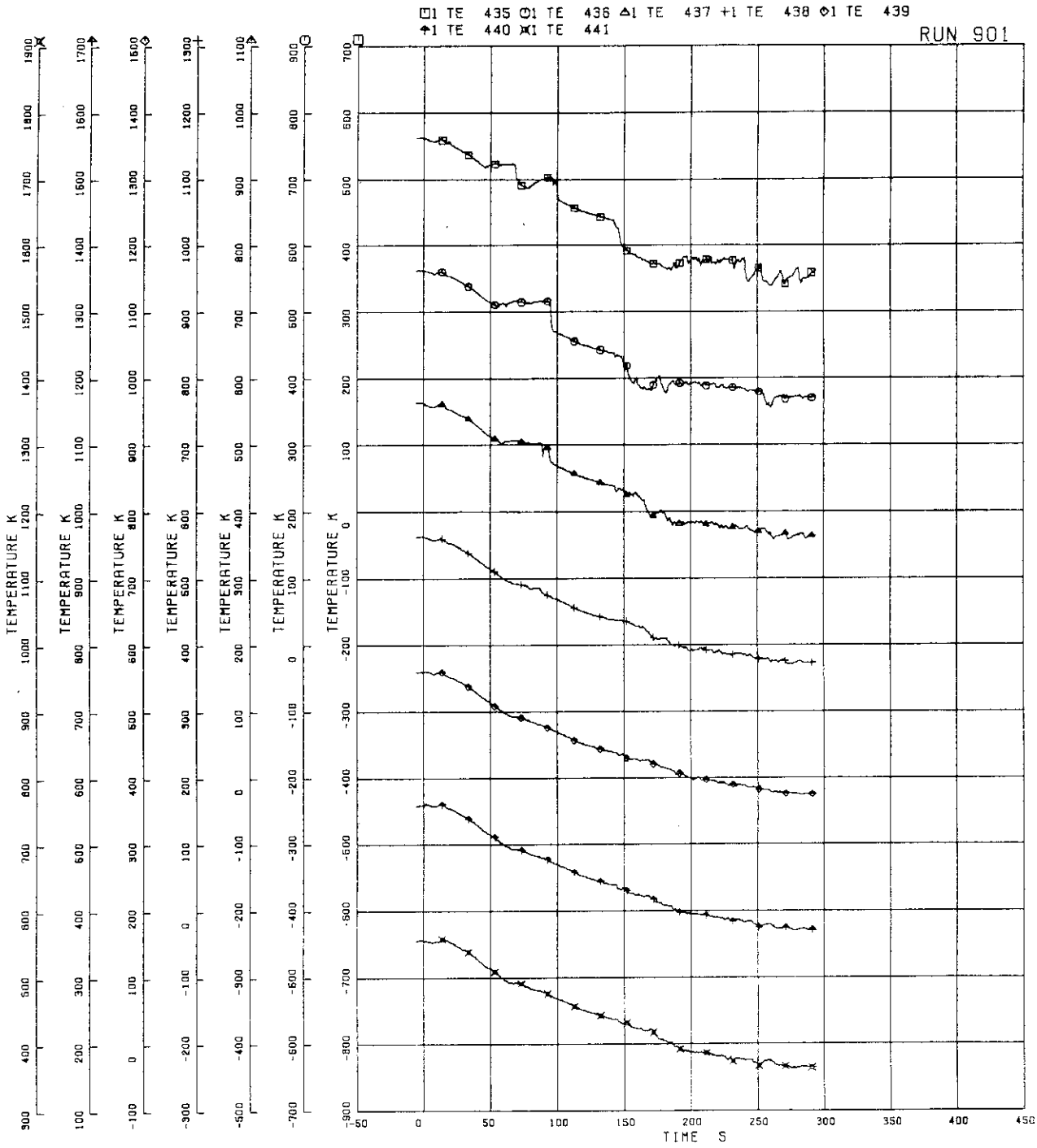


FIG.5.109 SURFACE TEMPERATURES OF WATER ROD SIMULATOR D45

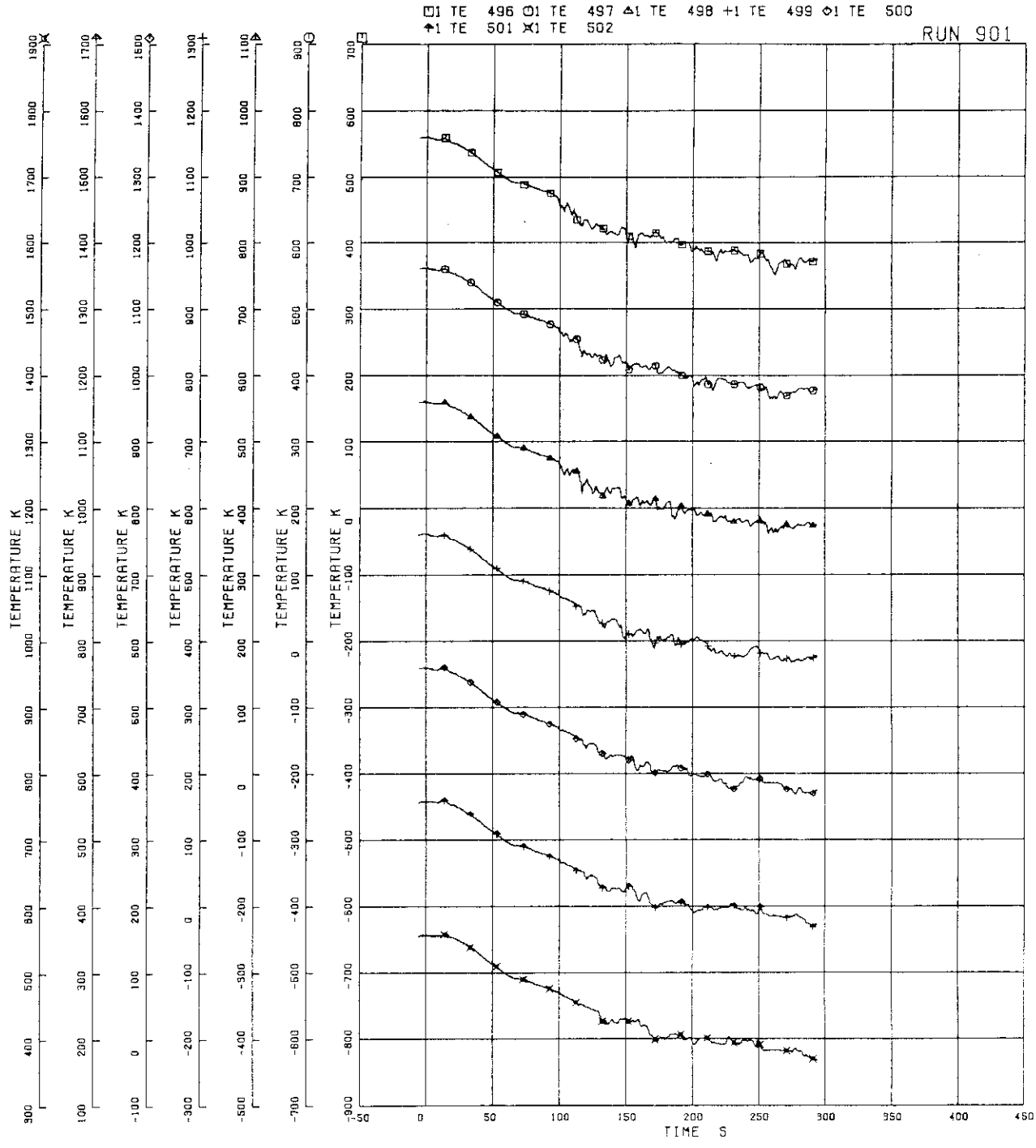


FIG.5.110 INNER SURFACE TEMPERATURES OF CHANNEL BOX A, LOCATION A1

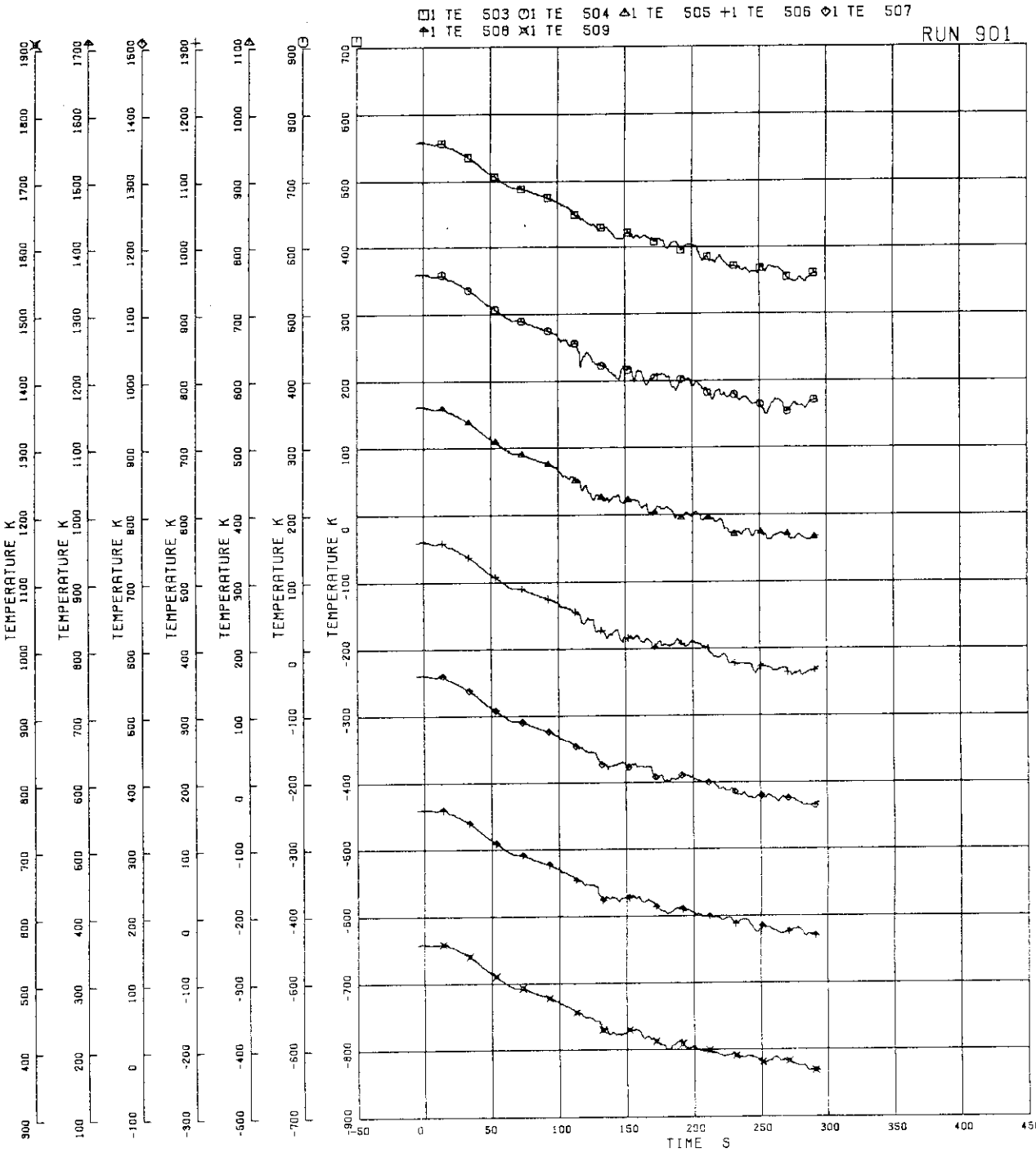


FIG.5.111 INNER SURFACE TEMPERATURES OF CHANNEL BOX A, LOCATION A2

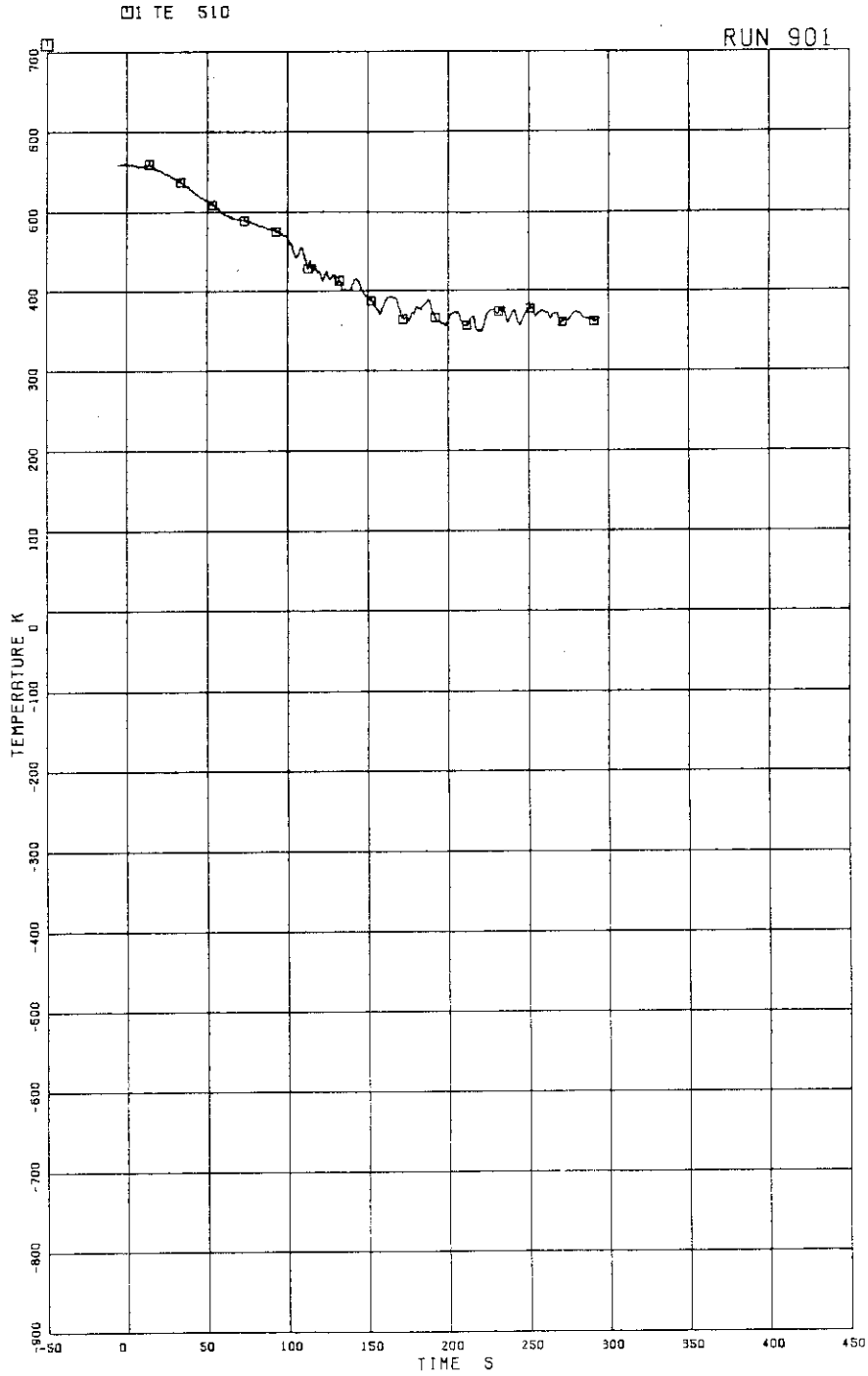


FIG.5.112 INNER SURFACE TEMPERATURE OF CHANNEL BOX B (POSITION 1)

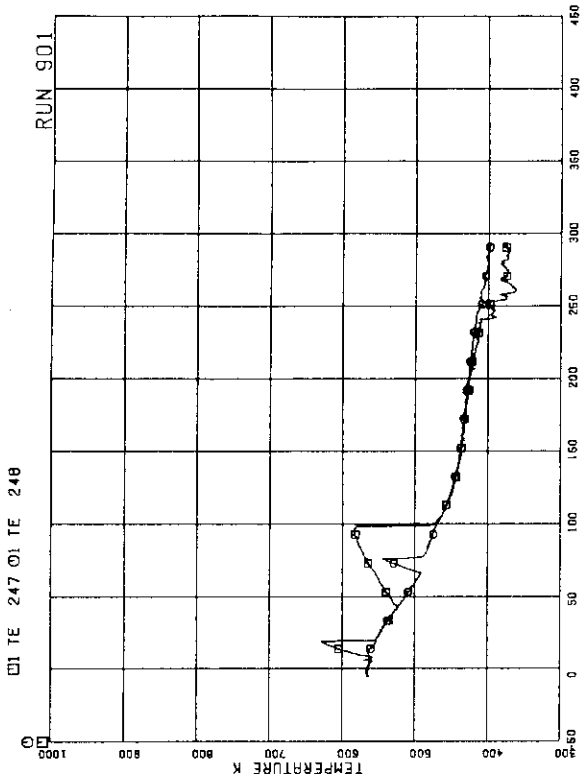


FIG.5.115 SURFACE TEMPERATURES OF FUEL ROD A26 AT POSITIONS 1 AND 4

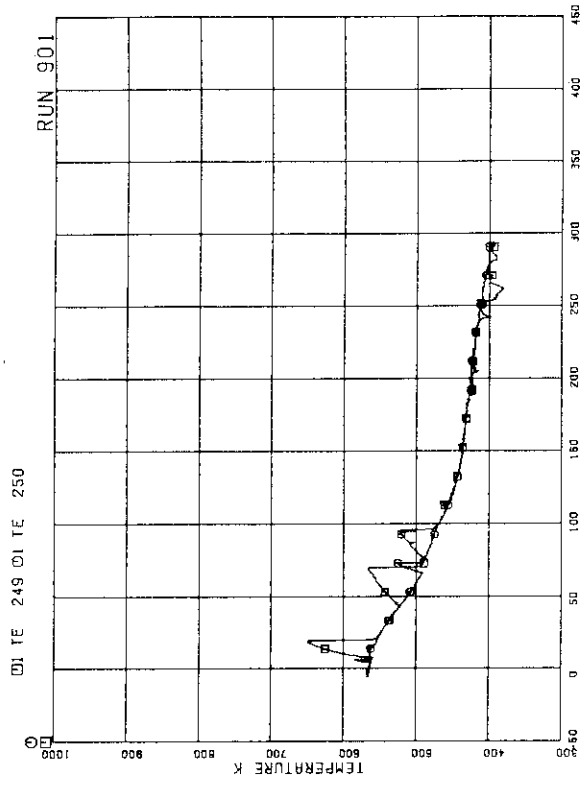


FIG.5.116 SURFACE TEMPERATURES OF FUEL ROD A28 AT POSITIONS 1 AND 4

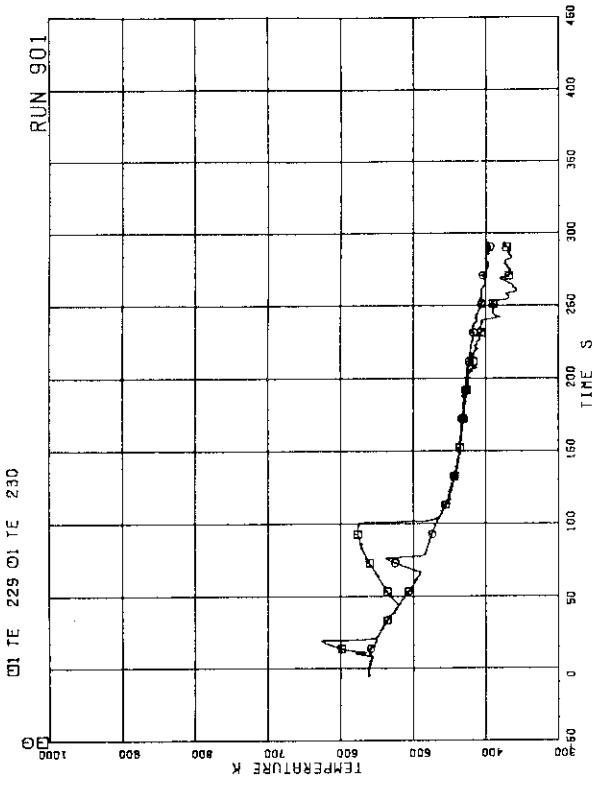


FIG.5.113 SURFACE TEMPERATURES OF FUEL ROD A15 AT POSITIONS 1 AND 4

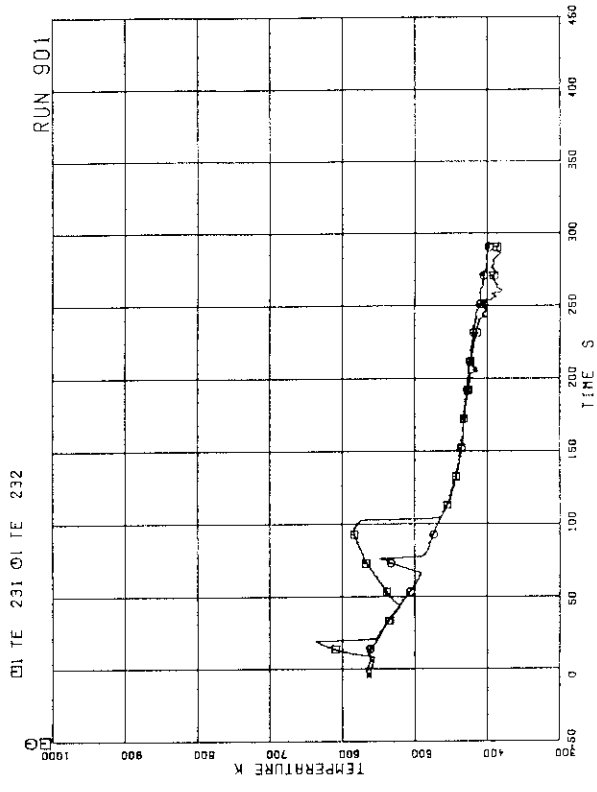


FIG.5.114 SURFACE TEMPERATURES OF FUEL ROD A17 AT POSITIONS 1 AND 4

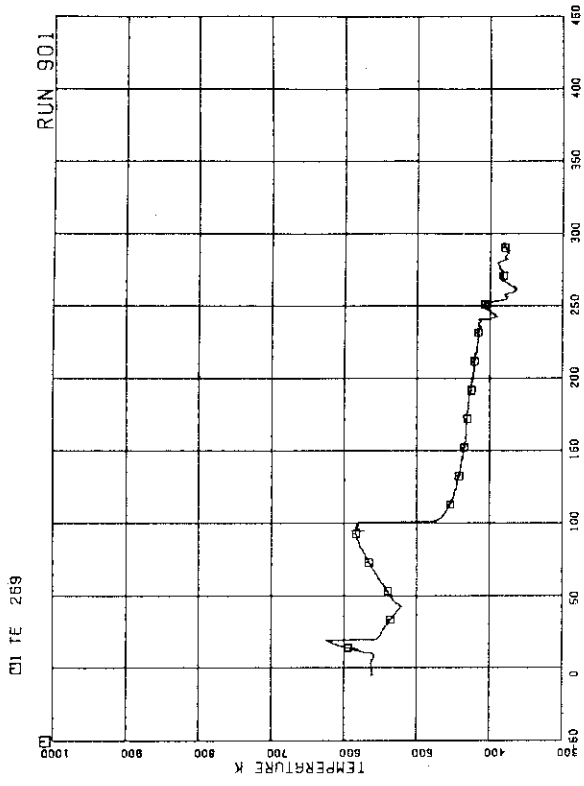


FIG.5.119 SURFACE TEMPERATURE OF FUEL ROD A42 AT POSITION 1

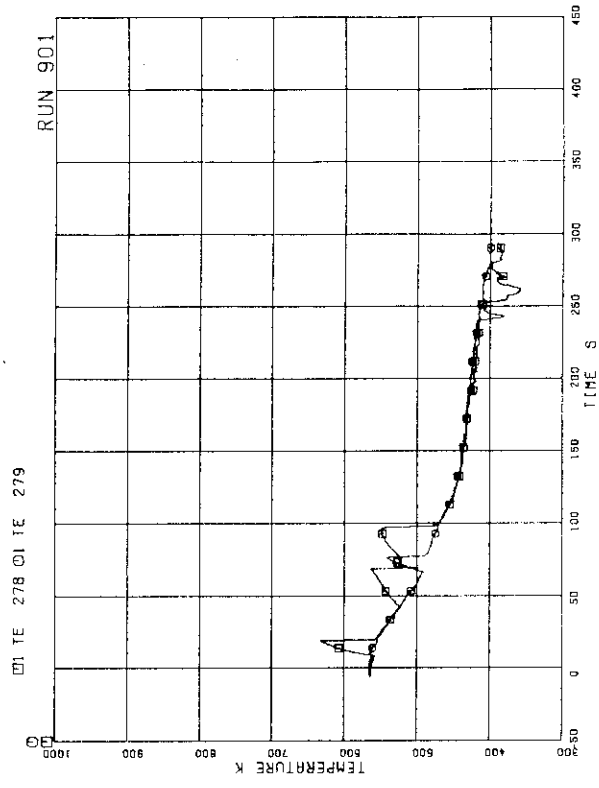


FIG.5.120 SURFACE TEMPERATURES OF FUEL ROD A48 AT POSITIONS 1 AND 4

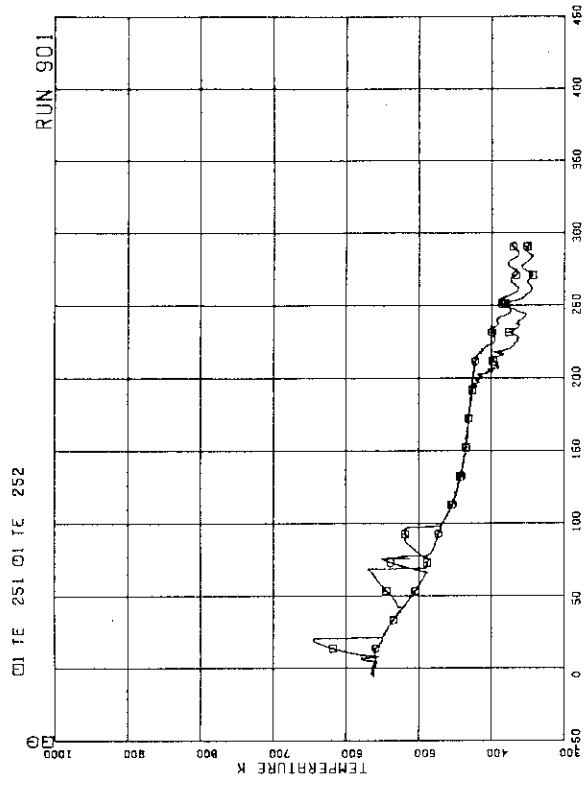


FIG.5.117 SURFACE TEMPERATURES OF FUEL ROD A31 AT POSITIONS 1 AND 4

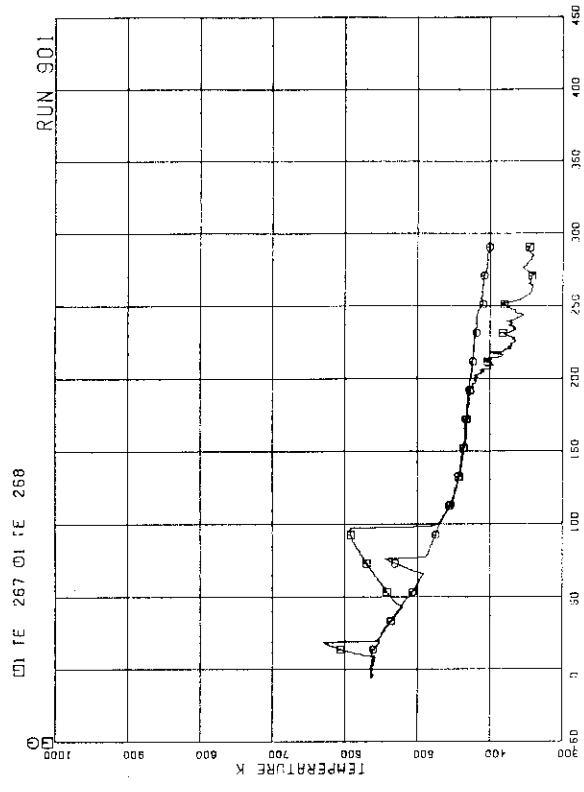


FIG.5.118 SURFACE TEMPERATURES OF FUEL ROD A37 AT POSITIONS 1 AND 4

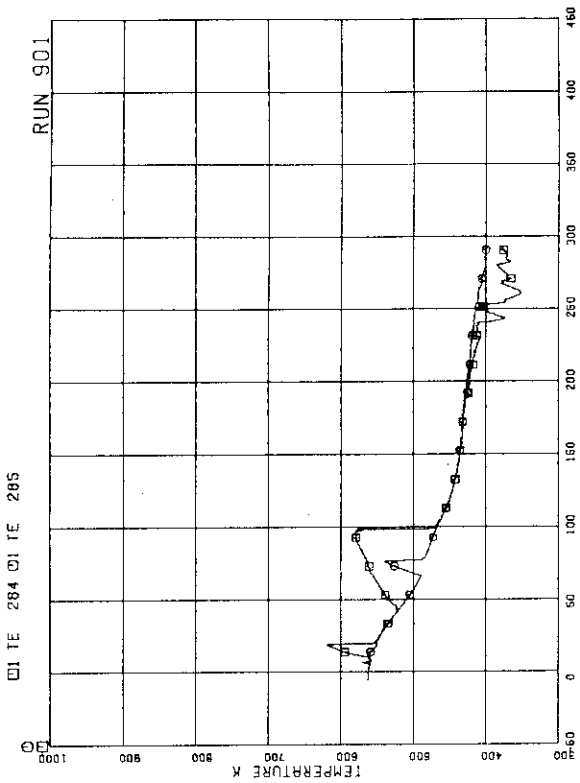


FIG.5.123 SURFACE TEMPERATURES OF FUEL ROD A57 AT POSITIONS 1 AND 4

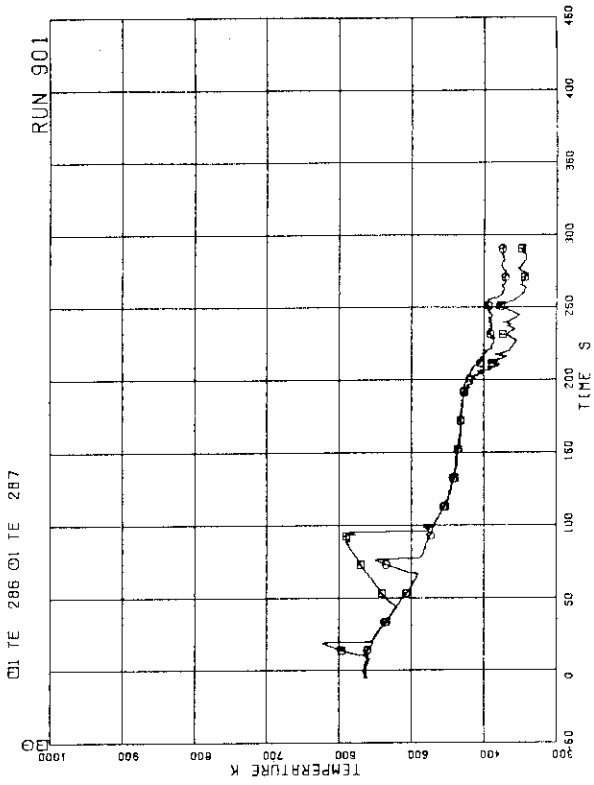


FIG.5.124 SURFACE TEMPERATURES OF FUEL ROD 962 AT POSITIONS 1 AND 4

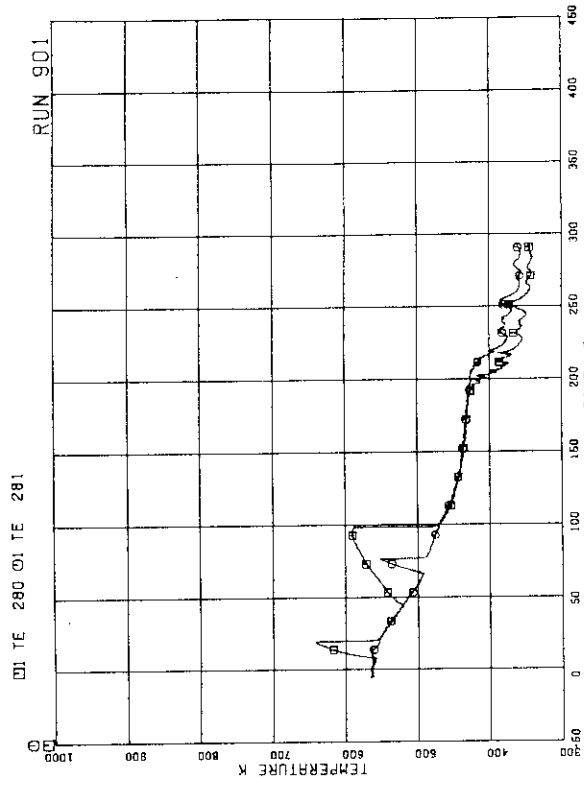


FIG.5.121 SURFACE TEMPERATURES OF FUEL ROD A51 AT POSITIONS 1 AND 4

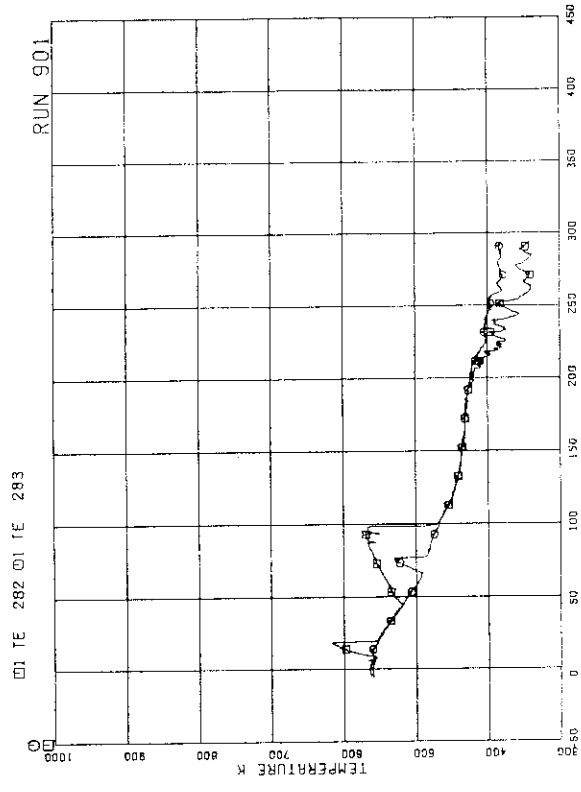


FIG.5.122 SURFACE TEMPERATURES OF FUEL ROD A53 AT POSITIONS 1 AND 4

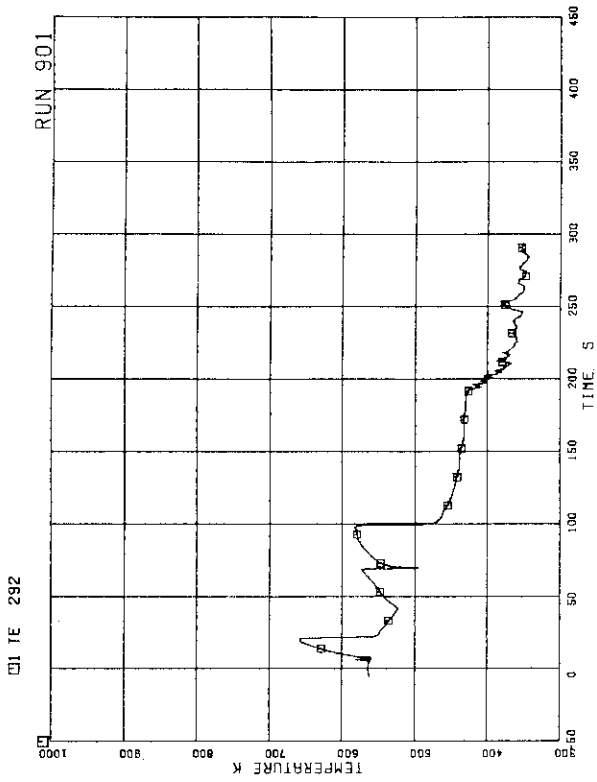


FIG.5.127 SURFACE TEMPERATURE OF FUEL ROD A71 AT POSITION 1

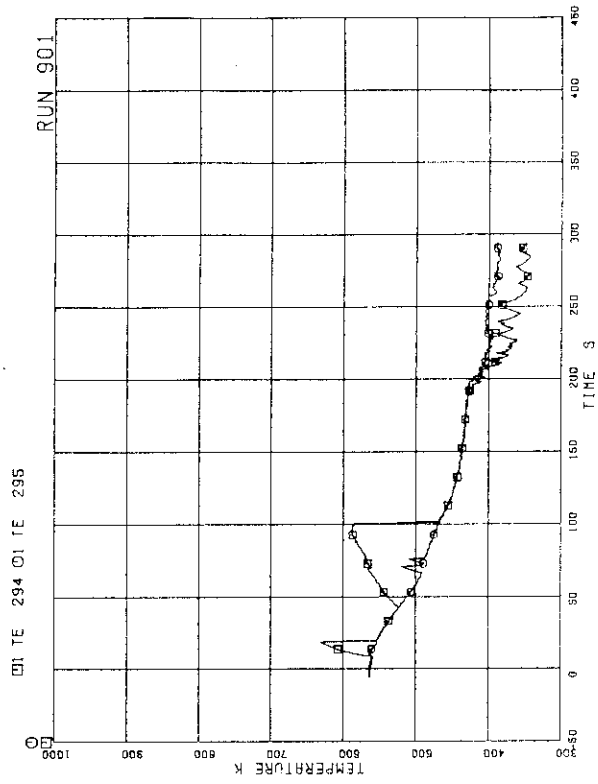


FIG.5.128 SURFACE TEMPERATURES OF FUEL ROD A73 AT POSITIONS 1 AND 4

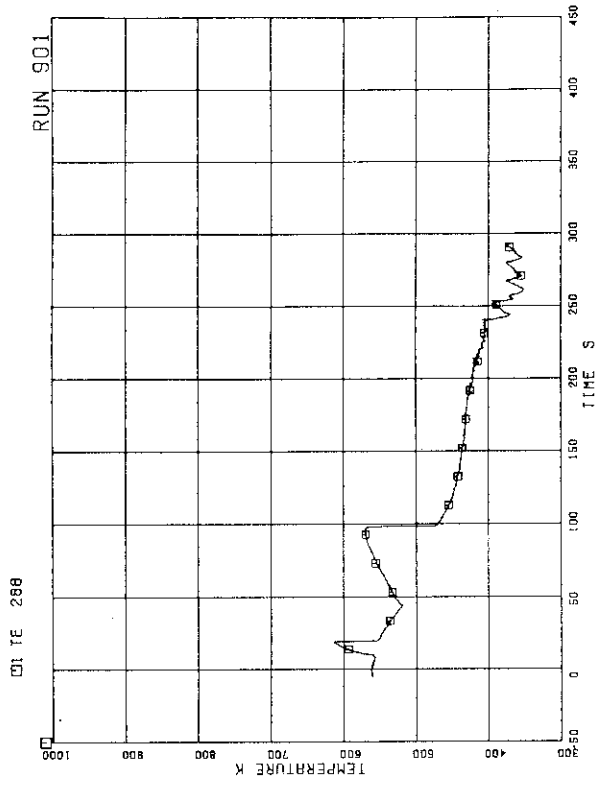


FIG.5.125 SURFACE TEMPERATURE OF FUEL ROD A66 AT POSITION 1

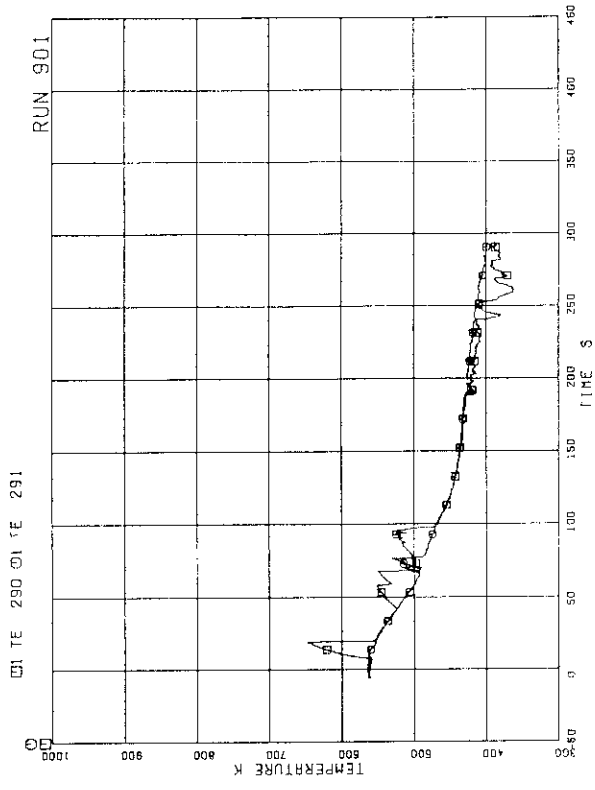


FIG.5.126 SURFACE TEMPERATURES OF FUEL ROD A68 AT POSITIONS 1 AND 4

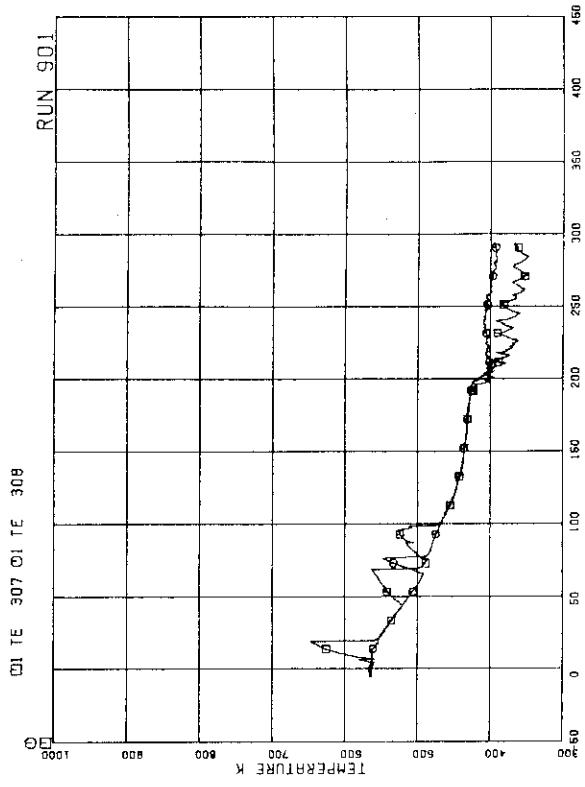


FIG.5.131 SURFACE TEMPERATURES OF FUEL ROD A84 AT POSITIONS 1 AND 4

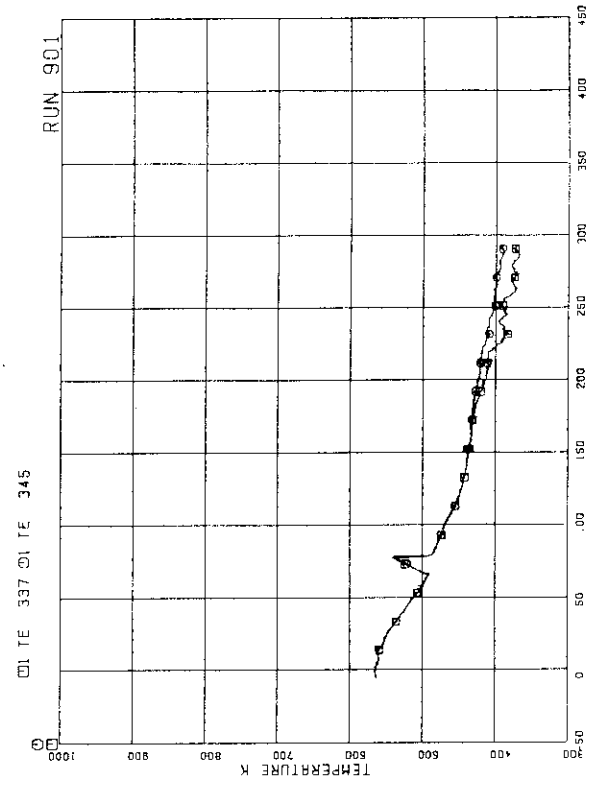


FIG.5.132 SURFACE TEMPERATURES OF FUEL RODS B13,B31 AT POSITION 4

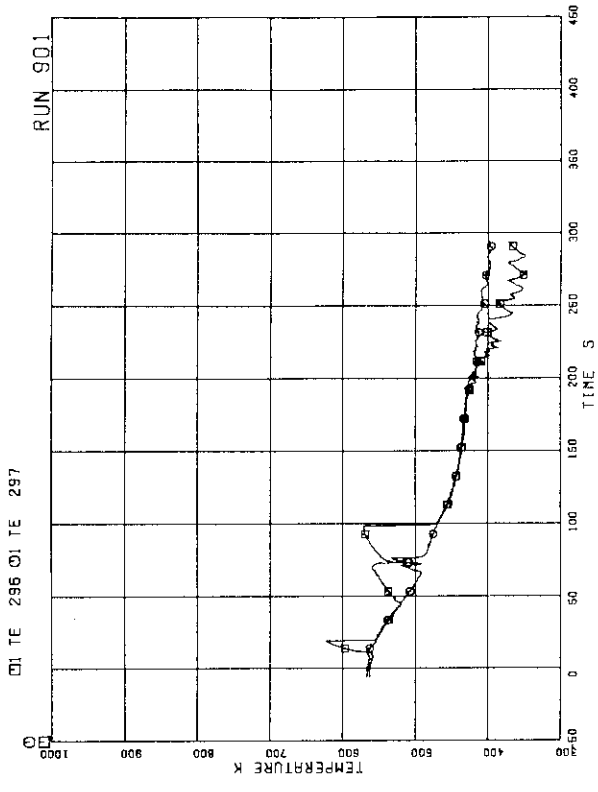


FIG.5.129 SURFACE TEMPERATURES OF FUEL ROD A75 AT POSITIONS 1 AND 4

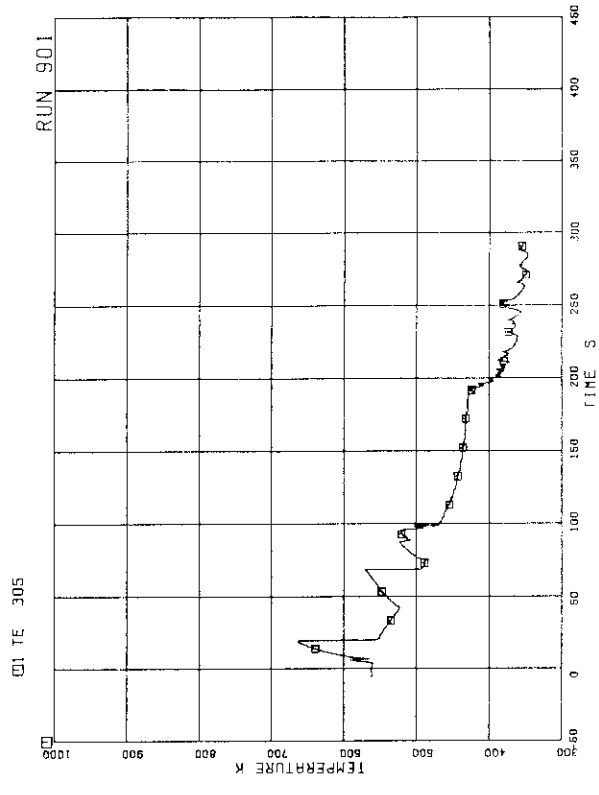


FIG.5.130 SURFACE TEMPERATURE OF FUEL ROD A82 AT POSITION 1

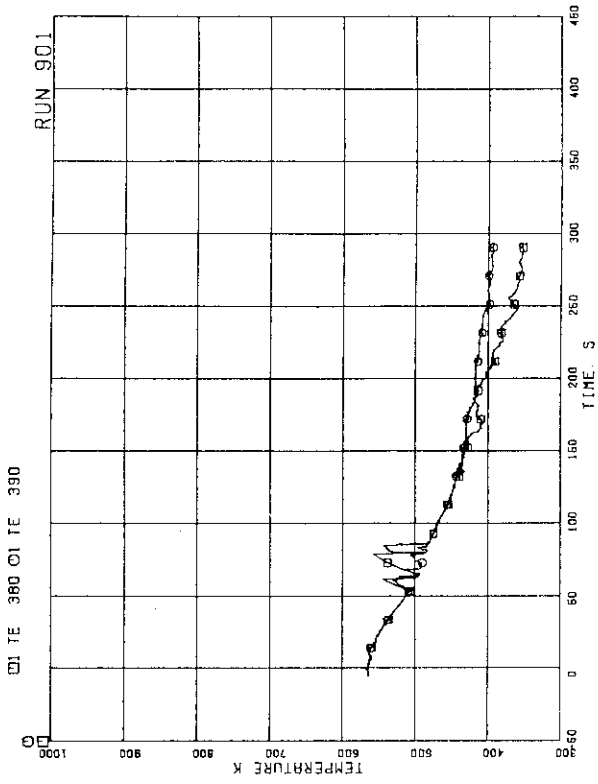


FIG.5.135 SURFACE TEMPERATURES OF FUEL RODS C31,C68 AT POSITION 4

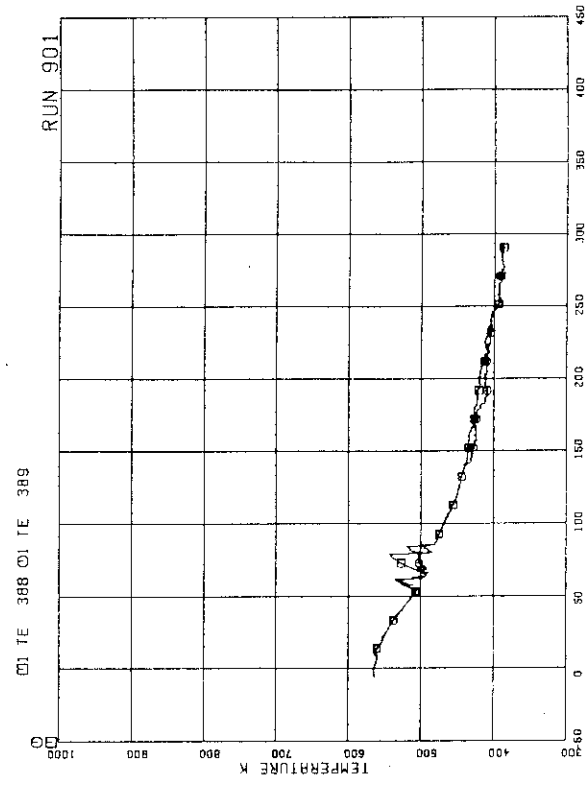


FIG.5.136 SURFACE TEMPERATURES OF FUEL RODS C35,C66 AT POSITION 4

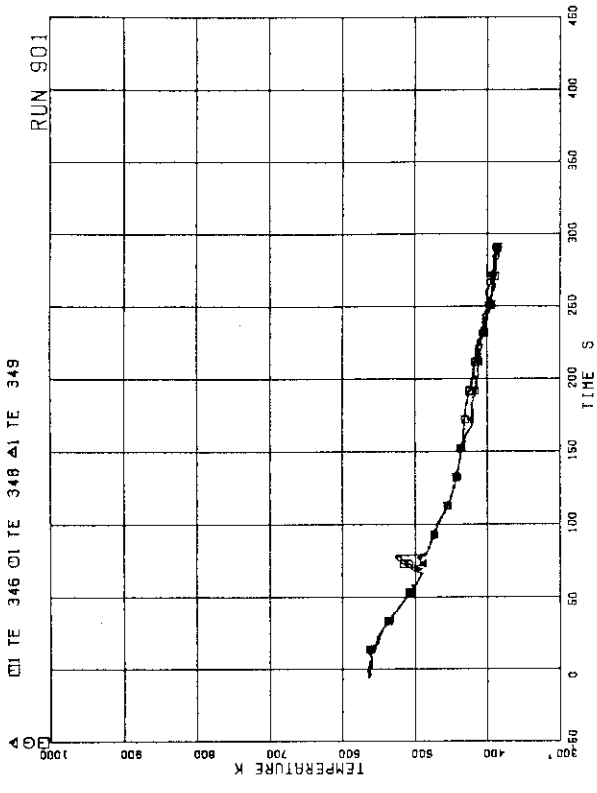


FIG.5.133 SURFACE TEMPERATURES OF FUEL RODS B33,B53,B66 AT POSITION 4

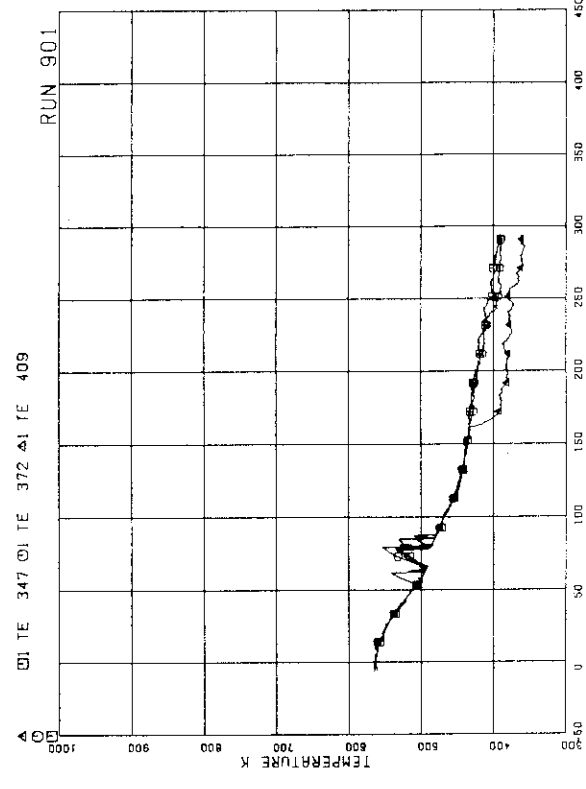


FIG.5.134 SURFACE TEMPERATURES OF FUEL RODS B51,C15,C51 AT POSITION 4

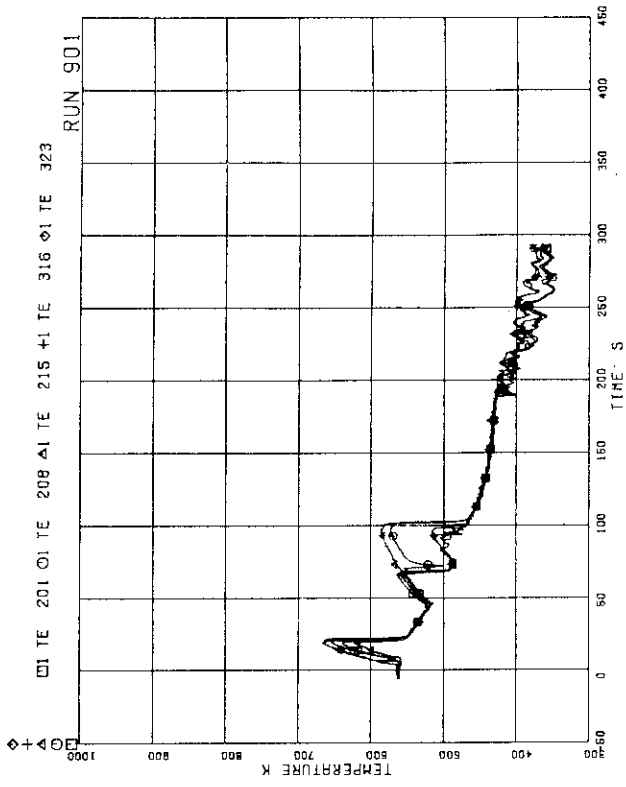


FIG.5.139 SURFACE TEMPERATURES OF FUEL RODS
A11,A12,A13,A87,A88 AT POSITION 1

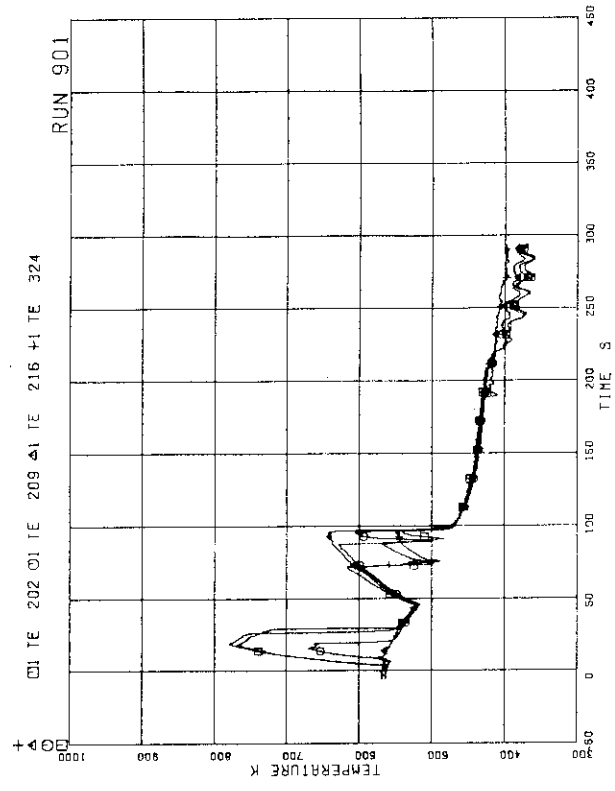


FIG.5.140 SURFACE TEMPERATURES OF FUEL RODS
A11,A12,A13,A88 AT POSITION 2

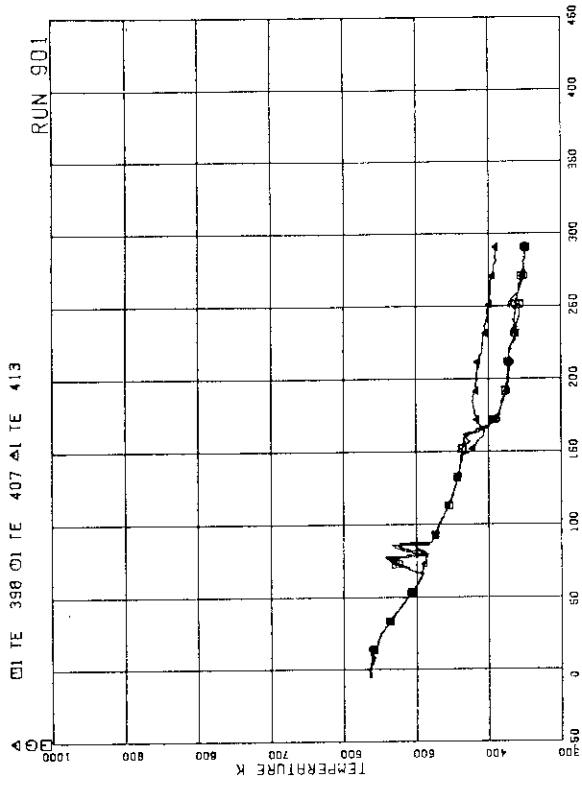


FIG.5.137 SURFACE TEMPERATURES OF FUEL RODS
D11,D31,D86 AT POSITION 4

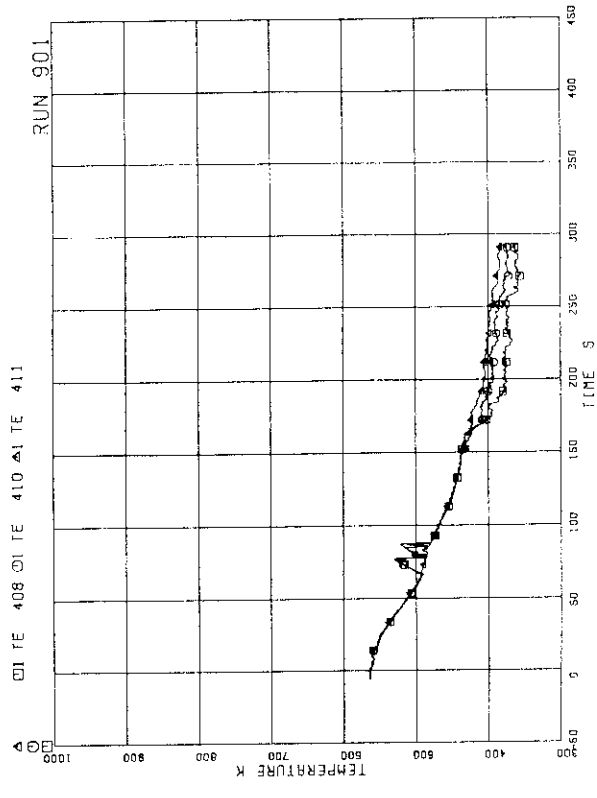


FIG.5.138 SURFACE TEMPERATURES OF FUEL RODS
D33,D53,D66 AT POSITION 4

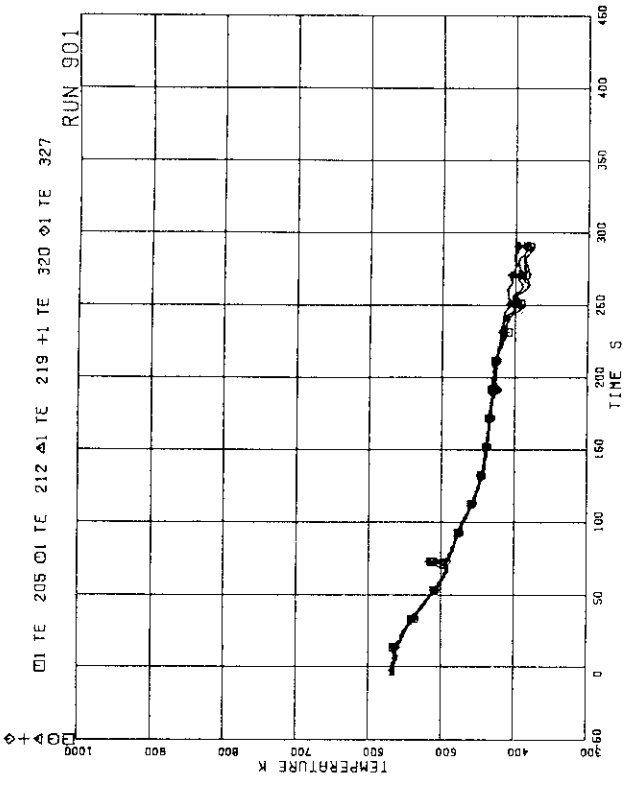


FIG.5.143 SURFACE TEMPERATURES OF FUEL RODS A11,A12,A13,A87,A88 AT POSITION 5

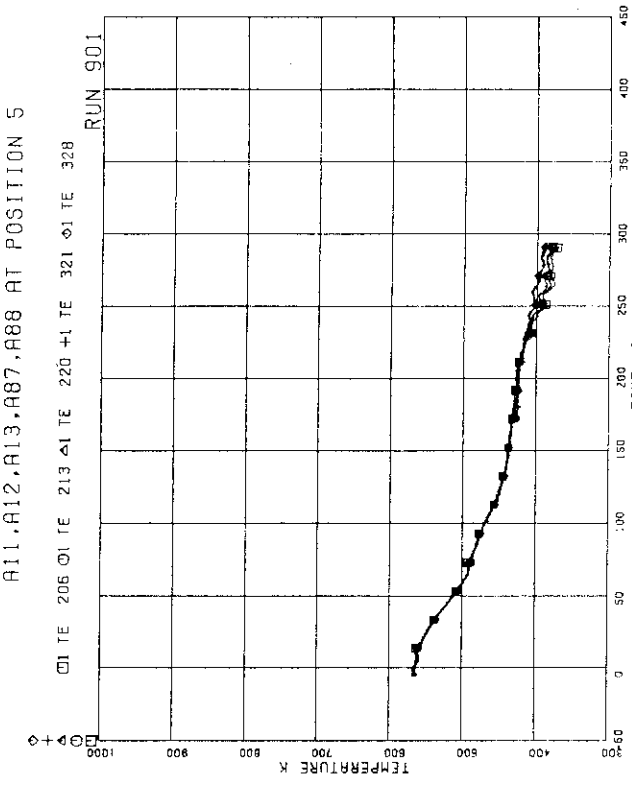


FIG.5.144 SURFACE TEMPERATURES OF FUEL RODS A11,A12,A13,A87,A88 AT POSITION 6

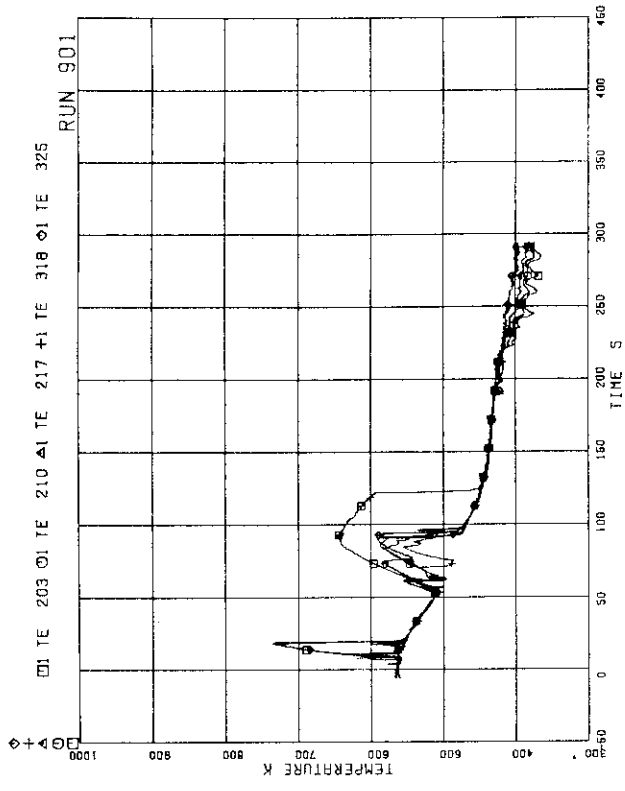


FIG.5.141 SURFACE TEMPERATURES OF FUEL RODS A11,A12,A13,A87,A88 AT POSITION 3

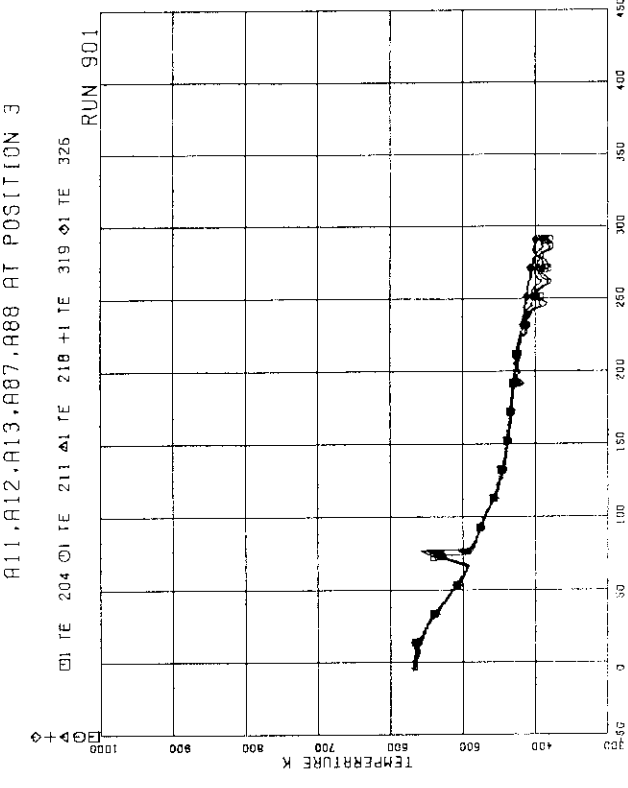


FIG.5.142 SURFACE TEMPERATURES OF FUEL RODS A11,A12,A13,A87,A88 AT POSITION 4

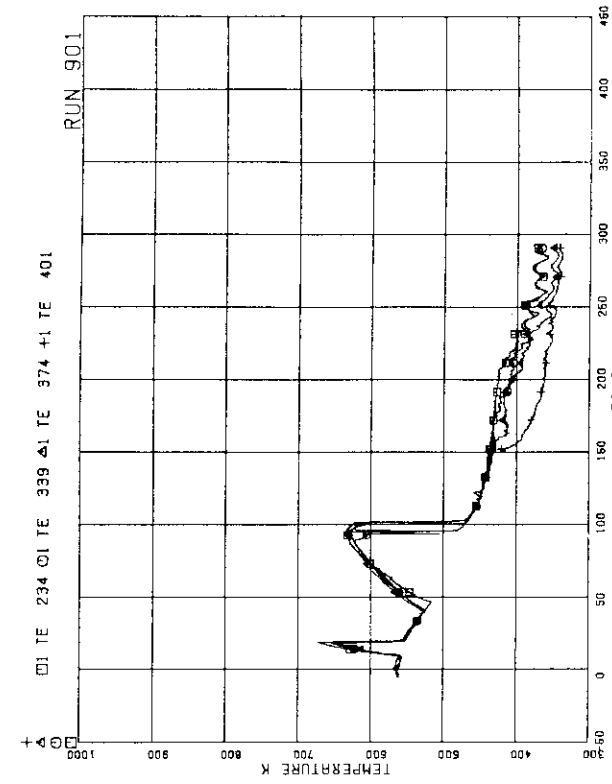


FIG.5.147 SURFACE TEMPERATURES OF FUEL RODS A22,B22,C22,D22 AT POSITION 2

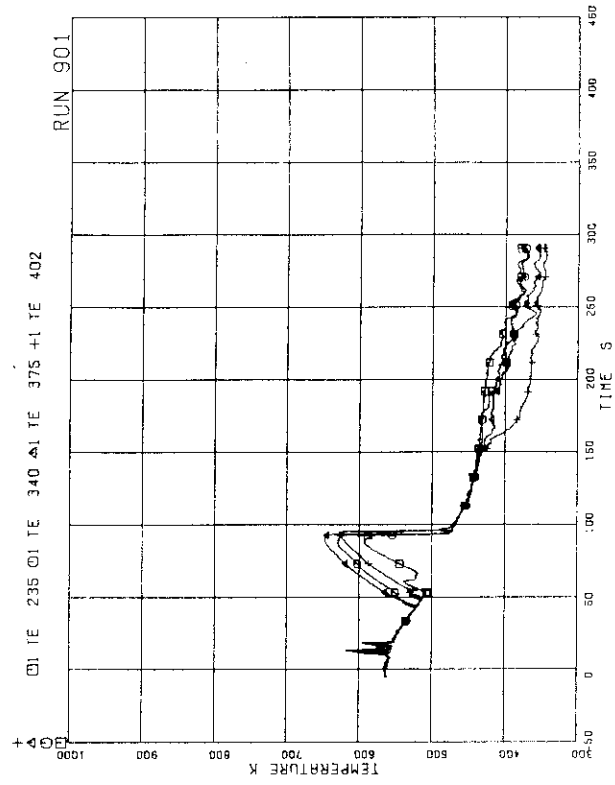


FIG.5.148 SURFACE TEMPERATURES OF FUEL RODS A22,B22,C22,D22 AT POSITION 3

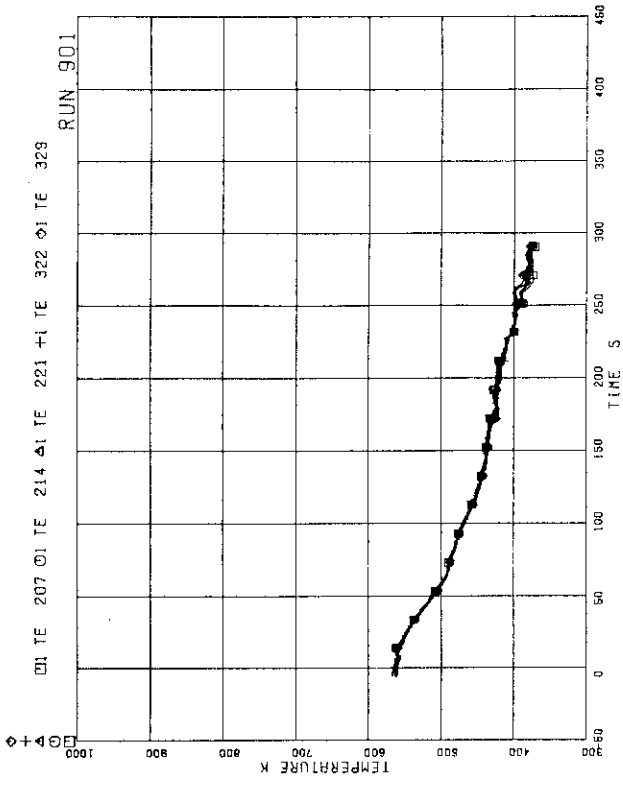


FIG.5.145 SURFACE TEMPERATURES OF FUEL RODS A11,A12,A13,A87,A88 AT POSITION 7

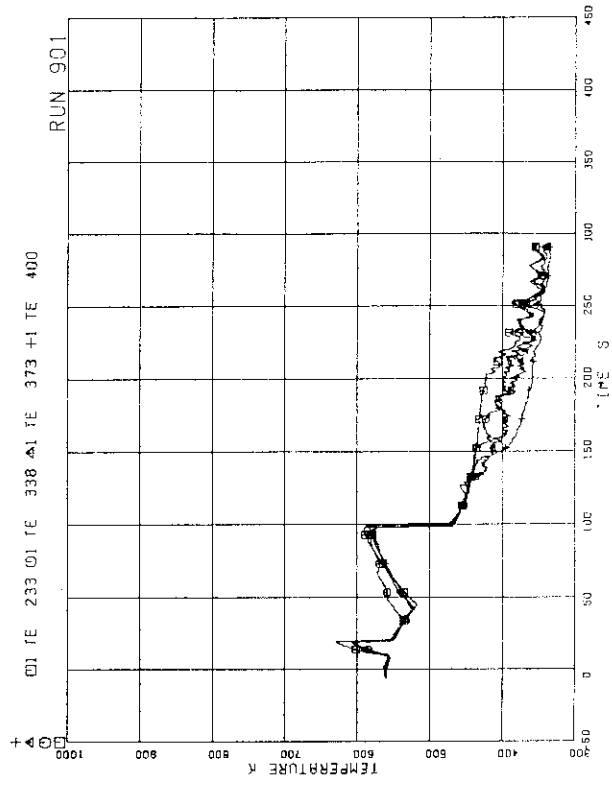


FIG.5.146 SURFACE TEMPERATURES OF FUEL RODS A22,B22,C22,D22 AT POSITION 1

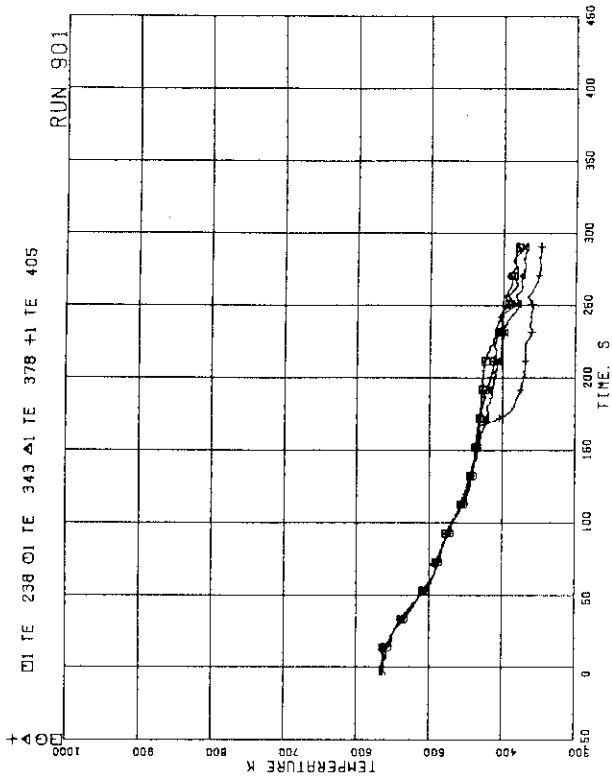


FIG.5.151 SURFACE TEMPERATURES OF FUEL RODS A22,B22,C22,D22 AT POSITION 6

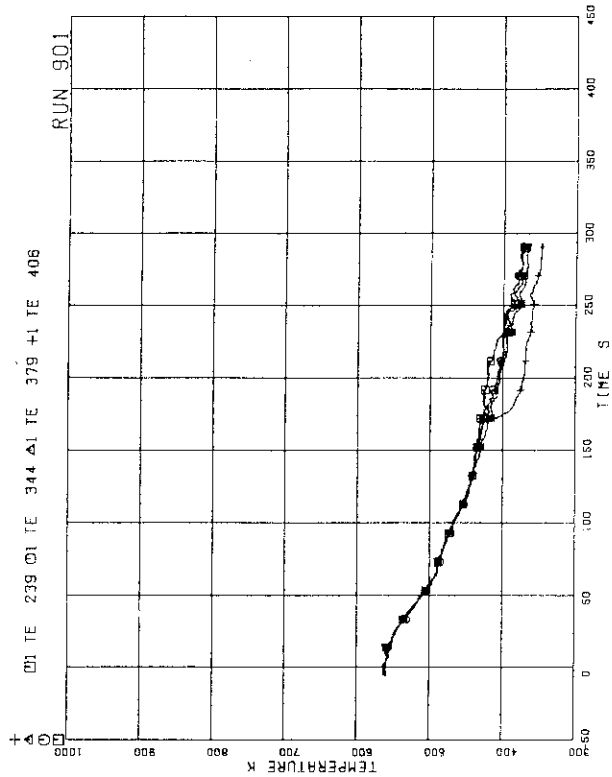


FIG.5.152 SURFACE TEMPERATURES OF FUEL RODS A22,B22,C22,D22 AT POSITION 7

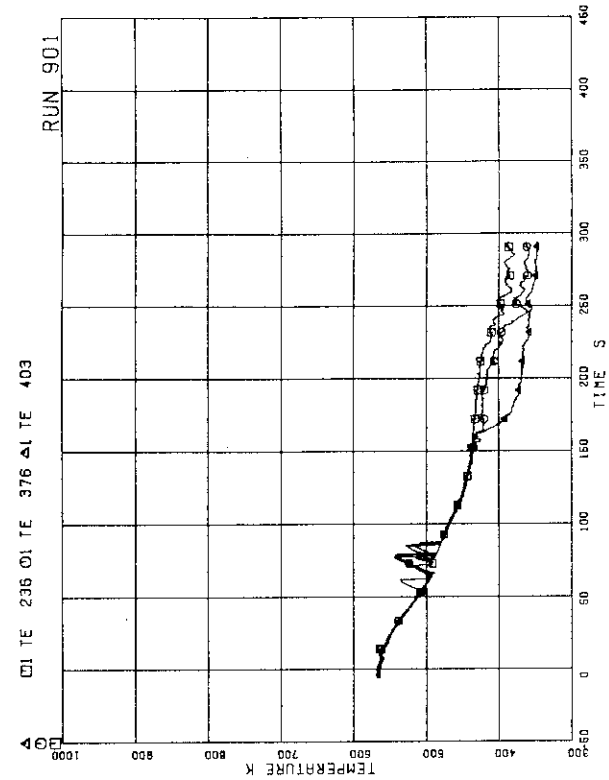


FIG.5.149 SURFACE TEMPERATURES OF FUEL RODS A22,C22,D22 AT POSITION 4

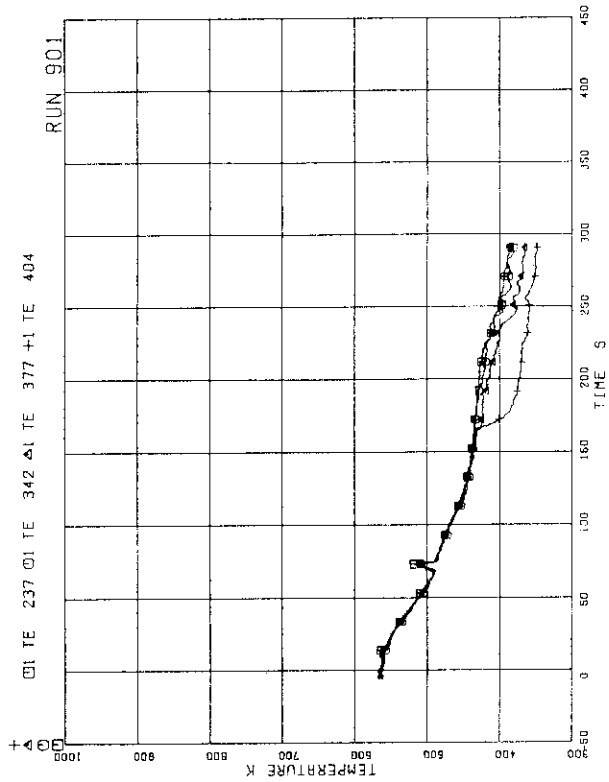


FIG.5.150 SURFACE TEMPERATURES OF FUEL RODS A22,B22,C22,D22 AT POSITION 5

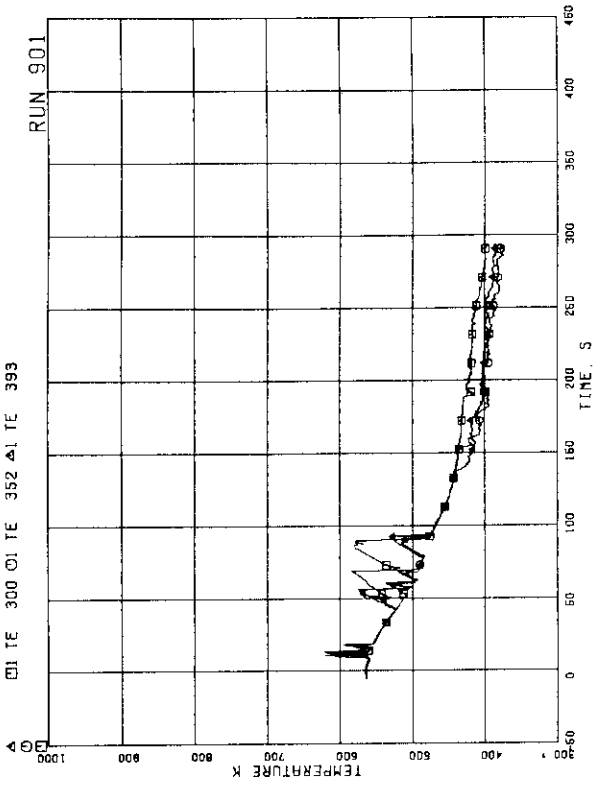


FIG.5.155 SURFACE TEMPERATURES OF FUEL RODS A77.877.C77 AT POSITION 3

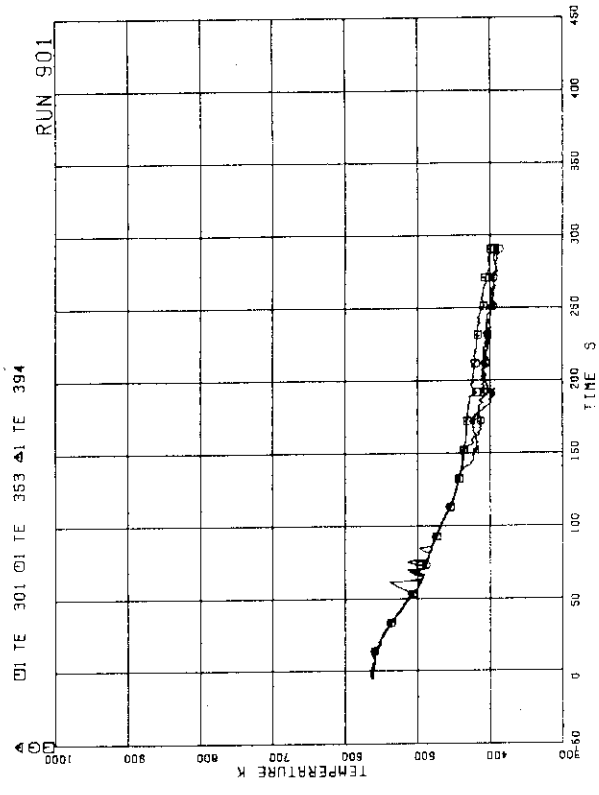


FIG.5.156 SURFACE TEMPERATURES OF FUEL RODS A77.877.C77 AT POSITION 4

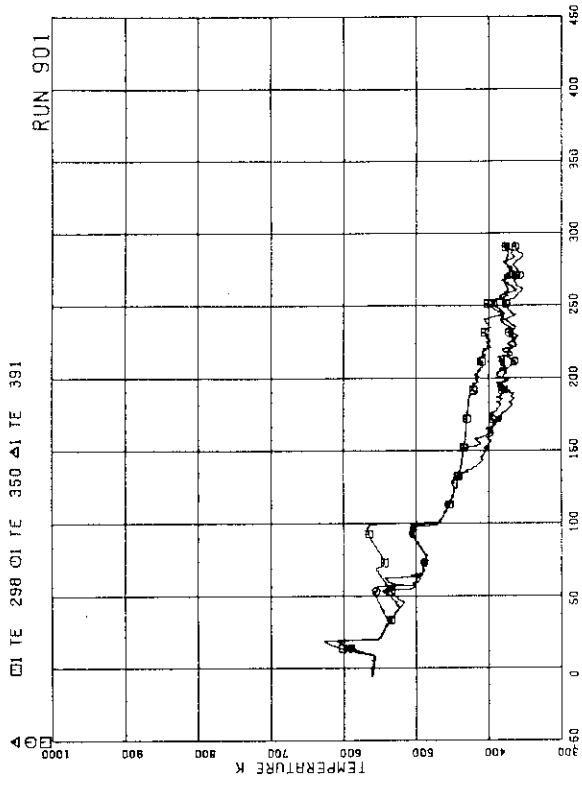


FIG.5.153 SURFACE TEMPERATURES OF FUEL RODS A77.877.C77 AT POSITION 1

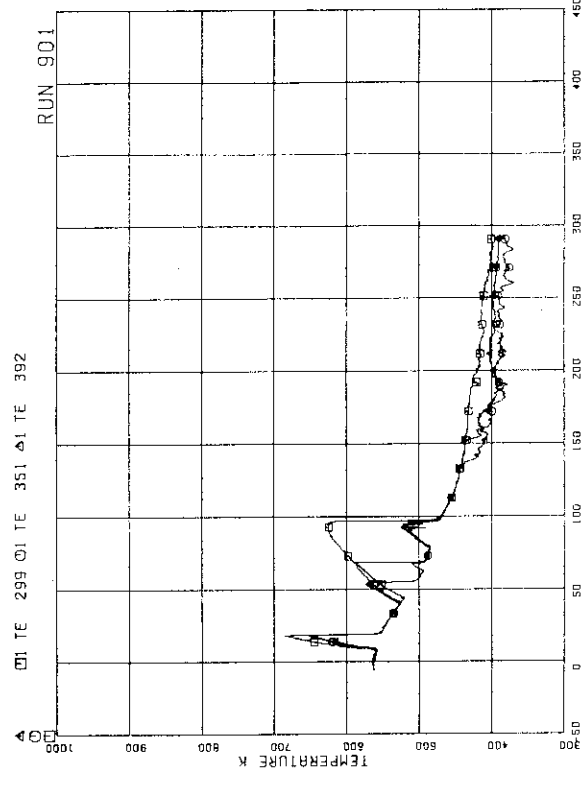


FIG.5.154 SURFACE TEMPERATURES OF FUEL RODS A77.877.C77 AT POSITION 2

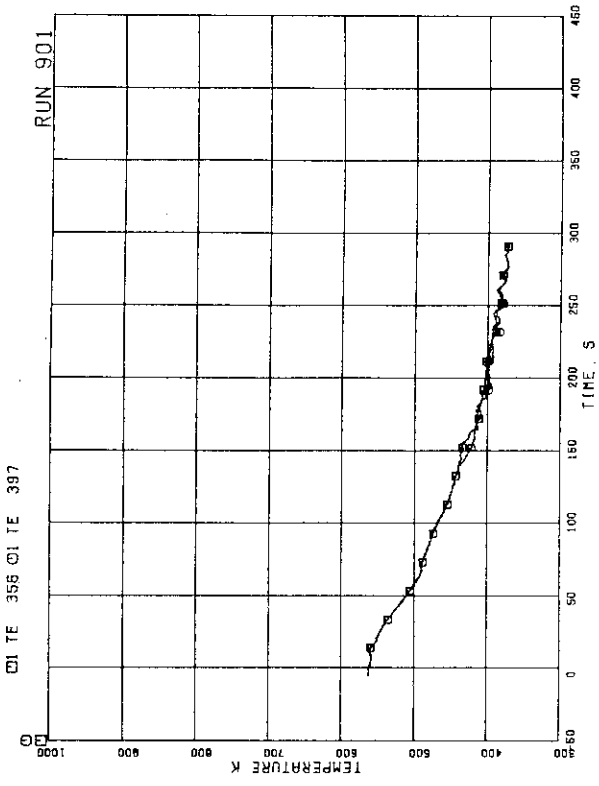


FIG.5.159 SURFACE TEMPERATURES OF FUEL RODS
B77,C77 RODS AT POSITION 7

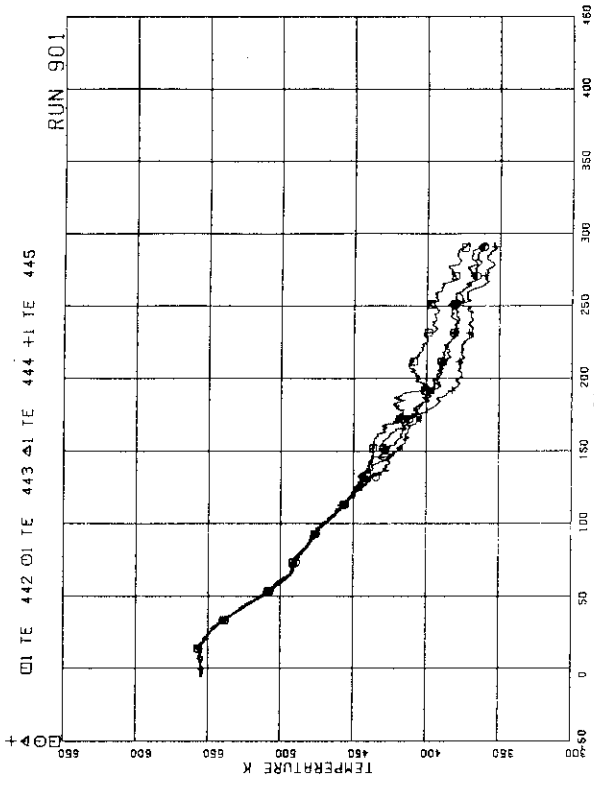


FIG.5.160 FLUID TEMPERATURES AT CHANNEL INLET

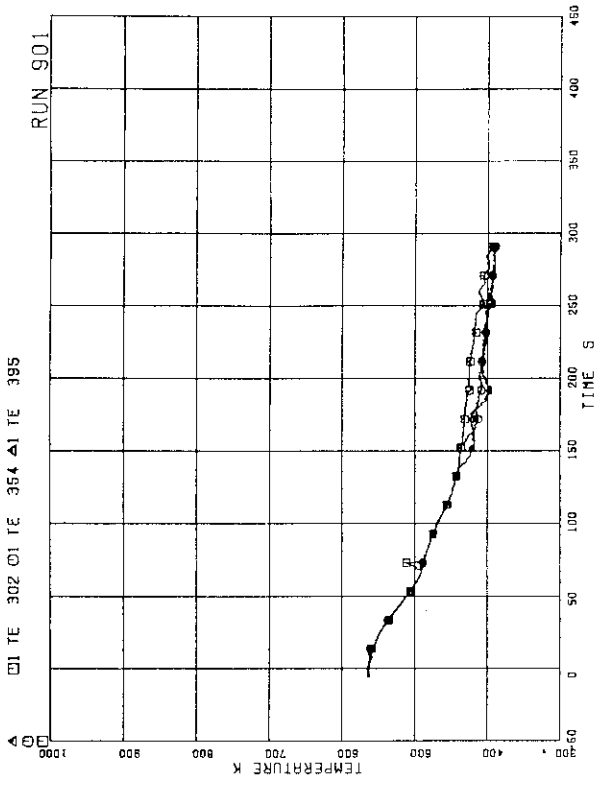


FIG.5.157 SURFACE TEMPERATURES OF FUEL RODS
A77,B77,C77 AT POSITION 5

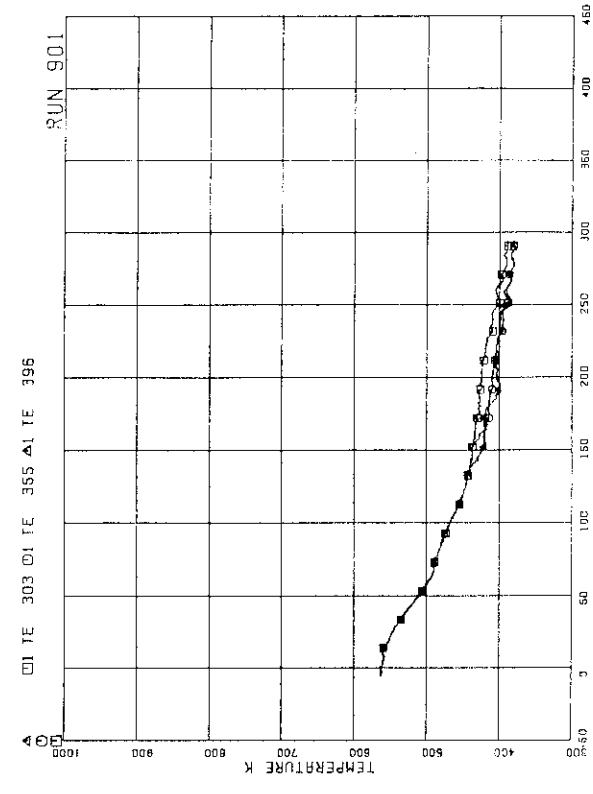


FIG.5.158 SURFACE TEMPERATURES OF FUEL RODS
A77,B77,C77 AT POSITION 6

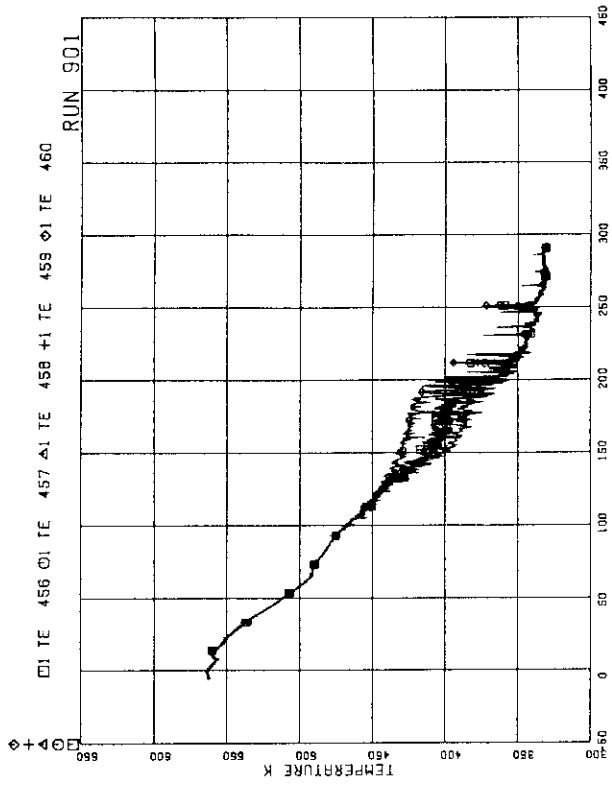


FIG.5.163 FLUID TEMPERATURES ABOVE UTP OF CHANNEL A, OPENINGS 1 TO 5

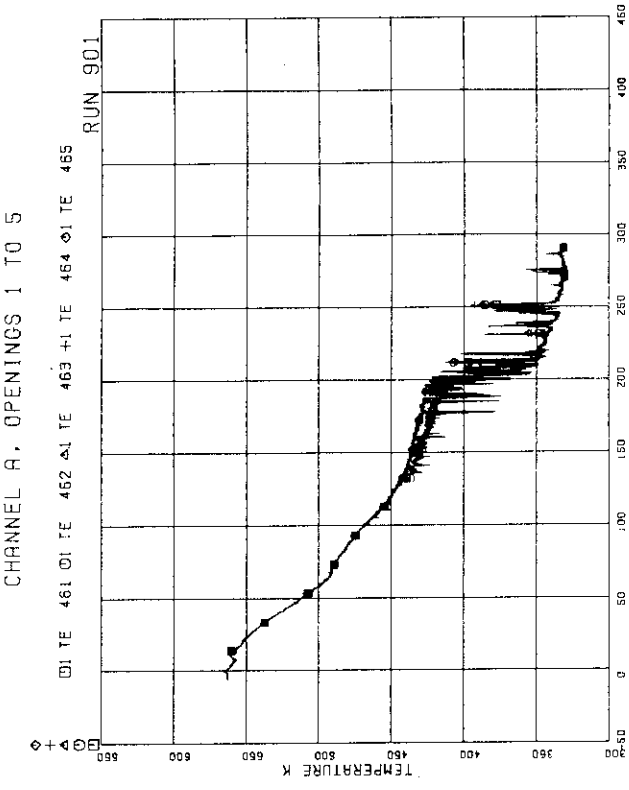


FIG.5.164 FLUID TEMPERATURES ABOVE UTP OF CHANNEL A, OPENINGS 6 TO 10

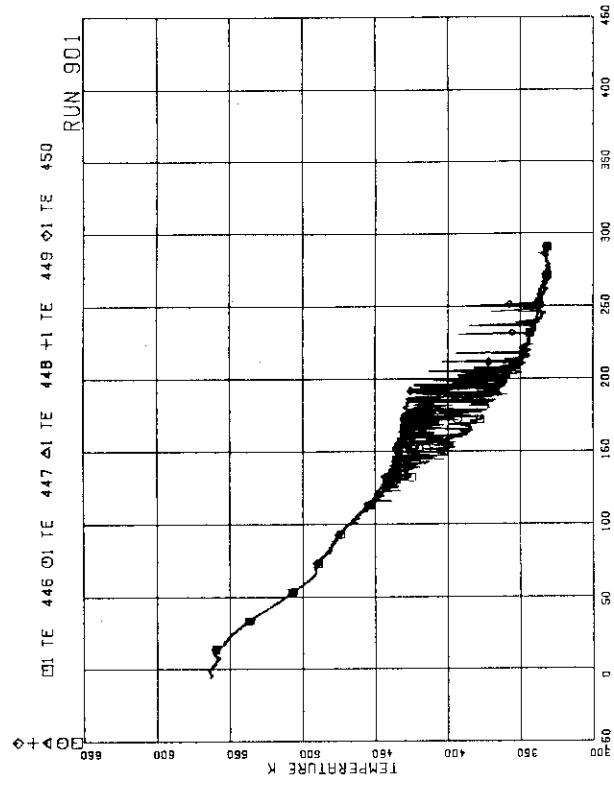


FIG.5.161 FLUID TEMPERATURES AT CHANNEL A OUTLET

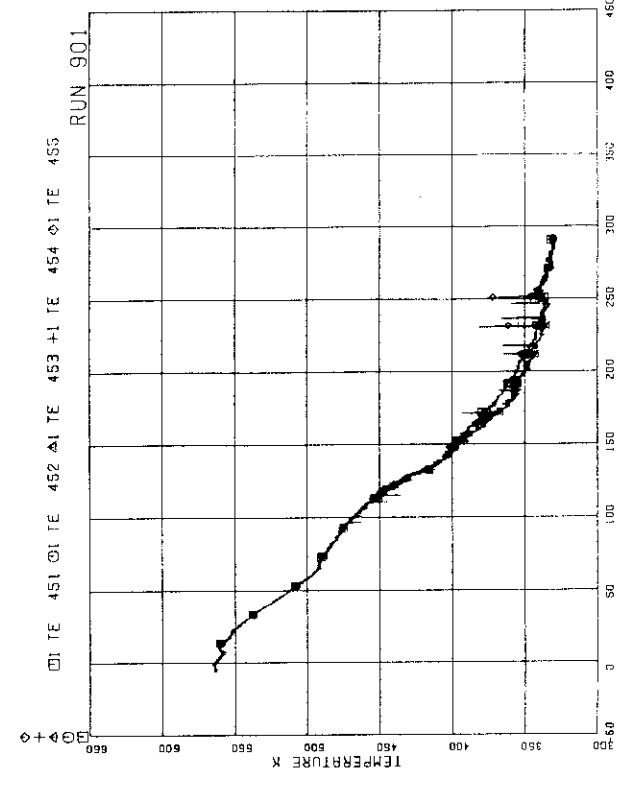


FIG.5.162 FLUID TEMPERATURES AT CHANNEL C OUTLET

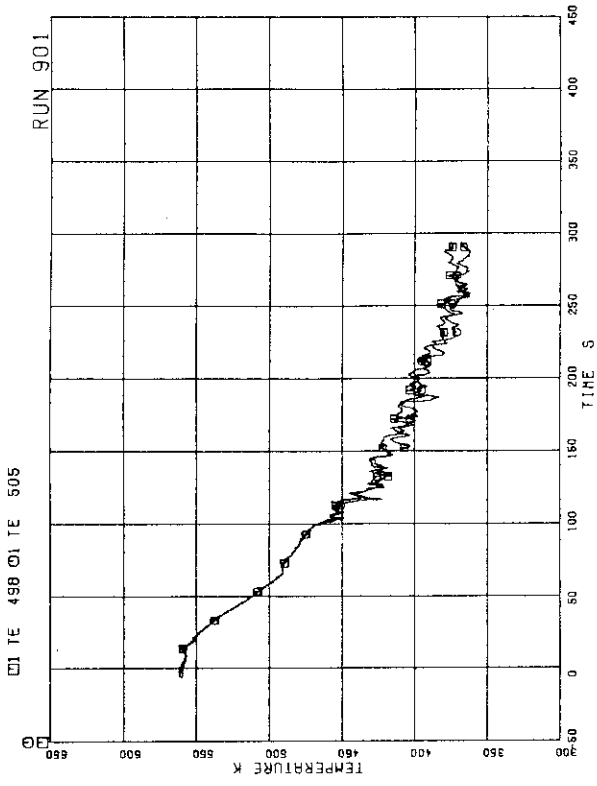


FIG.5.167 INNER AND OUTER SURFACE TEMPERATURES OF CHANNEL BOX AT POS.3

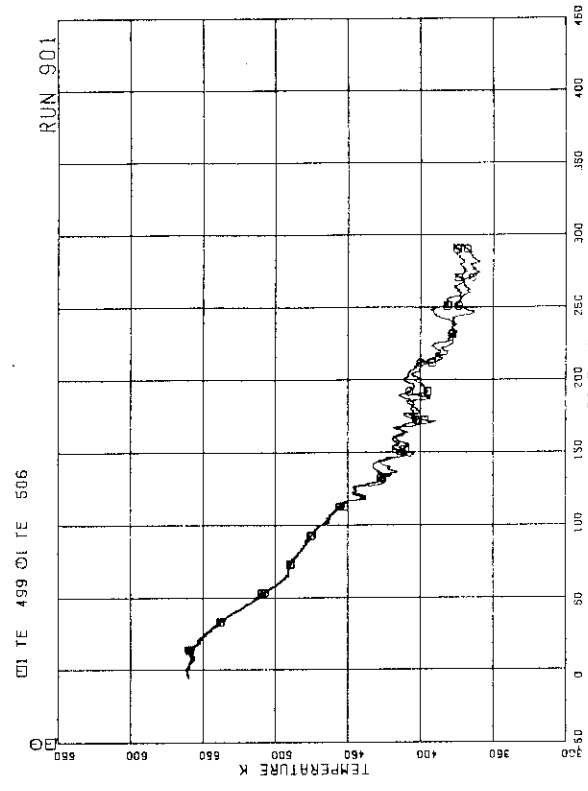


FIG.5.168 INNER AND OUTER SURFACE TEMPERATURES OF CHANNEL BOX AT POS.4

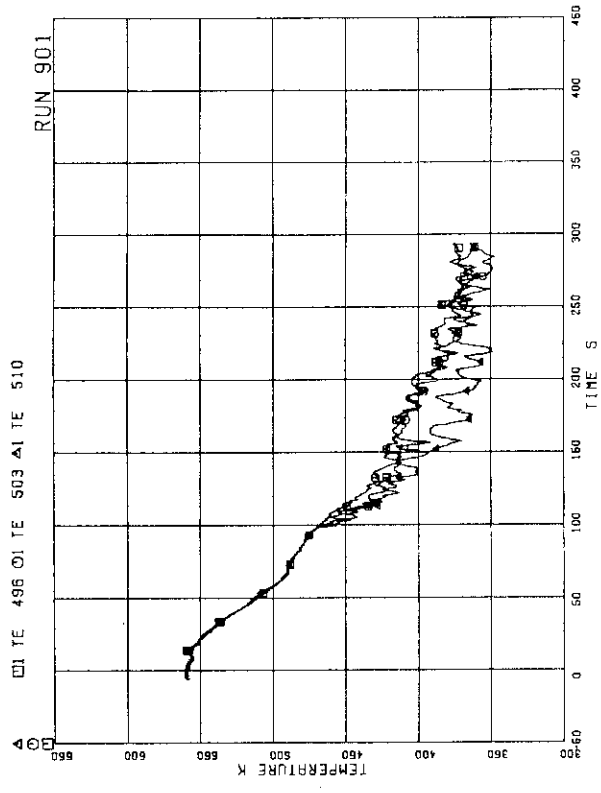


FIG.5.165 INNER AND OUTER SURFACE TEMPERATURES OF CHANNEL BOX AT POS.1

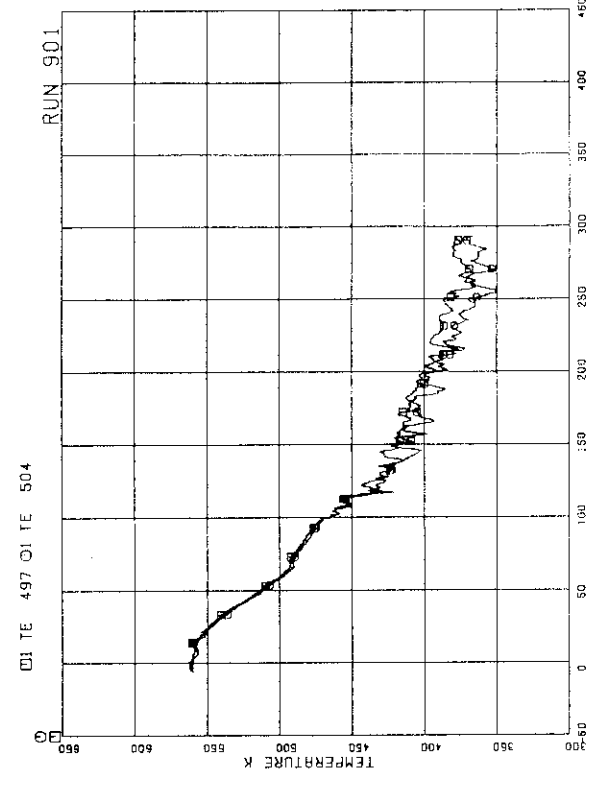


FIG.5.166 INNER AND OUTER SURFACE TEMPERATURES OF CHANNEL BOX AT POS.2

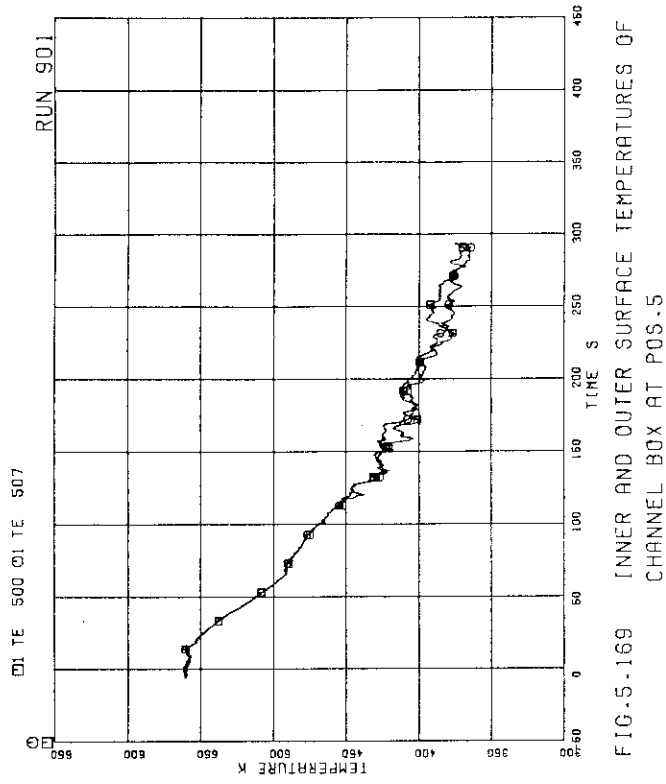


FIG.5.169 INNER AND OUTER SURFACE TEMPERATURES OF CHANNEL BOX AT POS.5

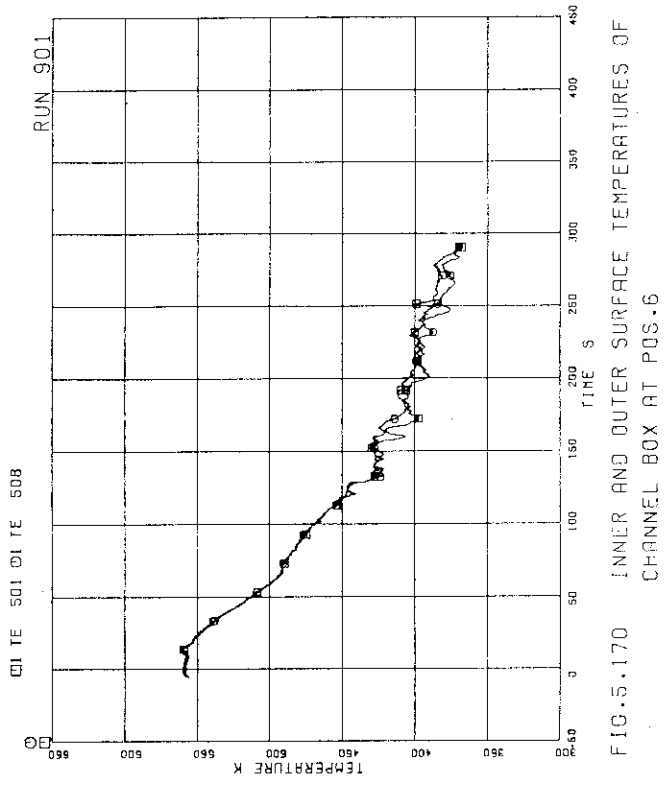


FIG.5.170 INNER AND OUTER SURFACE TEMPERATURES OF CHANNEL BOX AT POS.6

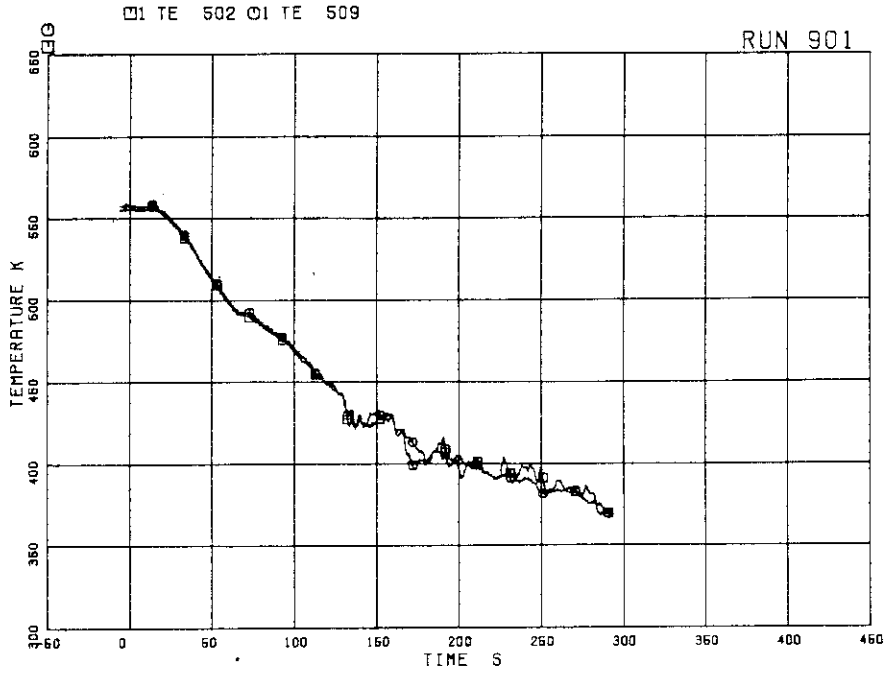


FIG.5.171 INNER AND OUTER SURFACE TEMPERATURES OF CHANNEL BOX AT POS.7

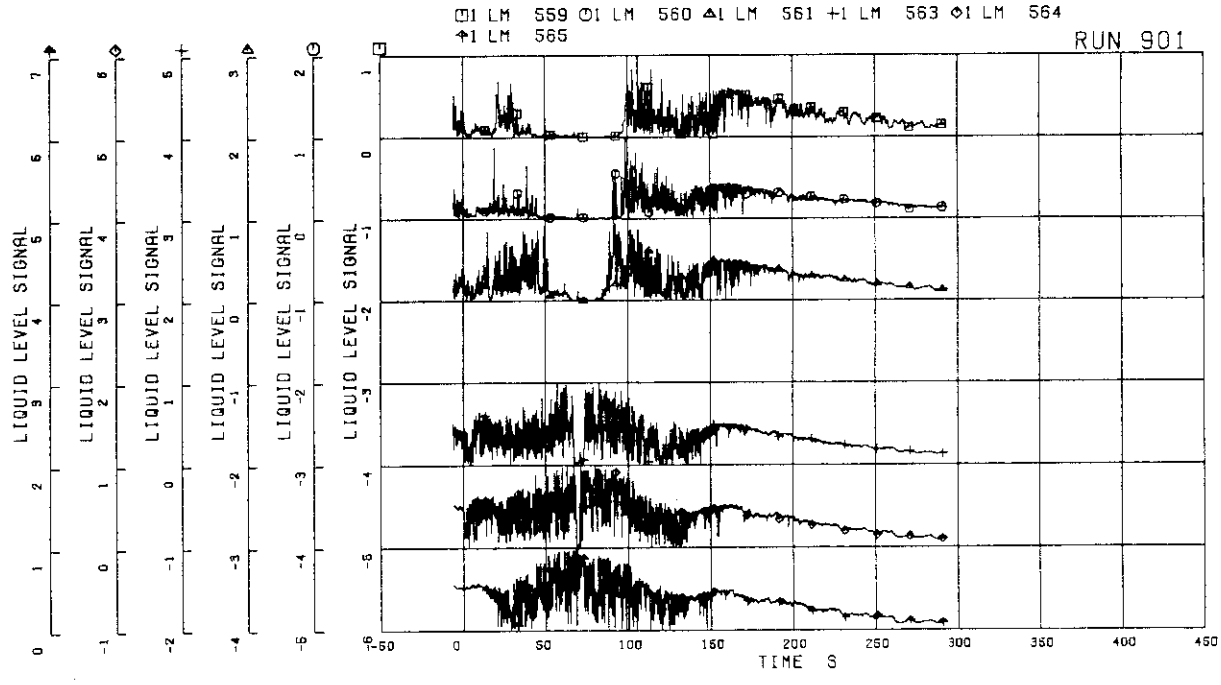


FIG.5.172 LIQUID LEVEL SIGNALS IN CHANNEL BOX A, LOCATION A1

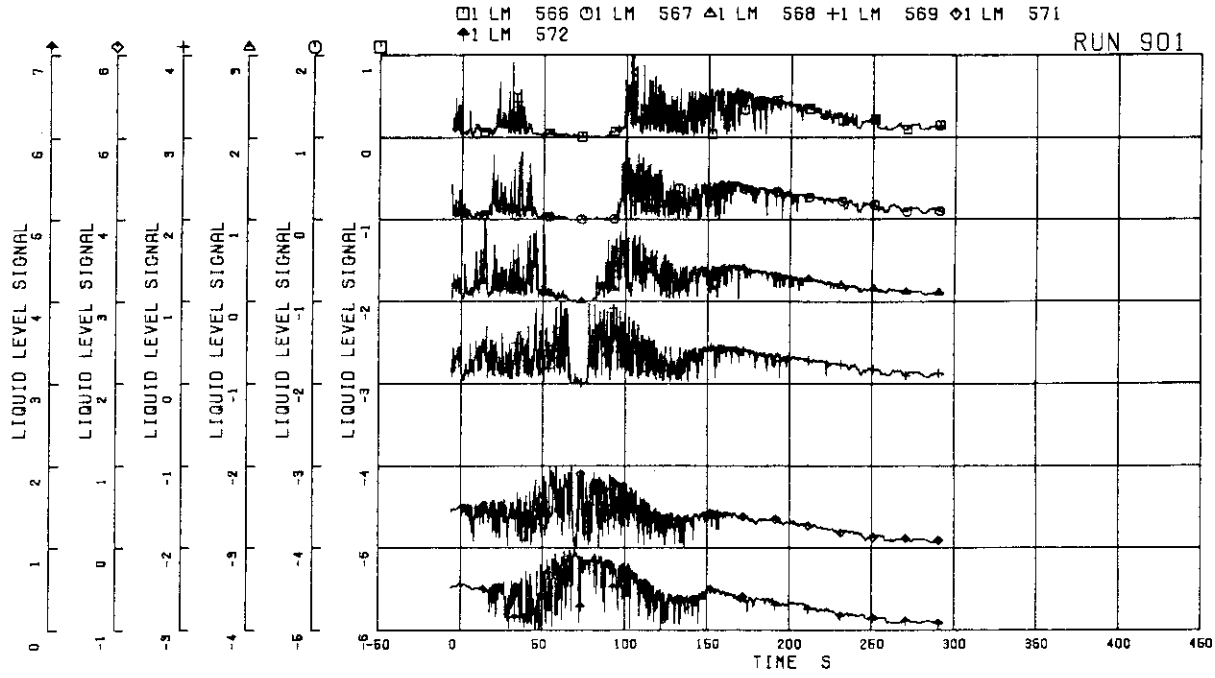


FIG.5.173 LIQUID LEVEL SIGNALS IN CHANNEL BOX A, LOCATION A2

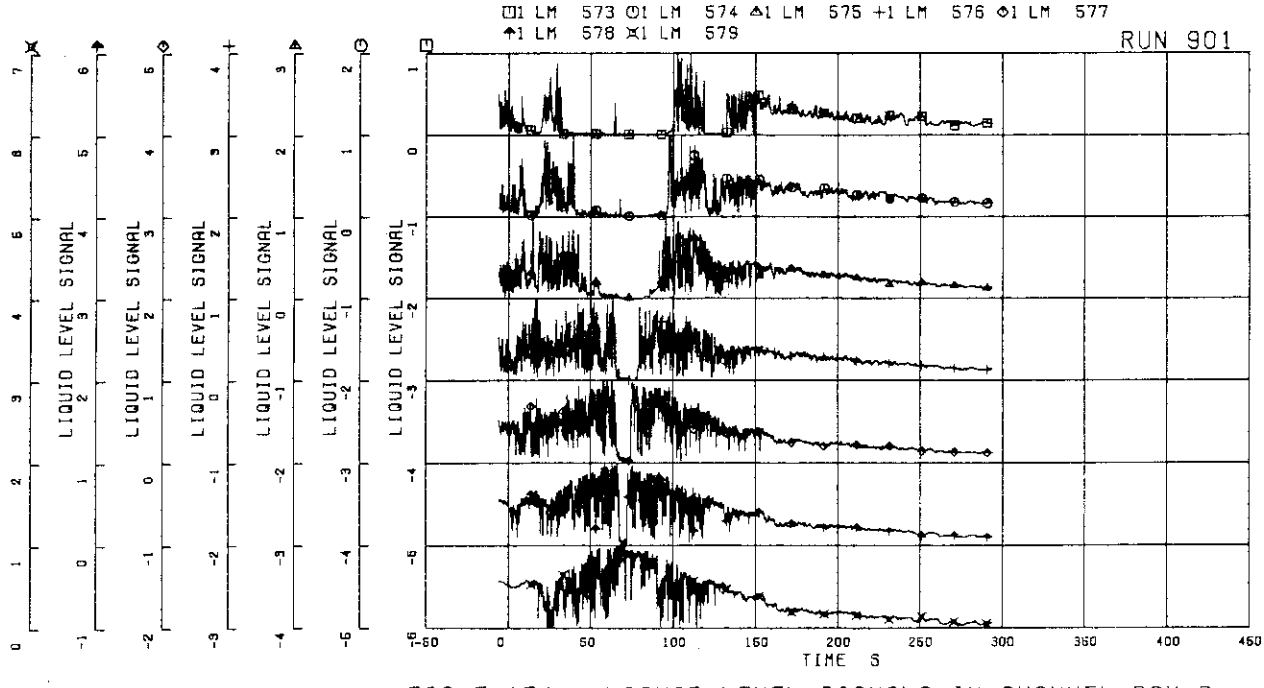


FIG.5.174 LIQUID LEVEL SIGNALS IN CHANNEL BOX B

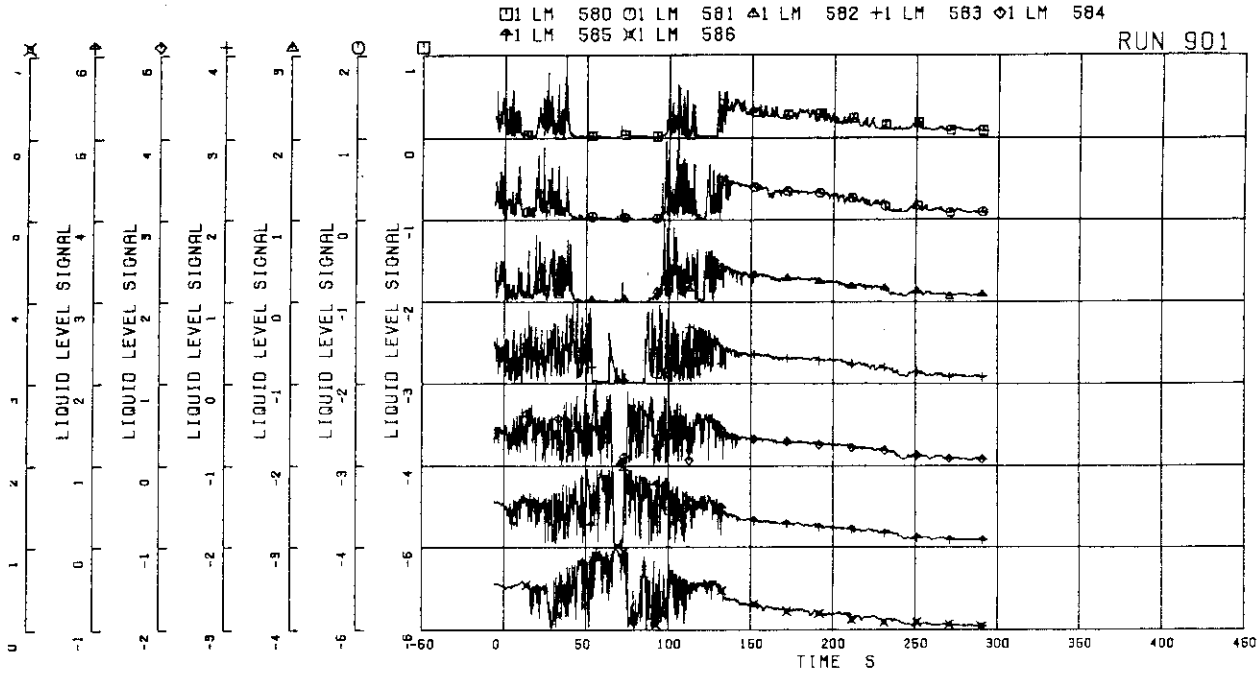


FIG.5.175 LIQUID LEVEL SIGNALS IN CHANNEL BOX C

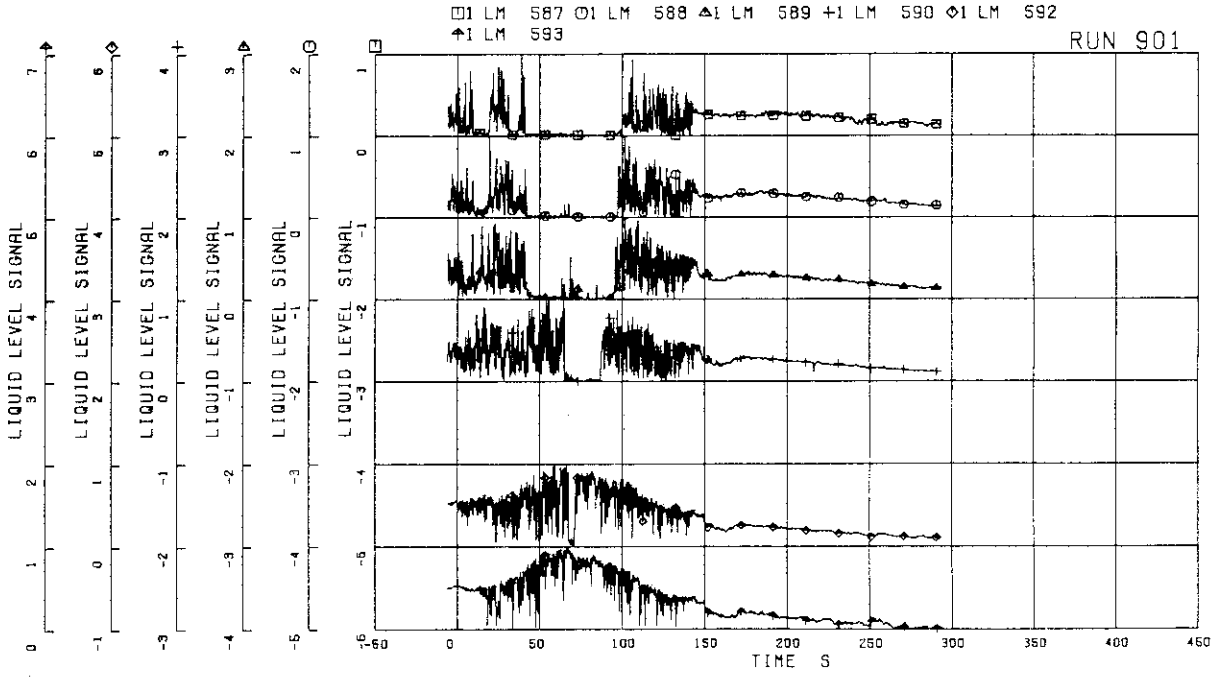


FIG.5.176 LIQUID LEVEL SIGNALS IN CHANNEL BOX D

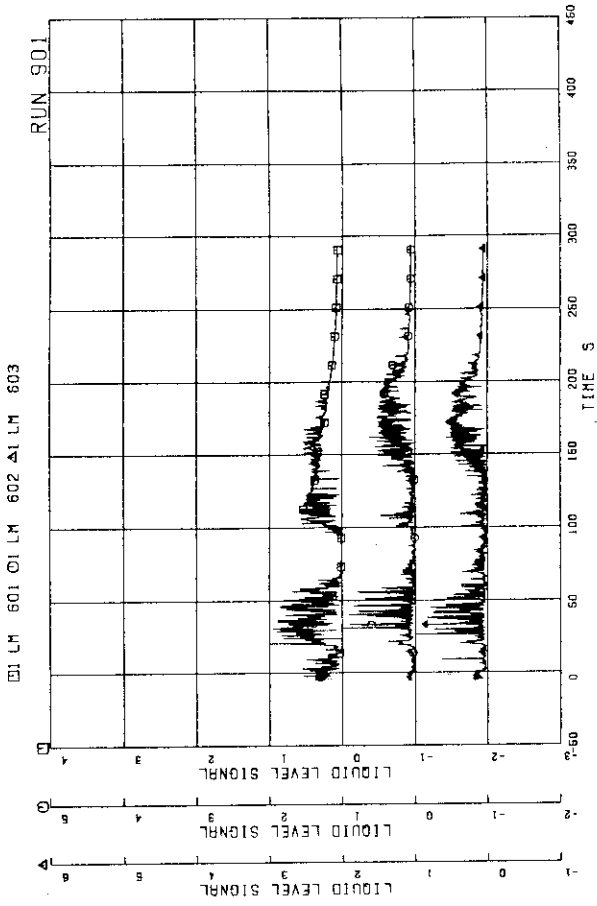


FIG.5.179 LIQUID LEVEL SIGNALS IN CHANNEL A OUTLET CENTER

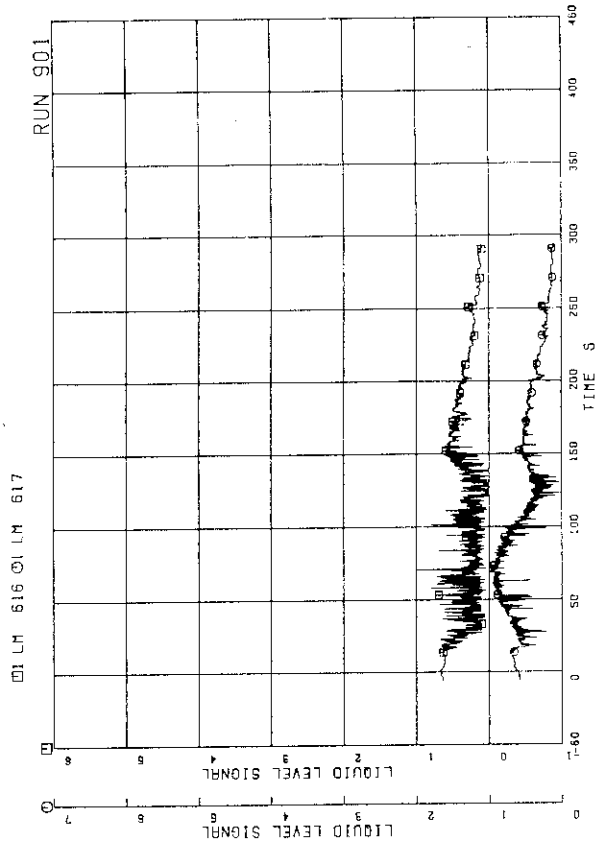


FIG.5.180 LIQUID LEVEL SIGNALS IN CHANNEL A INLET

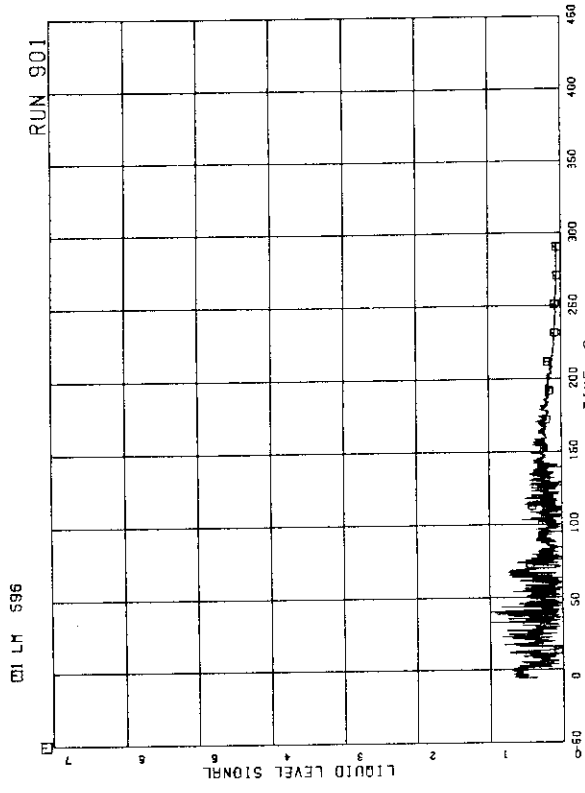


FIG.5.177 LIQUID LEVEL SIGNAL IN CHANNEL A OUTLET, LOCATION A1

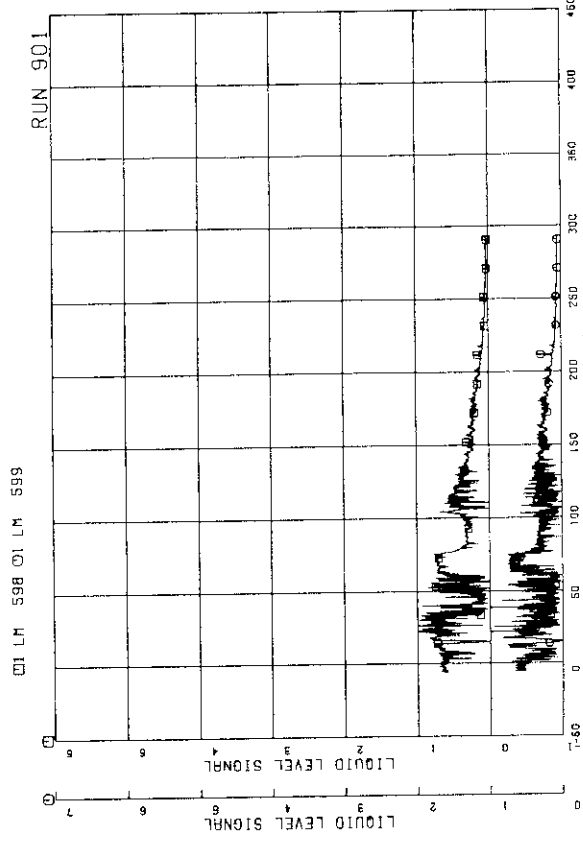


FIG.5.178 LIQUID LEVEL SIGNALS IN CHANNEL A OUTLET LOCATION A2

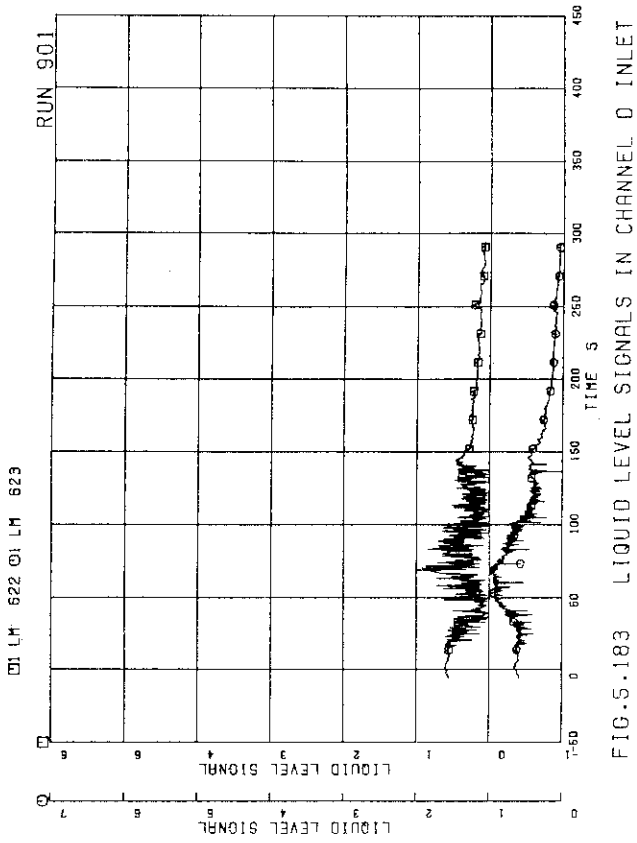


FIG.5.183 LIQUID LEVEL SIGNALS IN CHANNEL D INLET

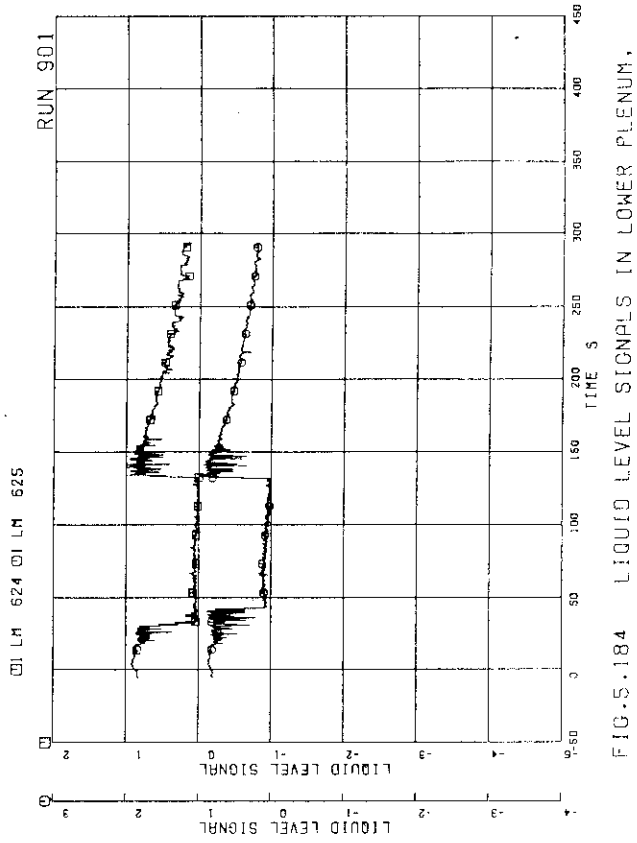


FIG.5.184 LIQUID LEVEL SIGNALS IN LOWER PLENUM, NORTH

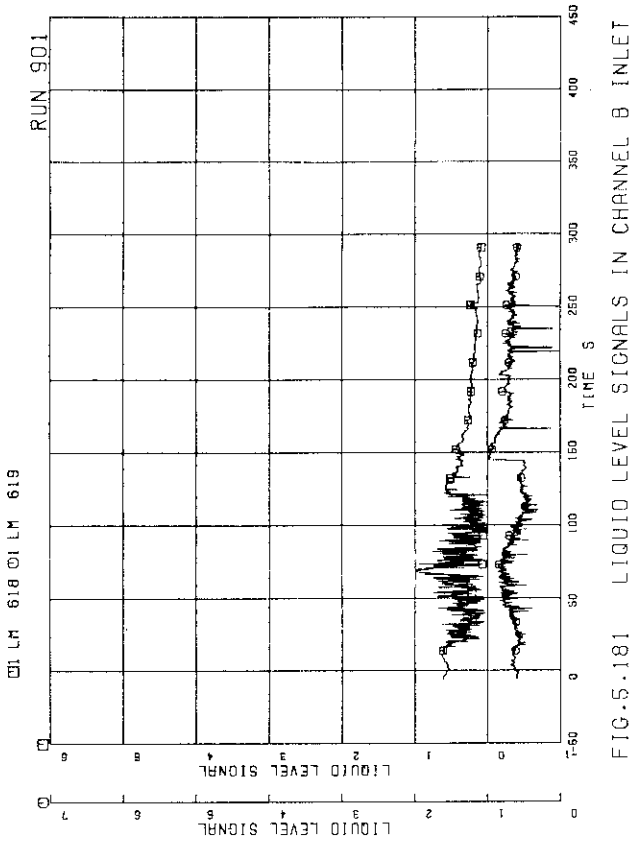


FIG.5.181 LIQUID LEVEL SIGNALS IN CHANNEL B INLET

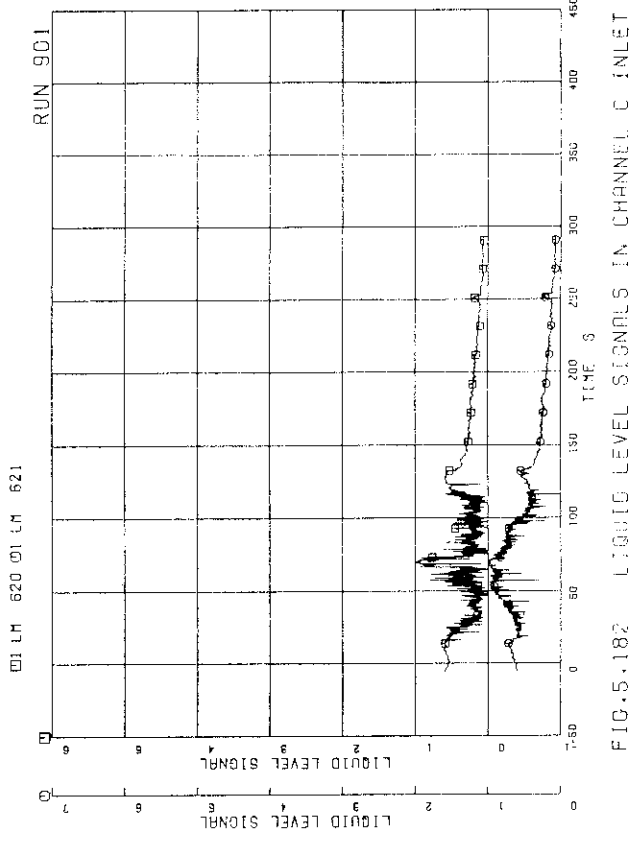


FIG.5.182 LIQUID LEVEL SIGNALS IN CHANNEL C INLET

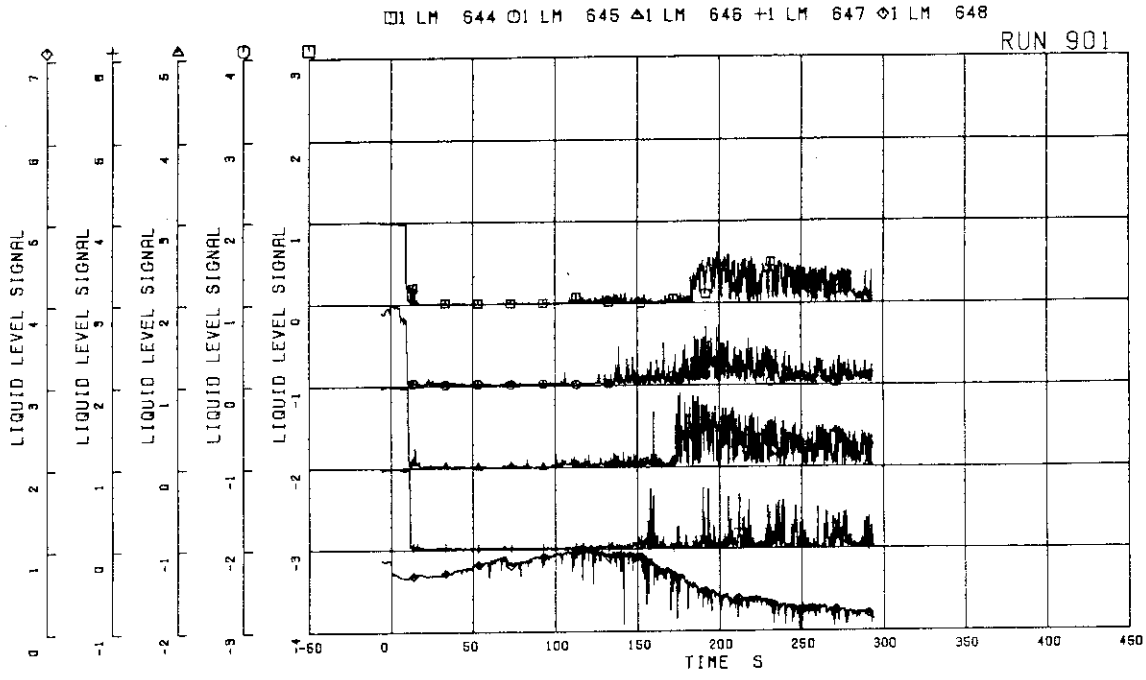


FIG.5.185 LIQUID LEVEL SIGNALS IN DOWNCOMER, D SIDE

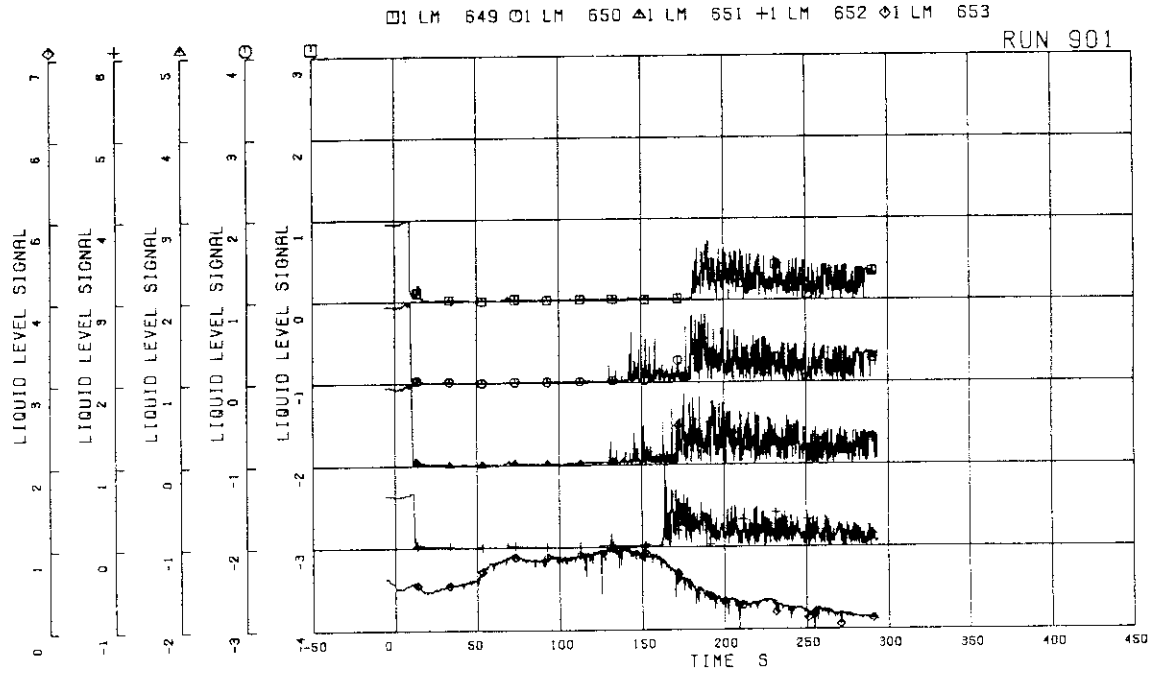


FIG.5.186 LIQUID LEVEL SIGNALS IN DOWNCOMER, B SIDE

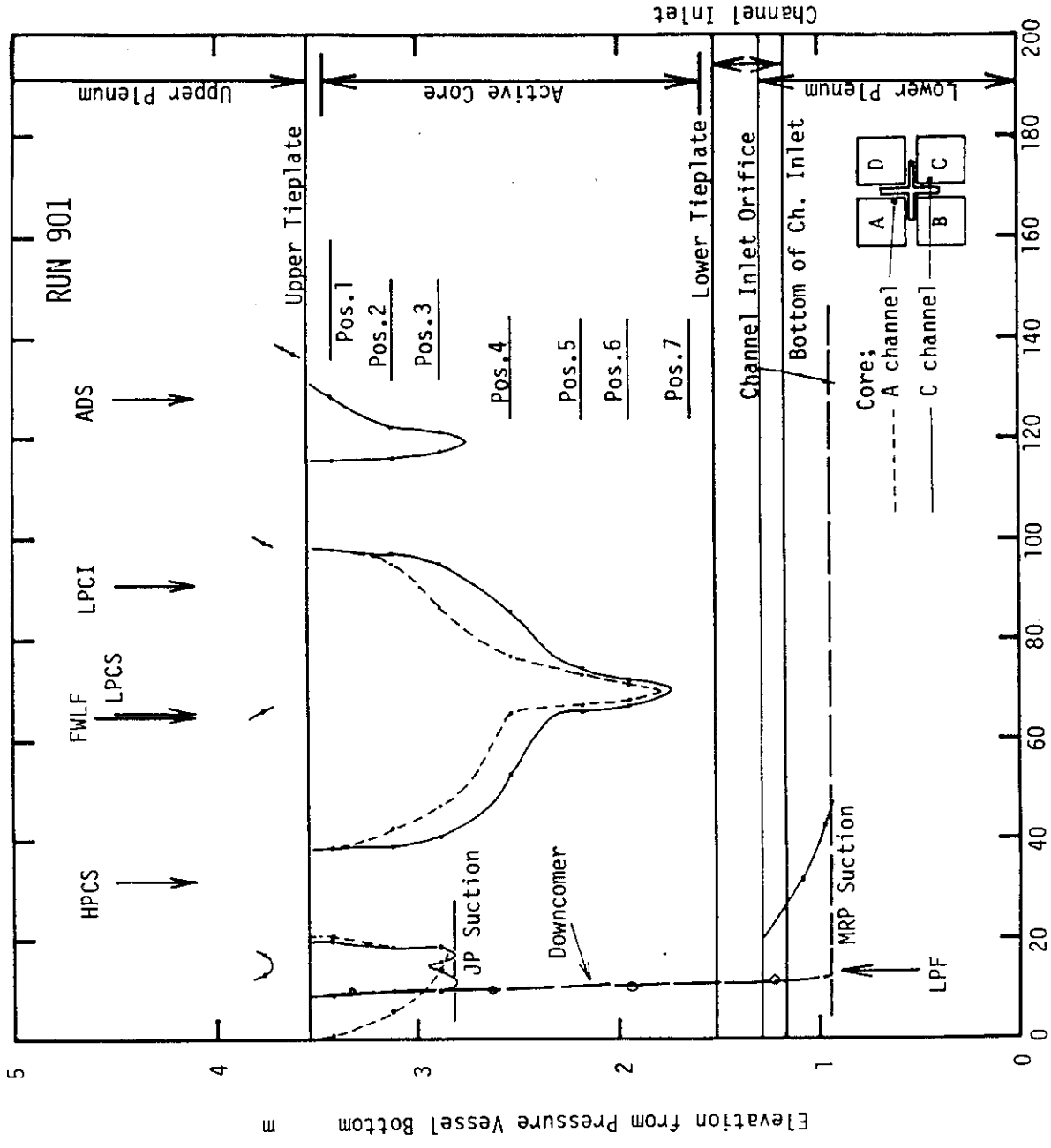


Fig. 5.187 Estimated Liquid Level in Pressure Vessel

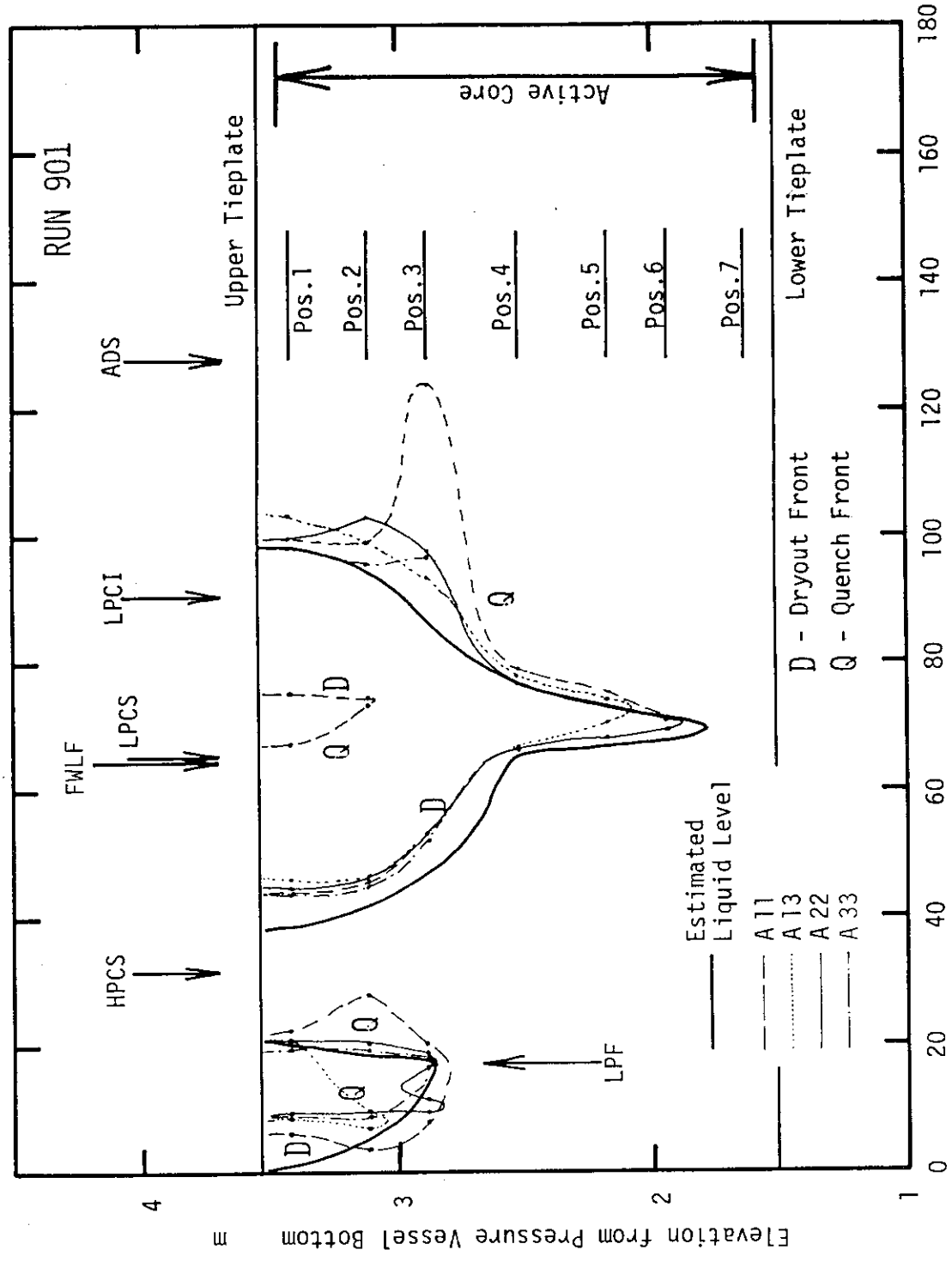


Fig. 5.188 Dryout and Quench Transients in Channel A

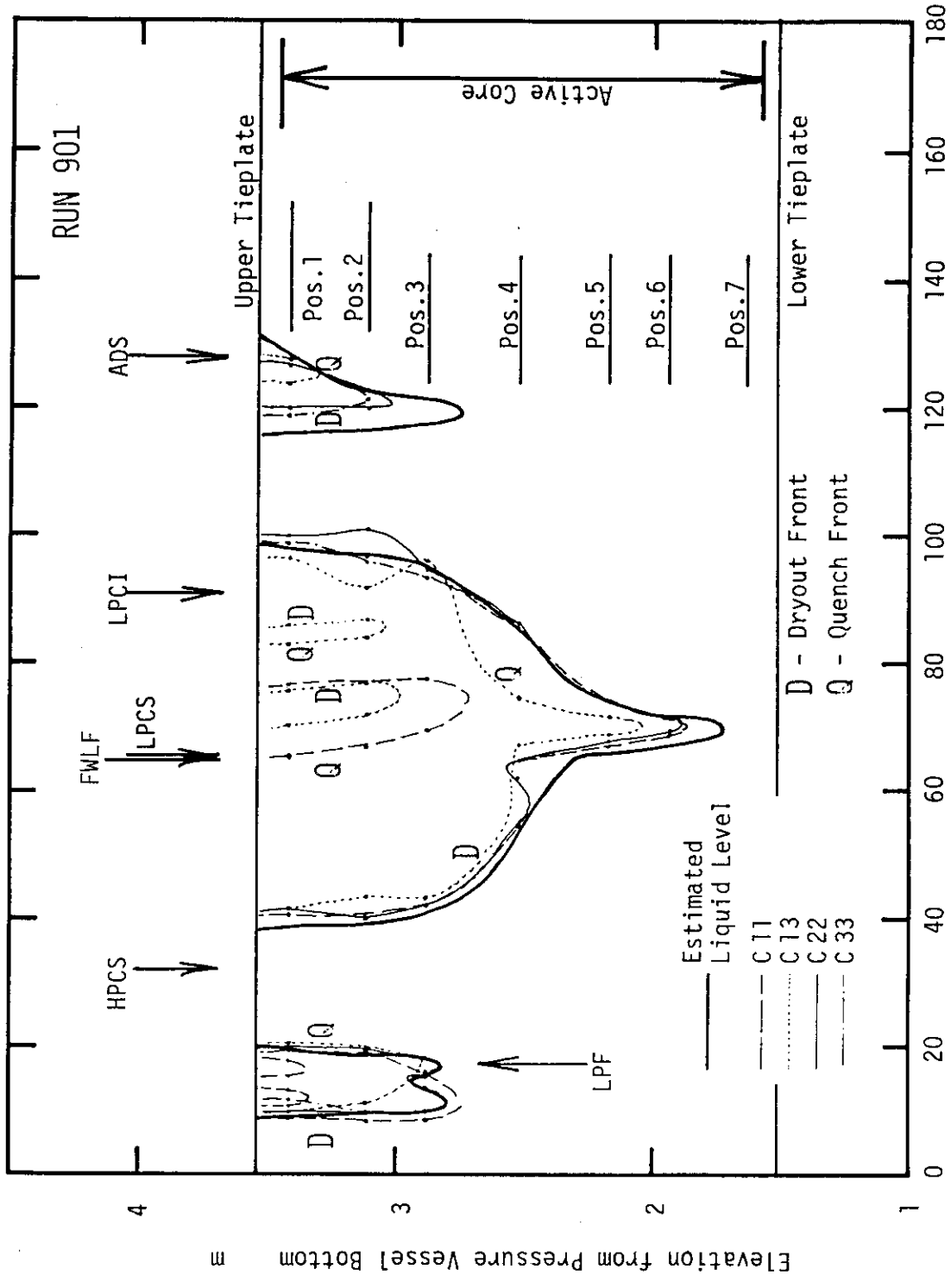


Fig. 5.189 Dryout and Quench Transients in Channel C

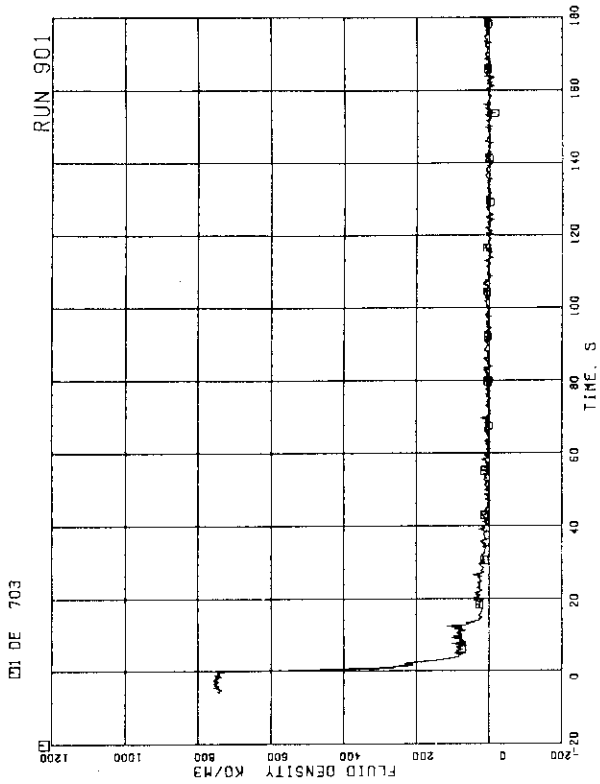


FIG.5.192 AVERAGE DENSITY AT MRP SIDE OF BREAK

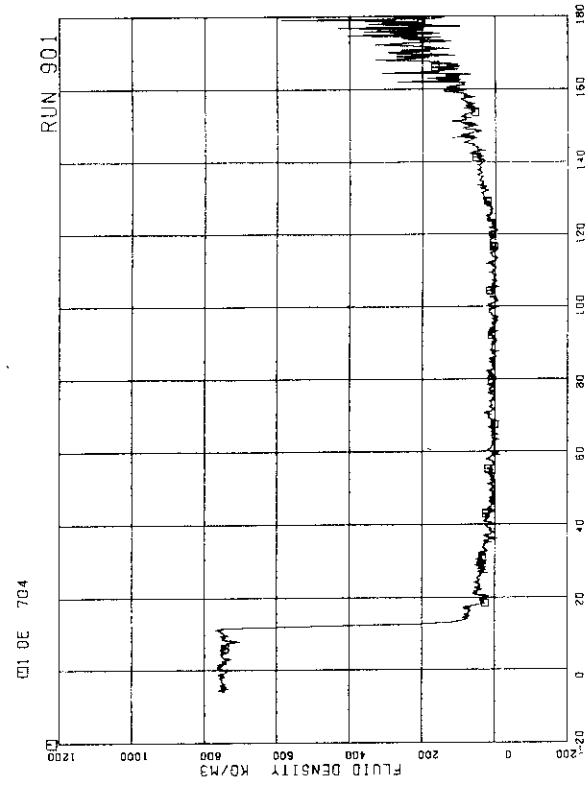


FIG.5.193 AVERAGE DENSITY AT PV SIDE OF BREAK

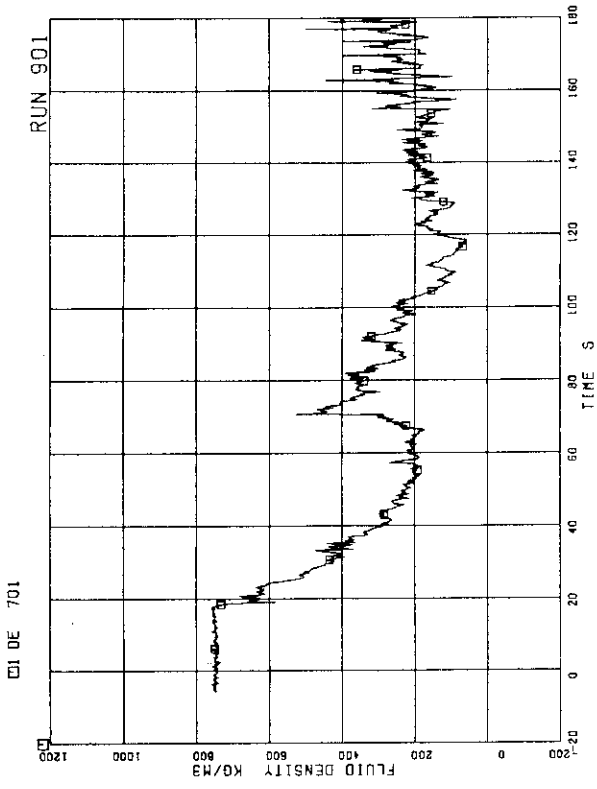


FIG.5.190 AVERAGE DENSITY AT JP-1.2 OUTLET

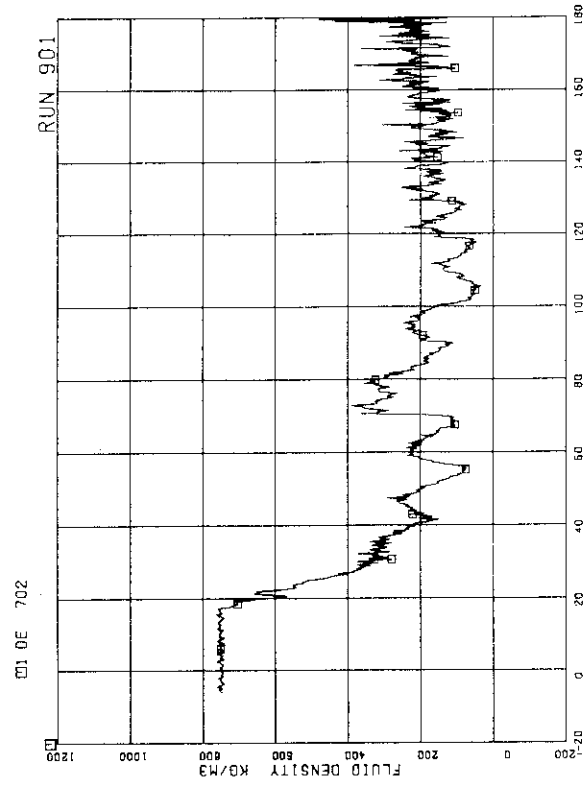


FIG.5.191 AVERAGE DENSITY AT JP-3.4 OUTLET

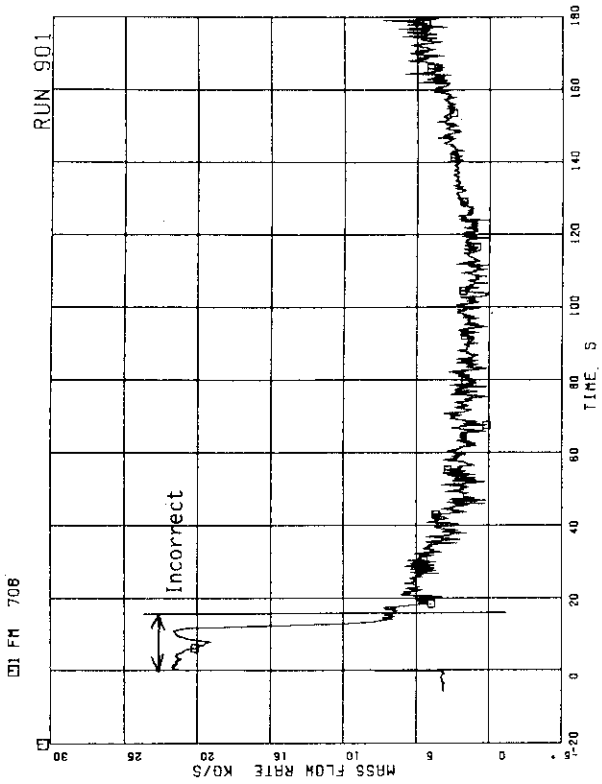


FIG.5.196 FLOW RATE AT PV SIDE OF BREAK
(BASED ON HIGH RANGE DRAG DISK DATA)

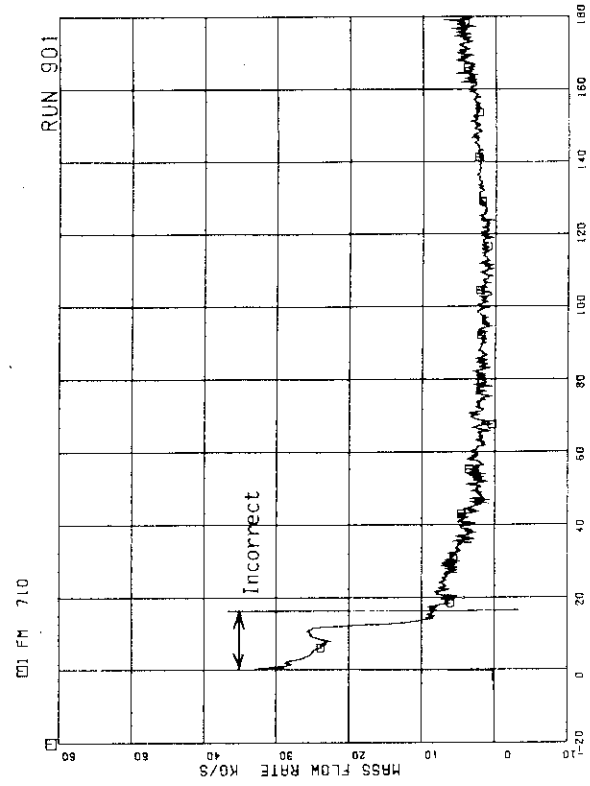


FIG.5.197 TOTAL DISCHARGE FLOW RATE FROM BREAK
(BASED ON HIGH RANGE DRAG DISK DATA)

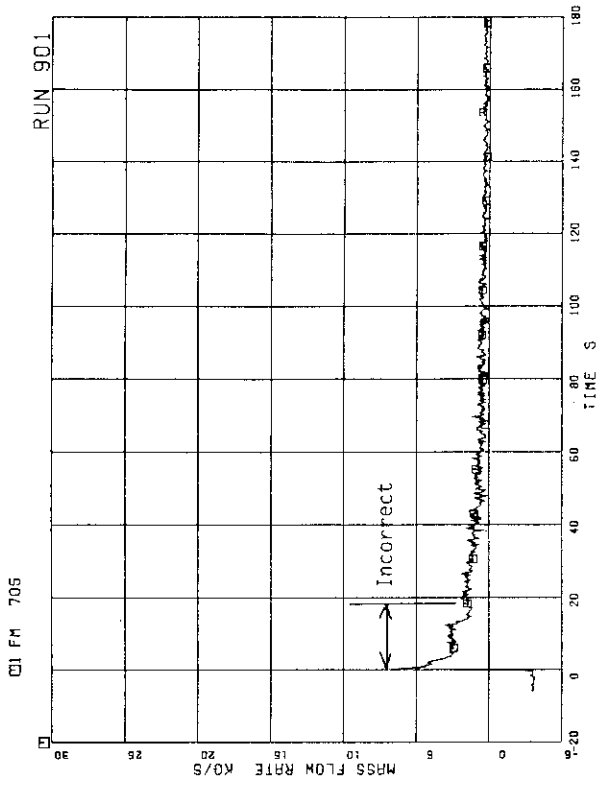


FIG.5.194 FLOW RATE AT MRP SIDE OF BREAK
(BASED ON LOW RANGE DRAG DISK DATA)

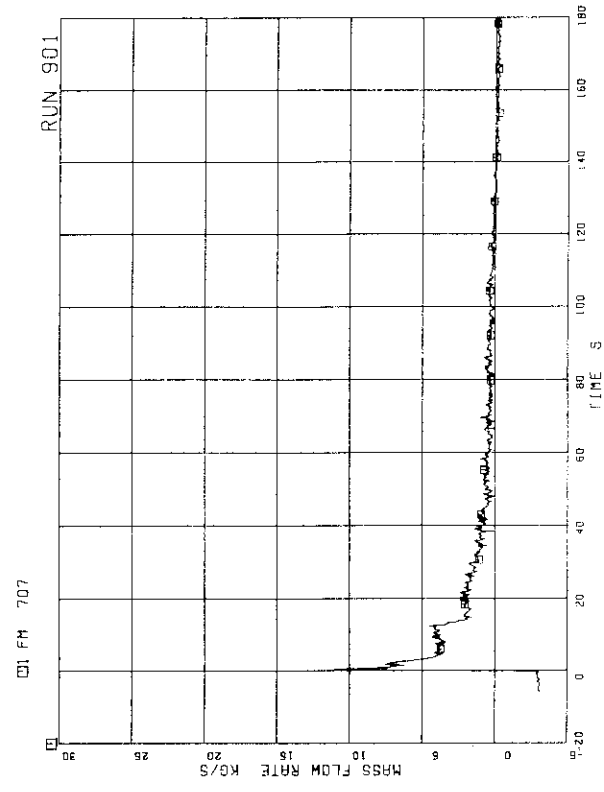


FIG.5.195 FLOW RATE AT MRP SIDE OF BREAK
(BASED ON HIGH RANGE DRAG DISK DATA)

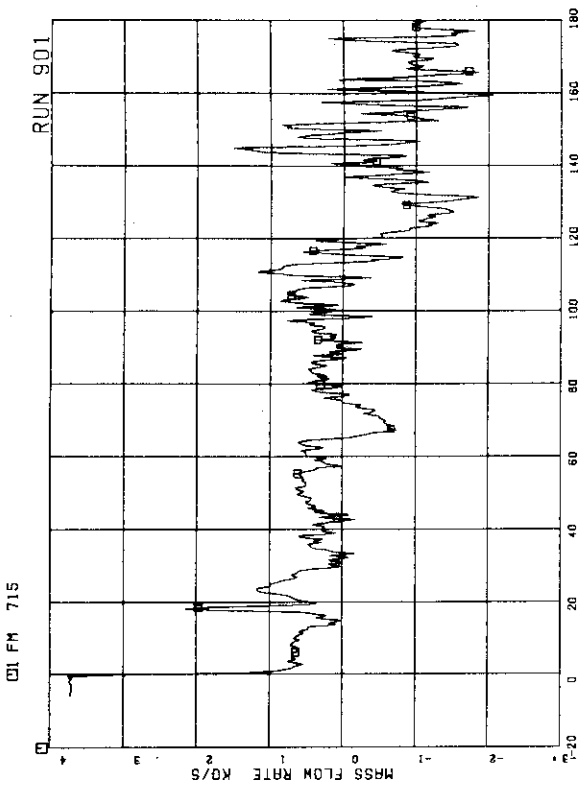


FIG.5.200 FLOW RATE AT CHANNEL B INLET

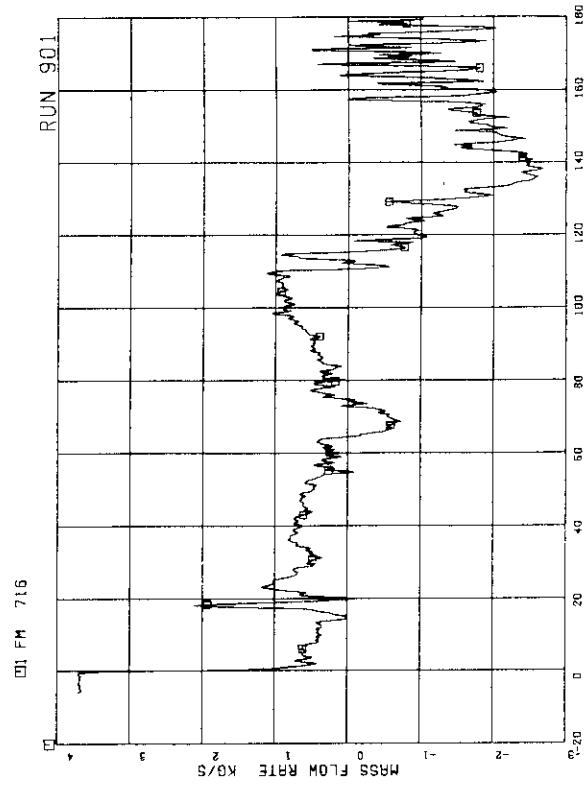


FIG.5.201 FLOW RATE AT CHANNEL C INLET

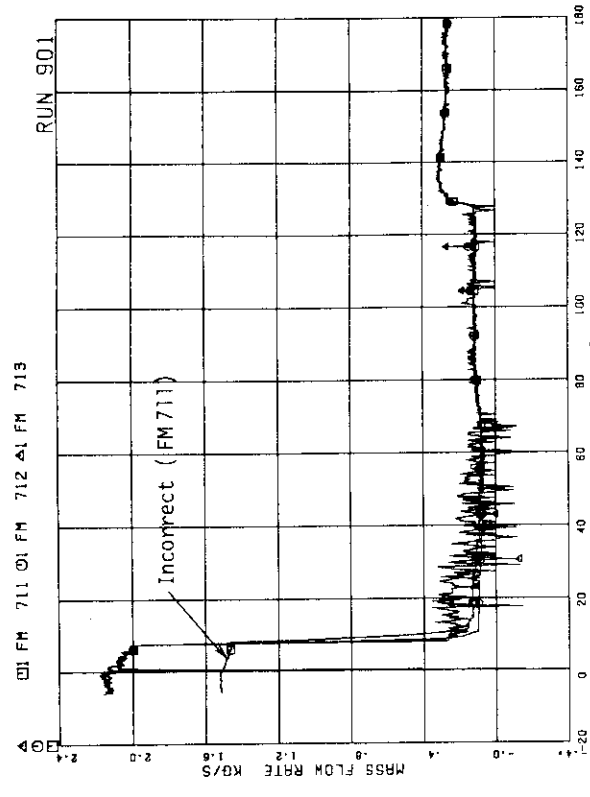


FIG.5.198 STEAM DISCHARGE FLOW RATE THROUGH MSL

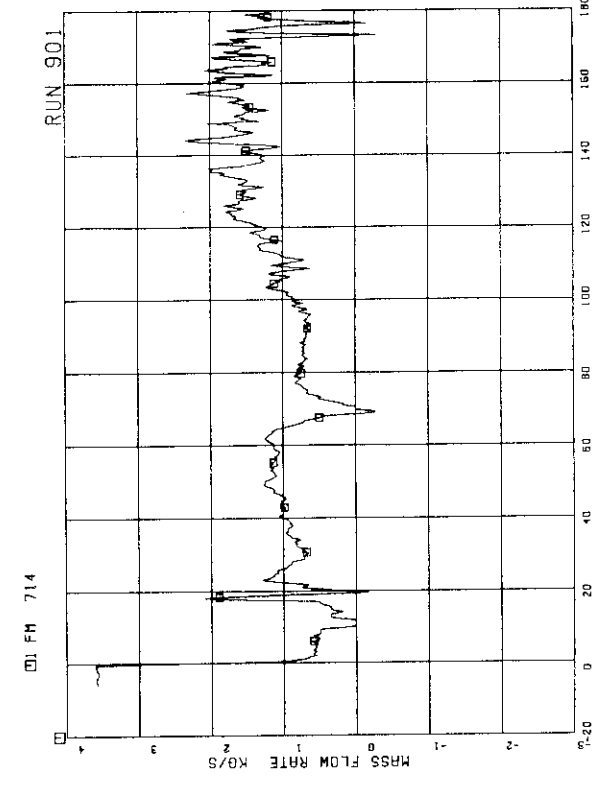


FIG.5.199 FLOW RATE AT CHANNEL A INLET

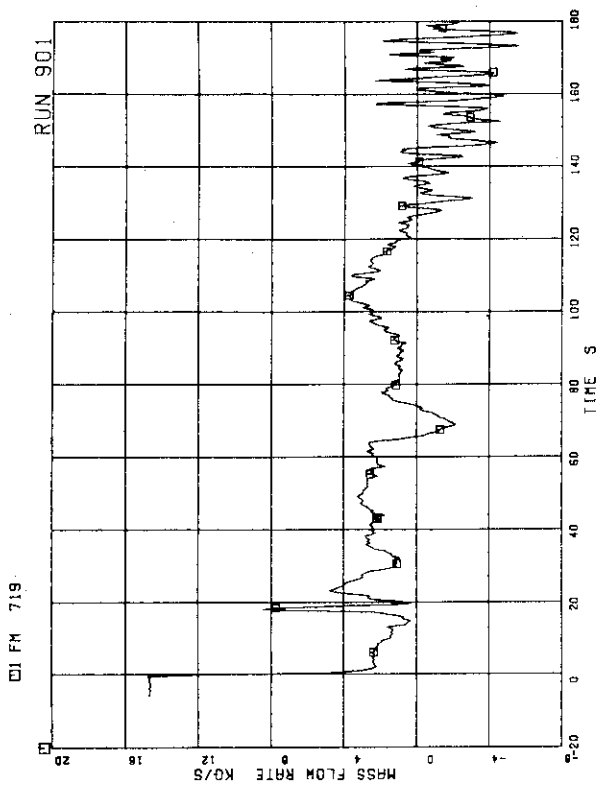


FIG.5.204 TOTAL CHANNEL INLET FLOW RATE

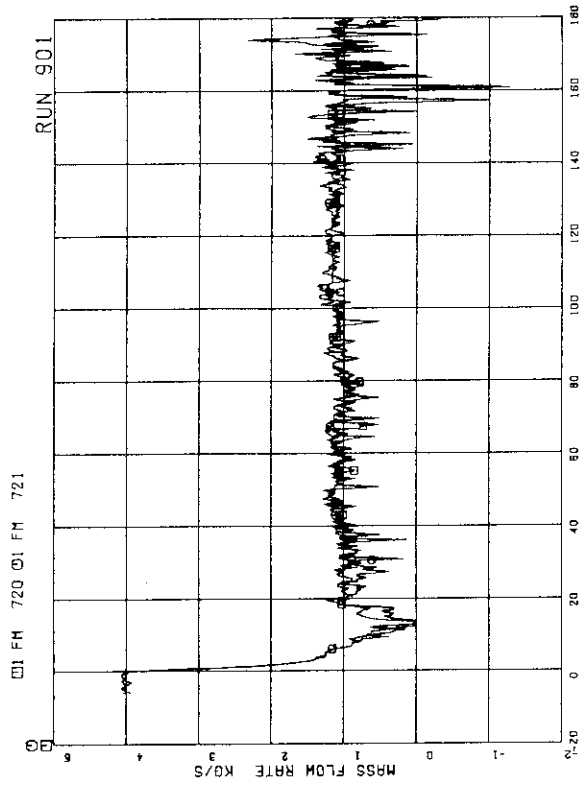


FIG.5.205 FLOW RATE AT JP-1,2 OUTLET (HIGH RANGE)

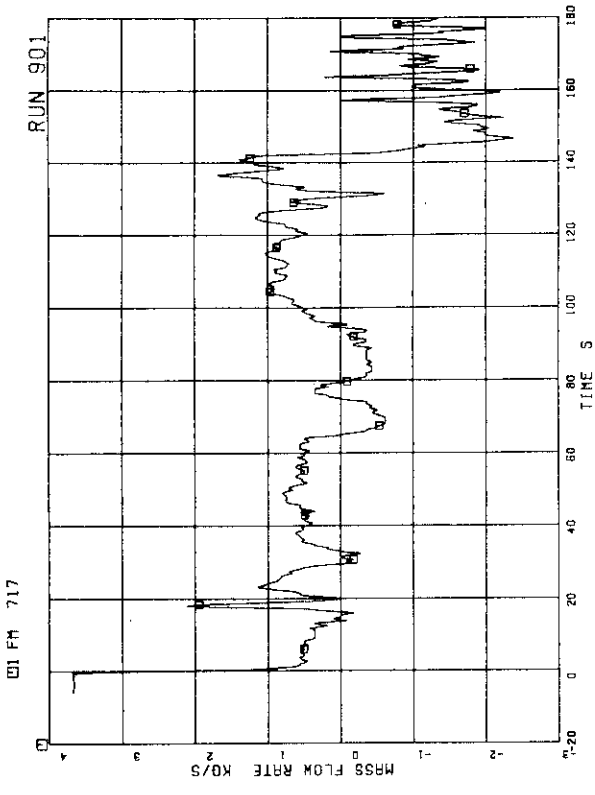


FIG.5.202 FLOW RATE AT CHANNEL D INLET

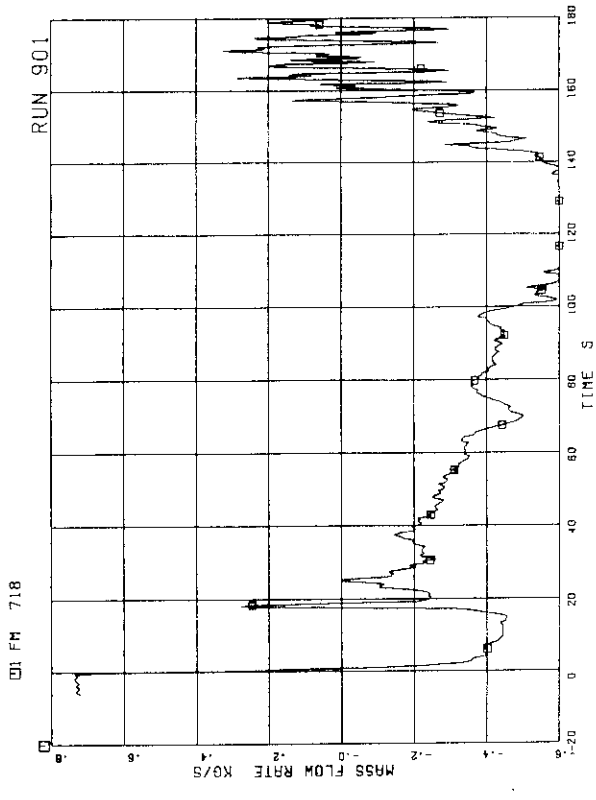


FIG.5.203 FLOW RATE AT BYPASS HOLE

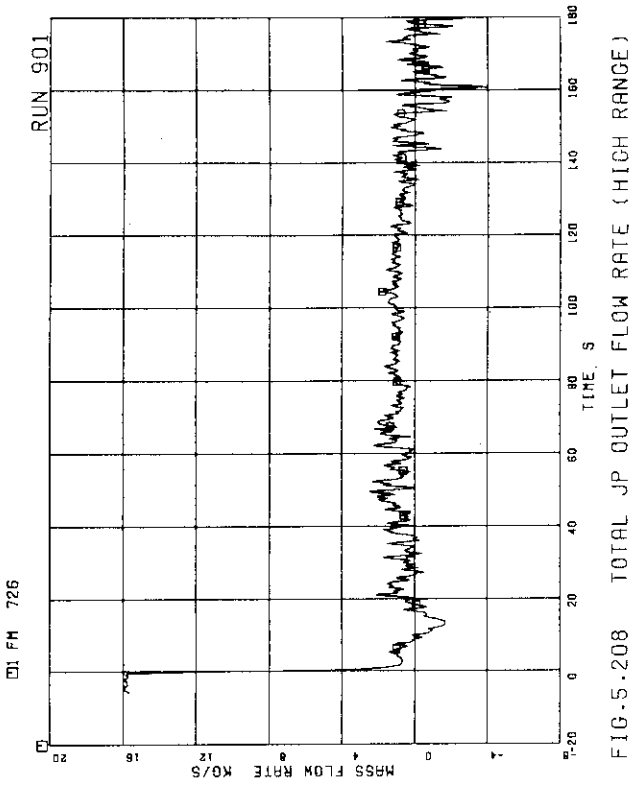


FIG.5.208 TOTAL JP OUTLET FLOW RATE (HIGH RANGE)

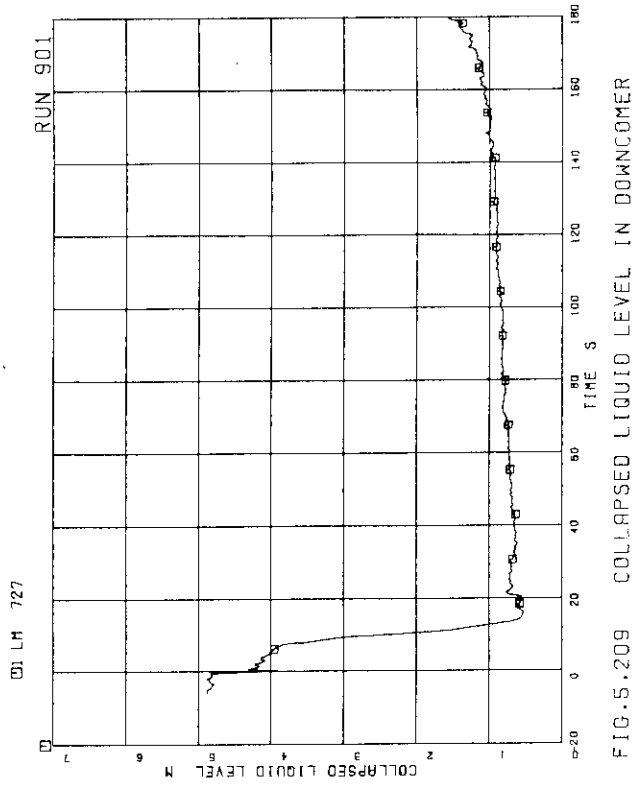


FIG.5.209 COLLAPSED LIQUID LEVEL IN DOWNCOMER

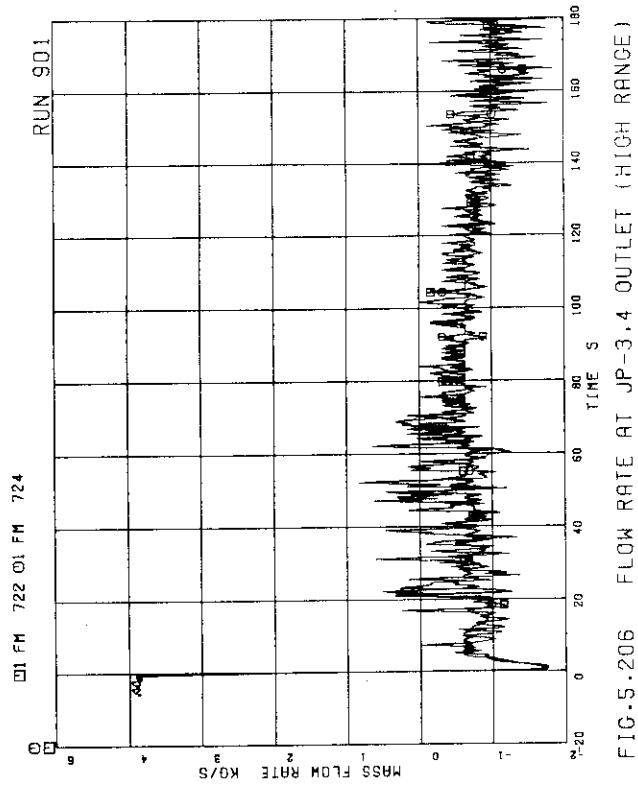


FIG.5.206 FLOW RATE AT JP-3,4 OUTLET (HIGH RANGE)

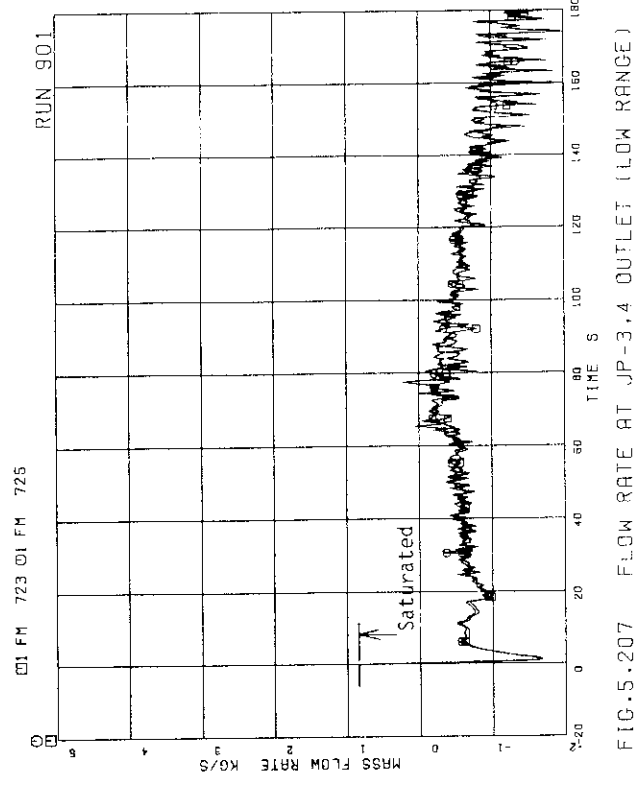


FIG.5.207 FLOW RATE AT JP-3,4 OUTLET (LOW RANGE)

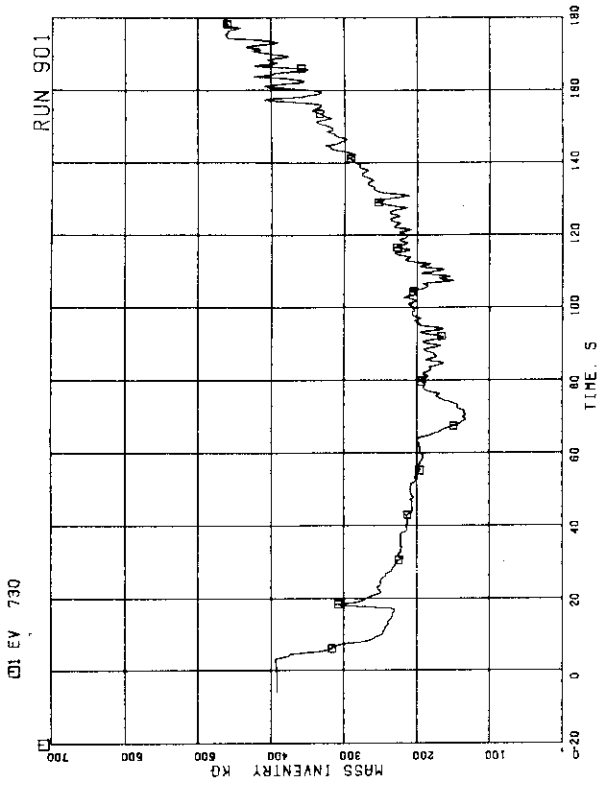


FIG.5.212 FLUID INVENTORY INSIDE CORE SHROUD

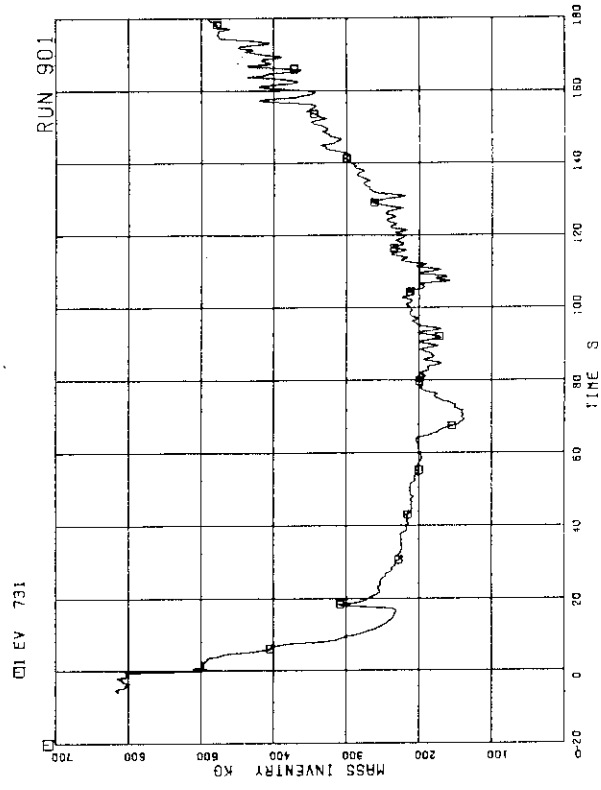


FIG.5.213 TOTAL FLUID INVENTORY IN PRESSURE VESSEL

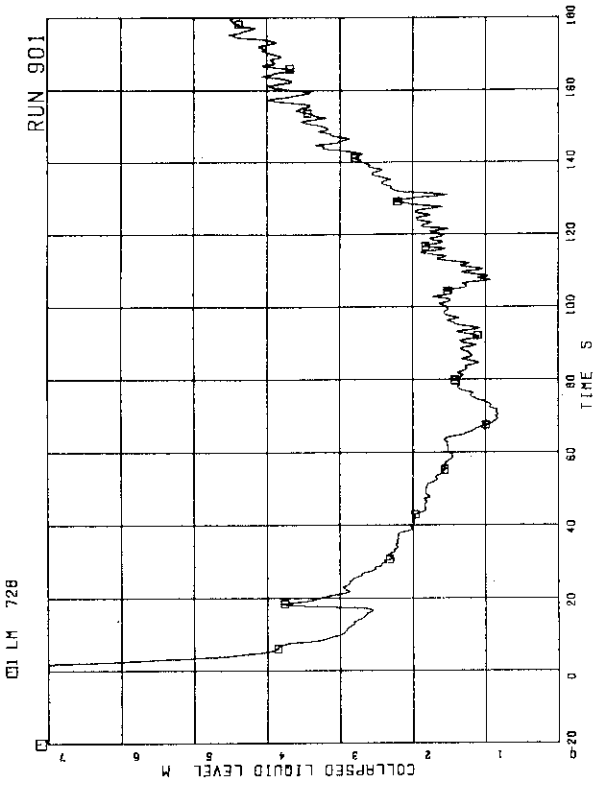


FIG.5.210 COLLAPSED LIQUID LEVEL INSIDE CORE SHROUD

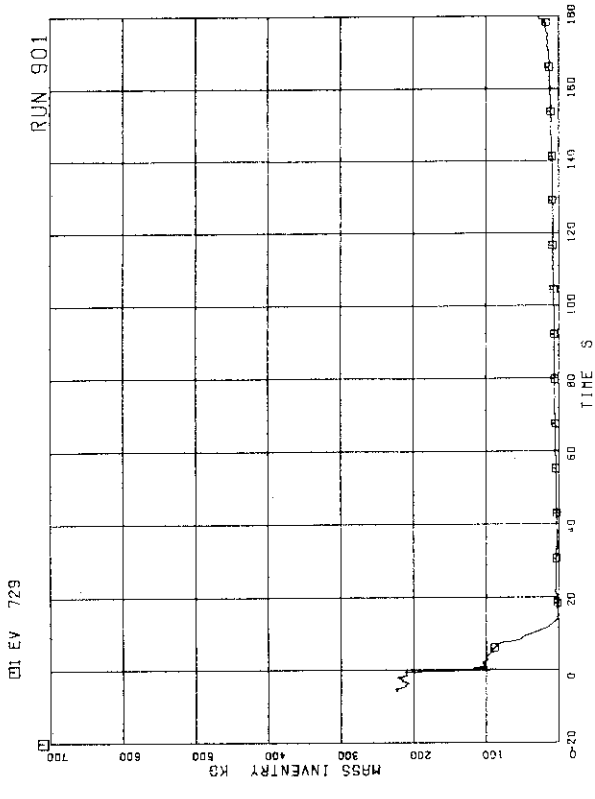


FIG.5.211 FLUID INVENTORY IN DOWNCOMER

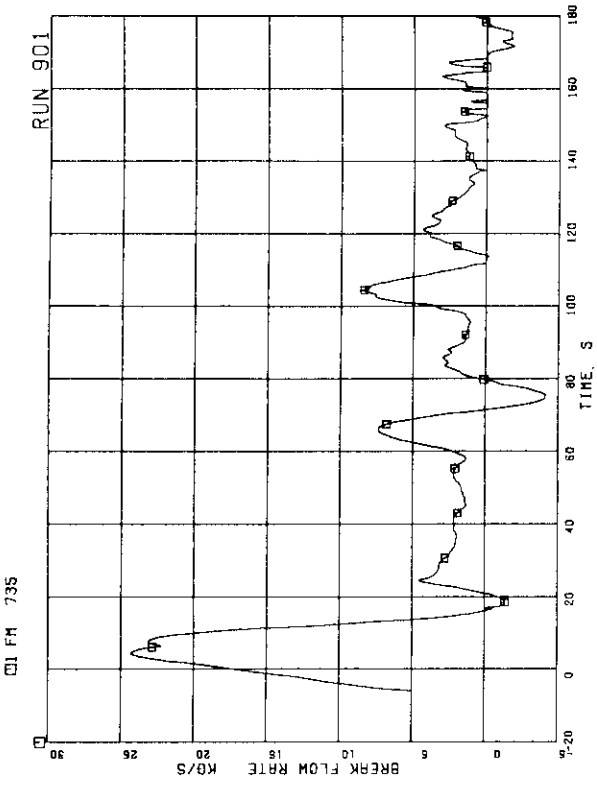


FIG.5.216 DISCHARGE FLOW RATE FROM THE BREAK

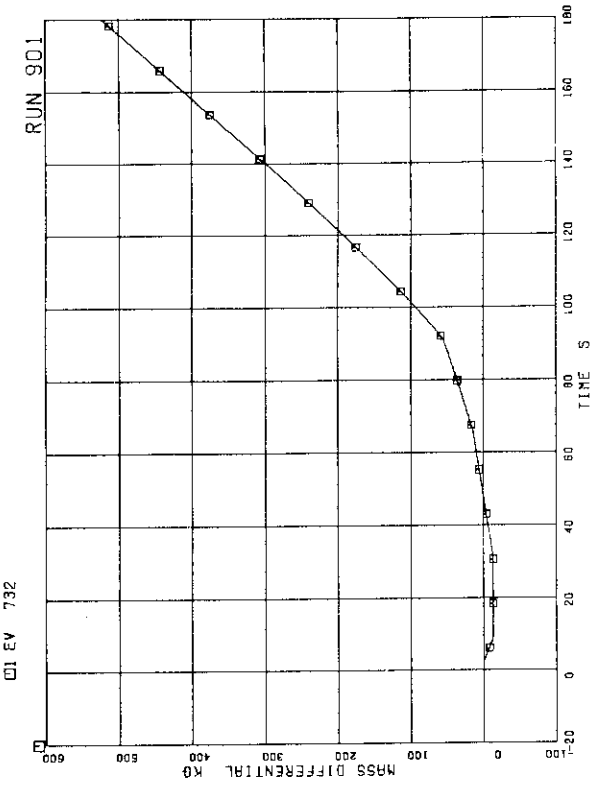


FIG.5.214 FLUID MASS INCREASE BY ECCS AND FW AND DECREASE BY STEAM DISCHARGE FLOW

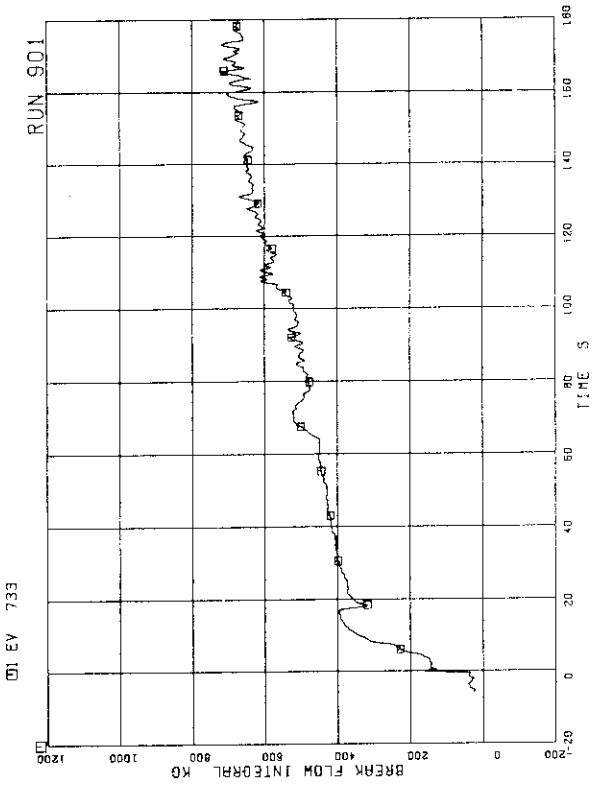


FIG.5.215 DISCHARGED FLUID MASS FROM THE BREAK

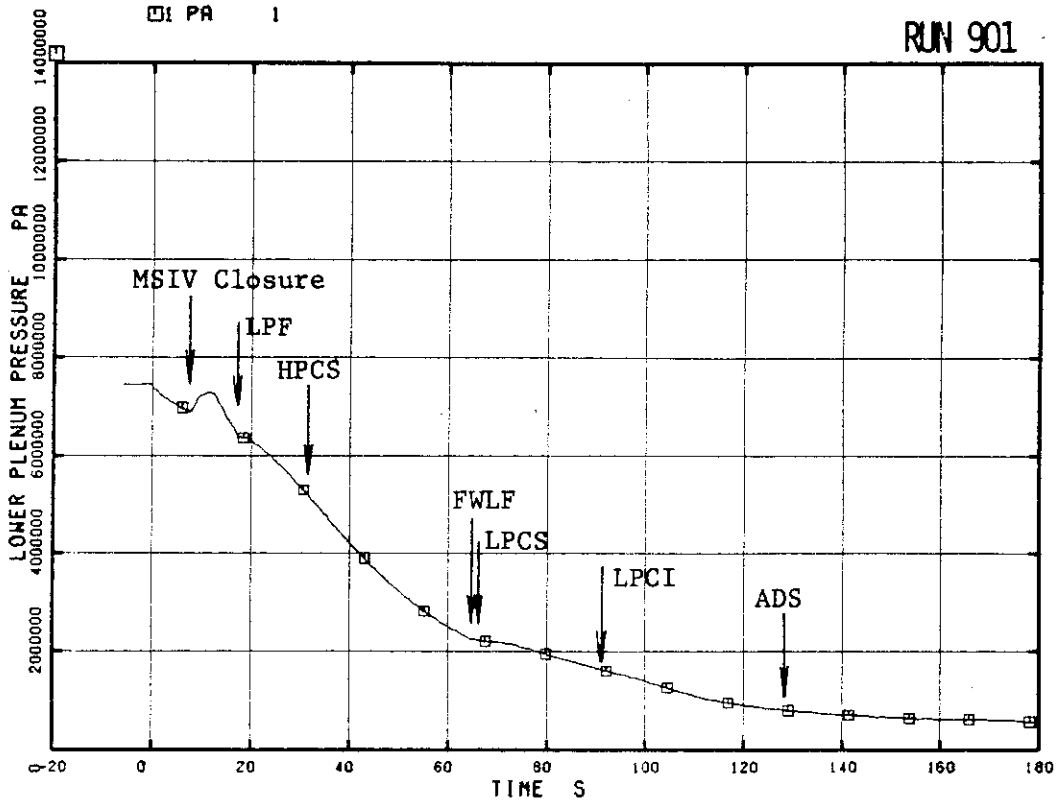


Fig. 6.1 Lower Plenum Pressure

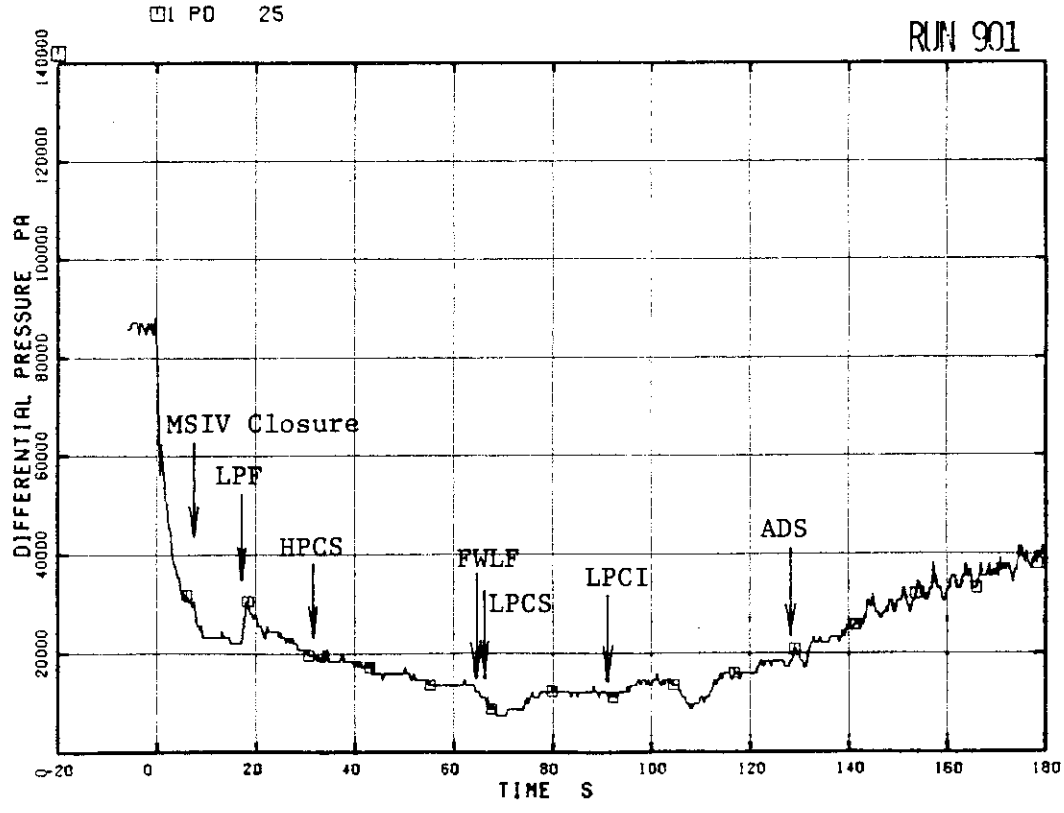


Fig. 6.2 Differential Pressure between Top and Bottom of Pressure Vessel

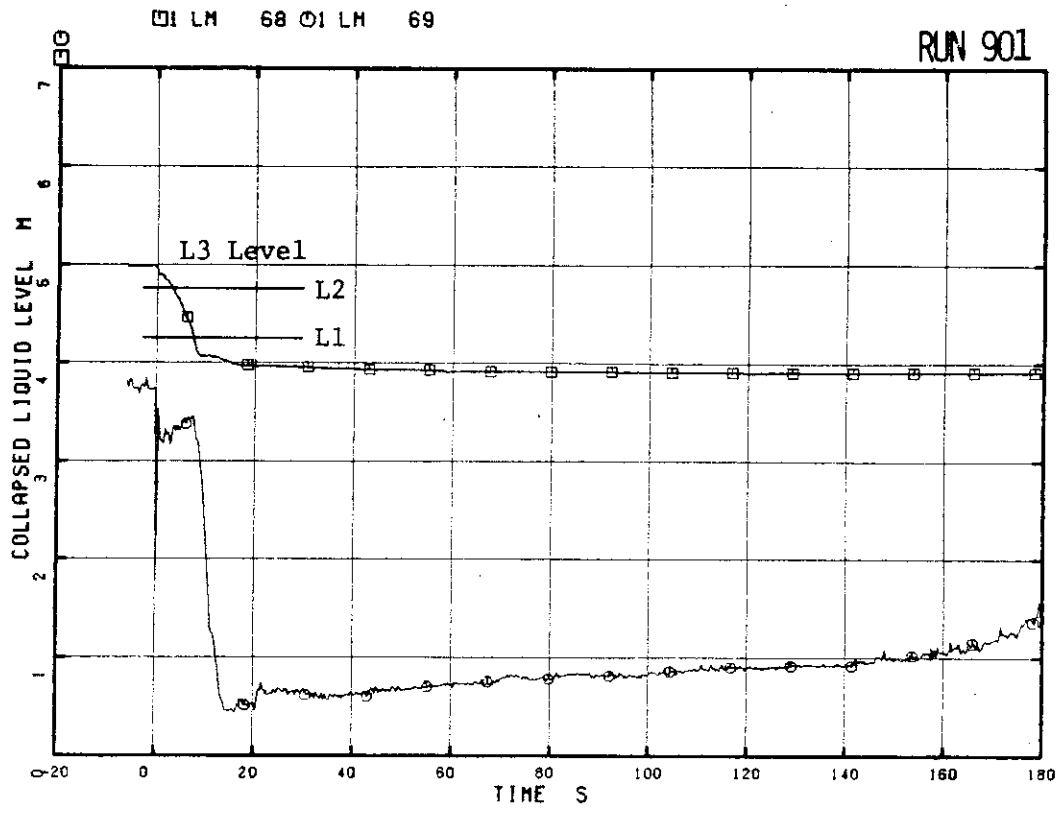


Fig. 6.3 Collapsed Liquid Level in Downcomer

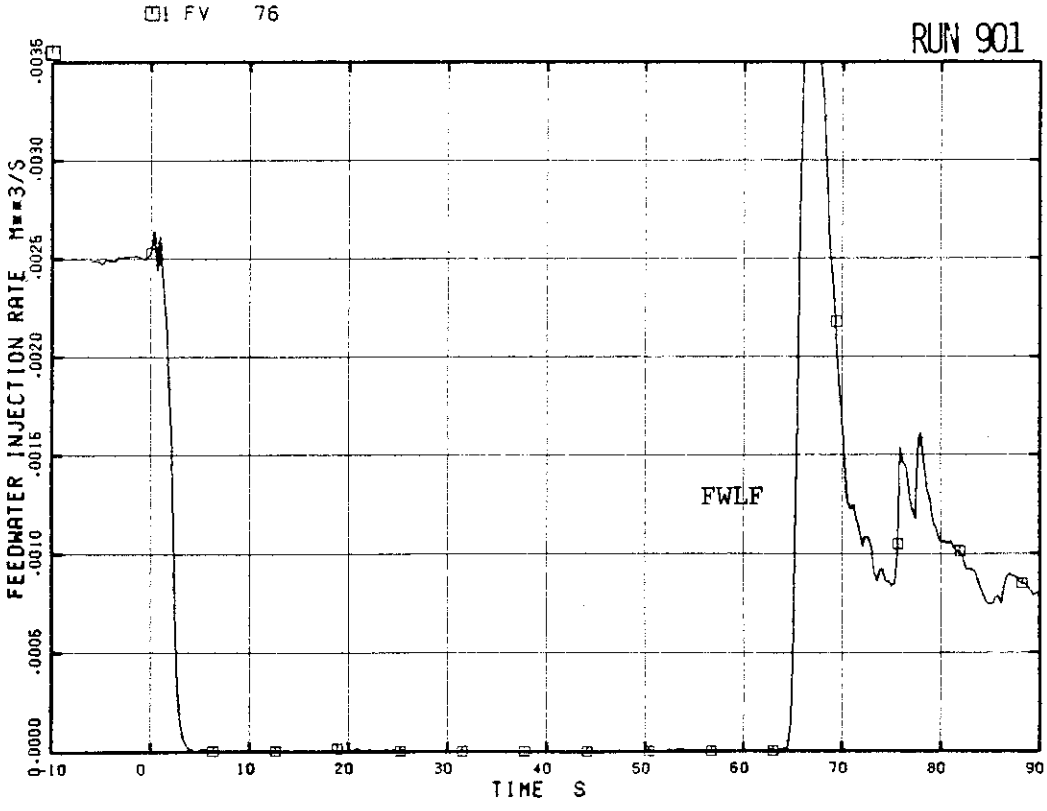


Fig. 6.4 Feedwater Injection Rate

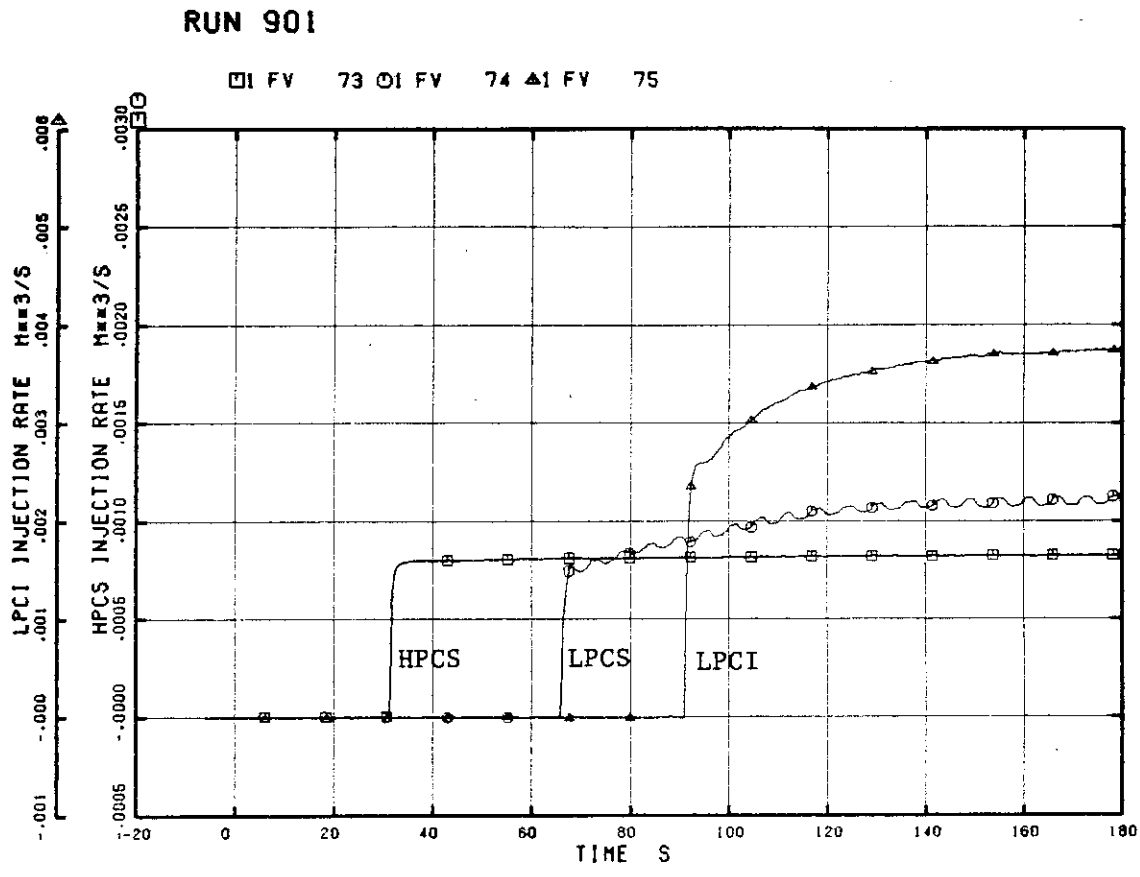


Fig. 6.5 ECCS Injection Rate